CO_2:O_2 balance in boreal freshwaters in a changing climate

Lina Allesson

Dissertation presented for the degree of
Philosophiae Doctor (PhD)
2022

Department of Biosciences
Faculty of Mathematics and Natural Sciences University of Oslo

Series of dissertations submitted to the
Faculty of Mathematics and Natural Sciences, University of Oslo
No. 2564

ISSN 1501-7710

.
Print production: Graphics Center, University of Oslo.

Acknowledgements

First, I would like to thank my supervisors. Dag and Tom for your valuable guidance and supervision of my research. For your doors always being open for a quick question (even if the answers are not always as quick) and for helping me balance in the world of perfect being the enemy of the good. Josefin, you do so much for the department, seeing everyone and considering their mental health, especially of the younger staff, and being the feminist voice in a male dominated world all while performing and supervising interesting research. You are a rock!

To my unofficial supervisors: Alexander, I am so grateful you came in, clickety clacketing in your biking shoes and with your knowledge, helping me improve my research. Thank you also to Peter, your help has been invaluable; the papers would not be as good without you. Per-Johan, your knowledge and problem-solving in the lab is invaluable, you are the MacGyver of AKVA.

I would also like to thank Martin who invited me to this world, I would not have considered research had it not been for you and our initial work in Lund.

To my dear friends and colleagues at AKVA; Jan, Raoul, Jan Erik, Torben, Andrea, Sabrina, Mette, Jonas, Zhanna, Ane, Fransisco, Clare, Julia, Luka, Silje, Lasse, Julie, Karoline, You-Ren, Even, Katrine, Bente, Stein, Stein, Ketil, and Berit; thank you for coffee breaks and after works, and for creating a friendly work environment. A special thank you to my dearest office mates Svenja, Jing and Laurent, thank you for the silence when we all needed to concentrate on work and for the chat breaks when we needed to solve the world's problems or just talk about a new book or TV series. Also, an extra thank you to Nico, I learnt a lot from you during my final year in Oslo.

To Ana, thank you for being a best friend and for pancake breakfasts and natural wine. To my best friend forever Maja, thank you for yearly visits to Oslo and gingerbread baking with a steady increasing number of children.

To my parents Stina and Jan-Inge, thank you for your everlasting love, support, and generosity. I am the luckiest daughter in the world! To my brothers Henrik and Jesper, thank you for the love, fun, and for the teasing, you have made me a stronger person.

To Selma, Finn and Liv, thank you for keeping things real and helping me get my priorities straight. You overwhelm me every day with your kindness and your wisdom. You are the coolest kids and you make me so proud. I cannot wait to see you grow and find out what life brings for you. I love you!

Finally, to Jonas, there is no way to put this. Thank you, life is better with you in it. You are everything!

Table of Contents

List of Papers

Paper I.

Allesson, L., Koehler, B., Thrane, J.E., Andersen, T. and Hessen, D.O., 2021. The role of photomineralization for CO_2 emissions in boreal lakes along a gradient of dissolved organic matter. *Limnology and Oceanography*, *66*(1), pp.158-170.

Paper II.

Allesson, L., Andersen, T., Dörsch, P., Eiler, A., Wei, J. and Hessen, D.O., 2020. Phosphorus availability promotes bacterial DOC-mineralization, but not cumulative CO_2production. *Frontiers in microbiology*, p.2272.

Paper III.

Allesson, L., Ström, L. and Berggren, M., 2016. Impact of photochemical processing of DOC on the bacterioplankton respiratory quotient in aquatic ecosystems. *Geophysical Research Letters*, *43*(14), pp.7538-7545.

Paper IV.

Allesson, L., Valiente, N., Dörsch, P., Eiler, A., Andersen, T., and Hessen. D.O. Drivers and variability of CO_2:O_2 along a gradient from boreal to Arctic lakes. Submitted to Biogeochemistry in May 2022.

Summary

Browning of lakes due to increasing concentration of coloured dissolved organic matter (CDOM), has become an increasingly studied topic over the past few decades. A large share of the CDOM consists of carbon (dissolved organic carbon; DOC), making browning of lakes associated with intensified carbon cycling in freshwater ecosystems. Affecting both microbial and photochemical mineralization of DOC and causing increasing light attenuation, lake browning may therefore regulate net heterotrophy by both inhibiting photosynthesis and stimulating DOC mineralization.

Using a combination of chemical, physical, and spectral data from lake surveys and in vitro measurements, this thesis presents an addition to the understanding of lake carbon cycling and the mechanisms behind the increasing CO_2 supersaturation in northern lakes. The research mainly focuses on DOC mineralization: both photochemical and microbial, and how this may vary with DOC quantity and quality, and nutrient availability.

In Paper I of this thesis, we study the contribution of photochemical DOC mineralization to total lake CO_2 production in Scandinavian lakes of different DOC concentration and colour. Although lakes differed substantially in color, depth-integrated photomineralization estimates were similar in all lakes, regardless of DOC concentrations and relative contribution of photochemical mineralization to total in-lake CO_2-production was small (about 3 %). DOC concentrations were positively related to CO_2-efflux and total in-lake CO_2 production but negatively related to primary production. We therefore conclude that enhanced rates of photochemical mineralization will be a minor contributor to increased heterotrophy under increased browning.

In vitro microbial DOC mineralization was studied in Paper II and III. In Paper II, we find cell specific respiration to be dependent on the carbon to phosphorus (P) ratio while total CO_2 production depended on DOC concentration and seemed to be unaffected by P additions.

P availability yields enhanced bacterial growth and lower cell specific respiration than under phosphorus limitation where the bacteria get rid of excess carbon via enhanced respiration. In addition to these P and DOC level effects, respiration rates responded in a non-monotonic fashion to temperature with increasing respiration rates from 15 to 25°C and a decrease above 30°C. This study highlight DOC as the major determinant of CO_2 production in boreal lakes, with P and temperature as significant modulators of respiration kinetics

Many studies assume a respiratory quotient (RQ = molar ratio of CO_2 produced to O_2 consumed) close to 1 when calculating bacterioplankton respiration. In Paper III, we find that the RQ is systematically higher than 1 when the bacterial metabolism in large part is based on photoproducts. By assuming an RQ of 1, bacterioplankton respiration in freshwater ecosystems may be greatly underestimated.

In Paper IV, we assess the drivers of CO_2 saturation in three groups of lakes separated by steps of approximately ten degrees latitude. CO_2 saturation was coupled to DOC concentrations and net heterotrophy in the southernmost boreal lakes with catchments dominated by coniferous forests. Contrastingly, further north in the arctic regime with sparsely- to unforested catchments, CO_2 saturation was instead tightly coupled to conductivity. This suggests that in the arctic, dissolved inorganic carbon inputs from the surrounding ecosystems and from carbonate weathering dominate as sources to lake CO_2 saturation. The results points to fundamentally different links between DOC and CO_2 in boreal and Arctic catchments, pinpointing the fundamental role of coniferous forests for organic and inorganic carbon dynamics in lakes.

Introduction

Over the past few centuries, the anthropogenic impact on Earth has grown increasingly heavy, making the footprint we leave on Earth's surface irreversible. The current interval of time on Earth is therefore commonly denoted the Anthropocene (Crutzen, 2006). The industrial revolution called for increased coal burning, marking the start of serious human influence on the environment. Since the end of the Second World War, both industry and the world's population have increased close to exponentially, resulting in a concomitant increase in human impact on the environment.

One notable anthropogenic change is the exponential increase in atmospheric CO_2 concentration. These concentrations are today more than 50 % higher than pre-industrial levels (NOAA, 2022) and they keep increasing, with the major share of the increase taken place since the mid 1900's (Change, 2018). As a direct result of these increases in atmospheric greenhouse gases, the global average temperature has increased with roughly 1 ^{o}C during the industrial era. At high latitudes, the increase in surface temperatures is about double that of the global mean (Change, 2018, Masson-Delmotte et al., 2021).

In addition to CO_2, burning of fossil fuels emits sulphur dioxide and nitrous oxides that, through chemical transformations in the atmosphere, form sulphuric acid and nitrous acid (Odén, 1968, Grennfelt and Hov, 2005, Reis et al., 2009). This has led to acid rains and thus a lowering of pH in soils and inland waters. Such acidification may cause severe damage to ecosystems with loss of acid-sensitive species and enhanced toxicity because of leaching metals (Raddum and Fjellheim, 1984, Lydersen et al., 2002). However, since the 1980s, the emissions of sulphur dioxide and nitrous oxides have decreased as the result of a number of successful measures taken. This reduction in emissions has led to a recover from acidification in northern soils and lakes over the past 30-40 years (Monteith et al., 2007).

Although we commonly speak about global warming; depending on geographic location, the ongoing climate change also leads to changes in precipitation patterns, and both intensified and increased numbers of extreme weather events and drought. In northern Europe, precipitation has increased during the past century (Dore, 2005), affecting the run-off from precipitation into the ground and within and between catchments.

Lakes are regarded as reflections of their catchments and react fast to changes in catchment characteristics such as catchment size, topography, geology, land use, vegetation, and soil properties. Lakes thus integrate catchment responses, serving as "sentinels" of changes at the catchment scale (Adrian et al., 2009). Additionally, lakes are sensitive to changes in temperature, precipitation patterns, cloudiness, and atmospheric composition, making lake properties respond rapidly to climate change (Assessment, 2004, Rosenzweig et al., 2007).

Higher temperatures and increased precipitation may be beneficial to plant growth. In fact, a so-called "greening" has been observed at high latitudes of Europe with increased forest biomass and an increased fraction of vegetation cover in the landscape (Tømmervik et al., 2009, Harsch et al., 2009, Larsen et al., 2011b, Myers-Smith et al., 2011, Berner and Goetz, 2022). However, enhanced movement of water leads to enhanced input of soluble minerals and substances from the terrestrial to the aquatic ecosystems. The enhanced biomass production together with enhanced movement of organic substances have led to increased inputs of terrestrially derived (allochthonous) dissolved organic matter (DOM), in northern inland waters (Larsen et al., 2011b, De Wit et al., 2016, Finstad et al., 2016). This DOM consists to a large part of dissolved organic carbon (DOC) and organic nutrients that may be recycled in the aquatic ecosystem by biogeochemical processes (Hessen and Tranvik, 1998).

Over the past few decades the view on lakes has shifted from being mere pipelines, transporting DOC from terrestrial ecosystems to the oceans, to active spots of carbon cycling,

and today we know lakes are a major component of the global carbon cycle (Cole et al., 2007, Tranvik et al., 2009). In lakes with high terrestrial influence, allochthonous DOC is a major source of energy to heterotrophs such that DOC increase has the potential to increase carbon mineralization rates (Hessen et al., 1990, Karlsson et al., 2007). Further, the brown colour of allochthonous DOC leads to lake browning and increased light attenuation (Kritzberg et al., 2020). Enhanced concentrations of allochthonous DOC thus has the potential to considerably perturb biogeochemical balances in lake ecosystems.

Changes in DOC and organic nutrient mineralization rates together with changes in light availability may alter the balance between autotrophic and heterotrophic processes and by extension also production further up the food web (Finstad et al., 2014).

This thesis revolves around the effects of enhanced inputs of allochthonous DOC on lake CO_2 and O_2 production and consumption. The results can contribute to predicting changes in lake ecology and biogeochemistry in a changing climate and environment.

Thesis Outline

Lake CO_2:O_2 balance depends on in-lake CO_2 and O_2 production and consumption. The main processes involved are DOC mineralization through heterotrophic respiration and photochemical processing on the one hand and primary production on the other. Further, DOC mineralization in the catchment may result in inputs of CO_2 to lakes via run-off and groundwater flow.

In this thesis, I focus on each mineralization process and aim to disentangle their relative importance to total lake CO_2 production and how this may change under an increasing DOC regime. In four chapters, I shed light on the different sources of CO_2 saturation in lake ecosystems, aiming to add to the knowledge of how northern lakes may

respond to the ongoing climate and environmental change. Although there is an overall agreement about the broad picture of how terrestrial DOC is cycled in lakes, there are still gaps to fill. Some of these gaps revolve around the relative importance between microbial and photochemical mineralization of DOC, and the relative importance of in-lake to CO_2 production to allochthonous CO_2 loadings for lake CO_2 saturation and evasion. Others revolve around how interacting factors such as substrate quantity and quality, nutrient availability, and temperature affect bacterial respiration, both on a cell-specific and on a community level. For a deeper understanding and to make reliable predictions of how future climate will affect aquatic ecosystems and, by extension, how to mitigate possible negative effects, more research on lake C cycling is needed.

In Paper I, we look at photochemical DIC production in boreal lakes of different DOC concentrations and colour. A few studies have estimated the relative importance of photomineralization to total lake DIC production and CO_2 evasion, mainly focusing on a single, or a limited set of lakes and the resulting estimates differ significantly (Granéli et al., 1996, Jonsson et al., 2001, Cory et al., 2014, Vachon et al., 2016, Groeneveld et al., 2016). One reason of the scarce number of large-scale studies is the need for specialized equipment and time-consuming experiments. We combined spectral data from the lakes with regression estimates between optical parameters and wavelength specific photochemical reactivity (Koehler et al., 2016) to estimate rates of photochemical DOC mineralization in 70 boreal lakes along an ecosystem gradient of DOC concentration. Further, we estimated total in-lake CO_2 production and efflux from lake chemical and physical data.

The aim is to find the relative importance of photochemical DOC mineralization to total in-lake CO_2 production in the study lakes. Shortwave radiation attenuates quickly in the water column and we expect all photo-reactive photons to be absorbed in all lakes. Although

the lakes differ substantially in DOC content and colour, we therefore hypothesise that the total amount of photochemical mineralization of DOC are similar in all lakes.

In Paper II, we focus on the biological mineralization of DOC via bacterioplankton respiration. The C to nutrient ratio of the substrate may have great implications on bacterioplankton metabolism (Hessen et al., 1994, Elser et al., 2009). At high ratios, the bacteria may dispose of excess C via increased CO_2 production (Hessen and Anderson, 2008), while at lower ratios, more C is allocated to growth (Hessen, 1992, Smith and Prairie, 2004). Furthermore, the temperature dependency of bacterioplankton metabolic rates interacts with the substrate quantity and quality (Apple et al., 2006). Microbial mineralization of DOC thus depends on several interacting factors. Although we can expect increases in bacterial growth and metabolism with increased temperatures and loadings of terrestrially DOC and nutrients, how the different environmental factors interact is still not fully elucidated.

Here we aim to fill in some of these knowledge gaps, studying heterotrophic respiration's dependence on additions of allochthonous DOC and P. We chemical and physical data from 75 boreal lakes to estimate in-lake CO_2 production. The lakes span close to orthogonal ecosystem gradients in DOC and TP, allowing us to assess the interactive effects of these two parameters. To test for dynamic responses of bacterioplankton respiration to allochthonous DOC concentrations, nutrient availability, and temperature, we additionally performed experimental incubations. We hypothesize that while the cell-specific respiration and growth depends on the nutrient availability, respiration on the community level may not differ substantially under nutrient poor and nutrient rich circumstances. The major difference being the number of respiring cells.

In Paper III we continue focusing on bacterioplankton respiration, studying biological DOC mineralization of photochemically altered humic substances. Bacterial respiration is

often measured as O_2 consumption and converted to CO_2 production via a conversion factor. This conversion factor is the respiratory quotient (RQ = unit CO_2 produced per unit O_2 consumed) and is often assumed to be one (1). However, true bacterioplankton RQ can vary greatly (Cimbleris and Kalff, 1998, Berggren et al., 2012, Romero-Kutzner et al., 2015). Especially importantly, RQ is strongly dependent on the composition of the assimilated organic substrate (Berggren et al., 2012, Romero-Kutzner et al., 2015). Assimilation of organic substrates with large O content and high O:H ratio requires less O_2 from the surroundings, and hence, respiration is performed at a relatively high RQ (Dilly, 2001). Several of the most common LMW compounds that are released from reactions between DOC and ultraviolet (UV) sunlight are theoretically oxidized at RQs between 1.3 and 4. Although photooxidation is known to be an important process in natural freshwater systems, its potential role as RQ regulator has to our knowledge never been addressed.

We therefore tested the impact of UV radiation on bacterioplankton RQ, hypothesizing that photo-chemically processed DOC is used at a higher RQ than non-irradiated DOC because bacteria assimilate highly oxidized photoproducts such as organic acids. To test this hypothesis, we perform biological incubations of both irradiated and non-irradiated samples of natural lake water, simultaneously measuring the changes in O_2 and CO_2.

Finally, in Paper IV, we take a step back and look at the broader picture, aiming to provide a better understanding of net heterotrophy and gas balance at the catchment scale. We aim to gain understanding on whether lake CO_2 saturation is dominated by in-lake processes or by allochthonous inputs and whether there is a latitudinal difference in drivers of lake CO_2:O_2 ratio, notably related to forested or unforested catchments. There are conflicting reports of whether the main regulator of lake CO_2 saturation is in-lake DOC mineralization or export from terrestrial environments (Larsen et al., 2011a, Weyhenmeyer et

al., 2015, Nydahl et al., 2020, Jonsson et al., 2001). Some of the contradictory findings likely depend on climate, local hydrology, catchment slopes, water retention time, and not the least catchment properties like lake size or fraction and type of forest, bogs and wetlands (Puts et al., 2022, Valiente et al., 2022). We couple surface CO_2 and O_2 concentrations in 103 Norwegian lakes to environmental variables along a geographical gradient ranging from the boreal zone in southern Norway (58^o N) through sub-Arctic northern Norway (69^o N) to the high Arctic at Svalbard (79^o N). The gradient reflects different catchment properties varying from dense spruce forest, via open birch forest to totally unforested catchments with thin soils in the high Arctic.

Lake Browning

Lake browning has been attributed to a number of drivers. One commonly suggested driver is the decline in atmospheric sulphur deposition. As acid rains have decreased during the last few decades, soil pH has increased, increasing the solubility and thereby mobility of soil organic matter (Monteith et al., 2007, Finstad et al., 2016, De Wit et al., 2016). If recovery from acidification were the only driver of browning, it would eventually level off and return to a state similar to before acidification started (De Wit et al., 2016).

However, there is a lack of long-term records to statistically confirm this return to previous water colour, and other factors should also be considered important drivers of browning. According to some existing historical records from southern Sweden, water colour was not primarily suppressed in response to increasing S deposition, suggesting that the change was rather a result of the transition in land use from agriculture to forestry (Kritzberg, 2017).

Forest type also has a key role in the level of browning. Litter from conifers is generally of lower quality for microbial processing and thereby more recalcitrant compared

to that from deciduous trees (Duan et al., 2014). More DOC thus leaches from coniferous forests than from deciduous forests, explaining higher levels of browning in boreal compared to temperate forests. Moreover, iron (Fe) is known to contribute to light absorption in freshwater systems and thus add to the water colour (Canfield Jr et al., 1984). Complexes between Fe and humic substances may in turn affect water colour more than DOC and Fe alone (Maloney et al., 2005, Kritzberg and Ekström, 2011, Weyhenmeyer et al., 2014). Increase in Fe concentrations are generally higher in lakes in forested areas dominated with coniferous trees than in lakes in deciduous forests (Li and Richter, 2012). Transition towards dominance of coniferous forests over deciduous forests due to forestry practices may thus also have an impact on browning.

Climate and land use change over the last century have caused an increasing trend in vegetation cover. Increased terrestrial biomass renders an increased source of organic matter to be exported to inland waters (Larsen et al., 2011b, Finstad et al., 2016). Time series analyses have shown that wetter periods may give rise to increased water colour compared to dryer periods (Erlandsson et al., 2008). Increased precipitation due to climate change may thus be a driver of increased browning of inland waters as it results in enhanced run-off and by that enhanced transport of DOC. However, in high precipitation areas a further increase in precipitation may likely result in shorter retention times and enhanced dilution of terrestrial DOC (De Wit et al., 2016).

The individual importance of each mechanism behind browning is difficult to disentangle and therefore also predicting future water colour. Climate and environmental change will however promote high concentrations and movement of DOC and Fe in the aquatic continuum, having the potential to further promote browning.

Lake CO_2 production

Light Attenuation and photochemical mineralization of DOC

Terrestrial DOC is high in aromatic humic compounds and therefore efficient in absorption of ultraviolet (UV) and visible light (Lindell et al., 1995). Several studies have shown that increased concentrations of terrestrial DOC in lakes leads to increased light attenuation in the water column and thus a decreased euphotic zone, constraining primary production to a thinner surface layer of the water body (Williamson et al., 1996, Thrane et al., 2014, Seekell et al., 2015). Consequently, browning regulates lake heterotrophy and net CO_2 efflux to the atmosphere.

Besides being an essential source of energy for bacterioplankton (Hessen, 1992), the chromophoric terrestrial DOC is highly photo-reactive, especially in the UV waveband (Lindell et al., 1995). Photochemical processing of DOC might therefore be a significant part of carbon cycling in humic lakes. This processing includes both photomineralization of DOC to dissolved inorganic carbon (DIC) and partial photooxidation of high molecular weight humic compounds to low molecular weight compounds available for bacterial metabolism (Kieber et al., 1989, Bertilsson and Tranvik, 1998, Berggren et al., 2012).

DOC photo-reactivity is highest at the shortest wavelengths and decreases close to exponentially towards longer wavelengths (Koehler et al., 2016). The apparent quantum yield (AQY) of photomineralization is the mole of photochemically produced DIC per mole of light quanta absorbed by the DOC pool (Miller et al., 2002) The AQY is thus highest in the UV – blue area of the spectrum which are also the wavelengths that are attenuated fastest in the water column (Koehler et al., 2016). In lakes with high concentrations of coloured DOM (CDOM) the majority of the photomineralization takes place near the surface, while in clearer lakes with lower CDOM concentrations, light penetrates further down in the water column, letting photochemical mineralization take place at greater depths. A few studies have estimated the relative importance of photomineralization to total lake DIC production and

CO_2 evasion. Most of the studies focus on a single, or a limited set of lakes and the resulting estimates differ significantly (Granéli et al., 1996, Cory et al., 2014, Vachon et al., 2016, Dempsey et al., 2020). One reason of the scarce number of large-scale studies is the need for specialized equipment and time-consuming experiments (Koehler et al., 2016). In a first global estimate, Koehler et al. (2014) found the annual photochemical mineralization to account for about 10 % of the total CO_2 emissions from inland waters. As loadings of photo-reactive DOC to lakes increase, the relative importance of photomineralization to lake C cycling may change (Cory et al., 2014, Dempsey et al., 2020).

To Paper I, we estimated the DIC photoproduction in 70 boreal lakes along an ecosystem gradient in DOC concentration and colour. The range in DOC concentrations spanned a wide range and the results could give a hint of what may be the role of phtotomineralization for CO_2 emissions in lakes undergoing browning. According to regression estimates from Koehler et al. (2016), we used optical parameters to estimate AQY spectra. Together with site-specific irradiance spectra we could estimate photochemical DIC production in the lakes (Figure 1).

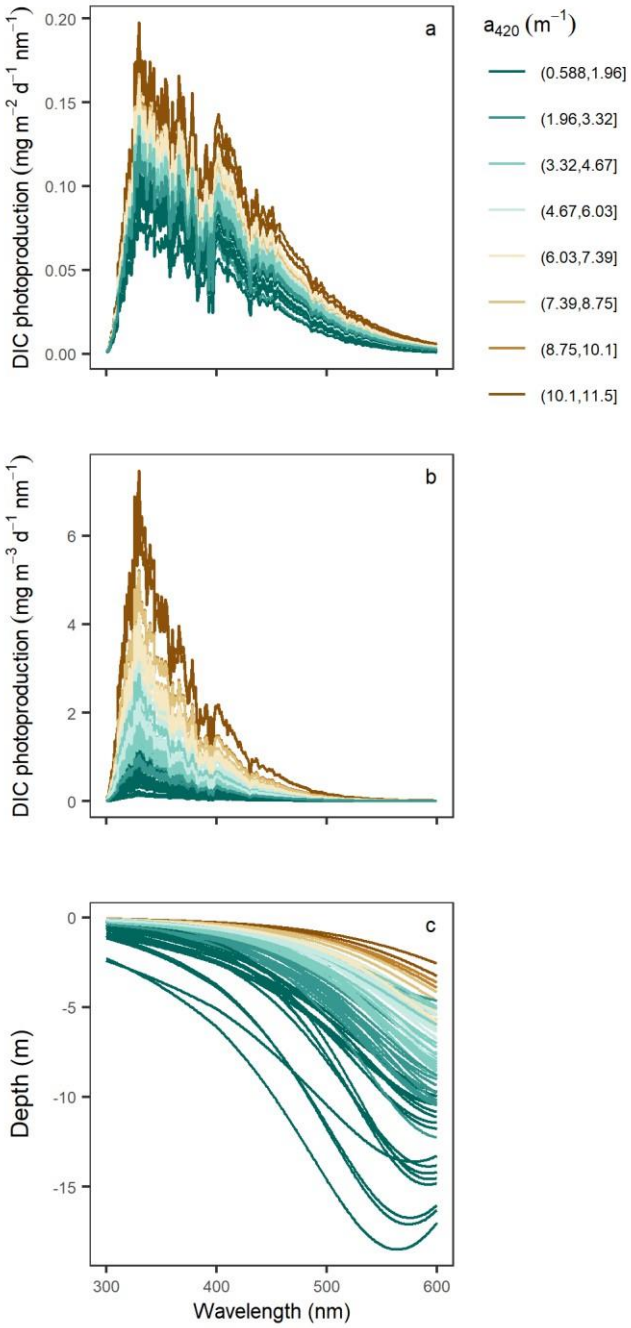

Figure 1. Estimated photoproduction spectra of dissolved inorganic carbon (DIC) from all 70 study lakes. In (a), the estimated areal DIC photoproduction (mg C m^{-2} d^{-1} nm^{-1}) spectra are shown; and (b) shows the estimated volumetric DIC photoproduction (mg C m^{-3} d^{-1} nm^{-1}) spectra just below the surface. In (c) the depth at which the volumetric DIC photoproduction (mg C m^{-3} d^{-1} nm^{-1}) is 1 % of that just below the surface is shown, indicating also the depth that receives 1 % of incoming radiation. The color gradient goes from dark blue for clear lakes with low a_{420} to brown for brown lakes with high a_{420}.

We found that close to all of the short wavelengths are absorbed within the top meters of the water column in most lakes regardless of water colour (Paper I; Figure 1c). The

browner the lake, the faster the wavelengths are absorbed. However, in lakes deeper than about five meters, all photo-reactive wavelengths are absorbed. This indicates that further browning would not result in higher amounts of photochemical DIC production but rather move the photochemical reactions further up in the water column. Further, we found depth-integrated photomineralization estimates to be similar in all lakes. There was thus little difference in the amount of photochemical DIC production per lake area among lakes of different colour. Rather, the difference was at which depth in the water column the photochemical reactions took place.

The relative contribution of DOC photomineralization to in lake carbon cycling has been shown to vary, both between systems (Granéli et al., 1996, Molot and Dillon, 1997, Cory et al., 2014), and temporally within the same system (Vachon et al., 2016, Groeneveld et al., 2016), depending mainly on DOC quantity and quality. However, in our study, where the studied lakes spanned a wide range in DOC concentration, the relative contribution of photochemical mineralization to total in-lake CO_2-production was about 3 ± 0.2% in all lakes with no significant difference between systems (Paper I; Figure 2). Rather than photochemical mineralization of DOC, heterotrophic respiration was thus the major CO_2 source in all lakes, regardless of water colour.

In the boreal biome, photochemical DIC production has been estimated to correspond to about 9-12% of the annual lake CO_2 emissions of 47 – 59 Tg C yr^{-1} (Kortelainen et al., 2006, Koehler et al., 2014). In accordance with these numbers, we estimated photochemically produced DIC to correspond on average to 9 ± 1% of the total CO_2-evasion from the study lakes. CO_2 evasion is generally higher in brown than in clear lakes (Sobek et al., 2003, Humborg et al., 2010, Larsen et al., 2011a) while the contribution of photochemically produced DIC to CO_2 evasion was highest in clear lakes (Paper I).

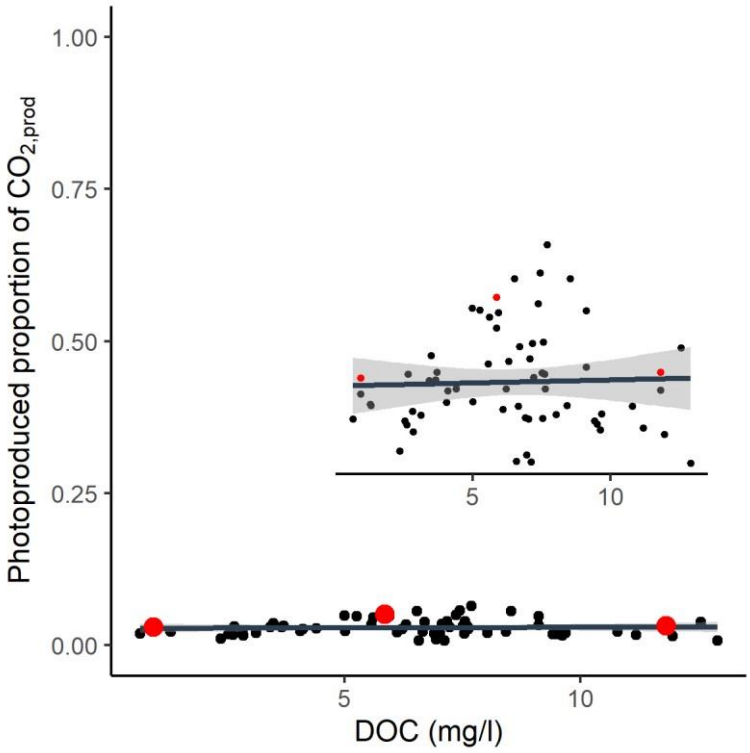

Figure 2. The relative proportion of photoproduced DIC to total CO_2 production in the 70 study lakes in Paper I (the inset figure is zoomed in on the y-axis). There was no significant difference between lakes of different DOC concentrations.

The lakes in Paper I differed widely in colour from clear to dark brown and both CO_2 efflux and total in-lake CO_2 production were positively related to DOC concentration. Although browner lakes most likely will result in enhanced CO_2 evasion, the contribution of enhanced rates of photochemical DIC production will presumably be minor.

Photochemical processing of DOC may however give other end-products than CO_2. Organic nutrients associated to DOC are photo-mineralized and made available for consumption by both aquatic autotrophs and heterotrophs. Further, partial photooxidation of DOC transforms recalcitrant DOC to more biologically available organic compounds such as carboxylic acids (Bertilsson and Tranvik, 1998, Bertilsson and Tranvik, 2000). Aquatic heterotrophs often preferentially consume such partially photooxidized compounds over the high molecular weight non-photodegraded compounds (Berggren et al., 2012). Although

most photochemical processes occur in the surface layer, downward mixing makes photochemically produced carboxylic acids a potential source of labile DOC in the entire mixed layer. Indirect microbial mineralization of partial photooxidation products may be as important as direct photomineralization (Bertilsson and Tranvik, 1998).

Finally, light absorption by DOC may be beneficial to aquatic organisms as it may protect from harmful UV-radiation (Williamson et al., 1996, Dillon and Molot, 2005). However, as the coloured DOC absorbs light, it re-emits heat. This may modify the stratification properties of the water column (Williamson et al., 2015). Shallower mixed layers and stronger and longer periods of stratification yields colder temperatures and anoxia in the hypolimnion (Couture et al., 2015). Anoxia in the hypolimnion controls lake productivity (Craig et al., 2015) and CH_4 production, which can be released to the atmosphere (Vuorenmaa et al., 2014). Moreover, a darker environment may disturb predator-prey interactions, especially for visual predators, potentially having great impacts on the ecosystem and its populations and individuals (Ranåker et al., 2012).

Heterotrophic respiration

Heterotrophic bacteria consume DOC and convert it to CO_2 through bacterial respiration (BR) (del Giorgio et al., 1997, Duarte and Prairie, 2005) and to biomass through bacterial production (BP) (Jansson et al., 2006, Berggren et al., 2010, Del Giorgio and Cole, 1998). Oceanic and freshwater BR together may represent the single largest sink of organic carbon worldwide and DOC constitutes a major part of the bulk organic carbon globally (Del Giorgio and Williams, 2005, Drake et al., 2018). Aquatic bacteria are thus an essential part of the global carbon cycle.

Most lakes on Earth are supersaturated with and net emitters of CO_2 to the atmosphere (Cole et al., 2007, Raymond et al., 2013). Several studies have reported a positive correlation

between lake CO_2 emission and DOC concentration (Sobek et al., 2003, Larsen et al., 2011a, Bogard and del Giorgio, 2016), indicating that bacterial respiration dominate as main CO_2 source. Autochthonous (in-lake) production is however not the only source of DIC. Lateral flux of inorganic carbon produced in the catchment may account for a sizeable share of lake CO_2, especially in small lakes with short retention times and long ice-free seasons (Weyhenmeyer et al., 2015).

Whether a lake is a net conduit of CO_2 is not necessarily a sign of net heterotrophy but could also reflect that catchment derived CO_2 exceeds photosynthetic uptake. Likewise, the magnitude of atmospheric CO_2 uptake in a net autotrophic system may be reduced by inputs of terrestrial CO_2. There are conflicting reports of whether CO_2 produced in aquatic environments via DOM mineralization or exported from terrestrial environments is the main regulator of lake CO_2 flux (Larsen et al., 2011a, Weyhenmeyer et al., 2015, Nydahl et al., 2020, Jonsson et al., 2001). Some of the contradictory findings likely depend on climate, local hydrology, catchment slopes, water retention time, and not the least catchment properties like lake size or fraction and type of forest, bogs and wetlands (Puts et al., 2022, Valiente et al., 2022).

In Paper I and II, we estimated in-lake CO_2 production in boreal lakes using chemical and physical data. The lakes spanned close to orthogonal ecosystem gradients in DOC and total phosphorus (TP), allowing us to assess the interactive effects of these two parameters on CO_2 production and on CO_2 and O_2 saturation deficits. We found a strong negative correlation between O_2 and CO_2 saturation deficits such that lakes saturated with O_2 were also saturated with CO_2 (Figure 3). Further, we saw no correlation between total inorganic carbon (TIC) and CO_2 deficit. This together indicates that in the sampled boreal lakes, processes within lakes, especially microbial respiration was the predominant source of CO_2 supersaturation.

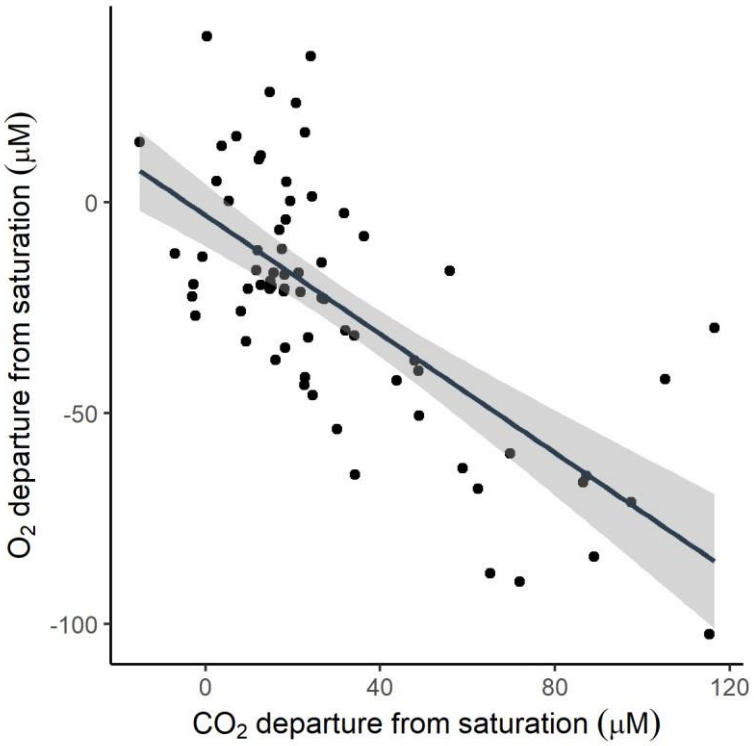

Figure 3. Lake O_2 departure from saturation with the atmosphere vs CO_2 departure from saturation with the atmosphere in 70 boreal lakes along an environmental gradient in DOC concentrations (Paper I; CI slope: (-9, -5); CI intercept: (-10, 4); $R^2 = 0.49$; $p << 0.001$).

There, however, seems to be a difference in dominating CO_2 source between systems of differing catchment type. In Paper IV, we coupled surface CO_2 and O_2 concentrations in 103 Norwegian lakes to environmental variables along a geographical gradient ranging from the boreal zone in southern Norway (58^o N) through sub-Arctic northern Norway (69 ^{o} N) to the high Arctic at Svalbard (79^o N). The gradient reflects different catchment properties varying from dense spruce forest, via open birch forest to unforested catchments with thin soils in the high Arctic.

We saw a clear distinction in drivers of CO_2 saturation between different regions. Boreal lakes, with catchments dominated by coniferous forests followed the expected pattern with both CO_2 and O_2 saturation being largely dependent on DOC concentrations and negatively related to one another, suggesting enhanced net heterotrophy with increased DOC inputs.

In Arctic lakes, despite differences between sub-Arctic and high-Arctic sites, we saw no correlation between DOC and CO_2, yet these sites were also to a large degree supersaturated with CO_2 and could be considered net heterotrophic. However, most Arctic lakes were also saturated or supersaturated with O_2, indicating low respiratory activity (Figure 4). This is in agreement with generally nutrient-poor conditions and low levels of primary production. We also saw a positive correlation between CO_2:O_2 ratio and conductivity, while the influence of DOC concentration was weak or non-significant. This may suggest that the major share of CO_2 in the Arctic lakes is of allochthonous origin, likely from organic carbon mineralization and carbonate weathering in the catchment soils, entering via groundwater flow (Rodríguez-Rodríguez et al., 2018, Puts et al., 2022). This points to fundamentally different links between DOC and CO_2 in boreal and Arctic catchments, pinpointing the role of coniferous forests for organic and inorganic carbon dynamics in lakes.

Although there may be pronounced regional differences within this vast area, the wide spatial gradient across climatic regions and catchment properties could provide insights relevant to larger parts of both the boreal and the arctic biome.

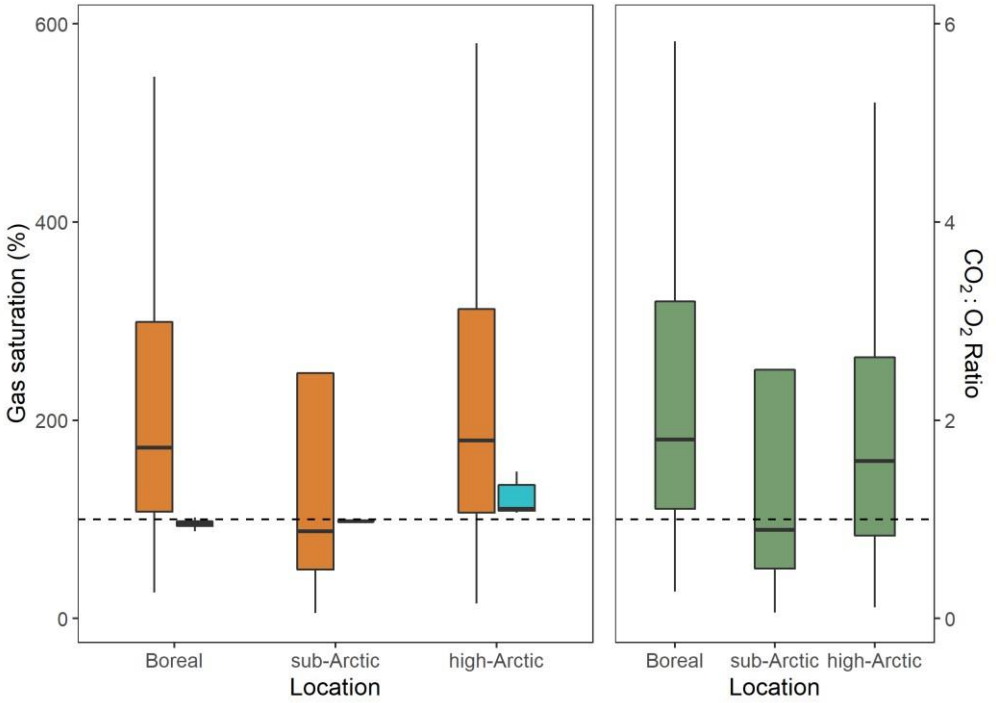

Figure 4. Box plot of lake CO_2 saturation (red), O_2 saturation (blue), and CO_2:O_2 ratio (green) in three different geographical regions. Dashed line represents the 100 % saturation (to the left) and a CO_2:O_2 ratio of 1 (to the right).

Substrate stoichiometry: nutrients

Heterotrophic respiration has a key role in C cycling in boreal lakes and will most likely increase with enhanced loadings of allochthonous DOC and enhanced temperatures (Apple et al., 2006, Larsen et al., 2011a, Lapierre et al., 2013). However, questions remain about bacterial metabolism's response to enhanced loadings of allochthonous DOC and nutrients and to increasing temperatures in a changing climate.

Current knowledge shows that nutrient stoichiometry, quantity and quality of the substrate, and temperature are main factors, governing bacterioplankton metabolism. Bacteria have a high nutrient demand and the C to nutrient ratio of the substrate and the availability to inorganic nutrients governs the carbon use efficiency (Hessen, 1992, Hessen et al., 1994, Elser et al., 2000). Low such C:nutrient regimes promote biomass production while under

high C:nutrient regimes, bacteria may dispose of excess C via enhanced respiration (Hessen, 1992, Hessen and Anderson, 2008).

The efficiency of bacterial carbon use can be approximated as the share of the total assimilated organic carbon used for BP (bacterial growth efficiency: BGE = BP / (BP + BR)). This determines to what degree bacterial metabolism results in bacterial biomass production or in mineralization of organic carbon (Del Giorgio and Cole, 1998).

The carbon to nutrient ratio therefore has great impact on the cycling and fate of carbon in a planktonic habitat. Phosphorus (P) is the most commonly reported limiting nutrient for BP and P availability thus regulates the use of DOC for growth (Vadstein, 2000). Planktonic DOC is generally more bioavailable and has a lower C:P ratio than allochthonous DOC. When DOC of both autochthonous and allochthonous origin is available, heterotrophic bacteria use the planktonic DOC for catabolic processes (Kritzberg et al., 2004).

Microorganism's activity and growth are constrained by temperature (Farrell and Rose, 1967, Madigan et al., 1997) with a general increase in metabolism with increased temperatures. However, studies show that the temperature dependency is stronger for bacterial respiration than for bacterial production (Rivkin and Legendre, 2001, Apple et al., 2006, Berggren et al., 2010, Kritzberg et al., 2010), and that this dependency may be constrained by nutrient availability. Furthermore, metabolic rates have been shown to be less temperature dependent for heterotrophic bacteria growing on labile autochthonous DOC than when growing on complex and recalcitrant allochthonous DOC (Ylla et al., 2012, Jane and Rose, 2018). Microbial mineralization of DOC thus depends on several interacting factors. Although we can expect an overall increased bacterial metabolism with increased temperatures and terrestrially derived DOC and nutrient loadings in lakes, there are still knowledge gaps of how the different environmental factors interact.

In Paper II, we coupled environmental factors to in situ CO_2 production rates in 75 Scandinavian lakes. The lakes spanned close to orthogonal ecosystem gradients in DOC and TP, allowing us to assess the interacting effect of these two parameters on CO_2 production. We found CO_2 production to have a unimodal response to increased DOC concentrations with a minimum around 5 mg DOC L^{-1}. This indicates a shift in DOC pool from primarily autochthonous at lower DOC concentrations to primarily allochthonous at higher DOC concentrations. After the turning point and as the concentration of allochthonous DOC increases, the CO_2 production rates increased linearly with increased DOC. This turning point corroborates with earlier observations of primary production rates increasing with increased DOC concentrations until around 5 mg C L^{-1}, after which they decline (Karlsson et al., 2007, Seekell et al., 2015, Tanentzap et al., 2017). The DOC concentration-specific CO_2 production, i.e., the rates of CO_2 production per unit of DOC concentration, was positively related to primary production rates. Further, the DOC:TP ratio had a negative effect on primary production, and consequently, the DOC:TP ratio also had a negative effect on the DOC concentration-specific CO_2 production. This implies a more bioavailable DOC pool in productive than in unproductive lakes (Søndergaard et al., 1995) and could also suggest that this is explained by a lower C:P ratio of the substrate.

To further assess the dependency of bacterial respiration on DOC and P, we monitored CO_2 production in incubations of water with a gradient of DOC crossed with two levels of inorganic P. Finally, we crossed DOC and P with a temperature gradient to test the temperature dependency of respiration rates. While the total amount of CO_2 produced during the incubations increased with DOC concentration, P additions had little to say for the cumulative CO_2 production (Figure 5a). On the other hand, respiration rates and bacterial growth yield were higher in P-spiked than in P-limited samples (Figure 5b), suggesting increased bacterial growth and decreased cell-specific respiration under non-limited P conditions. This is in accordance with earlier findings of negative relations between P supply

and cell-specific respiration (Smith and Prairie, 2004, Vikström and Wikner, 2019). DOC concentration hence regulates the overall respiratory output of CO_2 (and consumption of O_2), while additions of P changes the dynamics by boosting respiration.

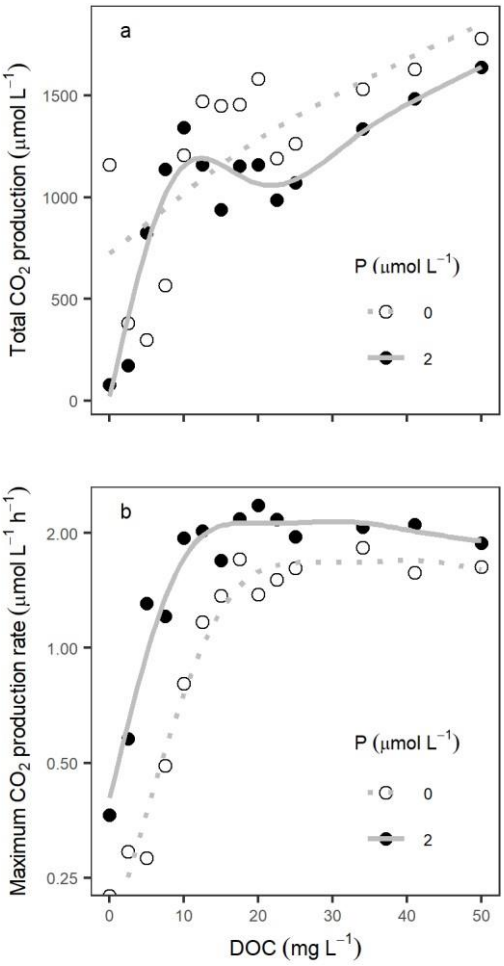

Figure 5. The response of a) total CO_2 production (µmol L^{-1}) during the entire incubation (240 h) and b) maximum CO_2 production rates (µmol L^{-1} h^{-1}) to increased DOC concentrations (mg L^{-1}). The solid and dotted lines are fitted gam curves (y ~ s(x)) to samples with and without P additions respectively.

Respiration rates showed a sigmoid response to increasing DOC availability reaching a plateau at about 20 mg C L^{-1} of initial DOC concentrations. This increase in respiration with DOC was in accordance with the increase in total CO_2 production rates at increased DOC concentration >5 mg L^{-1} found in the lake survey. Many boreal lakes have DOC

concentrations below 20 mg L^{-1} (e.g. the lake survey of Paper I and II had a maximum value of 12.9 mg C L^{-1} and Paper IV had a median value of 7.7 mg C L^{-1}) and a continued increase in BR with increased terrestrially derived DOC up to about 20 mg L^{-1} could be expected. In addition to these P and DOC level effects, respiration rates responded in a non-monotonic fashion to temperature with an increase in respiration rates by a factor of 2.6 from 15 to 25°C and a decrease at higher temperatures. This further reinforce the idea that net heterotrophy in lakes will increase with increasing temperatures, which also would lead to increased emissions of CO_2 (Sobek et al., 2003). The combined results from the survey and experiments highlight DOC as the major determinant of CO_2 production in boreal lakes, with P and temperature as significant modulators of respiration kinetics.

Substrate stoichiometry: oxygen

The DOC source we used in Paper II was a naturally isolated DOC, added at the beginning of the experiment. In a natural environment, the DOC pool would be constantly refreshed by new additions from the surrounding, not considered in our experiment. Further, recalcitrant DOC would undergo photochemical processing, breaking down high molecular weight humic acids to more bioavailable substrates (Bertilsson and Tranvik, 1998). When available, bacterioplankton preferentially use smaller fractions, easier to assimilate before the more recalcitrant humic fractions (Berggren et al., 2012).

Besides regulating bacterial respiration and growth, substrate composition may also regulate heterotrophic O_2 consumption. Assimilation of organic substrate of high O content and high O:H ratio requires less O_2 from the surroundings (Dilly, 2001). Under such circumstances, respiration is performed at a relatively high respiratory quotient (RQ = unit CO_2 produced per unit O_2 consumed).

High molecular weight humic substrates generally have low O:H ratios and respiration is performed at low RQ, requiring a relatively large amount of O_2 from the surroundings. However, partial oxidation of high molecular weight DOC, may produce compounds with high O content and high O:H ratio (Bertilsson and Tranvik, 1998). Assimilation of such photoproducts may thus be performed at a relatively high RQ (Berggren et al., 2012). Although photooxidation is known to be an important process in natural freshwater systems, its potential role as RQ regulator has to our knowledge never been addressed.

In Paper III, we therefore tested the impact of photochemical processing of DOC on bacterioplankton RQ. We monitored the bacterial RQ in bioassays of both irradiated and non-irradiated humic lake water. As expected, we found bacterioplankton RQ to be significantly higher in irradiated (3.4–3.5 ±0.4) than in non-irradiated samples (1.3 ±0.1). Both CO_2 production and O_2 consumption were higher in irradiated than in non-irradiated samples, indicating increased bacterial activity and a shift towards more labile substrate. The elevated RQ's found in irradiated samples could however not completely be explained by bacterial use of the photoproducts such that there must have been a broader modification of DOC molecules during irradiation. Further, anabolic metabolism is performed at a higher RQ than catabolic respiration alone (Dilly, 2003, Berggren et al., 2012) and bacterial consumption of a more bioavailable photo-altered substrate has been shown to result in enhanced biomass production compared to the more recalcitrant humic substances (Anesio et al., 2005, Amado et al., 2015). Enhanced biomass production in irradiated samples could thus have contributed to the elevated RQ's we observed.

The consistently much higher RQ values in irradiated samples reflect a mechanism that should be present in all light-exposed DOC-rich waters globally and photochemical processes thus have an important role in regulating bacterioplankton RQ.

When assessing BR in aquatic systems, O_2 measurements are often favoured over direct CO_2 measurements as dissolved O_2 can be measured on the aqueous phase, without gas extraction, and without the need to correct for changing equilibria in the inorganic carbon system. An RQ is thus needed as a conversion factor. Many such studies apply a fixed RQ value of 1 (del Giorgio et al., 1997, Koch et al., 2007), which is the theoretical value of complete oxidation of glucose. However, true bacterioplankton RQ can vary substantially (Cimbleris and Kalff, 1998, Berggren et al., 2012, Romero-Kutzner et al., 2015), for example by consumption of photo-altered DOC, as we showed in Paper III. By using the *a priori* assumption of an RQ value of 1 for inland waters, bacterioplankton CO_2 production may thus be greatly underestimated.

Lake O_2 production

Primary Production

Although enhanced inputs of allochthonous DOC primarily stimulates heterotrophic metabolism, DOM associated nutrients may also benefit autotrophs (Seekell et al., 2015, Tanentzap et al., 2017). Further, heterotrophic mineralization of DOC and the subsequent increase in heterotrophic CO_2 production may indirectly stimulate autotrophs by increasing CO_2 availability (Jansson et al., 2012). An increase in DOC concentrations in clear unproductive waters can therefore stimulate both primary and secondary production. However, as waters turn browner, increased light attenuation may suppress primary production overriding the positive effects of DOM as a nutrient supply (Thrane et al., 2014, Seekell et al., 2015). The relation between increased DOC concentrations and primary production is thus unimodal with a maximum typically around 5-10 mg l^{-1} (Seekell et al., 2015). A decrease in primary production propagates through the food web leading to lower overall production, including fish biomass (Karlsson et al., 2009). Finstad et al, (2014)

reported a unimodal response of fish production to increased DOM concentrations, similar to the response of primary production. In corroboration with this unimodality, we saw in Paper II a unimodal response of total CO_2 production to increased DOC concentration in the lakes, suggesting a shift in substrate from mainly autochthonous to predominantly allochthonous DOC.

In Paper I, II, and IV, we found similar drivers of O_2 saturation and estimated areal primary production rates as for CO_2 saturation and CO_2 production rates in boreal lakes. The major regulator of lake O_2 saturation was unsurprisingly the negative effect of DOC concentrations with browner lakes being undersaturated with O_2 while clearer lakes were at or close to O_2 saturation. Further, the DOC:TP ratio correlated negatively with areal primary production rates (Paper II), indicating increasing autotrophic activity with nutrient availability. This, together with the already discussed correlation between CO_2 and O_2 saturation deficits conform the common picture of DOM inputs regulating lake heterotrophy in boreal lakes.

On the contrary, the majority of the arctic lakes in Paper IV were saturated or supersaturated with both CO_2 and O_2 regardless of DOC concentrations. The CO_2 supersaturation in Arctic lakes would, at first thought, indicate net heterotrophy. However, high levels of O_2 saturation together with weak or non-significant influence of DOC concentration on CO_2 saturation rather indicate low respiratory activity in agreement with generally nutrient-poor conditions. High O_2 saturation levels together with a dominance of allochthonous input of CO_2 suggest autotrophy rather than heterotrophy in the artic lakes studied in Paper IV.

Closing Remarks

Allochthonous DOC stimulation of heterotrophic metabolism together with the subsequent reduction in primary production at high DOC concentrations make most lakes of high terrestrial influence net heterotrophic (Paper I, II, and IV) (Hessen et al., 1990, Cole et al., 1994, Sobek et al., 2003, Thrane et al., 2014). Lakes comprise only a small fraction of the global land surface (about 4 % (Verpoorter et al., 2014)) but intensive in-lake carbon processing together with inputs of allochthonous CO_2 make greenhouse gas emissions from lakes equivalent to up to 20 % of the global CO_2 emissions from fossil fuel combustion (DelSontro et al., 2018). Recovery from acidification, increased vegetation cover in catchments, land use change, and a wetter climate all together promote carbon export to lakes (Finstad et al., 2017, de Wit et al., 2018, Škerlep et al., 2020) contributing to enhanced browning (Kritzberg et al., 2020).

Bacterial metabolism depends on substrate quantity and quality, nutrient availability, and temperature (Farrell and Rose, 1967, Hessen et al., 1994, Smith and Prairie, 2004). Productive lakes have a more bioavailable DOC pool with lower C:P ratio, promoting bacterial growth and yielding high bacterial numbers with low per-cell respiration (Paper II) (Søndergaard et al., 1995). On the other hand, in unproductive lakes where the DOC pool is dominated by allochthonous DOC with high C:P ratio, fewer cells may be present but cell-specific respiration is elevated (Vikström and Wikner, 2019). The overall respiratory output of CO_2 is thus primarily regulated by DOC concentrations (Paper II).

While heterotrophic respiration is the dominant DOC mineralization process, photochemistry may have a significant role in processing DOC, both via photomineralization and via partially degrading DOC to smaller compounds (Granéli et al., 1996, Bertilsson and Tranvik, 2000, Cory et al., 2014). However, sunlight attenuates fast in the water column making photo-reactive wavelengths absorbed within the top few meters also in clear lakes

(Paper I). Photochemical processes will thus likely not increase as lakes turn browner but rather move upwards and take place closer to the surface. Decreasing primary production and increasing bacterial respiration due to increasing export of humic-rich DOC will thus enhance net heterotrophy (Paper I, II, and IV). The relative contribution of photomineralization to CO_2 evasion will most probably decline in a changing climate (Paper I).

Besides DOC mineralization and in-lake processing, DIC may also enter lakes via surface- and groundwater flow (Ojala et al., 2011, Vachon and Del Giorgio, 2014). Whether in-lake production or inputs of allochthonous CO_2 dominate as a cause of lake CO_2 saturation is dependent on the catchments characteristics with net heterotrophy tightly coupled to DOC inputs and coniferous forest coverage (Puts et al., 2022). Coniferous forests thus have a fundamental role, governing the organic and inorganic dynamics in lakes (Paper IV).

In the ongoing climate crisis, we can expect a decrease in lake productivity with decreased O_2 levels, having consequences throughout the entire food web. In a forest ecosystem with high lake abundance, including the evasion from lakes in the CO_2 budget of the forest lowers the effect of the vegetation as a net sink, with the potential to shift to a net source on the ecosystem level in a changing climate.

Selected Methods

Paper I: Estimating photochemical DIC production

In Paper I, we estimated the role of photochemical DOC mineralization for lake CO_2 emissions in 70 boreal lakes along a gradient in DOC concentrations. Simulation of photochemical mineralization of DOC requires knowledge of the photochemical reactivity of the DOC (apparent quantum yield; AQY, defined as moles photochemically produced DIC per mole photons absorbed by the DOC pool) across the whole spectrum of photochemically active wavelengths. The lakes from the data set we used for Paper I, was samples 2011 and did not include AQY measurements. However, Koehler et al. (2016) found positive linear correlations between AQY and the absorption coefficient at 420 nm (a420) and with specific UV absorption coefficients (SUVA254 and SUVA400). These correlations open up for possibilities to improve large-scale model estimates of photomineralization in inland waters based on water colour information.

For the lakes in Paper I, we only had optical data for wavelengths in the PAR band, and even though the correlation between AQY and SUVA 254 was stronger than between AQY and SUVA400, we instead used the relation between AQY and $SUVA_{400}$ (B. Koehler, unpublished data, 2016). We then used the lme4 package in R (Bates and al., 2014) for a linear mixed effects model with the measured AQY as response variable, a_{420}, $SUVA_{400}$, and wavelength as fixed effects, and intercept as a random effect.

In order to find whether we lost any using SUVA400 instead of SUVA254, we used the AQY model on data from the lakes in Koehler et al. (2016) using $SUVA_{254}$ and a_{420} and compared it to the model with $SUVA_{400}$ and a_{420}. The models resulted in close to exactly the same AQY spectra (Figure 6). Hence, we did not seem to lose any information by using extrapolated PAR spectra to predict the AQY spectra for the 70 study lakes.

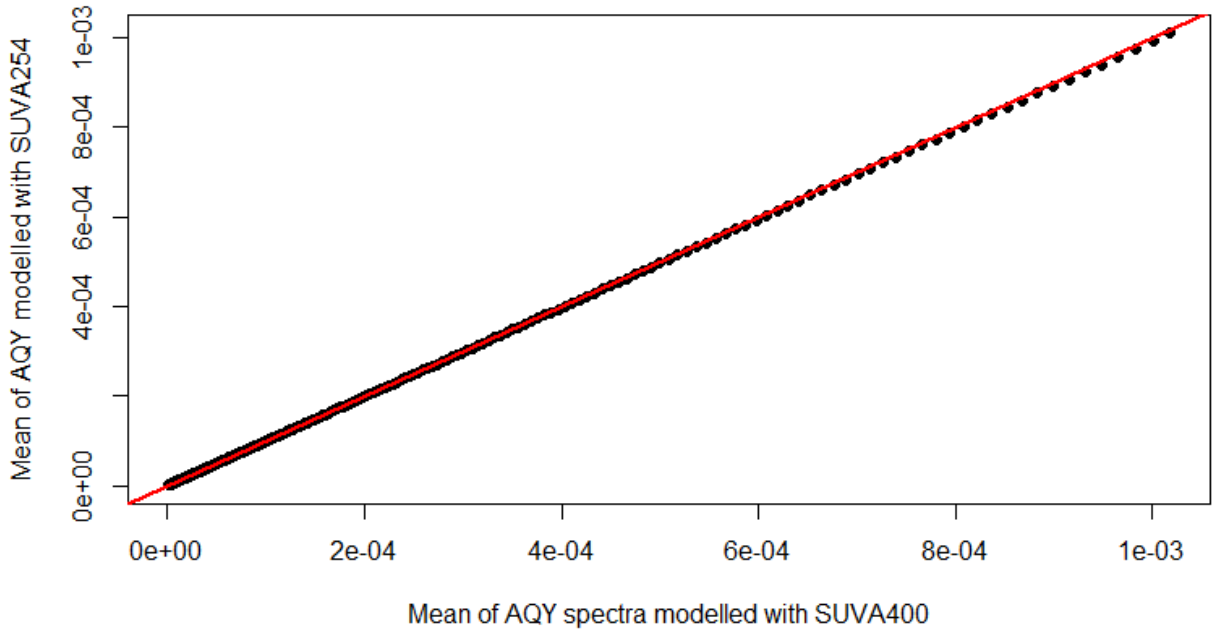

Figure 6. The mean values of each wavelength of the Monte Carlo samples in the AQY model using $SUVA_{254}$ and a_{420} versus the AQY model using $SUVA_{400}$ and a_{420}. The red line is the 1:1 line.

We then also modelled lake absorption spectra for the different compounds in the lake samples (Twardowski et al., 2004; Shen et al., 2012; Wozniak and Dera, 2007; Kirk, 1994) and calculated the relative contribution of DOC to total light absorption (Figure 7).

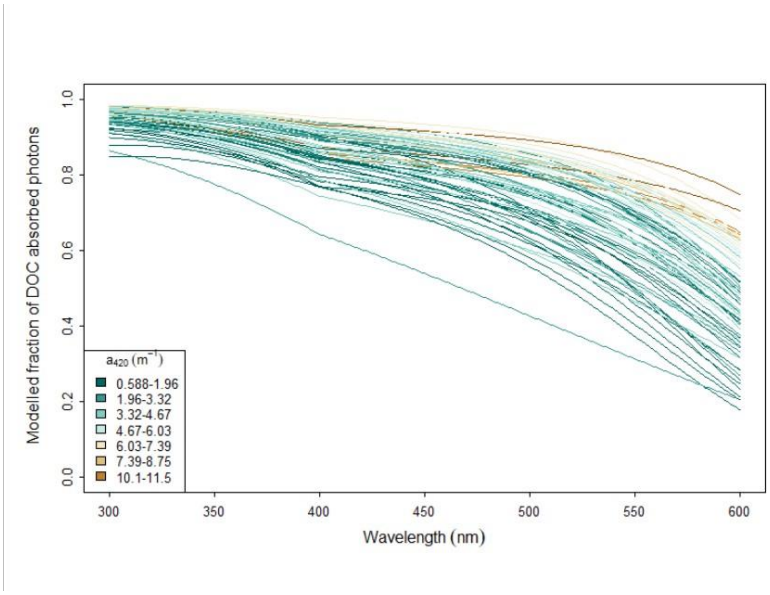

Figure 7. At short wavelengths the fraction of the photons absorbed by DOM is close to 1. The fraction decreases at longer wavelengths, where photochemical reactivity is lower. The color gradient goes from dark blue for clearer lakes with low a_{420} to brown for darker lakes with high a_{420}.

Finally, combining the AQY spectra with the absorption spectra and an irradiation model of incoming photon flux, we could calculate the wavelength-specific photoproduction of DIC per depth or per area unit. All absorption spectra were extrapolated from the measured PAR band to 300 nm using linear mixed effect models with prediction uncertainties propagated through Monte Carlo samples generated by the arm package in R (Gelman et al., 2018).

Paper I and II: Total CO_2 production in the lakes

For Papers I and II, we wanted an estimate of the CO_2 production I lakes. The data set we used included lake CO_2 concentrations. With these concentrations together with wind speed data (the Norwegian Reanalysis Archive (Furevik and Haakenstad, 2012)) we

calculated water-air flux of CO_2 using Henry's law to obtain the CO_2 deficit, and Fick's law of diffusion to obtain the net degassing from the surface. We also obtained necessary coefficients for the calculations according to Jähne et al (1987), Wanninkhof (1992), and Cole and Caraco (1998).

Further, in an earlier study of the same data set, Thrane et al (2014) calculated primary production rates in the lakes. Here, primary production is a measure of CO_2 consumption representing the CO_2 flux from water to primary producers.

The measured parameters included in the dataset did not allow for distinguishing between lateral input of CO_2 via surface- and ground water, and in-lake production of CO_2. We therefore used the sum of in-lake DOC mineralization and lateral input as an estimate of total CO_2 production. Assuming a steady state of the CO_2 saturation deficit, such that all production and input of CO_2 either evades from the surface or is consumed by autotrophs, we can estimate the mass balance due to production, lateral input, consumption, and evasion as the sum of CO_2 fluxes water-air and water-primary producers.

This is indeed a rather coarse estimate of CO2 production and does not give any exact values. However, it is useful and fits for our main purpose of finding the relative contribution of photomineralization to CO_2 production and evasion and whether this depends on the level of brownification of the lakes.

Paper II: Experimental determination of BR

To test for dynamic responses of bacterioplankton respiration to allochthonous DOC concentrations, nutrient availability, and temperature, we additionally performed experimental incubations. During 1-week incubations, we monitored respiration in two experimental set-ups, one addressing CO_2 production and the other O_2 consumption. A gradient of DOC concentrations was achieved by adding natural organic matter (NOM; isolates from a Norwegian humic lake obtained through reverse osmosis(see Gjessing (1999) and Vogt et al. (2001)) to clear lake water.

In the first experimental set-up, we monitored CO_2 concentraions by gas chromatography every 6 hours using the robotized setup described by Molstad et al. (2016) with some modifications. Since the vials contained 50 ml water and 70 ml air, the O_2 uptake was small relative to the large amount of O_2 in the headspace such that we could not measure uptake rates with sufficient precision.

In this set-up, we used 14 levels of DOC additions between 0 and 50 mg L^{-1}, crossing it with two levels of PO_4-P additions (0 and 2 µmol L^{-1}). To make sure that N was not limiting, we added 30 µmol L^{-1} each of NO_3-N and NH_4-N to all samples. The C:N:P ratio ranged between 82:30:1 and 2160:30:1 in samples with P additions.

At the end of the experiment, we aimed to assess biomass measurements using flowcytometry. However, the samples were obscured by background scatter from the added DOC and did not provide reliable counts. Instead, we assessed final microbial biomass from qPCR on filtered samples when terminating the experiment. We approximated bacterial growth yields we measured bacterial 16S rRNA gene copy numbers using a quantitative polymerase chain reaction (qPCR) protocol (Savio et al., 2015).

The main goal of the experiment was to assess BR and although it would have been ideal to verify the dynamic responses in CO_2 with bacterial counts and community response

by genetic screening and transcriptomic, this would have required a different set-up with larger volumes and more frequent sampling. The current set-up allowed us to prioritize the gas analysis while also assessing the final bacterial biomass in each incubation unit.

In the second experimental set-up, we used fewer DOC levels (0 mg L^{-1}, 25 mg L^{-1}, and 50 mg L^{-1}) but added an additional crossing with 4 temperatures (10 ºC, 15 ºC, 25 ºC, and 30 ºC). Concentration of dissolved oxygen was recorded automatically every 15 s using a SensorDish Reader (PreSens GmbH, Regensburg, Germany).

Paper III: Experimental determination of bacterioplankton respiratory quotient

In Paper III, we tested the impact of UV radiation on bacterioplankton RQ. To do so, we conducted incubations of both irradiated and non-irradiated samples of natural lake water from four humic-rich lakes in northern Sweden with catchments dominated by coniferous forest, simultaneously measuring changes in O_2 and CO_2.

We performed the experiment in three different parts. i) *Irradiated*: where we first irradiated the samples during 48 h and then incubated them for 48 h in the dark. ii*) Biological + irradiated*: where we first incubated the samples in the dark for 48 h followed by 48 h of UV-treatment and then finally another 48 h of biological incubation. iii) *Dark control*: where we incubated the samples in the dark for 144 h. In part *iii* we chose the longer incubation time to mirror the time of the second treatment, controlling that a possible change in RQ was due to bacterial consumption of photo-chemical processed DOC and not incubation time.

In this study, we measured CO_2 production through changes in pH (decreasing as CO_2 is produced) in the water samples. Depending on the alkalinity and pH in the system, a certain share of the respiratory CO_2 dissociates in the water, forming bicarbonate and carbonate ions (Stumm and Morgan, 1996). To cover the total CO_2 ($TCO_2 = CO_2 + HCO_3^- +$

CO_3^{2-}) production during BR measurements, the impact of the carbonate system on CO_2 hence needs to be corrected for.

Finally, to confirm that the photochemical processing of the samples contributed to increased concentrations of low molecular weight organic acids, we measured concentrations of common low molecular weight organic acids, before and after UV-treatment. To do so, we used a liquid ion chromatography-ionspray tandem mass spectrometry system (IC-MS). The method is described in further detail in Ström et al. (2012).

Paper I, II, and IV: Coupling lake CO_2 and O_2 to environmental variables

In Papers I, II, and IV, we analyzed environmental drivers of lake CO_2 and O_2 concentrations and saturation deficits. Besides *in situ* measurements of pH, temperature, and electrical conductivity, samples from all lakes were also analyzed total organic carbon, dissolved organic carbon, total nitrogen, total phosphorus. We analyzed dissolved gas concentration using the acidified headspace method (Åberg and Wallin, 2014). We then calculated the level of saturation of each gas relative to equilibrium with ambient air from measured concentrations using Henry's law with temperature-dependent solubility constants.

We used the open-source software R version 3.4.1 (Team, 2017) for all data analysis. For the statistical modelling in Paper II and IV, we used the mgcv package (Wood, 2011) fitting gam models for prediction of the dependent variables. To test dependency, we used a gam model with smoothers on each of the explanatory variables. Predictive variable selection was done by applying additional shrinkage on the null space of the penalty with the select=TRUE argument in the mgcv::gam function, as recommended by Marra and Wood (2011).

References

ADRIAN, R., O'REILLY, C. M., ZAGARESE, H., BAINES, S. B., HESSEN, D. O., KELLER, W., LIVINGSTONE, D. M., SOMMARUGA, R., STRAILE, D. & VAN DONK, E. 2009. Lakes as sentinels of climate change. *Limnology and oceanography,* 54**,** 2283-2297.

AMADO, A. M., COTNER, J. B., CORY, R. M., EDHLUND, B. L. & MCNEILL, K. 2015. Disentangling the interactions between photochemical and bacterial degradation of dissolved organic matter: amino acids play a central role. *Microbial ecology,* 69**,** 554-566.

ANESIO, A. M., GRANÉLI, W., AIKEN, G. R., KIEBER, D. J. & MOPPER, K. 2005. Effect of humic substance photodegradation on bacterial growth and respiration in lake water. *Applied and environmental microbiology,* 71**,** 6267-6275.

APPLE, J. K., DEL GIORGIO, P. A. & KEMP, W. M. 2006. Temperature regulation of bacterial production, respiration, and growth efficiency in a temperate salt-marsh estuary. *Aquatic Microbial Ecology,* 43**,** 243-254.

ASSESSMENT, A. C. I. 2004. *Impacts of a warming Arctic-Arctic climate impact assessment*.

BERGGREN, M., LAPIERRE, J.-F. & DEL GIORGIO, P. A. 2012. Magnitude and regulation of bacterioplankton respiratory quotient across freshwater environmental gradients. *The ISME journal,* 6**,** 984-993.

BERGGREN, M., LAUDON, H., HAEI, M., STRÖM, L. & JANSSON, M. 2010. Efficient aquatic bacterial metabolism of dissolved low-molecular-weight compounds from terrestrial sources. *The ISME Journal,* 4**,** 408-416.

BERNER, L. T. & GOETZ, S. J. 2022. Satellite observations document trends consistent with a boreal forest biome shift. *Global change biology*.

BERTILSSON, S. & TRANVIK, L. J. 1998. Photochemically produced carboxylic acids as substrates for freshwater bacterioplankton>. *Limnology and Oceanography,* 43**,** 885-895.

BERTILSSON, S. & TRANVIK, L. J. 2000. Photochemical transformation of dissolved organic matter in lakes. *Limnology and Oceanography,* 45**,** 753-762.

BOGARD, M. J. & DEL GIORGIO, P. A. 2016. The role of metabolism in modulating CO2 fluxes in boreal lakes. *Global Biogeochemical Cycles,* 30**,** 1509-1525.

CANFIELD JR, D. E., LINDA, S. B. & HODGSON, L. M. 1984. RELATIONS BETWEEN COLOR AND SOME LIMNOLOGICAL CHARACTERISTICS OF FLORIDA LAKES 1. *JAWRA Journal of the American Water Resources Association,* 20**,** 323-329.

CHANGE, I. P. O. C. 2018. *Global warming of 1.5° C: an IPCC special report on the impacts of global warming of 1.5° C above pre-industrial levels and related global greenhouse gas emission pathways, in the context of strengthening the global response to the threat of climate change, sustainable development, and efforts to eradicate poverty*, Intergovernmental Panel on Climate Change.

CIMBLERIS, A. C. & KALFF, J. 1998. Planktonic bacterial respiration as a function of C: N: P ratios across temperate lakes. *Hydrobiologia,* 384**,** 89-100.

COLE, J. J., CARACO, N. F., KLING, G. W. & KRATZ, T. K. 1994. Carbon dioxide supersaturation in the surface waters of lakes. *Science,* 265**,** 1568-1570.

COLE, J. J., PRAIRIE, Y. T., CARACO, N. F., MCDOWELL, W. H., TRANVIK, L. J., STRIEGL, R. G., DUARTE, C. M., KORTELAINEN, P., DOWNING, J. A., MIDDELBURG, J. J. & MELACK, J. 2007. Plumbing the Global Carbon Cycle: Integrating Inland Waters into the Terrestrial Carbon Budget. *Ecosystems,* 10**,** 172-185.

CORY, R. M., WARD, C. P., CRUMP, B. C. & KLING, G. W. 2014. Sunlight controls water column processing of carbon in arctic fresh waters. *Science,* 345**,** 925-928.

COUTURE, R. M., DE WIT, H. A., TOMINAGA, K., KIURU, P. & MARKELOV, I. 2015. Oxygen dynamics in a boreal lake responds to long-term changes in climate, ice phenology, and DOC inputs. *Journal of Geophysical Research: Biogeosciences,* 120**,** 2441-2456.

CRAIG, N., JONES, S. E., WEIDEL, B. C. & SOLOMON, C. T. 2015. Habitat, not resource availability, limits consumer production in lake ecosystems. *Limnology and Oceanography,* 60**,** 2079-2089.

CRUTZEN, P. J. 2006. The "anthropocene". *Earth system science in the anthropocene*. Springer.

DE WIT, H. A., COUTURE, R.-M., JACKSON-BLAKE, L., FUTTER, M. N., VALINIA, S., AUSTNES, K., GUERRERO, J.-L. & LIN, Y. 2018. Pipes or chimneys? For carbon cycling in small boreal lakes, precipitation matters most. *Limnology and Oceanography Letters,* 3**,** 275-284.

DE WIT, H. A., VALINIA, S., WEYHENMEYER, G. A., FUTTER, M. N., KORTELAINEN, P., AUSTNES, K., HESSEN, D. O., RÄIKE, A., LAUDON, H. & VUORENMAA, J. 2016. Current browning of surface waters will be further promoted by wetter climate. *Environmental Science & Technology Letters,* 3**,** 430-435.

DEL GIORGIO, P. & WILLIAMS, P. 2005. *Respiration in aquatic ecosystems*, OUP Oxford.

DEL GIORGIO, P. A. & COLE, J. J. 1998. Bacterial growth efficiency in natural aquatic systems. *Annual Review of Ecology and Systematics,* 29**,** 503-541.

DEL GIORGIO, P. A., COLE, J. J. & CIMBLERIS, A. 1997. Respiration rates in bacteria exceed phytoplankton production in unproductive aquatic systems. *Nature,* 385**,** 148-151.

DELSONTRO, T., BEAULIEU, J. J. & DOWNING, J. A. 2018. Greenhouse gas emissions from lakes and impoundments: Upscaling in the face of global change. *Limnology and Oceanography Letters,* 3**,** 64-75.

DEMPSEY, C. M., BRENTRUP, J. A., MAGYAN, S., KNOLL, L. B., SWAIN, H. M., GAISER, E. E., MORRIS, D. P., GANGER, M. T. & WILLIAMSON, C. E. 2020. The relative importance of photodegradation and biodegradation of terrestrially derived dissolved organic carbon across four lakes of differing trophic status. *Biogeosciences,* 17**,** 6327-6340.

DILLON, P. J. & MOLOT, L. A. 2005. Long-term trends in catchment export and lake retention of dissolved organic carbon, dissolved organic nitrogen, total iron, and total phosphorus: The Dorset, Ontario, study, 1978–1998. *Journal of Geophysical Research: Biogeosciences,* 110.

DILLY, O. 2001. Microbial respiratory quotient during basal metabolism and after glucose amendment in soils and litter. *Soil Biology and Biochemistry,* 33**,** 117-127.

DILLY, O. 2003. Regulation of the respiratory quotient of soil microbiota by availability of nutrients. *FEMS Microbiology Ecology,* 43**,** 375-381.

DORE, M. H. 2005. Climate change and changes in global precipitation patterns: what do we know? *Environment international,* 31**,** 1167-1181.

DRAKE, T. W., RAYMOND, P. A. & SPENCER, R. G. 2018. Terrestrial carbon inputs to inland waters: A current synthesis of estimates and uncertainty. *Limnology and Oceanography Letters,* 3**,** 132-142.

DUAN, S., DELANEY-NEWCOMB, K., KAUSHAL, S. S., FINDLAY, S. E. & BELT, K. T. 2014. Potential effects of leaf litter on water quality in urban watersheds. *Biogeochemistry,* 121**,** 61-80.

DUARTE, C. M. & PRAIRIE, Y. T. 2005. Prevalence of heterotrophy and atmospheric CO 2 emissions from aquatic ecosystems. *Ecosystems,* 8**,** 862-870.

ELSER, J. J., ANDERSEN, T., BARON, J. S., BERGSTRÖM, A.-K., JANSSON, M., KYLE, M., NYDICK, K. R., STEGER, L. & HESSEN, D. O. 2009. Shifts in lake N: P stoichiometry and nutrient limitation driven by atmospheric nitrogen deposition. *science,* 326**,** 835-837.

ELSER, J. J., FAGAN, W. F., DENNO, R. F., DOBBERFUHL, D. R., FOLARIN, A., HUBERTY, A., INTERLANDI, S., KILHAM, S. S., MCCAULEY, E. & SCHULZ, K. L. 2000. Nutritional constraints in terrestrial and freshwater food webs. *Nature,* 408**,** 578-580.

ERLANDSSON, M., BUFFAM, I., FÖLSTER, J., LAUDON, H., TEMNERUD, J., WEYHENMEYER, G. A. & BISHOP, K. 2008. Thirty-five years of synchrony in the organic matter concentrations of Swedish rivers explained by variation in flow and sulphate. *Global Change Biology,* 14**,** 1191-1198.

FARRELL, J. & ROSE, A. 1967. Temperature effects on microorganisms. *Annual Reviews in Microbiology,* 21**,** 101-120.

FINSTAD, A. G., ANDERSEN, T., LARSEN, S., TOMINAGA, K., BLUMENTRATH, S., DE WIT, H. A., TØMMERVIK, H. & HESSEN, D. O. 2016. From greening to browning: Catchment vegetation development and reduced S-deposition promote organic carbon load on decadal time scales in Nordic lakes. *Scientific Reports,* 6**,** 1-8.

FINSTAD, A. G., HELLAND, I. P., UGEDAL, O., HESTHAGEN, T. & HESSEN, D. O. 2014. Unimodal response of fish yield to dissolved organic carbon. *Ecology letters,* 17**,** 36-43.

FINSTAD, A. G., NILSEN, E. B., HENDRICHSEN, D. K. & SCHMIDT, N. M. 2017. Catchment vegetation and temperature mediating trophic interactions and production in plankton communities. *PLOS ONE,* 12**,** e0174904.

GRANÉLI, W., LINDELL, M. & TRANVIK, L. 1996. Photo-oxidative production of dissolved inorganic carbon in lakes of different humic content. *Limnology and Oceanography,* 41**,** 698-706.

GRENNFELT, P. & HOV, Ø. 2005. Regional air pollution at a turning point. *AMBIO: A Journal of the Human Environment,* 34**,** 2-10.

GROENEVELD, M., TRANVIK, L., NATCHIMUTHU, S. & KOEHLER, B. 2016. Photochemical mineralisation in a boreal brown water lake: considerable

temporal variability and minor contribution to carbon dioxide production. *Biogeosciences,* 13**,** 3931-3943.

HARSCH, M. A., HULME, P. E., MCGLONE, M. S. & DUNCAN, R. P. 2009. Are treelines advancing? A global meta-analysis of treeline response to climate warming. *Ecology letters,* 12**,** 1040-1049.

HESSEN, D., ANDERSEN, T. & LYEHE, A. 1990. Carbon metabolism in a humic lake: Pool sires and cycling through zooplankton. *Limnology and Oceanography,* 35**,** 84-99.

HESSEN, D. O. 1992. Dissolved organic carbon in a humic lake: effects on bacterial production and respiration. *Hydrobiologia,* 229**,** 115-123.

HESSEN, D. O. & ANDERSON, T. R. 2008. Excess carbon in aquatic organisms and ecosystems: physiological, ecological, and evolutionary implications. *Limnology and Oceanography,* 53**,** 1685-1696.

HESSEN, D. O., NYGAARD, K., SALONEN, K. & VÄHÄTALO, A. 1994. The effect of substrate stoichiometry on microbial activity and carbon degradation in humic lakes. *Environment international,* 20**,** 67-76.

HESSEN, D. O. & TRANVIK, L. J. 1998. *Aquatic Humic Substances: Ecology and Biogeochemistry,* Springer Science & Business Media.

HUMBORG, C., MÖRTH, C. M., SUNDBOM, M., BORG, H., BLENCKNER, T., GIESLER, R. & ITTEKKOT, V. 2010. CO2 supersaturation along the aquatic conduit in Swedish

watersheds as constrained by terrestrial respiration, aquatic respiration and weathering. *Global Change Biology,* 16**,** 1966-1978.
JANE, S. F. & ROSE, K. C. 2018. Carbon quality regulates the temperature dependence of aquatic ecosystem respiration. *Freshwater Biology,* 63**,** 1407-1419.
JANSSON, M., BERGSTRÖM, A.-K., LYMER, D., VREDE, K. & KARLSSON, J. 2006. Bacterioplankton growth and nutrient use efficiencies under variable organic carbon and inorganic phosphorus ratios. *Microbial ecology,* 52**,** 358-364.
JANSSON, M., KARLSSON, J. & JONSSON, A. 2012. Carbon dioxide supersaturation promotes primary production in lakes. *Ecology letters,* 15**,** 527-532.
JONSSON, A., MEILI, M., BERGSTRÖM, A.-K. & JANSSON, M. 2001. Whole-lake mineralization of allochthonous and autochthonous organic carbon in a large humic lake (örträsket, N. Sweden). *Limnology and Oceanography,* 46**,** 1691-1700.
KARLSSON, J., BYSTRÖM, P., ASK, J., ASK, P., PERSSON, L. & JANSSON, M. 2009. Light limitation of nutrient-poor lake ecosystems. *Nature,* 460**,** 506-9.
KARLSSON, J., JANSSON, M. & JONSSON, A. 2007. Respiration of allochthonous organic carbon in unproductive forest lakes determined by the Keeling plot method. *Limnology and Oceanography,* 52**,** 603-608.
KIEBER, D. J., MCDANIEL, J. & MOPPER, K. 1989. Photochemical source of biological substrates in sea water: implications for carbon cycling. *Nature,* 341**,** 637-639.
KOCH, R. W., BUKAVECKAS, P. A. & GUELDA, D. L. 2007. Importance of phytoplankton carbon to heterotrophic bacteria in the Ohio, Cumberland, and Tennessee rivers, USA. *Hydrobiologia,* 586**,** 79-91.
KOEHLER, B., BROMAN, E. & TRANVIK, L. J. 2016. Apparent quantum yield of photochemical dissolved organic carbon mineralization in lakes. *Limnology and Oceanography,* 61**,** 2207-2221.
KOEHLER, B., LANDELIUS, T., WEYHENMEYER, G. A., MACHIDA, N. & TRANVIK, L. J. 2014. Sunlight-induced carbon dioxide emissions from inland waters. *Global Biogeochemical Cycles,* 28**,** 696-711.
KORTELAINEN, P., RANTAKARI, M., HUTTUNEN, J. T., MATTSSON, T., ALM, J., JUUTINEN, S., LARMOLA, T., SILVOLA, J. & MARTIKAINEN, P. J. 2006. Sediment respiration and lake trophic state are important predictors of large CO2 evasion from small boreal lakes. *Global Change Biology,* 12**,** 1554-1567.
KRITZBERG, E. & EKSTRÖM, S. 2011. Increasing iron concentrations in surface waters--a factor behind brownification? *Biogeosciences Discussions,* 8.
KRITZBERG, E. S. 2017. Centennial-long trends of lake browning show major effect of afforestation. *Limnology and Oceanography Letters,* 2**,** 105-112.
KRITZBERG, E. S., ARRIETA, J. M. & DUARTE, C. M. 2010. Temperature and phosphorus regulating carbon flux through bacteria in a coastal marine system. *Aquatic Microbial Ecology,* 58**,** 141-151.
KRITZBERG, E. S., COLE, J. J., PACE, M. L., GRANÉLI, W. & BADE, D. L. 2004. Autochthonous versus allochthonous carbon sources of bacteria: Results from whole-lake 13C addition experiments. *Limnology and Oceanography,* 49**,** 588-596.
KRITZBERG, E. S., HASSELQUIST, E. M., ŠKERLEP, M., LÖFGREN, S., OLSSON, O., STADMARK, J., VALINIA, S., HANSSON, L.-A. & LAUDON, H. 2020. Browning of freshwaters: Consequences to ecosystem services, underlying drivers, and potential mitigation measures. *Ambio,* 49**,** 375-390.
LAPIERRE, J.-F., GUILLEMETTE, F., BERGGREN, M. & DEL GIORGIO, P. A. 2013. Increases in terrestrially derived carbon stimulate organic carbon processing and CO2 emissions in boreal aquatic ecosystems. *Nature communications,* 4**,** 1-7.

LARSEN, S., ANDERSEN, T. & HESSEN, D. 2011a. The pCO2 in boreal lakes: Organic carbon as a universal predictor? *Global Biogeochemical Cycles - GLOBAL BIOGEOCHEM CYCLE,* 25.

LARSEN, S., ANDERSEN, T. & HESSEN, D. O. 2011b. Climate change predicted to cause severe increase of organic carbon in lakes. *Global Change Biology,* 17**,** 1186-1192.

LI, J. & RICHTER, D. D. 2012. Effects of two-century land use changes on soil iron crystallinity and accumulation in Southeastern Piedmont region, USA. *Geoderma,* 173**,** 184-191.

LINDELL, M. J., GRANÉLI, W. & TRANVIK, L. J. 1995. Enhanced bacterial growth in response to photochemical transformation of dissolved organic matter. *Limnology and Oceanography,* 40**,** 195-199.

LYDERSEN, E., LÖFGREN, S. & ARNESEN, R. T. 2002. Metals in Scandinavian surface waters: effects of acidification, liming, and potential reacidification. *Critical reviews in environmental science and technology,* 32**,** 73-295.

MADIGAN, M. T., MARTINKO, J. M. & PARKER, J. 1997. *Brock biology of microorganisms,* Prentice hall Upper Saddle River, NJ.

MALONEY, K. O., MORRIS, D. P., MOSES, C. O. & OSBURN, C. L. 2005. The role of iron and dissolved organic carbon in the absorption of ultraviolet radiation in humic lake water. *Biogeochemistry,* 75**,** 393-407.

MASSON-DELMOTTE, V., ZHAI, P., PIRANI, A., CONNORS, S. L., PÉAN, C., BERGER, S., CAUD, N., CHEN, Y., GOLDFARB, L. & GOMIS, M. 2021. Climate change 2021: the physical science basis. *Contribution of working group I to the sixth assessment report of the intergovernmental panel on climate change***,** 2.

MOLOT, L. & DILLON, P. 1997. Photolytic regulation of dissolved organic carbon in northern lakes. *Global Biogeochemical Cycles - GLOBAL BIOGEOCHEM CYCLE,* 11.

MONTEITH, D. T., STODDARD, J. L., EVANS, C. D., DE WIT, H. A., FORSIUS, M., HØGÅSEN, T., WILANDER, A., SKJELKVÅLE, B. L., JEFFRIES, D. S. & VUORENMAA, J. 2007. Dissolved organic carbon trends resulting from changes in atmospheric deposition chemistry. *Nature,* 450**,** 537-540.

MYERS-SMITH, I. H., FORBES, B. C., WILMKING, M., HALLINGER, M., LANTZ, T., BLOK, D., TAPE, K. D., MACIAS-FAURIA, M., SASS-KLAASSEN, U. & LÉVESQUE, E. 2011. Shrub expansion in tundra ecosystems: dynamics, impacts and research priorities. *Environmental Research Letters,* 6**,** 045509.

NATIONAL OCEANIC AND ATMOSPHERIC ADMINISTRATION 2022. Cabbondioxide now more than 50% higher than pre-industrial levels. 100822 https://www.noaa.gov/news-release/carbon-dioxide-now-more-than-50-higher-than-pre-industrial-levels

NYDAHL, A. C., WALLIN, M. B. & WEYHENMEYER, G. A. 2020. Diverse drivers of long-term p CO2 increases across thirteen boreal lakes and streams. *Inland Waters,* 10**,** 360-372.

ODÉN, S. 1968. Acidification of air and precipitation and its consequences on the natural environment.

OJALA, A., BELLIDO, J. L., TULONEN, T., KANKAALA, P. & HUOTARI, J. 2011. Carbon gas fluxes from a brown-water and a clear-water lake in the boreal zone during a summer with extreme rain events. *Limnology and Oceanography,* 56**,** 61-76.

PUTS, I. C., ASK, J., SIEWERT, M. B., SPONSELLER, R., HESSEN, D. & BERGSTRÖM, A. K. 2022. Landscape determinants of pelagic and benthic primary production in northern lakes. *Global Change Biology*.

RADDUM, G. G. & FJELLHEIM, A. 1984. Acidification and early warning organisms in freshwater in western Norway: With 5 figures and 1 table in the text. *Internationale*

Vereinigung für theoretische und angewandte Limnologie: Verhandlungen, 22**,** 1973-1980.
RANÅKER, L., JÖNSSON, M., NILSSON, P. A. & BRÖNMARK, C. 2012. Effects of brown and turbid water on piscivore–prey fish interactions along a visibility gradient. *Freshwater biology,* 57**,** 1761-1768.
RAYMOND, P. A., HARTMANN, J., LAUERWALD, R., SOBEK, S., MCDONALD, C., HOOVER, M., BUTMAN, D., STRIEGL, R., MAYORGA, E., HUMBORG, C., KORTELAINEN, P., DÜRR, H., MEYBECK, M., CIAIS, P. & GUTH, P. 2013. Global carbon dioxide emissions from inland waters. *Nature,* 503**,** 355-359.
REIS, S., PINDER, R., ZHANG, M., LIJIE, G. & SUTTON, M. 2009. Reactive nitrogen in atmospheric emission inventories. *Atmospheric Chemistry and Physics,* 9**,** 7657-7677.
RIVKIN, R. B. & LEGENDRE, L. 2001. Biogenic carbon cycling in the upper ocean: effects of microbial respiration. *Science,* 291**,** 2398-2400.
RODRÍGUEZ-RODRÍGUEZ, M., FERNÁNDEZ-AYUSO, A., HAYASHI, M. & MORAL-MARTOS, F. 2018. Using water temperature, electrical conductivity, and pH to Characterize surface–groundwater relations in a shallow ponds system (Doñana National Park, SW Spain). *Water,* 10**,** 1406.
ROMERO-KUTZNER, V., PACKARD, T. T., BERDALET, E., ROY, S., GAGNÉ, J.-P. & GÓMEZ, M. 2015. Respiration quotient variability: bacterial evidence. *Marine Ecology Progress Series,* 519**,** 47-59.
ROSENZWEIG, C., CASASSA, G., KAROLY, D. J., IMESON, A., LIU, C., MENZEL, A., RAWLINS, S., ROOT, T. L., SEGUIN, B. & TRYJANOWSKI, P. 2007. Assessment of observed changes and responses in natural and managed systems.
SEEKELL, D. A., LAPIERRE, J.-F., ASK, J., BERGSTRÖM, A.-K., DEININGER, A., RODRÍGUEZ, P. & KARLSSON, J. 2015. The influence of dissolved organic carbon on primary production in northern lakes. *Limnology and Oceanography,* 60**,** 1276-1285.
ŠKERLEP, M., STEINER, E., AXELSSON, A. L. & KRITZBERG, E. S. 2020. Afforestation driving long-term surface water browning. *Global change biology,* 26**,** 1390-1399.
SMITH, E. M. & PRAIRIE, Y. T. 2004. Bacterial metabolism and growth efficiency in lakes: the importance of phosphorus availability. *Limnology and Oceanography,* 49**,** 137-147.
SOBEK, S., ALGESTEN, G., BERGSTRÖM, A. K., JANSSON, M. & TRANVIK, L. J. 2003. The catchment and climate regulation of pCO2 in boreal lakes. *Global Change Biology,* 9**,** 630-641.
SØNDERGAARD, M., HANSEN, B. & MARKAGER, S. 1995. Dynamics of dissolved organic car-bon lability in a eutrophic lake. *Limnology and Oceanography,* 40**,** 46-54.
TANENTZAP, A. J., KIELSTRA, B. W., WILKINSON, G. M., BERGGREN, M., CRAIG, N., DEL GIORGIO, P. A., GREY, J., GUNN, J. M., JONES, S. E. & KARLSSON, J. 2017. Terrestrial support of lake food webs: Synthesis reveals controls over cross-ecosystem resource use. *Science advances,* 3**,** e1601765.
THRANE, J.-E., HESSEN, D. O. & ANDERSEN, T. 2014. The Absorption of Light in Lakes: Negative Impact of Dissolved Organic Carbon on Primary Productivity. *Ecosystems,* 17**,** 1040-1052.
TRANVIK, L. J., DOWNING, J. A., COTNER, J. B., LOISELLE, S. A., STRIEGL, R. G., BALLATORE, T. J., DILLON, P., FINLAY, K., FORTINO, K. & KNOLL, L. B. 2009. Lakes and reservoirs as regulators of carbon cycling and climate. *Limnology and oceanography,* 54**,** 2298-2314.
TØMMERVIK, H., JOHANSEN, B., RISETH, J., KARLSEN, S., SOLBERG, B. & HØGDA, K. 2009. Above ground biomass changes in the mountain birch forests and mountain

heaths of Finnmarksvidda, northern Norway, in the period 1957–2006. *Forest Ecology and Management,* 257**,** 244-257.

VACHON, D. & DEL GIORGIO, P. A. 2014. Whole-lake CO 2 dynamics in response to storm events in two morphologically different lakes. *Ecosystems,* 17**,** 1338-1353.

VACHON, D., LAPIERRE, J.-F. & DEL GIORGIO, P. A. 2016. Seasonality of photochemical dissolved organic carbon mineralization and its relative contribution to pelagic CO2 production in northern lakes. *Journal of Geophysical Research: Biogeosciences,* 121**,** 864-878.

VADSTEIN, O. 2000. Heterotrophic, planktonic bacteria and cycling of phosphorus. *Advances in microbial ecology.* Springer.

VALIENTE, N., EILER, A., ALLESSON, L., ANDERSEN, T., CLAYER, F., CRAPART, C., DÖRSCH, P., FONTAINE, L., HEUSCHELE, J. & VOGT, R. D. 2022. Catchment properties as predictors of greenhouse gas concentrations across a gradient of boreal lakes. *Frontiers in Environmental Science***,** 1668.

VERPOORTER, C., KUTSER, T., SEEKELL, D. A. & TRANVIK, L. J. 2014. A global inventory of lakes based on high-resolution satellite imagery. *Geophysical Research Letters,* 41**,** 6396-6402.

VIKSTRÖM, K. & WIKNER, J. 2019. Importance of bacterial maintenance respiration in a subarctic estuary: a proof of concept from the field. *Microbial ecology,* 77**,** 574-586.

VUORENMAA, J., SALONEN, K., ARVOLA, L., MANNIO, J., RASK, M. & HORPPILA, P. 2014. Water quality of a small headwater lake reflects long-term variations in deposition, climate and in-lake processes.

WEYHENMEYER, G., KOSTEN, S., WALLIN, M., TRANVIK, L., JEPPESEN, E. & ROLAND, F. 2015. Significant fraction of CO2 emissions from boreal lakes derived from hydrologic inorganic carbon inputs. *Nature Geoscience,* 8**,** 933-936.

WEYHENMEYER, G. A., PRAIRIE, Y. T. & TRANVIK, L. J. 2014. Browning of boreal freshwaters coupled to carbon-iron interactions along the aquatic continuum. *PloS one,* 9**,** e88104.

WILLIAMSON, C., STEMBERGER, R., MORRIS, D. & PAULSEN, S. 1996. Ultraviolet radiation in North American lakes: Attenuation estimates from DOC measurements and implications for plankton communities. *Limnology and Oceanography,* 41.

WILLIAMSON, C. E., OVERHOLT, E. P., PILLA, R. M., LEACH, T. H., BRENTRUP, J. A., KNOLL, L. B., METTE, E. M. & MOELLER, R. E. 2015. Ecological consequences of long-term browning in lakes. *Scientific reports,* 5**,** 18666.

YLLA, I., ROMANÍ, A. M. & SABATER, S. 2012. Labile and Recalcitrant Organic Matter Utilization by River Biofilm Under Increasing Water Temperature. *Microbial Ecology,* 64**,** 593-604.

Paper I

LIMNOLOGY and OCEANOGRAPHY

ASLO

Limnol. Oceanogr. 66, 2021, 158–170

doi: 10.1002/lno.11594

The role of photomineralization for CO_2 emissions in boreal lakes along a gradient of dissolved organic matter

Lina Allesson,[1*] **Birgit Koehler**,[2] **Jan-Erik Thrane**,[3] **Tom Andersen**,[1] **Dag O. Hessen**[1]

[1]Department of Biosciences, University of Oslo, Oslo, Norway
[2]Department of Ecology and Genetics/Limnology, Uppsala University, Uppsala, Sweden
[3]Norwegian Institute for Water Research, Oslo, Norway

Abstract

Many boreal lakes are experiencing an increase in concentrations of terrestrially derived dissolved organic matter (DOM)—a process commonly labeled "browning." Browning affects microbial and photochemical mineralization of DOM, and causes increased light attenuation and hence reduced photosynthesis. Consequently, browning regulates lake heterotrophy and net CO_2-efflux to the atmosphere. Climate and environmental change makes ecological forecasting and global carbon cycle modeling increasingly important. A proper understanding of the magnitude and relative contribution from CO_2-generating processes for lakes ranging in dissolve organic carbon (DOC) concentrations is therefore crucial for constraining models and forecasts. Here, we aim to study the relative contribution of photomineralization to total CO_2 production in 70 Scandinavian lakes along an ecosystem gradient of DOC concentration. We combined spectral data from the lakes with regression estimates between optical parameters and wavelength specific photochemical reactivity to estimate rates of photochemical DOC mineralization. Further, we estimated total in-lake CO_2-production and efflux from lake chemical and physical data. Photochemical mineralization corresponded on average to 9% ± 1% of the total CO_2-evasion, with the highest contribution in clear lakes. The calculated relative contribution of photochemical mineralization to total in-lake CO_2-production was about 3% ± 0.2% in all lakes. Although lakes differed substantially in color, depth-integrated photomineralization estimates were similar in all lakes, regardless of DOC concentrations. DOC concentrations were positively related to CO_2-efflux and total in-lake CO_2-production but negatively related to primary production. We conclude that enhanced rates of photochemical mineralization will be a minor contributor to increased heterotrophy under increased browning.

Most lakes worldwide are supersaturated with carbon dioxide (CO_2), emitting 0.32–0.53 Pg CO_2-C yr^{-1} to the atmosphere on a global scale (Cole et al. 2007; Raymond et al. 2013). A major part of the CO_2 emitted from lakes is produced through mineralization of dissolved organic matter (DOM) (Vachon et al. 2016). DOM in freshwaters originates both from in situ primary production and from the surrounding terrestrial ecosystems, with a general dominance of the latter (Karlsson et al. 2009). Terrestrially derived DOM consists primarily of high molecular weight humic substances. These substances make the majority of the dissolved organic carbon (DOC) pool in most lakes and thus we will primarily refer to DOC, hence using C as a common currency, through the following text. DOC poses a multitude of partly contrasting impacts on the physical and chemical properties of water, as well as on the biota (Hessen and Tranvik 1998).

Humic substances are a major source of energy to heterotrophs in aquatic ecosystems with high terrestrial influence and the subsequent increase in heterotrophic CO_2 production may indirectly stimulate autotrophs. Nutrients associated with DOC may stimulate both heterotrophic and autotrophic productivity in nutrient-poor regions. Further, humic substances are often highly aromatic and can protect aquatic organisms from harmful UV-radiation (Dillon and Molot 2005; Kritzberg and Ekström 2011). On the other hand, at a certain threshold concentration (possibly around 5 mg l^{-1}; Seekell et al. 2015), terrestrial DOC may shift from acting as a nutrient subsidy to suppressing primary production due to light attenuation (Thrane et al. 2014; Seekell et al. 2015). Lakes with high inputs of terrestrial DOC are often to a larger degree supersaturated with CO_2 than lakes where the major part of the DOC pool originates from in-lake production (Cole et al. 2000; Larsen et al. 2011*a*).

*Correspondence: lina.allesson@ibv.uio.no

Additional Supporting Information may be found in the online version of this article.

Besides being an essential source of energy for bacterioplankton (Hessen 1992), this terrigenous DOC is highly chromophoric and photo-reactive, especially in the UV waveband (Lindell et al. 1995). Photomineralization of DOC to dissolved inorganic carbon (DIC) might therefore be a significant part of the DIC production and carbon cycling in humic lakes, adding to the high respiratory activity of heterotrophic prokaryotes and low autotrophic CO_2-fixation. The annual photochemical mineralization has been estimated to account for 9–12% of the total lake CO_2 emission in the boreal biome, and amount to 13–35 Tg C yr^{-1} from inland waters worldwide (Koehler et al. 2014). However, the relative contribution of photochemical mineralization to in-lake carbon cycling varies significantly both between systems (Granéli et al. 1996; Molot and Dillon 1997; Cory et al. 2014) and temporally within the same system (Groeneveld et al. 2016; Vachon et al. 2016).

In order to simulate photochemical mineralization, knowledge of the reactivity across the whole spectrum of photochemically active wavelengths is needed. This photochemical reactivity or apparent quantum yield (AQY) of DIC photoproduction is defined as moles photochemically produced DIC per mole photons absorbed by the DOC pool (Miller et al. 2002). Besides the quantity of DOC, studies have found photochemical DIC production rates to be dependent on its quality, as well as on water chemistry, such as pH and iron concentration (Lindell et al. 1995; Bertilsson and Tranvik 2000; Panneer Selvam et al. 2019) while other studies have found no such relationships (Cory et al. 2014). A significant share of the AQY variability between lakes can be explained by simple optical parameters (Koehler et al. 2016), allowing for estimates of photochemical DIC production when system-specific AQY spectra are not available.

In this study, we used data of such optical parameters from 70 Scandinavian lakes along a gradient of DOC concentrations, together with correlation estimates between the absorption coefficient at 420 nm (a_{420}) and the specific UV absorption coefficient at 400 nm ($SUVA_{400}$) and the AQY (Koehler et al. 2016) to estimate the lakes' wavelength specific AQY spectra. Together with atmospheric radiative modeling, we then simulated the photochemical DIC production in the study lakes. We further estimated the lakes' primary production using lake-specific phytoplankton absorption coefficients and in situ irradiance. Finally, we calculated the air-water CO_2 flux through surface water CO_2 concentrations, temperature and wind speed, using Fick's law of diffusion and Henry's law to find the CO_2 deficit from concentrations at equilibrium with the atmosphere. Assuming that the deviation of CO_2 from saturation is kept at steady state due to production, lateral input, evasion, and consumption we estimated the sum of total lake CO_2 production and the lateral input as the sum of the consumption and evasion. This allowed us to calculate the relative contribution of photochemical DIC production to lake carbon cycling. As shortwave radiation attenuates quickly in the water column of lakes, we expect all incoming photochemically reactive photons to be absorbed within the top few meters of all lakes, even the clear ones. Therefore, we hypothesized that the total amount of photomineralization of DOC would be similar in all lakes regardless of their CDOM concentrations.

Methods

Study sites

During July and August of 2011, 77 lakes along a geographical gradient between western Norway and eastern Sweden were sampled (Fig. 1). The lakes were chosen to represent gradients in DOC and total phosphorus (TP), aiming for an orthogonal gradient between these parameters, and to avoid strong temperature gradients with respect to latitude and altitude. All lakes met the following criteria: latitude 57–64°N, altitude < 600 m, surface area > 1 km^2, pH > 5, TP < 30 μg l^{-1}, and DOC < 30 mg l^{-1}.

Field sampling

Composite samples (15 L in total) were taken from 0 to 5 m in the central part of each lake during daytime, using an integrating water sampler (Hydro-BIOS, Germany). Water temperatures were measured using XRX-620 10-channel CTD (RBR Ltd., Canada). Vertical temperature profiles indicated that the thermocline was deeper than 5 m in all lakes (Fig. S1) and the integrated 0–5 m samples could be considered representative of the entire mixed layer of the lakes. Vertical profiles of scalar irradiance in the photosynthetically active radiation (PAR) region (400–700 nm; E_d) were measured using a spherical irradiance sensor (BioSpherical instruments) attached to a 10 channel CTD profiler (WRW620. RBR Ltd., Canada). The sensor was lowered at a rate of approximately 20 cm s^{-1} with a sampling rate of 6 Hz. The vertical attenuation coefficient for scalar PAR (K_dPAR) was estimated by taking the median of the distribution of slopes obtained from regressing natural log-transformed E_d against depth (z) for each 10 sampling points (i.e., sliding windows). This was done to correct for temporal changes in irradiance caused by for example wave action and clouds during the haul. pH in the samples was measured within 1 h after sampling using a handheld pH-meter (PHM201, Radiometer Analytical, France).

Laboratory analyses

Concentrations of total phosphorus (TP), total organic carbon (TOC), and total nitrogen (TN) were measured in two accredited laboratories, at the Norwegian Institute for Water Research (NIVA) and at the University of Oslo (UiO). Differences between laboratories were small for TOC and TN but slightly higher for TP. Regressions of UiO vs. NIVA measurements had the following statistics: TP: $R^2 = 0.77$, residual standard error (RSE) = 2.27 μg l^{-1}; TOC: $R^2 = 0.99$, RSE = 0.25 mg l^{-1}; TN: $R^2 = 0.91$, RSE = 81 μg l^{-1}. There were no systematic differences between the laboratories and the averages of the results were used in the subsequent analysis. DOC was calculated as the difference between the total organic carbon (TOC) and particulate organic carbon (POC). TOC was

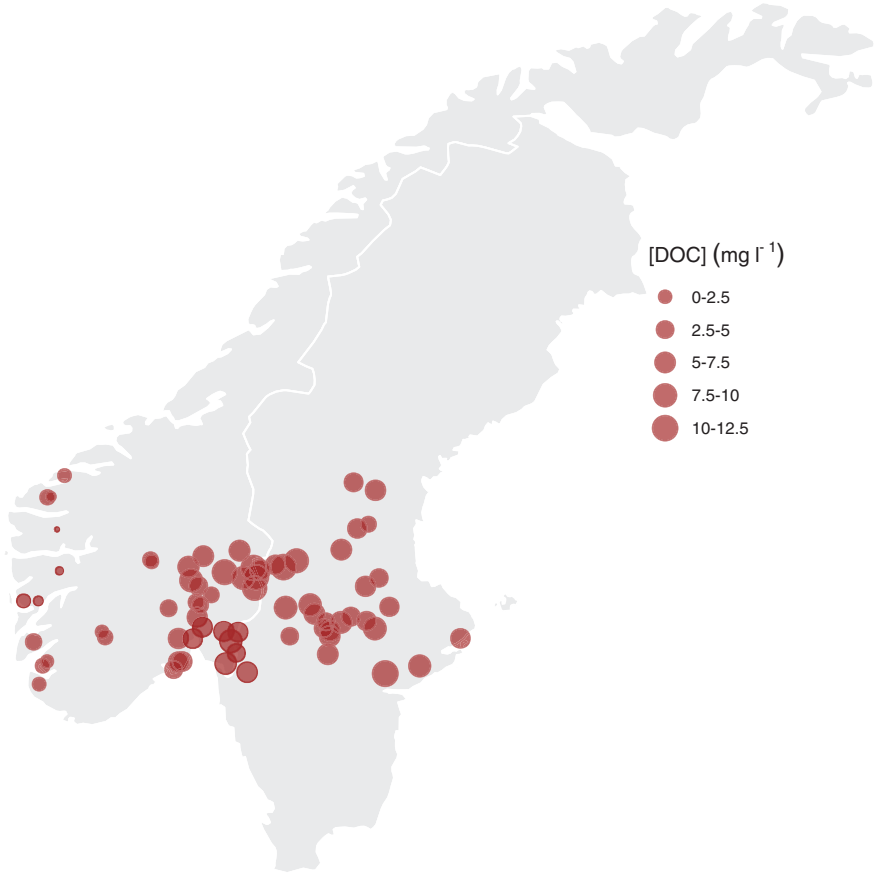

Fig. 1. Lakes included in the survey. The sizes of the symbols scale with the concentration of dissolved organic carbon (DOC; mg l^{-1}).

measured by infrared CO_2 detection after catalytic high temperature combustion (Shimadzu TOC-VWP analyzer (UiO), or Phoenix 8000 TOC-TC analyzer (NIVA)). On average, >95% of the TOC was in dissolved form (DOC). POC was measured on an elemental analyzer (Flash EA 1112 NC, Thermo Fisher Scientific, Waltham, Massachusetts) through rapid combustion in pure oxygen of a pre-combusted GF/C-filter with particulates. TP was measured on an auto-analyzer as phosphate after wet oxidation with peroxodisulfate in both laboratories. TN was measured on unfiltered samples by detecting nitrogen monoxide by chemiluminescence using a TNM-1 unit attached to the Shimadzu TOC-VWP analyzer (UiO), or detection of nitrate after wet oxidation with peroxodisulfate in a segmented flow auto-analyzer (NIVA). Concentrations of CO_2 and O_2 were determined by automated gas chromatography (GC) analysis with back-flushing H_2O (see Yang et al. 2015 for details). Total iron (Fe) was measured using an inductively coupled plasma mass spectrometer (ICP-MS, PerkinElmer NexION 300, Norwalk, Connecticut) equipped with three quadrupole mass analyzers, a cyclonic spray chamber, and a concentric nebulizer. Three subsamples from each lake were measured to evaluate the analytical precision.

For measurements of particulate absorbance spectra, water samples (150–170 mL, depending on particle load) were filtered onto 25 nm Whatman GF/C glass filters under low vacuum. The filters were placed in the entrance of an integrating sphere (ISR 2200, Shimadzu scientific instruments, Columbia, Maryland) attached to a double beam Shimadzu UV-2550 spectrophotometer, and optical density was measure for each nm from 400 to 800 nm. After the first measurement, the sample filters were bleached with sodium hypochlorite (Tassan and Ferrari 1995). The bleaching oxidizes all pigments, leaving only organic and inorganic detritus, including de-pigmented algal remains, unbleached. The optical density of this nonalgal particulate (NAP) matter was then measured and the absorption coefficients (m^{-1}) of total particulate matter and nonalgal particulate matter were calculated according to Mitchell et al. (2002), using the algorithm of Bricaud and Stramski (1990) to estimate the path-length amplification factor (β). Finally, the absorption coefficient spectra of phytoplankton pigments were calculated as the difference between the total particulate and the NAP absorption coefficient spectra. DOC absorbance spectra from 400 to 700 nm (1 nm resolution) were measured in 0.2 µm filtered water samples

(Acrodisc 0.2 μm polyethersulfone membrane syringe filter, Pall Life Sciences, Port Washington, NY) using a 50 mm quartz cuvette. Absorption coefficient spectra were calculated according to Mitchell et al. (2002). Due to missing values of some of the absorbance measurements, seven lakes had to be omitted, giving a data set of 70 lakes for further analysis.

Primary production calculations

Area-specific primary production (PP_A; mg C m^{-2} d^{-2}) was calculated using a bio-optical model based on lake-specific phytoplankton absorption coefficients, in situ irradiance, and the light dependent quantum yield of photosystem II measured by a Pulse Amplitude Modulated (PAM) fluorometer (AquaPen, PSI Czech Republic). In brief, this bio-optical model is based on estimating the in vivo rate of light absorption by phytoplankton, and subsequently electron transport rates (ETRs) through photosystem II (PSII) using information about the light-dependent quantum yield of photochemistry in PSII. ETR can further be converted to a rate of gross carbon fixation by assuming an appropriate value for the quantum yield of CO_2 fixation (Kromkamp and Forster 2003; Suggett et al. 2010). While the method could be sensitive to phytoplankton community composition related to their pigments and light capturing properties, it has gained increased interest over the last two decades because it offers a fast and inexpensive way of obtaining PP estimates (see Thrane et al. 2014 for details). A comparison of this method and empirical estimates for PP in boreal lakes demonstrates a good accordance (Thrane et al. 2014). The method is thus a feasible tool for assessment of primary production across a large number of sites. It also avoids many of the pitfalls of ^{14}C-bottle incubation, which in any case could not have been applied in this kind of synoptic, snapshot survey with sampling from a plane spanning many lakes over a large geographical area.

Wavelength-specific AQY spectrum

Koehler et al. (2016) found the strongest predictors of AQY to be the Napierian absorption coefficient at 420 nm (a_{420}; m^{-1}) and specific UV absorption coefficient at 254 nm ($SUVA_{254}$; L mg C^{-1} m^{-1}) (Kirk 1994). The data set in this study only contained optical data for wavelengths in the PAR band and therefore the relation between AQY and $SUVA_{400}$ (B. Koehler, unpublished data, 2016) (Table S2) was used instead of $SUVA_{254}$.

A linear mixed effects model with the measured AQY as the response variable, a_{420}, $SUVA_{400}$, and wavelength as fixed effects, and intercept as a random effect was run for the lakes in Koehler et al. (2016) using the lme4 package in R (Bates et al. 2014).

$$\ln(\Phi) \sim a_{420} + SUVA_{400} + \lambda + (1|lake) \quad (1)$$

Where Φ is AQY for DIC photoproduction, λ is the wavelengths in the measured wavelength region (400–700 nm in steps of 1 nm), and the (1|lake) term captures other between-lake variations not related to chromophoric DOM (CDOM) quality. The Napierian absorption coefficient at 420 nm (a_{420}) is a proxy for CDOM content, such that the higher the a_{420}, the browner the lake. We used the AQY model on data from the lakes in Koehler et al. (2016) using $SUVA_{254}$ and a_{420} and compared it to the model with $SUVA_{400}$ and a_{420}. The models resulted in close to exactly the same AQY spectra (Fig. S4) and hence we did not lose information modeling the AQY from $SUVA_{400}$ instead of $SUVA_{254}$. The model was then used to predict the AQY spectra for the 70 study lakes.

The arm package in R (Gelman et al. 2018) was used to generate Monte Carlo samples of fixed effect parameters of the linear model, which was used to propagate model uncertainties to the estimated lake specific AQYs over the entire spectrum (300–600 nm; Figs. S2 and S3). AQY spectra were extrapolated to wavelengths < 400 nm using the exponential model (Eq. 1). The irradiation model included wavelengths between 300 and 600 nm and therefore the AQY spectra were also cut at 600 nm.

Irradiation model

Daily integrated downwelling scalar irradiation spectra (300–600 nm) just below the water surface were obtained using the libRadtran model (version 1.6) for radiative transfer (Mayer and Kylling 2005), parameterized and cloud corrected as described in Koehler et al. (2014). The clear-sky spectra were integrated with calculated solar zenith angles and measurements of ozone column fields in hourly time steps at the coordinates of each lake. The true solar zenith angle was calculated with hourly time step for each lake and day for a month between early July and early August of 2011 (i.e., the time period of field sampling), using approximations in the Astronomical Almanac (Michalsky 1988). The actual ozone column fields for the same time were extracted from the archive operational runs of the Integrated Forecasting System at the European Centre for Medium-Range Weather Forecasts (http://www.ecmwf.int/research/ifsdocs/CY33r1/index.html). To correct for attenuation by clouds, total cloud cover data were retrieved for the requested time period at the lakes coordinates from the archive of the operational mesoscale analysis system at the Swedish Meteorological and Hydrological Institute (Häggmark et al. 2000).

Photochemical DIC production in the lakes

According to the photon budget approach (Kirk 1994), absorption spectra for the lakes were modeled for DOC ($a_{DOC}[\lambda]$; m^{-1}) (Twardowski et al. 2004), nonalgal particles ($a_{NAP}[\lambda]$; m^{-1}) (Shen et al. 2012), phytoplankton ($a_{PP}[\lambda]$; m^{-1}), all from lake samples and for standardized water ($a_{water}[\lambda]$; m^{-1}) (Wozniak and Dera 2007). All absorption spectra were extrapolated from the measured PAR band to 300 nm using linear mixed effect models with prediction uncertainties

propagated through Monte Carlo samples generated by the arm package in R (Gelman et al. 2018).

The total absorption coefficient spectrum ($a_{\text{total}}[\lambda]$; m^{-1}) was calculated as the sum of $a_{\text{DOC}}(\lambda)$, $a_{\text{NAP}}(\lambda)$, $a_{\text{water}}(\lambda)$, and $a_{\text{PP}}(\lambda)$ (Kirk 1994) and the relative contribution of DOC to the total absorption ($k_{\text{DOC}}(\lambda)$) was calculated as the $a_{\text{DOC}}(\lambda)$ to $a_{\text{total}}(\lambda)$ quotient (Fig. S5). Finally, the wavelength-specific photon absorption by DOC per depth unit ($E_{\text{abs,p}}$ [λ, z]; mol m^{-3} d^{-1} nm^{-1}) was calculated as the depth derivative of the attenuation profile, weighted by the relative DOC contribution:

$$E_{abs,p}(\lambda, z) = E_p(\lambda) e^{-a_{total}(\lambda) z} a_{DOC}(\lambda) \quad (2)$$

where E_{p} is the photon flux ($E_{\text{p}}(\lambda)$; mol m^{-2} d^{-1} nm^{-1}) at the lake surface from the modeled irradiation spectra and z is depth (m). Solving Eq. (2) for $z \rightarrow 0$, i.e., just below the surface, the DOC absorbed photons per unit volume is given by:

$$E_{abs,p}(\lambda, 0) = E_p(\lambda) a_{DOC}(\lambda) \quad (3)$$

Boreal lakes generally absorb all incoming irradiation (Kirk 1994; Koehler et al. 2014; Thrane et al. 2014). Assuming that this also is the case for the lakes in this study, integrating Eq. (3) over the entire water column ($\int_0^\infty E_{abs,p}(\lambda, z) dz$), DOC absorbed photons per unit surface area ($E_{\text{abs,p}}(\lambda)$; mol m^{-2} d^{-1} nm^{-1}) is given by:

$$E_{abs,p}(\lambda) = E_p(\lambda) k_{DOC}(\lambda) \quad (4)$$

Wavelength-specific photochemical DIC production could then be calculated as either volumetric rates at the surface ($\psi_{\text{DIC}}[\lambda, 0]$; mol m^{-3} d^{-2} nm^{-1}) or as production rates per unit area ($\psi_{\text{DIC}}(\lambda)$; mol m^{-2} d^{-2} nm^{-1}), multiplying the photon absorption by DOC by the AQY (Φ):

$$\psi_{DIC}(\lambda, z) = E_{abs,p}(\lambda, z) \Phi_{DIC}(\lambda) \quad (5)$$

CO_2 flux

Air-water flux of CO_2 (F_{CO2}; mmol m^{-2} d^{-1}) was calculated from the surface CO_2 concentrations in each lake using Fick's law of diffusion:

$$F_{CO2} = k_{CO2} \Delta_{CO2} \quad (6)$$

where k_{CO2} (m d^{-1}) is the CO_2 gas exchange coefficient at a given temperature and Δ_{CO2} (mmol m^{-3}) is the CO_2 deficit from concentrations at equilibrium with the atmosphere, obtained using Henry's law. k_{CO2} was estimated for each lake using the gas transfer velocity (cm h^{-1}) for a gas-temperature combination with a Schmidt number of 600 (k_{600}; CO_2 at 20°C) according to Jähne et al. (1987):

$$k_{CO2} = k_{600} \left(\frac{Sc_{CO2}}{600} \right)^{-x} \quad (7)$$

where x = 2/3 if wind speed ≤ 3 ms^{-1} and x = 0.5 if wind speed > 3 ms^{-1}, Sc is the temperature dependent Schmidt number for CO_2 (Wanninkhof 1992). k_{600} is estimated from the wind speed according to Cole and Caraco (1998):

$$k_{600} = 2.07 + 0.215\, U_{10}^{1.7} \quad (8)$$

Hourly wind speed data at 10 m above ground (U_{10} in Eq. 9) at all 70 lakes were received from the Norwegian Reanalysis Archive (Furevik and Haakenstad 2012) and aggregated into July–August means.

Lake pelagic CO_2 production

From the dataset, it was not possible to distinguish between lateral input of CO_2 (surface- and ground water flow) and in-lake production of CO_2 (microbial and photochemical mineralization of DOC). Lake pelagic CO_2 production ($CO_{2,\text{prod}}$; mg C m^{-2} d^{-1}) will therefore be used as a term for the sum of the in situ DOC mineralization and the lateral input. Assuming that the deviation of CO_2 from saturation is kept at steady state due to production, lateral input, consumption and evasion, the air-water flux of CO_2 (F_{CO2}; mg C m^{-2} d^{-1}) can be written as:

$$F_{CO2} = CO_{2,prod} - PP_A \quad (9)$$

Positive and negative values of F_{CO2} are evasion and invasion across the air–water interface, respectively. Rearranging Eq. (9), we estimate $CO_{2,\text{prod}}$ as the sum of F_{CO2} and PP_A.

Statistical analysis

All data analysis was performed using the open-source software R version 3.4.1 (R Development Core Team, 2017). For linear modeling of the CO_2 production, consumption, and evasion in the lakes the explanatory variables were DOC (mg l^{-1}), TP (µg l^{-1}) and TN (mg l^{-1}). The predictors were chosen using AICc in backwards stepwise regression. For estimation of the best predictor, the largest value of the standardized regression coefficients was used. All error estimates are given in standard errors (standard deviation divided by the square root of the number of observations: $SE = SD/\sqrt{n}$).

Results

Modeling the AQY spectra

The optical parameters a_{420} and $SUVA_{400}$ explained 26–64% of the variation in AQY across lakes. The variation in AQY explained by the parameters decreased with wavelength giving a higher percentage explained at shorter wavelengths where AQY variability between lakes is larger (Table S2; data from Koehler et al. (2016)). The relative magnitude of the

sums of squares (SS) of the fixed terms in the model (Eq. 1) can be used to rank their contribution to the variance of the predicted AQY. While wavelength was by far the largest variance contribution (SS = 48.9; $p << 0.001$), a_{420} contributed about five times (SS = 0.87; p = 0.023) as much to the variance in modeled AQY as $SUVA_{400}$ (SS = 0.18; p = 0.027). Monte Carlo simulations of the AQY spectra based on these regression relationships (n = 70) resulted in a SE ranging between 0.9% and 1.8% of the wavelength integrated AQY's. The SE was negatively related to a_{420} (r = −0.73; data not shown), indicating that the model fits brown lakes somewhat better than clear ones. The SE of the AQY had an almost one to one fit with the SE of the DIC photoproduction. The uncertainty of the modeled AQY thus propagated through to the DIC photoproduction estimate and the uncertainties of the absorption spectra or the downwelling irradiation did not contribute substantially.

CO_2 saturation

Out of the 70 lakes in this study, 62 were supersaturated with CO_2 while 6 lakes were close to saturation or slightly undersaturated and 2 were clearly undersaturated with CO_2. DOC concentrations were strongly related to a_{420} (r = 0.88), and the CO_2 saturation deficit was positively related to both DOC and a_{420} (r = 0.50 and 0.61 for DOC and a_{420}, respectively). The CO_2 and O_2 saturation deficits were negatively correlated (r = −0.70), and the O_2 saturation deficit was negatively related to DOC concentrations and a_{420} (r = −0.74 and −0.69, respectively; Fig. S6).

Photochemical DIC production

a_{420} and $SUVA_{400}$ in the sampled lakes varied between 0.60 and 11.47 m^{-1}, and 0.16 and 1.33 L mg C^{-1} m^{-1}, respectively (Table S1). Integrating the estimated areal photochemical production of DIC (Fig. 2a), over wavelengths (300–600 nm) gave a range in photoproduced DIC between 8.4 mg C m^{-2} d^{-1} ± 1.5% and 21.4 mg C m^{-2} d^{-1} ± 1.0%; Table S1) in the lakes. Both $SUVA_{400}$ and a_{420} were negatively related to pH (r = −0.51 and r = −0.28, respectively; Fig. S7) and positively related to iron concentrations (Fe; r = 0.35 and r = 0.74 for $SUVA_{400}$ and a_{420} respectively; Fig. S7). A multiple linear regression model showed equal sized but opposite effects of pH and Fe concentrations on the estimated DIC photoproduction rates (R^2 = 0.31, Table S3). The interaction term between the predictor variables was nonsignificant (p > 0.05, Table S3).

In lakes with high a_{420}, the shorter wavelengths are absorbed at the surface, resulting in high DIC photoproduction in the top layer compared to lakes with lower a_{420} (Fig. 2b). While in the brownest lakes irradiance of all photochemically active wavelengths was absorbed within the first meter, this irradiance penetrated further in clearer lakes, allowing for DIC photoproduction to take place at greater depth. Most DIC photoproduction is induced by absorption of photons with wavelengths in the UV and violet part of the spectrum (Vähätalo et al. 2000). Of the estimated areal photochemical DIC production in all lakes 85% ± 0.1% and 93% ±

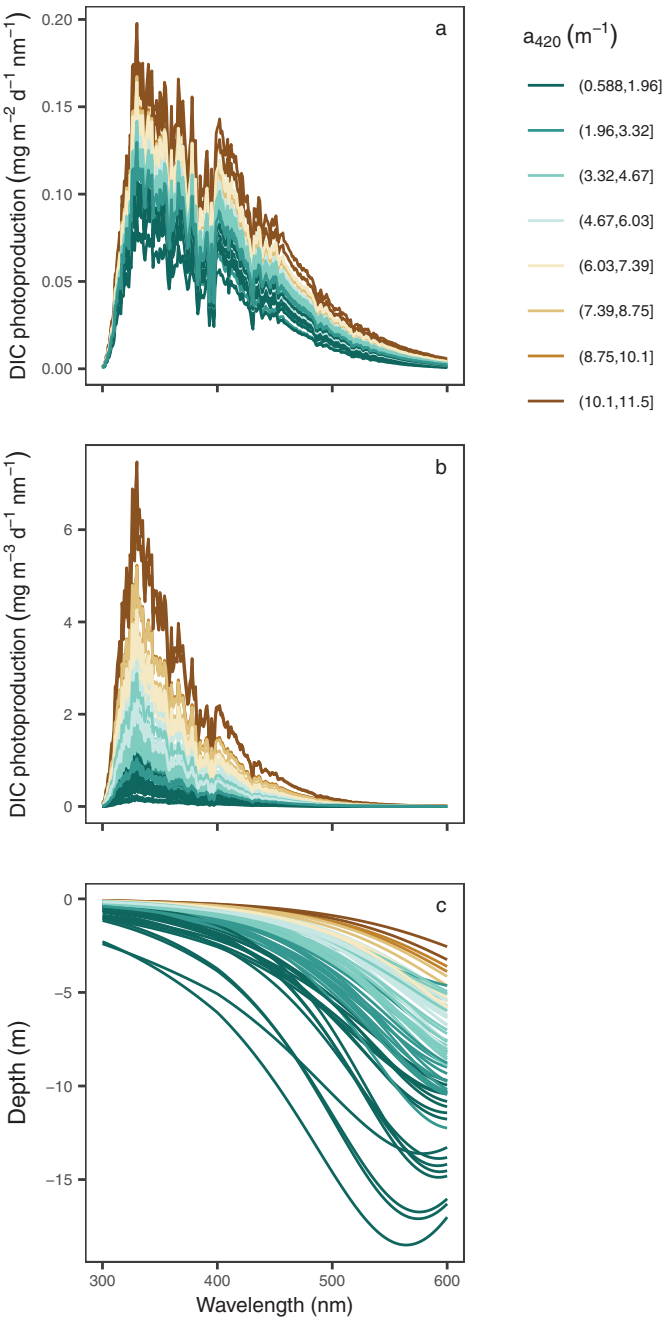

Fig. 2. Estimated photoproduction spectra of dissolved inorganic carbon (DIC) from all 70 study lakes. In **(a)**, the estimated areal DIC photoproduction (mg C m^{-2} d^{-1} nm^{-1}) spectra are shown; and **(b)** shows the estimated volumetric DIC photoproduction (mg C m^{-3} d^{-1} nm^{-1}) spectra just below the surface. In **(c)** the depth at which the volumetric DIC photoproduction (mg C m^{-3} d^{-1} nm^{-1}) is 1% of that just below the surface is shown, indicating also the depth that receives 1% of incoming radiation. The color gradient goes from dark blue for lakes with low a_{420} to brown for lakes with high a_{420}.

Table 1. Regression coefficients for regressions predicting lake pelagic CO_2 production, consumption, and evasion.

Response	Predictors	Coefficient estimates (SE, significance levels)	R^2
Lake pelagic CO_2 production	TP + TN	29.9 (±6.6***), 338.0 (±116.9**)	0.47
Areal primary production (PP_A)	DOC + TP + TN	−29.2 (±7.4***), 21.9 (±4.6***), 174.8 (±75.7*)	0.47
CO_2 flux	DOC + TP	35.4 (±8.9***), 11.2 (±4.9*)	0.33

Significance codes:
***$p < 0.001$,
**$p < 0.01$,
*$p < 0.05$.

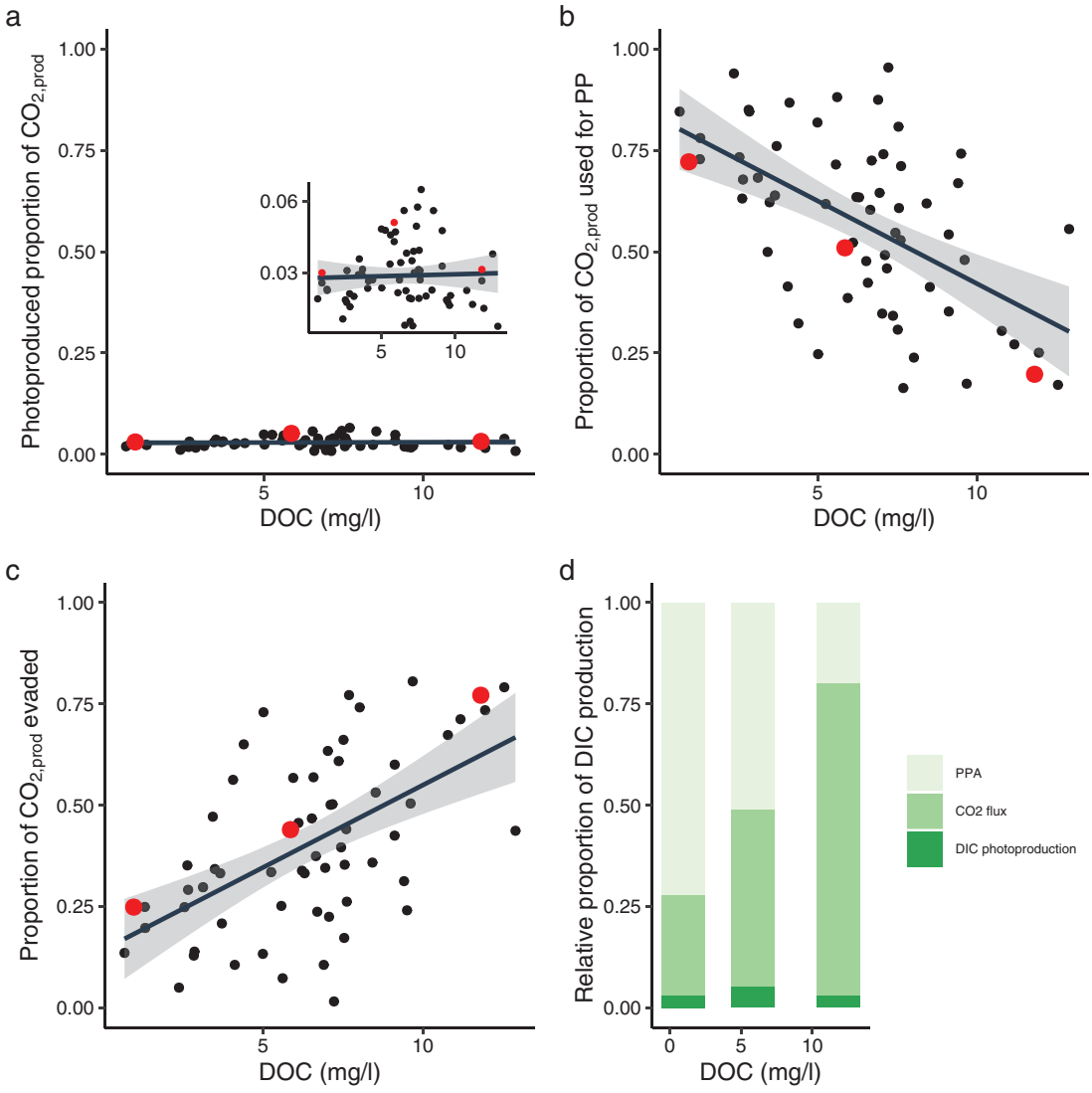

Fig. 3. The relative proportions of **(a)** DIC photoproduction (the inset figure is zoomed in on the *y*-axis); **(b)** CO_2 flux and; **(c)** areal primary production (PP_A) to total lake pelagic CO_2 production ($CO_{2,prod} = F_{CO2} + PP_A$; Eq. 9). In **(d)** is an example of the relative proportion of DIC production for three lakes with low (0.95 mg C l^{-1}), medium (5.85 mg C l^{-1}), and high (11.84 mg C l^{-1}) DOC concentrations. Red dots in the regression plots indicate the three example lakes.

0.1% was induced by wavelengths shorter than 465 and 500 nm, respectively (Fig. S5). Therefore, almost all DIC photoproduction took place in the top 5 m of all lakes, regardless of their color (Fig. 2c). In some of the clearest lakes, light of wavelengths > 500 nm penetrated as deep as 15–20 m (Fig. 2c). The contribution to total DOC photomineralization by wavelengths > 500 nm was minor (Figs. 2a and S3), and the majority of DIC photoproduction thus occurred in the top 5 m of the water column, even in the clearest lakes. The estimated percentage of the DOC standing stock that was photomineralized each day averaged about 2% (0.2–3%) at the surface and 0.3% (0.1–1%) at 1-m depth (Fig. S8). At the surface, the photomineralized share of the standing stock of DOC increased somewhat with increased DOC concentration, while at one meter the relationship was the opposite.

Lake pelagic CO_2 production and consumption

Estimations of summer lake pelagic CO_2 production (photochemical and biological mineralization + lateral input of CO_2) in the studied lakes ranged between 120 and 1770 mg C m^{-2} d^{-1}. The best predictors for lake pelagic CO_2 production were TP (μg P l^{-1}) and TN (mg N l^{-1}; Table 1). The relative contribution of DIC photoproduction to lake pelagic CO_2 production averaged 3.0% ± 0.2% regardless of DOC concentration (Fig. 3a,d). Primary production in the lakes was negatively related to DOC concentration and positively related to nutrient content, mainly TP (Table 1). The share of lake pelagic CO_2 production used for primary production was thus smaller in lakes with a high DOC concentration than in lakes with a low DOC concentration (Fig. 3b,d).

CO_2 flux

The majority of the lakes were net sources of CO_2 to the atmosphere. The CO_2 flux ranged from –0.12 to 1.0 g C m^{-2} d^{-1}. CO_2 evasion from lakes was best explained by DOC concentration, followed by TP (Table 1). Assuming that all photochemically produced DIC was emitted as CO_2 from supersaturated lakes, the relative contribution of estimated DIC photoproduction to total CO_2 efflux ranged between 1.4% and 36%, averaging 9% ± 1%, and with higher contribution in lakes with low than in lakes with high DOC concentrations (Fig. S7). The source of the remaining CO_2 efflux must be attributed to respiration and lateral CO_2 input. Of the total DIC production in the lakes, a larger share was emitted as CO_2 in lakes with high than in lakes with low DOC concentrations (Fig. 3c,d).

Discussion

We estimated DIC photoproduction in boreal lakes using modeled spectra of irradiance and AQY, and spectra of attenuation coefficients and absorption extrapolated from the measured PAR to the UV region from 70 lakes in Norway and Sweden. We found that DIC photoproduction contributed on average 9% ± 1% to the CO_2 emission from the lakes. Regarding that this percentage decreases with increased DOC concentrations and that water temperatures as well as DOC and nutrient concentrations in boreal lakes are increasing (Larsen et al. 2011*b*; O'Reilly et al. 2015), we expect that the relative contribution of sunlight for CO_2 production in boreal lakes may decline in the future.

The AQY spectra were modeled using regressions between AQY at discrete wavelengths and the optical parameters $SUVA_{400}$ and a_{420}, which were set up based on AQY spectral measurements of 25 lakes worldwide (Koehler et al. 2016). While a_{420} is a proxy for CDOM content, $SUVA_{400}$ is well correlated with DOC aromaticity, and both parameters describe absorbing properties of the DOC. (Koehler et al. 2016). Even though $SUVA_{400}$ is well correlated with DOC aromaticity, $SUVA_{254}$ is usually a better indication of DOC aromaticity. Likewise, in the study by Koehler et al. (2016), $SUVA_{254}$ was somewhat better correlated with AQY than $SUVA_{400}$ was. However, the difference in R^2 between $SUVA_{400}$ and $SUVA_{254}$ as linear predictors of AQY was minor (Table S2). Running the AQY model (Eq. 1) on the data from Koehler et al. (2016) with $SUVA_{254}$ produced similar spectra as with $SUVA_{400}$, mean values of the Monte Carlo simulations had a one to one fit (Fig. S4) and there were no significant differences in SEs between the two. We therefore used the measured $SUVA_{400}$ instead of an extrapolated value of $SUVA_{254}$. The uncertainty in the modeled AQY spectra propagated through to the DIC photoproduction estimates. The SEs in the modeled AQY's were however small (1.2% ± 0.02%) and the errors in the estimated DIC photoproduction were therefore also small. Additionally, the AQY spectra estimated in this study match spectra from other studies on boreal lakes well (Koehler et al. 2014; Groeneveld et al. 2016; Vachon et al. 2016).

Estimated DIC photoproduction contributed about 3% (1–5%) of the total production and lateral inflow of CO_2 in the 62 lakes supersaturated with CO_2. Further, assuming that all photochemically produced of DIC is outgassed from the lakes, the relative share of DIC photoproduction to total CO_2 emission averaged about 9% across the 70 study lakes. These results conform to earlier studies on photomineralization of DOC and CO_2 flux from boreal lakes. For example, the contribution of DIC photoproduction to total DOC mineralization in two Swedish humic lakes amounted to about 7% (Jonsson et al. 2001) and 6% (Chmiel et al. 2016). In a third lake, the mean contribution of DIC photoproduction to CO_2 out flux was 1–8%, depending on the time of the year (Groeneveld et al. 2016). Or, in a large-scale modeling study for 1086 Swedish lakes, the mean contribution of DIC photoproduction to out flux of CO_2 was about 12% and upscaling to the entire boreal region about 9–12% (Koehler et al. 2014). However, in other aquatic systems than boreal lakes, photochemical degradation has been found to have an important role in aquatic carbon cycling. In arctic surface waters photochemical reactions accounted for 75% of the total DOC processed (Cory et al. 2014) and in a number of boreal streams photochemical

degradation accounted for more than 60% of DOC losses (Molot and Dillon 1997).

Rates of DIC photoproduction in lakes are controlled by three wavelength-dependent processes: the amount of sunlight reaching the lake surface; the fraction of this that is absorbed by CDOM across wavelengths; and the amount of DIC produced per unit absorbed light (AQY) (Cory and Kling 2018). The latter two processes had the largest variations between our 70 study lakes while the solar irradiation spectra were similar, owing to the fact that we sampled in a similar geographic region and time, and that cloud cover variability was low. Both AQY and the CDOM fraction of absorbed irradiance are dependent on the quantity and quality of CDOM in the water. Volumetric DIC photoproduction rates at specific depths are therefore closely related to CDOM content.

While the variability in absorption coefficients between lakes was substantial, the total estimated areal photochemical production of DIC did not differ as much, as similarly shown in earlier studies (Granéli et al. 1996; Koehler et al. 2014). Lower a_{420} allows light to penetrate deeper down in the water column and DIC photoproduction to take place at greater depths compared to waters with higher a_{420}. In the latter, all short wavelength photons are strongly absorbed by the DOC and therefore all photoproduction occurs close to the water surface. The absolute areal DIC photoproduction rates were similar whether they were integrated over the entire lake depth or over five meters, indicating that even in the clearest lakes all photochemical production of DIC takes place in the top five meters, where the sampling took place. Both $SUVA_{400}$ and a_{420} were negatively related to pH, and positively related to Fe concentrations (Fig. S9). This implies that the effect of extrinsic variables may affect the intrinsic properties of the DOC and therefore the DIC photoproduction rates. A positive correlation between Fe concentrations and CDOM absorption (e.g., a_{420}) has been shown before (Kritzberg and Ekström 2011). $SUVA_{400}$ was principally related to pH. As $SUVA_{400}$ is a measure of the aromatic character of the DOC, this implies that aromaticity is increasing at decreasing pH. In acidic waters, DIC photoproduction rates have frequently been reported to increase with decreasing pH (Panneer Selvam et al. 2019). In alkaline waters, the relationship between photochemical degradation of DOC and pH is less certain. While some studies find photomineralization rates to keep decreasing as pH increases (Bertilsson and Tranvik 2000; Molot et al. 2005), others report that they start increasing as pH increases above 7 (Pace et al. 2012; Panneer Selvam et al. 2019). Iron concentrations are also known to interact with pH, having a stronger positive effect on CDOM absorption and hence DIC photoproduction rate under acidic conditions (Gu et al. 2017). However, the pH in the study lakes ranged between 6.3 and 8.0 with two outliers at 5.4 and 8.9 and was thus close to neutral, possibly explaining why the interaction term between Fe and pH in our model was not significant.

Photons entering the water column are likely to be absorbed, if not by DOC, by phytoplankton, nonalgal particles, or by the water itself. Lake absorption spectra show that close to all the photons in the UV region and the largest fraction of the photons in the PAR region were absorbed by DOM, and only a small number were absorbed by other chromophoric compounds (Fig. S3; see also Thrane et al. (2014)). In this study, absorption spectra were only measured in the PAR region. Since the major part of absorption by DOC and thereby the major part of photochemical mineralization of DOC takes place in the UV region, we extrapolated the absorption spectra to wavelengths < 400 nm. We acknowledge that the extrapolation may have led to increased uncertainties of the absorption estimates and through that to increased uncertainties of the DIC photoproduction estimates. However, DOC absorption is rather well studied and the spectra are known to be approximately exponential (Bricaud et al. 1981). Therefore, the mean value of the Monte Carlo simulated spectra and their SE can be assumed to capture most of the uncertainty of the absorption and its propagation through to the DIC photoproduction estimates. For wavelengths between 280 and 400 nm, the DOC absorption fraction in boreal lakes is generally close to 1, and the DOC concentrations are often sufficient for absorption of all incoming photons in this waveband in the top meters of the water column (Williamson et al. 1996). In lakes with high a_{420}, primary production is constrained to the surface layer due to high light attenuation, resulting in lower rates of primary production on the whole-lake scale (Thrane et al. 2014). However, in regard to the areal photochemical DIC production, the critical limitation is the total amount of DOM-absorbed photons regardless of where in the water column they are absorbed. The major part of the estimated photoproduction of DIC took place above 5 m (Fig. 2c) and was therefore within the mixed zone of the lakes (Fig. S1). The photic zone is deeper in clear than in brown lakes and we can expect that some DIC photoproduction might take place below the mixed zone. However, the photons reaching depths deeper than 5 m are of longer, less photoreactive wavelengths and the contribution of DIC photoproduction at such depth to total lake DIC photoproduction is minor.

While some studies have reported that the vast majority of the CO_2 evasion from boreal lake surfaces is explained by pelagic respiration (Jonsson et al. 2001), others have shown that input of DIC has a larger role than previously thought (Weyhenmeyer et al. 2015). In this study, it was not possible to distinguish between lateral flow and respiration; lake pelagic CO_2 production is therefore used as a common term for the sum of the two. There was, however, a strong relationship between O_2 and CO_2 saturation deficits ($r = -0.70$; Fig. 4). The intercept was not significantly different from 0, meaning that lakes that were saturated with O_2 were also saturated with CO_2. This relationship indicates that microbial respiration was the predominant source of CO_2 in the lakes. Furthermore, both O_2 and CO_2 concentrations correlated well with DOC,

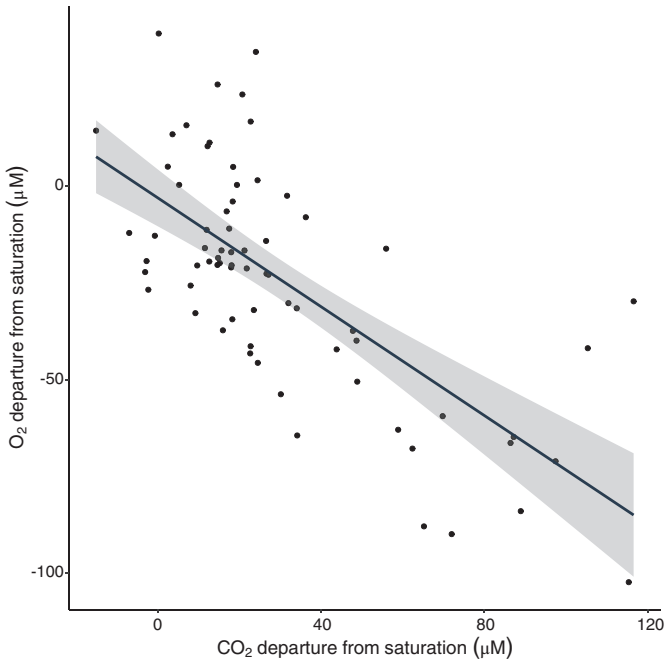

Fig. 4. Lake O_2 departure from saturation with the atmosphere vs. CO_2 departure from saturation with the atmosphere ($y = -0.70x - 3.02$, $R^2 = 0.49$, $p << 0.001$).

but not with chlorophyll *a* (Fig. S10). This suggests that the major DOC source for microbial degradation was of terrestrial origin. The strong relationship between DOC concentrations and a_{420} confirms that the dominant part of the DOC pool in the lakes originated from the terrestrial surroundings.

Sampling of the lakes used in this study was performed during mid-summer in July and August. Our results cannot be extrapolated to estimate annual rates, but rather present a picture of summer conditions. Photochemical reactivity of DOC depends on the degree of aromaticity (Bertilsson and Tranvik 2000). As DOC leaves the soil and enters the aquatic systems, it will be altered through both biological and photochemical reactions and lose aromaticity (Brinkmann et al. 2003), becoming less photoreactive. Hence, the DOC photochemical reactivity is linked to light exposure time. AQY spectra of photochemical DOC mineralization show pronounced seasonal variability. Photomineralization rates were found to be higher during seasons with high inputs of DOC to lakes, after snowmelt during spring flood (Vachon et al. 2016), and in connection to rain events in autumn, and lower in summer when DOC inputs are low (Groeneveld et al. 2016; Vachon et al. 2016). Photochemical DIC production is dependent on both irradiation and on DOC composition. The AQY might thus be higher in autumn than in summer but due to less sunlight in autumn than in summer, the amount of DIC photoproduction does not necessarily differ substantially between the two seasons. However, increased light absorption due to brownification may lead to enhanced lake stratification (Williamson et al. 2015), and especially it may give rise to microlayers of stratification at the surface where most irradiance is absorbed. The CO_2 concentrations in these microlayers could thus be much higher than in the underlying water, causing increased rates of photochemically induced CO_2 emissions from brown lakes, especially during the summer months when daily irradiation rates are high. We did not see any indication of increased thermal stratification with increased CDOM content in the study lakes. The CO_2 concentrations of the composite samples can therefore be assumed to represent the concentrations in the entire mixed layers.

On the other hand, pelagic respiration is strongly related to temperature and, therefore, also has a seasonal pattern with higher rates during summer than the rest of the year (Vachon et al. 2016). The relative contribution of photomineralization to total pelagic CO_2 production can thus be assumed to be lower during summer. This was confirmed by Vachon et al. (2016) where the relative contribution of photochemical DIC production to total pelagic CO_2 production in three lakes averaged 14% over the year with larger contribution in spring (26%) than in summer (7.6%) and autumn (12%). The mean value of lake pelagic CO_2 production in the 70 lakes in our study was 616.4 mg C m^{-2} d^{-1}, ranging from 118.7 to 1769.1 mg C m^{-2} d^{-1}. These numbers accord with measurements of DOC mineralization in other boreal lakes at summer conditions (Jonsson et al. 2001; Vachon et al. 2016). The DIC photoproduction rates and their relative contribution to lake CO_2 production and evasion also correspond to measures and estimates in previous studies (Jonsson et al. 2001, Vachon et al. 2016). The typical seasonal variations in both microbial and photochemical mineralization rates reported from other lakes make it likely that the role of DIC photoproduction also in the 70 boreal lakes of this study is larger during spring and autumn conditions than found here at summer conditions.

In this study, we estimated photochemical mineralization of DOC. Other photochemical processes in the water column may also have a large impact on the aquatic carbon cycle. Such processes are photomineralization of organic nutrients and partial photooxidation of DOC (Bertilsson and Tranvik 2000). In the latter processes, recalcitrant DOC is transformed to more biologically available organic compounds (Bertilsson and Tranvik 1998). Microbial consumption of such photodegraded compounds is thus often preferred over the nonphotodegraded compounds (Allesson et al. 2016). Although most photochemical processes take place near the surface, photochemically produced carboxylic acids may mix downwards and be a source of labile DOC in the entire mixed layer (Bertilsson and Tranvik 1998). Enhanced microbial degradation of photodegraded DOC may have an impact on aquatic carbon cycling as large as photomineralization.

Post-acidification recovery, increased vegetation cover in catchments, and a wetter climate promote carbon export to

lakes (Finstad et al. 2017; de Wit et al. 2018). Concentrations of allochthonous DOC are thus predicted to increase in most boreal lakes (Larsen et al. 2011*b*). Input of DOC in boreal lakes is correlated with export of TP and TN (Dillon and Molot 2005), and the predicted increased nutrient levels will most likely promote microbial activity and thus pelagic CO_2 production. Although DOC and TP have contrasting effects on primary production, the net effect of enhanced levels will probably be a reduced primary production due to light attenuation in most lakes with initial moderate to high DOC concentrations (Thrane et al. 2014). In lakes with low initial levels of DOC, an increase in DOC and nutrient levels could lead to enhanced primary production, and thus an enhanced level of autochthonous DOC which in turn could result in enhanced microbial respiration (Lapierre and del Giorgio 2014). Increased DOC input will thus most likely lead to enhanced levels of heterotrophy in boreal lakes (Larsen et al. 2011*a*). Moreover, higher levels and more frequent input of fresh, photolabile, DOC are to be expected and therefore the AQY and by that DIC photoproduction can be expected to increase as well. However, the rather small difference in estimated areal DIC photoproduction between lakes compared to the wide ranges in DOC and a_{420} indicates that enhanced rates of photochemical mineralization will not be a major contributor to shifting levels of boreal lake net heterotrophy. In all lakes, all photons active to DOC photochemistry were absorbed within the top five meters, regardless of DOC concentration. This suggests that the contribution of enhanced rates of DIC photoproduction to lake net heterotrophy will probably be largest when clear, shallow lakes undergo browning. While the observed strong increase in surface water temperatures (O'Reilly et al. 2015) will promote microbial respiratory activity, photomineralization is only weakly temperature dependent (Chatwal and Arora 2007), hence the relative contribution of DIC photoproduction to total CO_2 production will most likely decrease in boreal lakes under a changing climate.

References

Allesson, L., L. Ström, and M. Berggren. 2016. Impact of photochemical processing of DOC on the bacterioplankton respiratory quotient in aquatic ecosystems. Geophys. Res. Lett. **43**: 7538–7545.

Bates, D., Mächler, M., Bolker, B. & Walker, S. 2014. Fitting linear mixed-effects models using lme4. **67**: 1–48.

Bertilsson, S., and L. J. Tranvik. 1998. Photochemically produced carboxylic acids as substrates for freshwater bacterioplankton. Limnol. Oceanogr. **43**: 885–895.

Bertilsson, S., and L. J. Tranvik. 2000. Photochemical transformation of dissolved organic matter in lakes. Limnol. Oceanogr. **45**: 753–762.

Bricaud, A., A. Morel, and L. Prieur. 1981. Absorption by dissolved organic matter of the sea (yellow substance) in the UV and visible domains 1. Limnol. Oceanogr. **26**: 43–53.

Bricaud, A., and D. Stramski. 1990. Spectral absorption coefficients of living phytoplankton and nonalgal biogenous matter: A comparison between the Peru upwelling areaand the Sargasso Sea. Limnol. Oceanogr. **35**: 562–582.

Brinkmann, T., D. Sartorius, and F. H. Frimmel. 2003. Photobleaching of humic rich dissolved organic matter. Aquat. Sci. **65**: 415–424.

Chatwal, G. R., and M. Arora. 2007. Organic photochemistry. Himalaya Publishing House. Mumbay, India.

Chmiel, H. E., et al. 2016. The role of sediments in the carbon budget of a small boreal lake. Limnol. Oceanogr., **61**, 1814–1825.

Cole, J. J., and N. F. Caraco. 1998. Atmospheric exchange of carbon dioxide in a low-wind oligotrophic lake measured by the addition of SF6. Limnol. Oceanogr. **43**: 647–656.

Cole, J. J., M. L. Pace, S. R. Carpenter, and J. F. Kitchell. 2000. Persistence of net heterotrophy in lakes during nutrient addition and food web manipulations. Limnol. Oceanogr. **45**: 1718–1730.

Cole, J. J., and others. 2007. Plumbing the global carbon cycle: Integrating inland waters into the terrestrial carbon budget. Ecosystems, **10**, 172–185.

Cory, R. M., and G. W. Kling. 2018. Interactions between sunlight and microorganisms influence dissolved organic matter degradation along the aquatic continuum. Limnol. Oceanogr. Lett. **3**: 102–116.

Cory, R. M., C. P. Ward, B. C. Crump, and G. W. Kling. 2014. Sunlight controls water column processing of carbon in arctic fresh waters. Science **345**: 925–928.

de Wit, H. A., R.-M. Couture, L. Jackson-Blake, M. N. Futter, S. Valinia, K. Austnes, J.-L. Guerrero, and Y. Lin. 2018. Pipes or chimneys? For carbon cycling in small boreal lakes, precipitation matters most. Limnol. Oceanogr. Lett. **3**: 275–284.

Dillon, P. J., and L. A. Molot. 2005. Long-term trends in catchment export and lake retention of dissolved organic carbon, dissolved organic nitrogen, total iron, and total phosphorus: The Dorset, Ontario, study, 1978–1998. J. Geophys. Res. Biogeo. **110**.

Finstad, A. G., E. B. Nilsen, D. K. Hendrichsen, and N. M. Schmidt. 2017. Catchment vegetation and temperature mediating trophic interactions and production in plankton communities. PLOS One **12**: e0174904.

Furevik, B. R., and H. Haakenstad. 2012. Near-surface marine wind profiles from rawinsonde and NORA10 hindcast. J. Geophys. Res. Atmos. **117**.

Gelman, A., et al. 2018. Package 'arm'.

Granéli, W., M. Lindell, and L. Tranvik. 1996. Photo-oxidative production of dissolved inorganic carbon in lakes of different humic content. Limnol. Oceanogr. **41**: 698–706.

Groeneveld, M., L. Tranvik, S. Natchimuthu, and B. Koehler. 2016. Photochemical mineralisation in a boreal brown water lake: Considerable temporal variability and minor contribution to carbon dioxide production. Biogeosciences **13**: 3931–3943.

Gu, Y., A. Lensu, S. Perämäki, A. Ojala, and A. V. Vähätalo. 2017. Iron and pH regulating the photochemical mineralization of dissolved organic carbon. ACS Omega **2**: 1905–1914.

Häggmark, L., K.-I. Ivarsson, S. Gollvik, and P.-O. Olofsson. 2000. Mesan, an operational mesoscale analysis system. Tellus A Dynam. Meteorol. Oceanogr. **52**: 2–20.

Hessen, D. O. 1992. Dissolved organic carbon in a humic lake: Effects on bacterial production and respiration. Hydrobiologia **229**: 115–123.

Hessen, D. O., and L. J. Tranvik. 1998. Aquatic humic substances: Ecology and biogeochemistry. Springer Science & Business Media. Berlin Heidelberg: Springer.

Jähne, B., K. O. Münnich, R. Bösinger, A. Dutzi, W. Huber, and P. Libner. 1987. On the parameters influencing air-water gas exchange. J. Geophys. Res. Oceans **92**: 1937–1949.

Jonsson, A., M. Meili, A.-K. Bergström, and M. Jansson. 2001. Whole-lake mineralization of allochthonous and autochthonous organic carbon in a large humic lake (örträsket, N. Sweden). Limnol. Oceanogr. **46**: 1691–1700.

Karlsson, J., P. Byström, J. Ask, P. Ask, L. Persson, and M. Jansson. 2009. Light limitation of nutrient-poor lake ecosystems. Nature **460**: 506–509.

Kirk, J. T. O. 1994. Light and photosynthesis in aquatic ecosystems. Cambridge, England: Cambridge Univ. Press.

Koehler, B., E. Broman, and L. J. Tranvik. 2016. Apparent quantum yield of photochemical dissolved organic carbon mineralization in lakes. Limnol. Oceanogr. **61**: 2207–2221.

Koehler, B., T. Landelius, G. A. Weyhenmeyer, N. Machida, and L. J. Tranvik. 2014. Sunlight-induced carbon dioxide emissions from inland waters. Global Biogeochem. Cycles **28**: 696–711.

Kritzberg, E., and S. Ekström. 2011. Increasing iron concentrations in surface waters—A factor behind brownification? Biogeosciences Discussions **8**: 12285–12316.

Kromkamp, J. C., and R. M. Forster. 2003. The use of variable fluorescence measurements in aquatic ecosystems: Differences between multiple and single turnover measuring protocols and suggested terminology. Eur. J. Phycol. **38**: 103–112.

Lapierre, J. F., and P. A. del Giorgio. 2014. Partial coupling and differential regulation of biologically and photochemically labile dissolved organic carbon across boreal aquatic networks. Biogeosciences **11**: 5969–5985.

Larsen, S., T. Andersen, and D. hessen. 2011*a*. The pCO2 in boreal lakes: Organic carbon as a universal predictor? Global Biogeochem. Cycle **25**.

Larsen, S., T. Andersen, and D. O. Hessen. 2011*b*. Climate change predicted to cause severe increase of organic carbon in lakes. Glob. Chang. Biol. **17**: 1186–1192.

Lindell, M. J., W. Granéli, and L. J. Tranvik. 1995. Enhanced bacterial growth in response to photochemical transformation of dissolved organic matter. Limnol. Oceanogr. **40**: 195–199.

Mayer, B., and A. Kylling. 2005. Technical note: The libRadtran software package for radiative transfer calculations—Description and examples of use. Atmos. Chem. Phys. **5**: 1855–1877.

Michalsky, J. 1988. The astronomical Almanac's algorithm for approximate solar position (1950–2050). Solar Energy **40**: 227–235.

Miller, W. L., M. Moran, W. M. Sheldon, R. G. Zepp, and S. Opsahl. 2002. Determination of apparent quantum yield spectra for the formation of biologically labile photoproducts. Limnol. Oceanogr. **47**: 343–352.

Mitchell, B., Kahru, M., Wieland, J. & Stramska, M. 2002. Determination of spectral absorption coefficients of particles, dissolved material and phytoplankton for discrete water samples. Ocean Opt. Protoc. Satell. Ocean Color Sens. Valid. Revis. **3**: 231–257.

Molot, L., and P. Dillon. 1997. Photolytic regulation of dissolved organic carbon in northern lakes. Global Biogeochem. Cycle **11**: 357–365.

Molot, L. A., J. J. Hudson, P. J. Dillon, and S. A. Miller. 2005. Effect of pH on photo-oxidation of dissolved organic carbon by hydroxyl radicals in a coloured, softwater stream. Aquat. Sci. **67**: 189–195.

O'Reilly, C. M., and others. 2015. Rapid and highly variable warming of lake surface waters around the globe. Geophys. Res. Lett., **42**, 10773-10781.

Pace, M. L., I. Reche, J. J. Cole, A. Fernández-Barbero, I. P. Mazuecos, and Y. T. Prairie. 2012. pH change induces shifts in the size and light absorption of dissolved organic matter. Biogeochemistry **108**: 109–118.

Panneer Selvam, B., J.-F. Lapierre, A. R. A. Soares, D. Bastviken, J. Karlsson, and M. Berggren. 2019. Photo-reactivity of dissolved organic carbon in the freshwater continuum. Aquat. Sci. **81**: 57.

Raymond, P. A., and others. 2013. Global carbon dioxide emissions from inland waters. Nature, **503**, 355–359.

Seekell, D. A., J.-F. Lapierre, J. Ask, A.-K. Bergström, A. Deininger, P. Rodríguez, and J. Karlsson. 2015. The influence of dissolved organic carbon on primary production in northern lakes. Limnol. Oceanogr. **60**: 1276–1285.

Shen, F., Y. X. Zhou, and G. L. Hong. 2012. Absorption property of non-algal particles and contribution to Total light absorption in optically complex waters, a case study in Yangtze estuary and adjacent coast. Adv. Intell. Soft Comput. **141**: 61–66.

Suggett, D. J., O. Prášil, and M. A. Borowitzka. 2010. Chlorophyll a fluorescence in aquatic sciences: Methods and applications. Dordrecht, Netherlands: Springer.

Tassan, S., and G. M. Ferrari. 1995. An alternative approach to absorption measurements of aquatic particles retained on filters. Limnol. Oceanogr. **40**: 1358–1368.

Thrane, J.-E., D. O. Hessen, and T. Andersen. 2014. The absorption of light in lakes: Negative impact of dissolved organic carbon on primary productivity. Ecosystems **17**: 1040–1052.

Twardowski, M. S., E. Boss, J. M. Sullivan, and P. L. Donaghay. 2004. Modeling the spectral shape of absorption by chromophoric dissolved organic matter. Mar. Chem. **89**: 69–88.

Vachon, D., J.-F. Lapierre, and P. A. del Giorgio. 2016. Seasonality of photochemical dissolved organic carbon mineralization and its relative contribution to pelagic CO2 production in northern lakes. J. Geophys. Res. Biogeosci. **121**: 864–878.

Vähätalo, A. V., M. Salkinoja-Salonen, P. Taalas, and K. Salonen. 2000. Spectrum of the quantum yield for photochemical mineralization of dissolved organic carbon in a humic lake. Limnol. Oceanogr. **45**: 664–676.

Wanninkhof, R. 1992. Relationship between wind speed and gas exchange over the ocean. J. Geophys. Res. Oceans **97**: 7373–7382.

Weyhenmeyer, G., S. Kosten, M. Wallin, L. Tranvik, E. Jeppesen, and F. Roland. 2015. Significant fraction of CO_2 emissions from boreal lakes derived from hydrologic inorganic carbon inputs. Nat. Geosci. **8**: 933–936.

Williamson, C., R. Stemberger, D. Morris, and S. Paulsen. 1996. Ultraviolet radiation in North American lakes: Attenuation estimates from DOC measurements and implications for plankton communities. Limnol. Oceanogr. **41**: 1024–1034.

Williamson, C. E., E. P. Overholt, R. M. Pilla, T. H. Leach, J. A. Brentrup, L. B. Knoll, E. M. Mette, and R. E. Moeller. 2015. Ecological consequences of long-term browning in lakes. Sci. Rep. **5**: 18666.

Wozniak, B., and J. Dera. 2007. Light absorption in sea water. NY, USA: Springer.

Yang, H., T. Andersen, P. Dörsch, K. Tominaga, J.-E. Thrane, and D. O. Hessen. 2015. Greenhouse gas metabolism in Nordic boreal lakes. Biogeochemistry **126**: 211–225.

Acknowledgments

The study was funded by the Department of Biosciences, University Oslo, and two projects funded by the Research Council of Norway: COMSAT, grant 196336/S30 to T. Andersen and ECCO, grant 224779 to D.O. Hessen. We are most indebted to our colleagues in these projects.

Conflict of interest

None declared.

Submitted 26 November 2019
Revised 05 May 2020
Accepted 16 August 2020

Associate editor: David Antoine

Table S1. Measured and modelled lake parameters for the 70 lakes used in this study. The first 11 parameters from the left are measured while the last 4 are modelled or calculated as described under methods.

Abbreviations. a_{420}: absorption coefficient at 420 nm; $SUVA_{400}$: Specific ultraviolet absorbance at 400 nm; PP_A: Areal primary production

Lake	Area (km2)	Depth (m)	pH	O_2 (µmol/l)	CO_2 (µmol/l)	TOC (mg/l)	TN (mg/l)	TP (µg/l)	Fe (µg/l)	a_{420} (m^{-1})	$SUVA_{400}$ (L mgC^{-1} m^{-1})	PP_A (mg C m^{-2} d^{-1})	CO_2 flux (mg C m^{-2} d^{-1})	Lake pelagic CO_2 production (mg C m^{-2} d^{-1})	Areal DIC photoproduction (mg C m^{-2} d^{-1} ± se)
Gjersjøen	2.64	22.0	7.69	265.7	24.8	6.90	1.28	9.8	162.4	3.41	0.71	581.3	85.6	666.9	12.3 (± 1.2 %)
Øgderen	12.7	9.5	7.23	266.6	63.8	6.94	0.33	19.2	270.0	3.78	0.76	776.0	428.4	1204.4	13.3 (± 1.3 %)
Krøderen	43.9	14.0	6.70	305.5	73.4	4.40	0.25	3.55	97.0	3.09	1.00	181.2	380.2	561.5	12.9 (± 1.1 %)
Rødbyvatnet	1.2	10.0	7.54	258.7	40.5	6.65	0.97	9.35	287.3	3.27	0.70	322.4	214.3	536.7	11.6 (± 1.1 %)
Gjesåssjøen	4.0	3.5	7.07	258.7	64.2	9.61	0.39	15.1	1537.5	5.62	0.83	382.1	415.9	798.0	15.2 (± 1.3 %)
Osensjøen	43.6	70.0	6.56	297.8	52.2	7.69	0.28	3.05	172.7	6.77	1.24	48.2	245.1	293.3	12.0 (± 1.1 %)
Rokossjøen	3.8	9.0.	6.71	220.4	81.6	11.81	0.33	8.25	830.7	7.92	0.96	122.6	499.6	622.1	13.0 (± 1.0 %)
Sør Mesna	6.9	17.0	6.71	270.2	66.3	7.51	0.25	6.7	174.8	6.03	1.13	1.3	378.3	546.8	17.7 (± 1.0 %)
Vermundsjøen	3.3	12.0	6.29	219.9	132.9	11.95	0.36	9.25	1333.8	9.07	1.08	283.8	848.7	1132.5	12.5 (± 1.2 %)
Gjønvatnet	2.9	46.0	6.44	352.9	38.9	1.30	0.24	2	7.2	0.60	0.64	330.6	126.3	456.9	15.6 (± 1.1 %)
Kalandsvatnet	3.4	43.0	6.90	337.9	31.3	2.85	0.35	3.8	70.4	2.03	1.00	711.0	129.5	840.5	19.2 (± 1.3 %)
Myrkdalsvatnet	1.6	76.0	6.36	358.2	42.0	0.95	0.09	1	21.0	0.74	1.06	348.4	133.8	482.2	16.6 (± 0.9 %)
Engsetdalsvatnet	4.4	13.0	6.87	310.9	34.6	2.66	0.20	1.15	25.0	1.80	0.95	305.3	145.3	450.6	10.7 (± 1.3 %)
Rotevatnet	1.4	23.0	6.74	315.1	48.8	3.43	0.17	2.55	50.2	2.49	1.05	255.3	255.5	510.8	17.2 (± 1.2 %)
Vatnevatnet	2.0	25.0	6.66	362.2	42.1	1.31	0.17	4.7	24.8	1.34	1.33	539.6	148.9	688.5	17.1 (± 0.9 %)
Einavatnet	13.7	24.0	7.43	292.9	31.4	5.57	1.09	3	73.4	3.13	0.79	292.2	118.3	410.4	10.5 (± 1.4 %)
Ringsjøen	1.2	19.0	7.19	260.5	105.0	8.02	0.56	5.55	383.0	5.62	0.99	188.5	602.3	790.7	13.3 (± 1.4 %)
Sæbufjorden	1.5	18.4	7.08	298.8	39.2	3.66	0.36	3.1	82.0	2.21	0.84	278.3	158.7	437.0	12.4 (± 1.6 %)
Strondafjorden	13.4	34.0	7.22	329.9	29.9	2.83	0.35	2	41.3	1.89	0.91	525.8	93.3	619.0	15.6 (± 1.1 %)
Trevatna	4.8	17.0	6.47	239.8	106.6	9.68	0.35	4.3	422.8	6.54	0.96	136.8	649.8	786.6	13.9 (± 1.4 %)
Bogstadvannet	1.1	8.0	6.94	266.3	87.6	7.03	0.39	6.6	348.1	4.74	0.96	274.4	516.6	790.9	14.9 (± 1.4 %)
Rødenessjøen	16.0	20.0	7.04	279.3	43.0	9.11	0.98	12.2	279.1	6.72	1.04	285.2	240.2	525.4	10.3 (± 1.3 %)

Rømsjøen	13.7	30.0	6.83	291.7	27.9	6.69	0.40	1.2	65.0	3.96	0.85	277.9	106.8	384.7	14.5 (± 1.2 %)
Edlandsvatnet	2.1	8.0	6.94	316.5	41.4	2.63	0.79	3.85	52.7	1.47	0.79	418.0	245.8	663.8	13.5 (± 1.1 %)
Hetlandsvatn	2.1	33.0	7.19	327.0	23.7	2.37	1.01	2.35	25.0	1.20	0.68	993.0	66.0	1059.0	17.7 (± 1.2 %)
Vatsvatnet	2.2	18.0	7.53	355.6	17.3	4.09	0.48	18.9	168.8	2.39	0.83	673.0	2.4	675.3	15.7 (± 1.8 %)
Vostervatnet	2.7	60.0	6.97	304.0	34.7	3.12	0.61	3.6	31.7	1.66	0.72	427.4	201.2	628.7	13.9 (± 1.2 %)
Jølstravatnet	39.3	46.0	6.33	356.2	40.0	0.66	0.29	0.5	13.0	0.60	1.11	565.5	102.2	667.7	19.8 (± 1.0 %)
Grungevatnet	1.6	27.0	6.75	293.9	41.4	2.54	0.15	1.55	42.2	1.52	0.83	486.8	178.4	665.2	16.4 (± 1.1 %)
Vinjevatn	3.2	13.0	6.68	316.8	37.0	3.49	0.17	1.05	35.0	1.29	0.53	190.2	119.8	310.0	15.6 (± 1.1 %)
Åsrumvatnet	1.1	20.0	7.07	268.3	121.8	7.11	1.12	20.2	359.4	4.61	0.91	869.1	900.0	1769.1	14.8 (± 1.1 %)
Bergsvannet	3.0	12.1	8.88	317.1	0.8	7.07	0.37	17.85	288.8	4.05	0.82	450.2	-120.7	329.5	15.4 (± 1.1 %)
Goksjø	3.4	16.0	7.23	278.3	132.9	6.58	1.53	27.45	342.6	4.10	0.87	739.4	1009.0	1748.3	15.7 (± 1.1 %)
Hallevatnet	3.7	45.0	6.92	297.9	52.4	5.01	0.74	2	141.3	2.30	0.67	133.3	409.8	543.1	12.6 (± 1.2 %)
Dagarn	1.7	5.5	7.10	276.9	30.8	6.22	0.25	3	50.9	2.12	0.49	260.3	154.1	414.4	13.5 (± 1.2 %)
Langen	1.4	14.0	8.00	277.4	7.8	6.39	0.35	4.9	63.6	0.74	0.16	303.4	-77.3	226.1	11.7 (± 1.1 %)
Rotnessjøen	1.1	26.0	6.64	244.2	114.4	11.18	0.28	4.55	778.3	8.93	1.13	286.1	768.1	1054.2	15.9 (± 1.1 %)
Mylla	1.7	33.0	7.59	287.6	24.9	4.11	0.21	2.45	102.5	2.35	0.78	407.7	63.9	471.7	14.6 (± 1.2 %)
Femsjøen	10.7	18.5	7.02	274.1	42.0	8.42	0.82	7.45	228.6	5.25	0.90	423.7	261.7	685.4	12.7 (± 1.1 %)
Klämmingen	10.0	35.0	7.82	270.9	12.1	8.83	0.43	11.45	118.1	2.44	0.40	582.2	-30.3	551.9	21.4 (± 1.0 %)
Torrsjøn	1.8	25.0	7.21	290.1	34.3	7.62	0.37	2.35	57.2	4.93	0.91	409.9	167.3	577.2	17.4 (± 1.0 %)
Visten	32.0	10.0	7.20	278.2	14.2	4.86	0.25	6	27.1	1.43	0.42	269.0	-6.7	262.3	17.7 (± 1.1 %)
Stora Le	84.9	52.0	6.97	287.1	28.9	5.25	0.51	1.9	44.6	3.04	0.82	0.7	117.5	304.6	14.7 (± 1.2 %)
Näsrämmen	2.7	9.0	7.02	255.7	38.2	7.60	0.22	5.85	203.2	3.82	0.73	229.9	207.7	437.6	13.8 (± 1.2 %)
Rangsjön	2.7	9.0	7.01	258.8	46.9	7.37	0.22	3.2	169.9	5.99	1.14	122.1	234.0	356.1	11.4 (± 1.3 %)
Tisjön	27.1	17.0	6.88	287.8	31.5	6.53	0.21	4.55	168.1	3.82	0.83	118.3	131.3	249.6	16.0 (± 1.1 %)
Halsjøen	5.2	14.0	5.41	244.3	103.0	12.28	0.27	5.8	1249.5	11.05	1.25	NA	694.6	NA	10.8 (± 1.3 %)
Jangen	4.5	8.0	7.04	237.4	50.0	9.41	0.24	5.25	245.3	6.40	0.96	590.9	292.5	883.4	13.0 (± 1.1 %)
Sör-älgen	15.5	32.0	7.11	301.8	17.9	7.22	0.29	5.85	164.0	4.70	0.92	496.2	24.3	520.4	12.9 (± 1.3 %)
Möckeln	18.0	22.0	7.27	275.5	30.0	7.54	0.47	12.6	204.3	4.97	0.93	618.3	146.9	765.2	13.2 (± 1.3 %)
Ljusnaren	9.6	20.0	6.94	287.7	32.1	8.52	0.30	6.75	441.8	5.43	0.91	113.2	161.9	275.1	16.1 (± 1.0 %)
Halvarsnoren	16.9	26.0	7.23	305.3	27.5	7.44	0.29	5.4	252.1	4.84	0.92	148.8	124.2	273.0	15.1 (± 1.1 %)
Nätsjön	2.9	20.0	7.15	297.2	20.7	4.99	0.19	3.45	44.8	2.35	0.65	212.3	50.1	262.4	15.1 (± 1.2 %)

Saxen	7.0	14.0	7.33	309.9	19.0	5.61	0.25	4.85	63.2	2.99	0.76	259.3	37.1	296.4	14.6 (± 1.2 %)
Långbjörken	1.7	4.0	7.16	281.7	32.6	9.50	0.31	9.65	285.9	3.82	0.58	490.8	174.2	665.0	17.3 (± 1.1 %)
Skattungen	19.5	17.5	7.18	277.9	33.6	7.55	0.23	4.25	329.1	5.34	1.00	244.8	158.0	402.8	14.7 (± 1.1 %)
Bäsingen	12.7	10.5	7.25	264.2	47.2	6.11	0.26	8.5	370.7	4.28	0.99	351.1	321.2	672.4	11.7 (± 1.3 %)
Tisken	63.4	8.0	7.30	273.6	24.9	7.06	0.48	8	206.5	3.36	0.68	268.9	97.0	365.9	11.3 (± 1.3 %)
Stora Almsjön	2.0	17.0	6.98	251.9	75.8	12.55	0.27	5.55	537.5	11.47	1.27	2.3	465.2	561.7	10.0 (± 1.3 %)
Dragsjön	1.4	3.5	6.71	241.2	78.8	10.78	0.23	7.25	755.1	8.57	1.12	234.7	535.7	770.5	12.6 (± 1.3 %)
Milsjön	3.3	18.0	6.86	286.4	42.3	9.12	0.25	3.75	220.1	6.86	1.06	130.3	239.0	369.3	12.8 (± 1.6 %)
Stora Korslängen	3.5	15.0	6.70	289.2	37.4	5.94	0.24	2.05	78.3	3.64	0.87	1.1	192.9	313.1	12.4 (± 1.3 %)
Hinsen	11.9	9.0	7.18	275.4	12.4	5.49	0.22	3.55	41.0	1.84	0.49	195.7	-28.9	166.8	11.0 (± 1.3 %)
Storsjön	1.9	9.0	7.19	276.3	13.6	3.77	0.17	3.15	32.3	1.43	0.50	138.1	-19.4	118.7	13.8 (± 1.1 %)
Grycken	3.2	9.0	6.94	264.9	31.8	6.30	0.20	3.3	221.7	3.36	0.75	240.3	140.8	381.1	12.8 (± 1.1 %)
Holmsjön	50.7	8.0	7.33	268.0	34.1	5.86	0.20	3.1	156.2	4.01	0.96	178.0	171.8	349.8	14.0 (± 1.1 %)
Stornaggen	3.0	7.0	7.08	263.4	38.8	7.17	0.21	4.7	138.2	4.28	0.85	171.2	203.3	374.5	12.8 (± 1.2 %)
Forsjösjön	1.9	14.0	7.52	204.1	87.1	12.90	0.91	16.3	149.3	4.74	0.54	895.0	719.5	1614.5	11.1 (± 1.2 %)
Hurdalsjøen	32.8	20.0	6.87	296.6	28.3	3.71	0.41	1.6	51.9	1.84	0.71	296.9	96.0	392.9	12.2 (± 1.1 %)
Harestuvatnet	2.0	13.0	7.37	277.1	61.1	4.06	0.37	4.35	154.8	2.53	0.86	233.7	332.0	565.6	8.4 (± 1.5 %)

Supplementary information

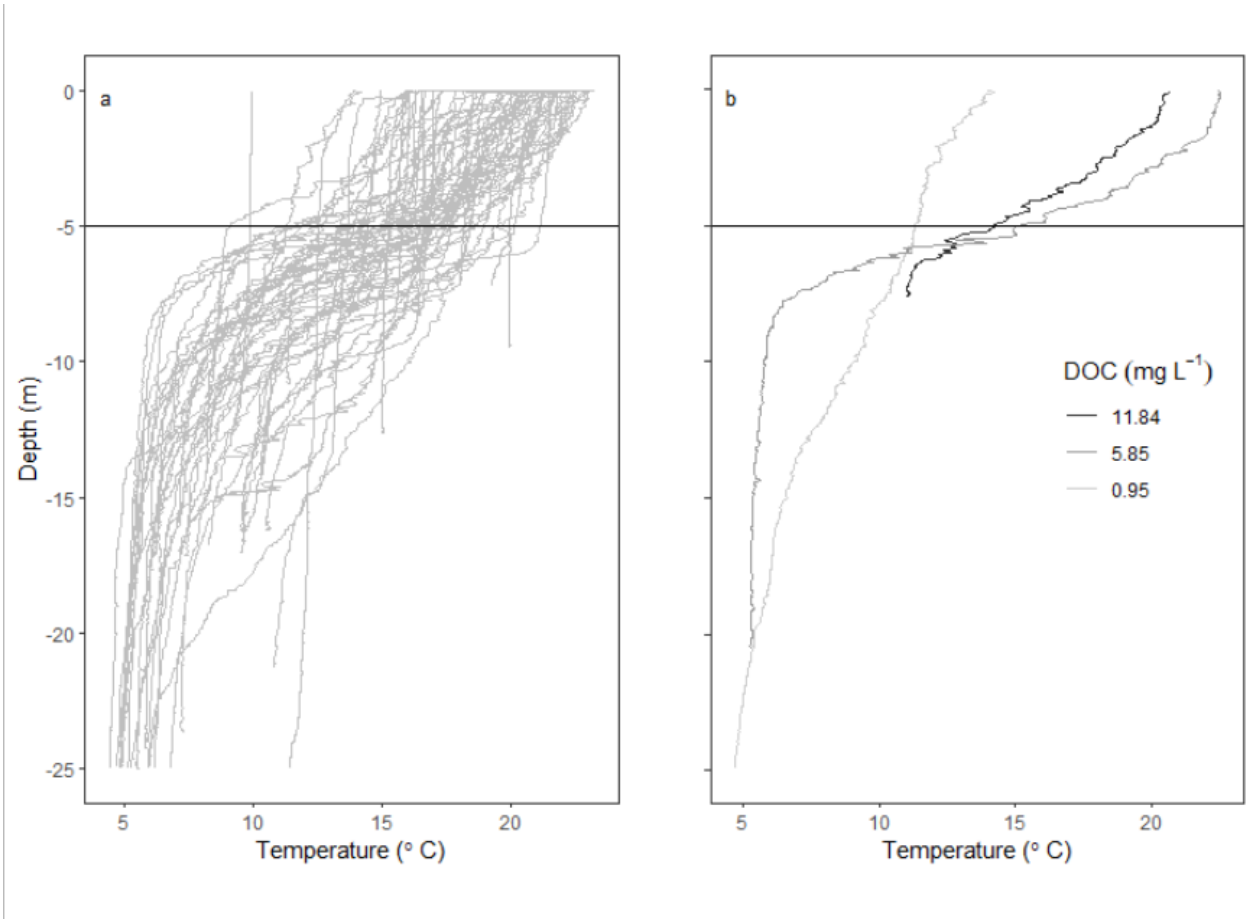

Figure S1. a) Temperature profiles in all the surveyed lakes. b) Temperature profiles of three example lakes with low (0.95 mg C l^{-1}), medium (5.85 mg C l^{-1}), and high (11.84 mg C l^{-1}) DOC concentrations. Samples were taken over the period of July-August during summer stratification, as a single snap-shot record during daytime.

Modelling apparent quantum yield

Table S2. Parameter estimates and model statistics for the linear regression equations between the apparent quantum yield (AQY) and specific UV absorption coefficient at 400 nm ($SUVA_{400}$) as well as the Napierian absorption coefficient at 420 nm (a_{420}) for AQY integrated across 300–500 nm and at eight wavelengths between 300 and 440 nm. Data from Koehler et al. (2016).

Predictor variable	Wavelength (nm)	Intercept $\cdot 10^{-6}$	Slope $\cdot 10^{-6}$	R^2
$SUVA_{400}$	300	282.0	933.4	0.55
	320	203.1	638.6	0.54
	340	149.8	437.7	0.51
	360	113.2	300.0	0.47
	380	87.4	205.3	0.42
	400	68.9	140.0	0.36
a_{420}	300	528.1	55.5	0.64
	320	387.8	36.7	0.59
	340	288.7	24.1	0.52
	360	217.4	15.8	0.43
	380	165.4	10.3	0.35
	400	126.8	6.6	0.26
$SUVA_{254}$	300	-206.7	163.3	0.56
	320	-139.5	112.7	0.56
	340	-88.8	77.7	0.53
	360	-52.0	53.4	0.49
	380	-26.1	36.6	0.44
	400	-8.5.	25.0	0.38

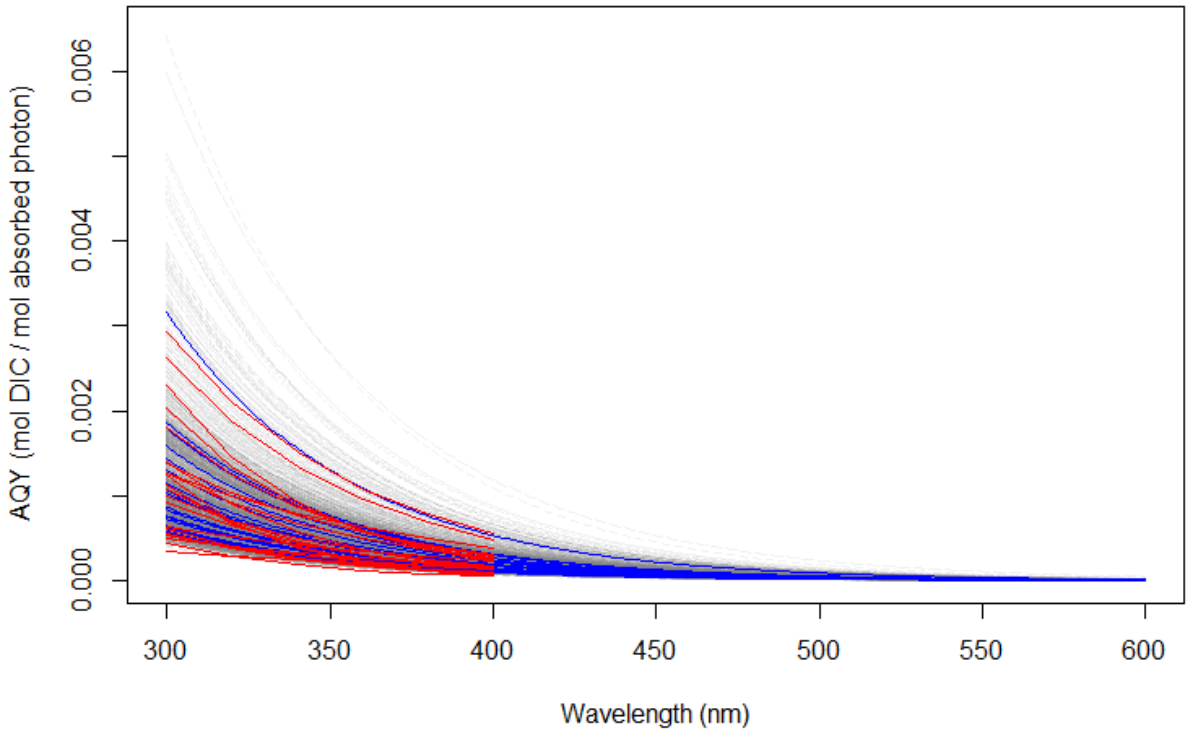

Figure S2. Monte Carlo samples of AQY spectra for the lakes used to derive the predictive regression relationships (Table S2; data from Koehler et al. (2016). The blue lines are the mean spectra and the red lines are the measured AQY's at six discrete wavelengths between 300 and 400 nm.

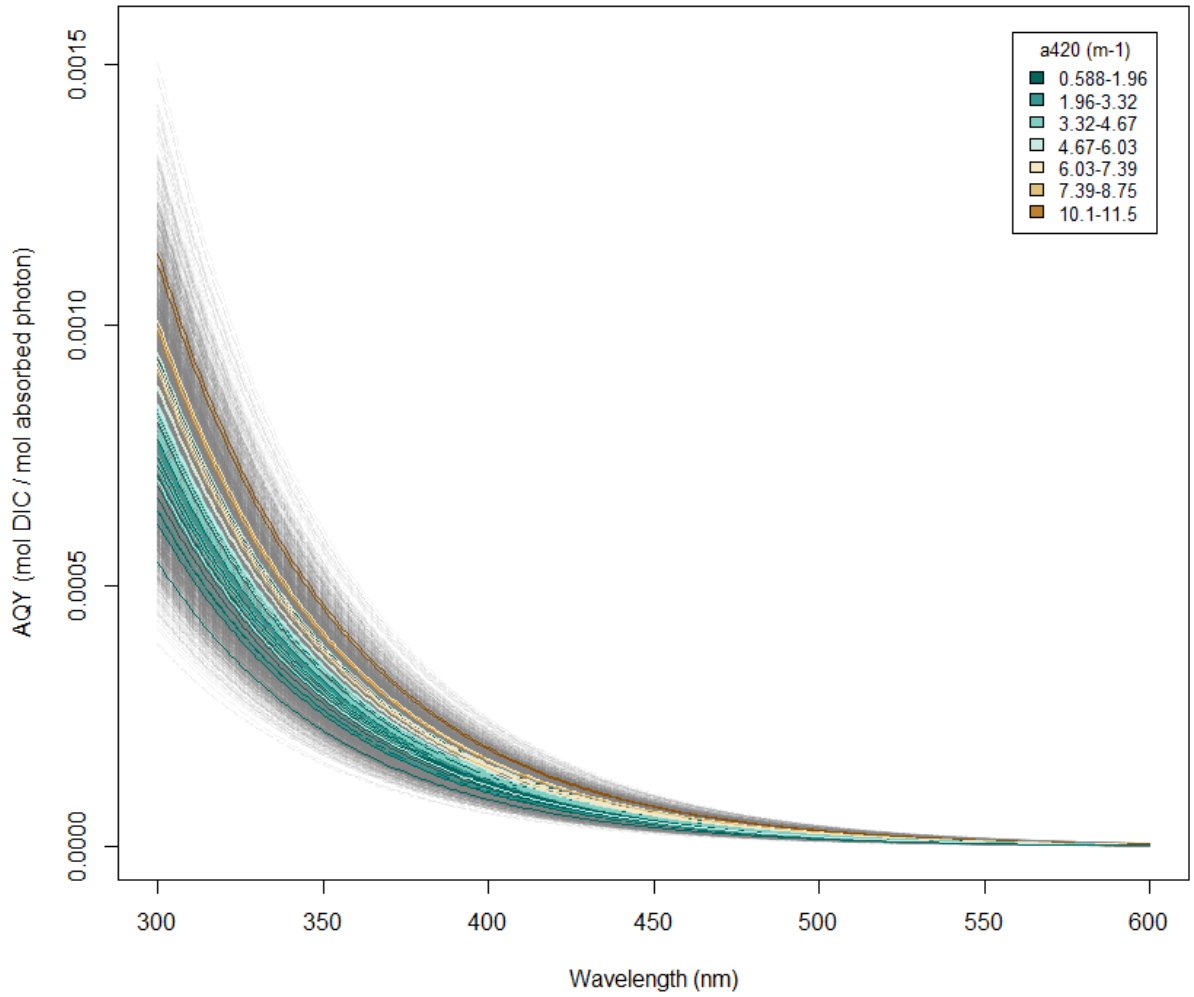

Figure S3. Monte Carlo samples of AQY spectra for all sampled lakes, the colored lines represent the mean spectra of each lake.

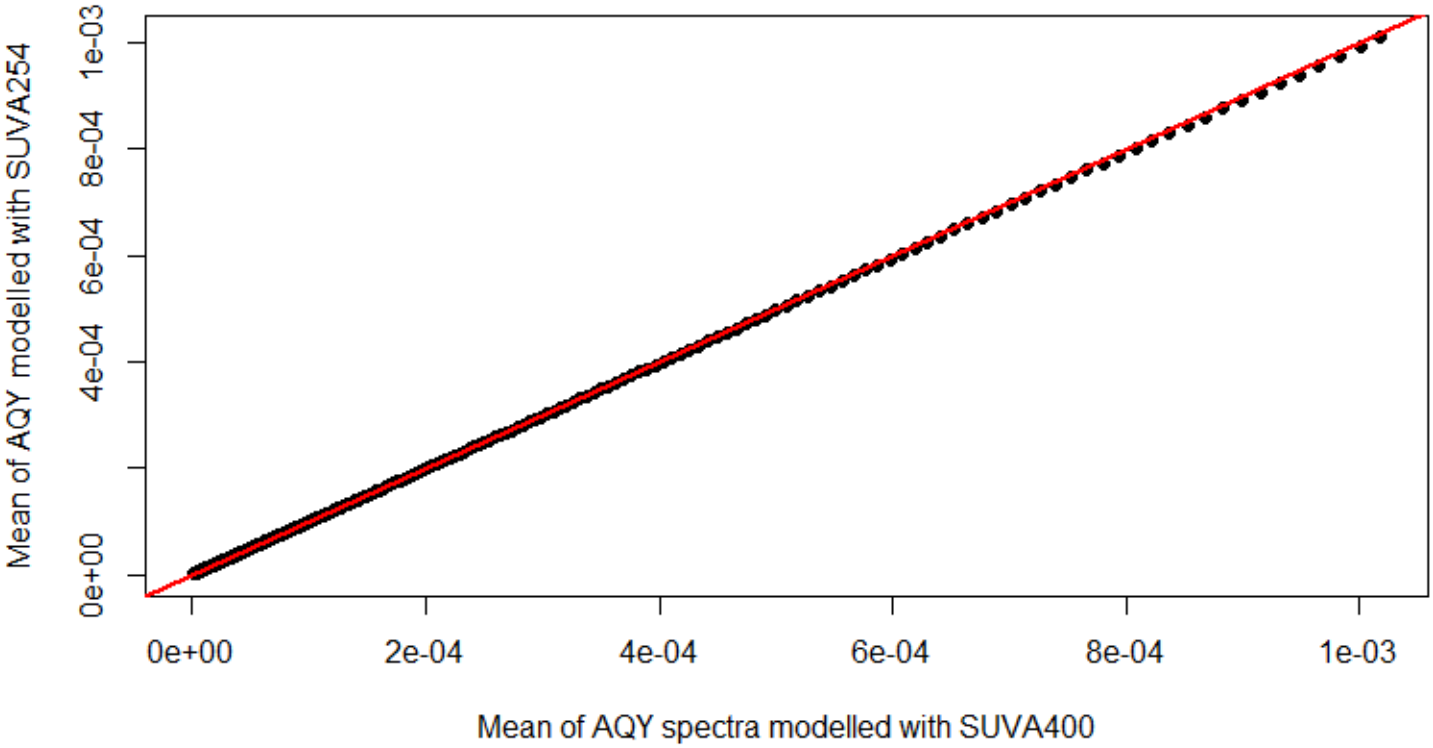

Figure S4. The mean values of each wavelength of the Monte Carlo samples in the AQY model using SUVA254 and a420 versus the AQY model using SUVA400 and a420 (equation 1 in main text). The red line is the 1:1 line.

Irradiance

The irradiance in the model (mWh m^{-2} d^{-1} nm^{-1}) was converted to photon flux (mole photons m^{-2} d^{-1} nm^{-2}). The irradiance energy was first converted from mWh to J by multiplication with 3.6 and was then divided by the amount of energy one mole photons contain, using Planck's law and Avogadro's constant:

$$photon\ flux = \frac{irradiance \cdot 3.6}{\frac{hc}{\lambda} \cdot N_A}$$

where h is Planck's constant (Js), c is speed of light (m/s), λ is wave length (nm) and N_A is Avogadro's number (mol^{-1}).

Error propagation

The uncertainty in DIC photoproduction was calculated through the uncertainties of the absorption and AQY spectra. First the uncertainties (δ) were calculated as the standard error of the mean of the Monte Carlo samples from the standard deviation (σ) and the sample size (n).

$$\delta x = \frac{\sigma x}{\sqrt{n}}$$

The uncertainty of the total absorption coefficient spectrum is the combination of the uncertainties of all absorption coefficient spectra.

$$\delta a_{total} = \sqrt{(\delta a_{NAP})^2 + (\delta a_{PP})^2 + (\delta a_{DOM})^2 + (\delta a_{water})^2}$$

The fraction of the DOM absorbance to total absorption (k_{DOM}) had thus the following uncertainty.

$$\frac{\delta k_{DOM}}{\langle k_{DOM} \rangle} = \sqrt{\left(\frac{\delta a_{DOM}}{\langle a_{DOM} \rangle}\right)^2 + \left(\frac{\delta a_{total}}{\langle a_{total} \rangle}\right)^2}$$

And finally the uncertainty of the DIC photoproduction becomes the combination of the uncertainties of k_{DOM} and AQY for DIC production (Φ_{DIC}).

$$\frac{\delta \psi_{DIC}}{\langle \psi_{DIC} \rangle} = \sqrt{\left(\frac{\delta k_{DOM}}{\langle k_{DOM} \rangle}\right)^2 + \left(\frac{\delta \Phi_{DIC}}{\langle \Phi_{DIC} \rangle}\right)^2}$$

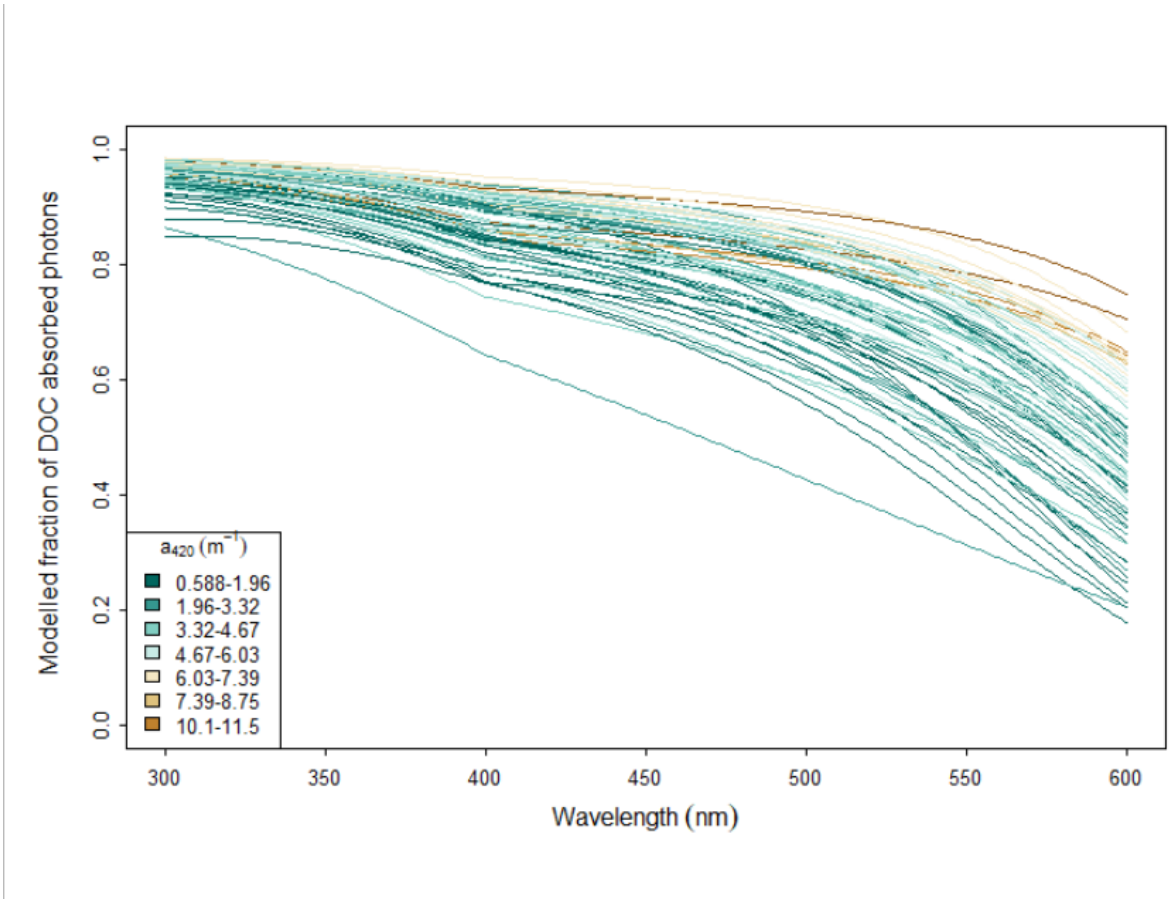

Figure S5. At short wavelengths the fraction of the photons absorbed by DOM is close to 1. The fraction decreases at longer wavelengths, where photochemical reactivity is lower.

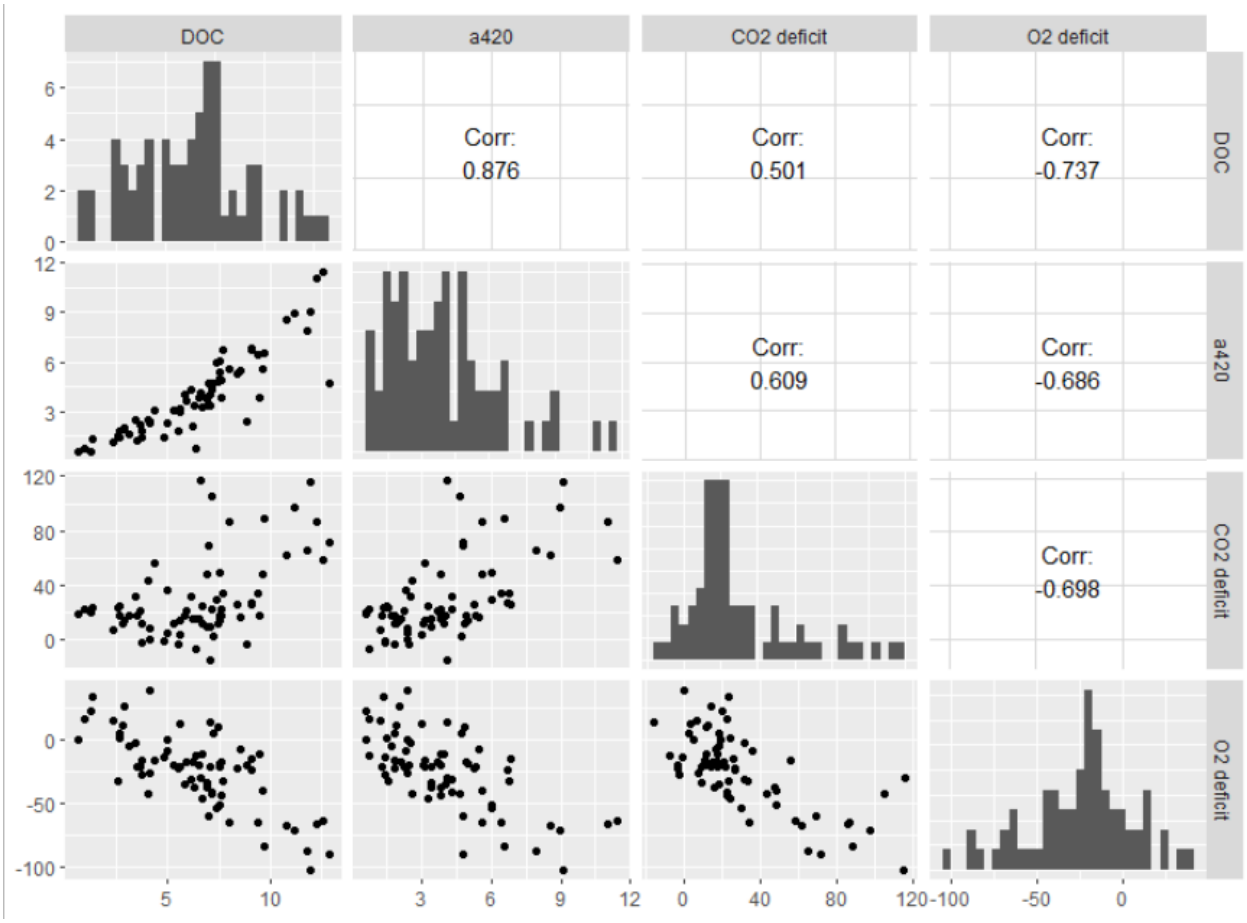

Figure S6. Correlation matrix plot with DOC (mg L^{-1}), a_{420} (m^{-1}), CO_2 saturation deficit (µmol L^{-1}) and O_2 saturation deficit (µmol L^{-1}) concentrations. There was a significant negative correlation between CO_2 and O_2 saturation deficits (r = -0.70) and saturation deficits of both CO_2 and O_2 were significantly correlated with TOC concentration (r = 0.50 and r = -0.74 respectively) and with a_{420} (r = 0.61 and r = -0.69 respectively). DOC concentrations were strongly related to a_{420} (r = 0.88).

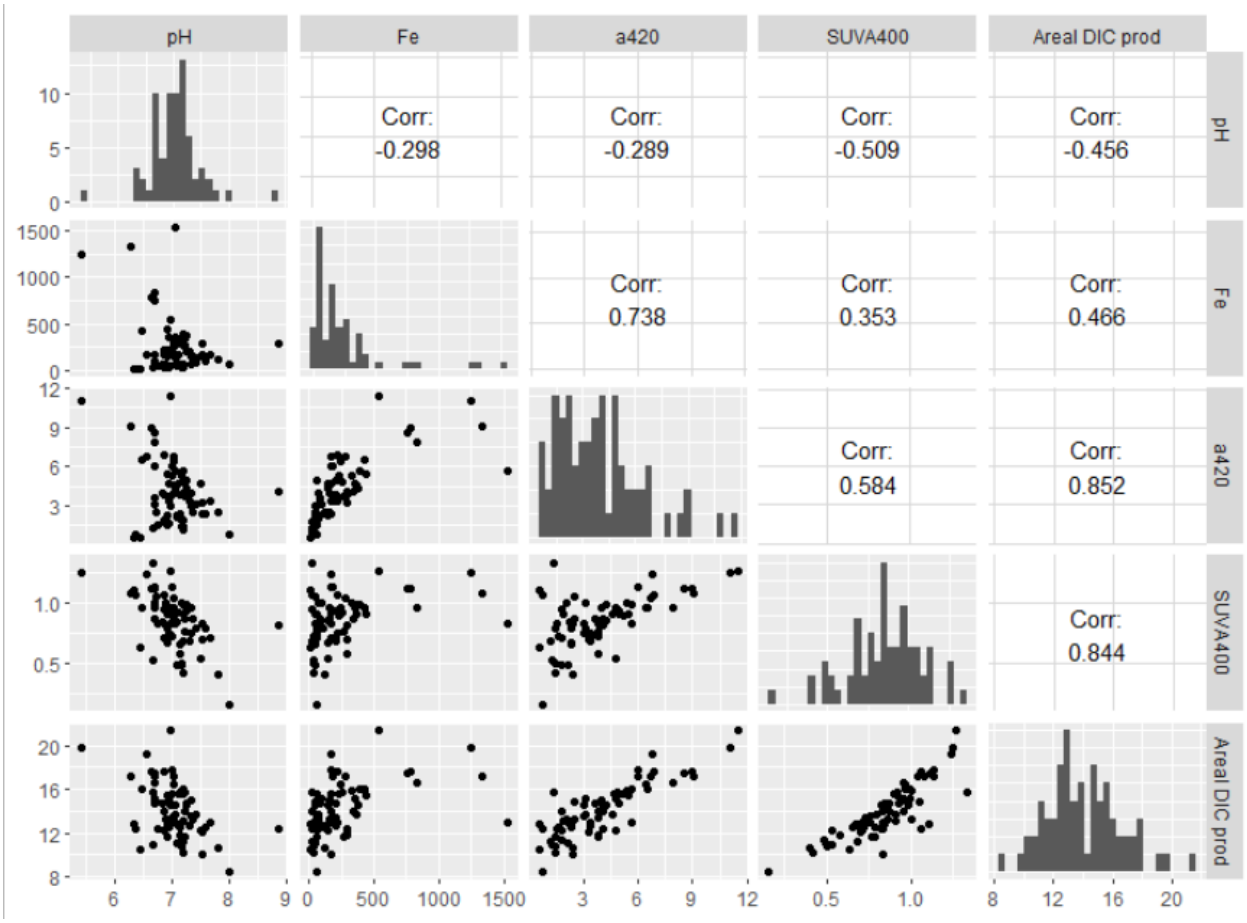

Figure S7. Correlation matrix plot with pH, Fe (µg/L), a_{420} (m^{-1}), $SUVA_{400}$ (L mg C^{-1} m^{-1}) and estimated areal DIC photoproduction (mg C m^{-2} d^{-1}). $SUVA_{400}$ and a_{420} were negatively related to pH and positively related to Fe. These relations propagated through to the areal DIC photoproduction rates.

Table S3. Regression coefficients for multiple linear regressions predicting areal DIC photoproduction rates from Fe concentrations (µg L^{-1}) and pH. Significance codes: *** p < 0.001, ** p < 0.01, * p < 0.05, $^{non\text{-}sig}$ p > 0.05.

Response	**Predictors**	**Estimates (se, significance levels)**	**R^2_{adj}**
Areal DIC photoproduction	pH + Fe	-1.9(0.6, **), 0.003(0.0009, ***)	0.31
	pH + Fe + pH:Fe	-2.1(0.8, ***), -0.0004(0.01, $^{non\text{-}sig}$), 0.0005 (0.001, $^{non\text{-}sig}$)	0.30

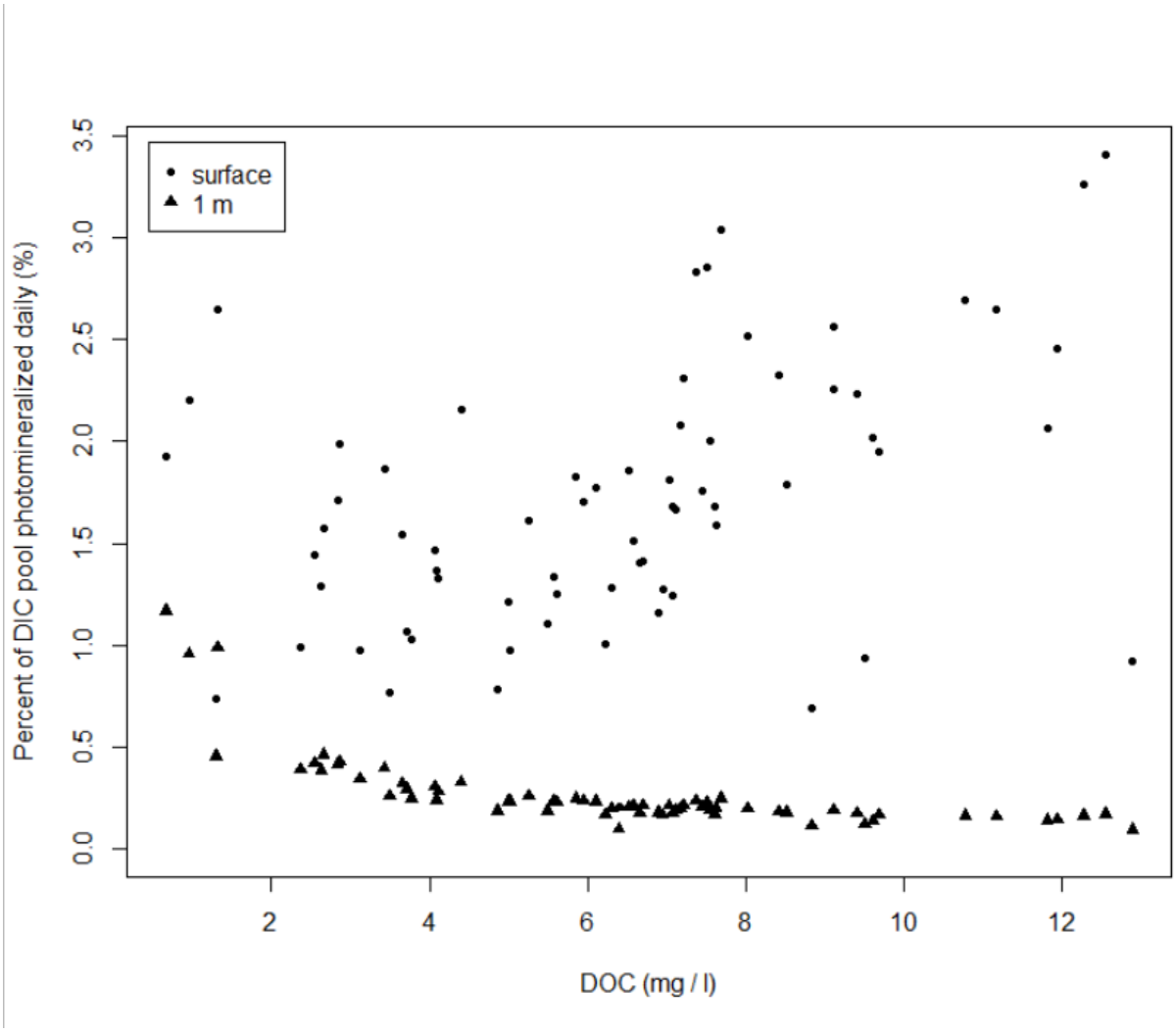

Figure S8. The percentage of the DOC pool that was photomineralized each day as a function of DOC concentration. At the surface, the photomineralized share of the DOC pool increased with DOC concentration, while the opposite was true further down in the water column.

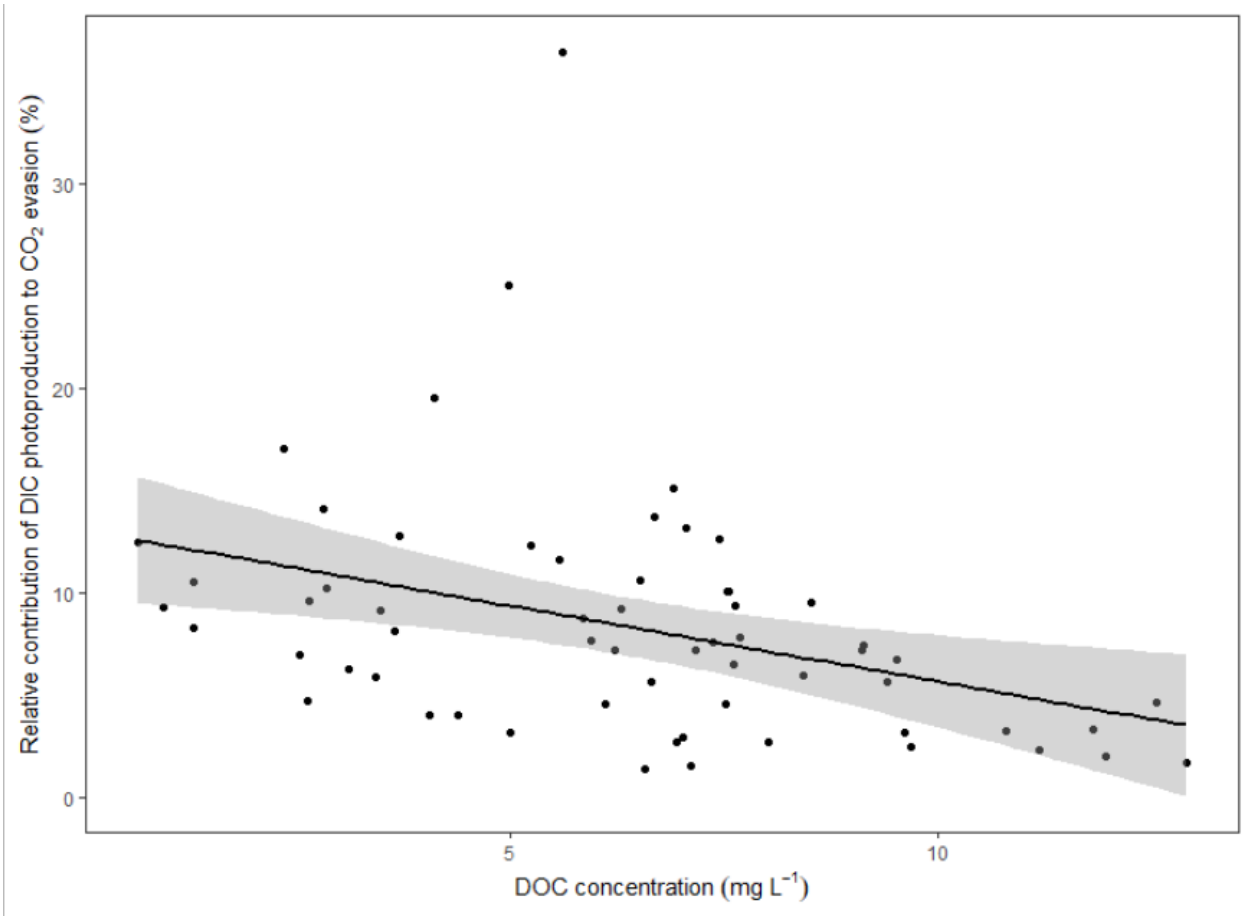

Figure S9. Relative contribution of photoproduced DIC to CO_2 evasion from the lakes as a function of DOC concentration. Assuming that all photochemically produced DIC was emitted as CO_2 from the supersaturated lakes, the relative contribution of estimated DIC photoproduction to total CO_2 efflux decreased with DOC concentration.

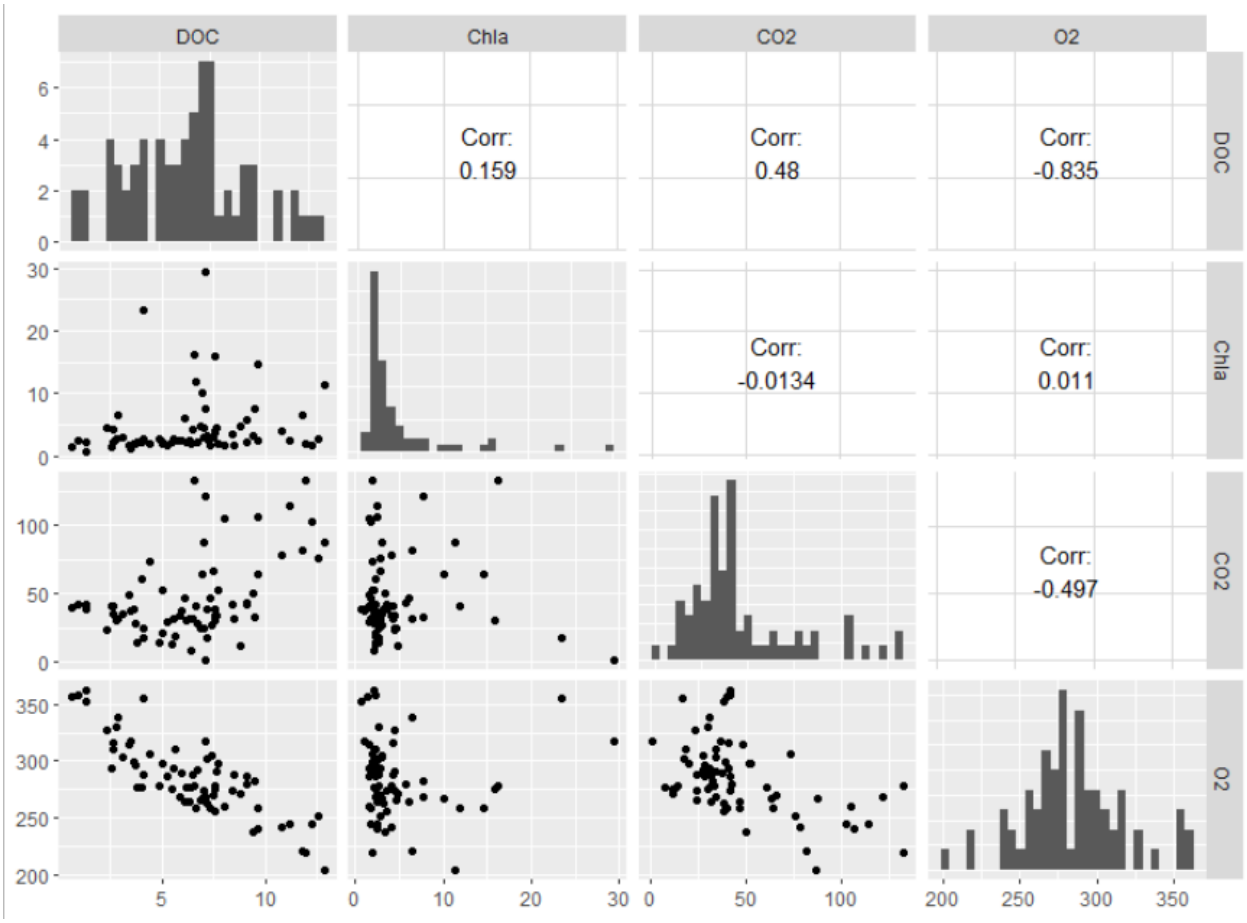

Figure S10. Correlation matrix plot with DOC (mg/L), chlorophyll *a* (µg L^{-1}), CO_2 (µmol L^{-1}) and O_2 (µmol L^{-1}) concentrations. There was a negative relation between CO_2 and O_2 concentrations (r = 0.50) and both CO_2 and O_2 were significantly but opposite correlated with TOC concentration (r = 0.48 and r = -0.83 respectively). There was no correlation between CO_2 or O_2 concentrations and chlorophyll *a*.

KOEHLER, B., BROMAN, E. & TRANVIK, L. J. 2016. Apparent quantum yield of photochemical dissolved organic carbon mineralization in lakes. *Limnology and Oceanography,* 61**,** 2207-2221.

Paper II

frontiers in Microbiology

ORIGINAL RESEARCH
published: 24 September 2020
doi: 10.3389/fmicb.2020.569879

Phosphorus Availability Promotes Bacterial DOC-Mineralization, but Not Cumulative CO_2-Production

*Lina Allesson[1], Tom Andersen[1], Peter Dörsch[2], Alexander Eiler[1], Jing Wei[1] and Dag O. Hessen[1]**

[1]Department of Biosciences and Centre for Biogeochemistry in the Anthropocene, University of Oslo, Oslo, Norway,
[2]Faculty of Environmental Sciences and Natural Resource Management, Norwegian University of Life Sciences, Ås, Norway

The current trend of increasing input of terrestrially derived dissolved organic carbon (DOC) to boreal freshwater systems is causing increased levels of carbon dioxide (CO_2) supersaturation and degassing. Phosphorus (P) is often the most limiting nutrient for bacterial growth and would thus be expected to increase overall mineralization rates and CO_2 production. However, high carbon (C) to P ratios of terrestrially derived DOC could also cause elevated cell-specific respiration of the excess C in heterotrophic bacteria. Using data from a survey of 75 Scandinavian lakes along an ecosystem gradient of DOC, we estimated *in situ* CO_2 production rates. These rates showed a unimodal response with DOC-specific CO_2 production negatively related to DOC:total phosphorus (TP) ratio, and a turning point at 5 mg C L^{-1}, indicating higher DOC turnover rates in productive than in unproductive lakes. To further assess the dependency of bacterial respiration (BR) on DOC and P, we monitored CO_2 production in incubations of water with a gradient of DOC crossed with two levels of inorganic P. Finally, we crossed DOC and P with a temperature gradient to test the temperature dependency of respiration rates [as oxygen (O_2) consumption]. While total CO_2 production seemed to be unaffected by P additions, respiration rates, and growth yields, as estimated by ribosomal gene copy numbers, suggest increased bacterial growth and decreased cell-specific respiration under non-limited P conditions. Respiration rates showed a sigmoid response to increasing DOC availability reaching a plateau at about 20 mg C L^{-1} of initial DOC concentrations. In addition to these P and DOC level effects, respiration rates responded in a non-monotonic fashion to temperature with an increase in respiration rates by a factor of 2.6 (±0.2) from 15 to 25°C and a decrease above 30°C. The combined results from the survey and experiments highlight DOC as the major determinant of CO_2 production in boreal lakes, with P and temperature as significant modulators of respiration kinetics.

Keywords: dissolved organic carbon-mineralization, lake metabolism, response curves, phosphorus addition, stoichiometry

OPEN ACCESS

Edited by:
Johanna Sjöstedt, Lund University, Sweden

Reviewed by:
Joanna Paczkowska, Centro Nacional Patagónico, Argentina
O. Roger Anderson, Lamont Doherty Earth Observatory (LDEO), United States

****Correspondence:***
Dag O. Hessen
d.o.hessen@mn.uio.no

Specialty section:
This article was submitted to Aquatic Microbiology, a section of the journal Frontiers in Microbiology

Received: *05 June 2020*
Accepted: *25 August 2020*
Published: *24 September 2020*

Citation:
Allesson L, Andersen T, Dörsch P, Eiler A, Wei J and Hessen DO (2020) Phosphorus Availability Promotes Bacterial DOC-Mineralization, but Not Cumulative CO_2-Production. Front. Microbiol. 11:569879. doi: 10.3389/fmicb.2020.569879

INTRODUCTION

Heterotrophic bacteria play a key role in aquatic ecosystems, consuming dissolved organic carbon (DOC) and converting it to carbon dioxide (CO_2) through bacterial respiration (BR; Del Giorgio et al., 1997; Duarte and Prairie, 2005) and biomass through bacterial production (BP; Del Giorgio and Cole, 1998; Jansson et al., 2006; Berggren et al., 2010).

Bacterial respiration is probably the largest biotic sink of organic carbon on Earth and DOC constitutes a major part of the bulk organic carbon globally (Del Giorgio and Williams, 2005; Drake et al., 2018). Together this makes aquatic bacteria an essential part of the global carbon (C) budget.

The DOC sustaining heterotrophic bacterial metabolism in aquatic ecosystems originates either from primary production within the system (autochthonous DOC) or from terrestrial primary production in the catchment (allochthonous DOC). There is a current trend of increasing transport of terrestrial DOC, to some extent also of total phosphorus (TP) and total nitrogen (TN), to inland waters, caused by factors such as recovery from acidification, climate change, and land use change (Monteith et al., 2007; Kellerman et al., 2015; Finstad et al., 2016; Kritzberg, 2017; Škerlep et al., 2020).

Allochthonous DOC contains a mixture of substances with a variety of molecular size, age, and bioavailability (Neff and Asner, 2001). A large portion of the allochthonous DOC is composed of humic substances, containing aromatic hydrocarbons of high C to nutrient ratios (Mcknight and Aiken, 1998). In humic-rich, low-productive lakes, typical for the boreal zone terrestrially derived substrates often make up the main source of energy and nutrients for bacterial maintenance and growth (Hessen et al., 1990; Karlsson et al., 2007). This decouples the microbial metabolism from the conventional "microbial loop" fueled by autochthonous DOC from algal exudates. In such DOC-rich systems, BR and BP are positively correlated to concentrations of allochthonous DOC rather than to primary production (Jones, 1992; Jansson et al., 2000; Karlsson et al., 2007).

The aromaticity of humic substances causes efficient light absorption and renders DOC prone to photochemical degradation. Allochthonous DOC thus attenuates light and reduces CO_2 uptake through primary production, while promoting CO_2 production through both biological and photochemical mineralization. Allochthonous DOC is a key driver of the in-lake partial pressure of CO_2 (Sobek et al., 2003; Humborg et al., 2010; Larsen et al., 2011). High DOC input renders most boreal lakes net heterotrophic, serving as major conduits of CO_2 to the atmosphere (Hessen et al., 1990; Cole et al., 1994; Sobek et al., 2003).

The share of the total assimilated organic carbon used for BP is given by the bacterial growth efficiency [BGE = BP/(BP + BR)], determining to what degree bacterial metabolism results in bacterial biomass production or in mineralization of organic carbon (Del Giorgio and Cole, 1998). In planktonic communities, BGE varies substantially and has been shown to depend on the quality rather than the quantity of the DOC (Vallino et al., 1996).

Bacterial carbon utilization efficiency is governed by the nutrient to C ratio of the substrate and availability of inorganic nutrients. Bacteria have a high nutrient demand, such that heterotrophic bacteria may dispose of "excess C" under high C-to-nutrient regimes (Hessen, 1992; Hessen and Anderson, 2008). While bacterial metabolism is often limited by C, N, and P, bacterial biomass accumulation is primarily limited by P and N as these are essential building blocks for RNAs and proteins (Sterner and Elser, 2002). However, there is a trade-off in microbial response to substrate C:P ratios. High C:P promotes increased cell-specific respiration, while elevated P support increased growth and biomass accumulation, thus increasing community respiration while the cell-specific respiration still may be reduced and BGE high (Hessen, 1992). Bacterial degradation of DOC at nutrient sufficiency will most likely result in C allocation to bacterial growth, while nutrient limitation may result in higher respiratory rates as the bacteria dispose of excess C (Smith and Prairie, 2004; Hessen and Anderson, 2008; Berggren et al., 2010).

The C to nutrient ratio thus has great implications for the BGE and the cycling and fate of C in a planktonic habitat. Inorganic P is the most frequently reported limiting nutrient for BP (Vadstein, 2000) and it is mainly the P availability that regulates the use of DOC for growth. Experiments of adding DOC and inorganic P to oligotrophic lake waters have shown that low BGE's accompanying increased C:P ratios do not necessarily mean that BP is decreasing but rather that BR is increasing (Jansson et al., 2006).

Together with increased run-off and biomass production, air and water temperatures are increasing with the ongoing climate warming (Schneider and Hook, 2010; O'Reilly et al., 2015). Temperature has a fundamental role in regulating the activity and growth of microorganisms (Farrell and Rose, 1967; Madigan et al., 1997). While it can be broadly stated that metabolism increases with temperature up to a certain level, the rate of the exponential increase differs between organisms, reactions, and temperature ranges. Although the rates of both BP and BR increase with temperature, several studies have reported that the temperature dependency of BR is stronger than that of BP and as a consequence, BGE has often been shown to decrease at increasing temperatures (Rivkin and Legendre, 2001; Apple et al., 2006; Berggren et al., 2010; Kritzberg et al., 2010).

Furthermore, the temperature dependency of bacterioplankton metabolic rates interacts with the substrate quantity and quality. Metabolic rates have been shown to be less temperature dependent for heterotrophic bacteria growing on labile autochthonous DOC than when growing on complex and recalcitrant allochthonous DOC (Ylla et al., 2012; Jane and Rose, 2018). In aquatic systems with a DOC pool heavily influenced by terrestrial inputs, increased temperatures are expected to further enhance BR, expanding the role of heterotrophic bacteria as CO_2 conduits to the atmosphere.

Microbial mineralization of DOC thus depends on several interacting factors. Although we can expect that increased loadings of terrestrially derived DOC and nutrients and enhanced temperatures increase bacterial growth and

metabolism, more studies are needed to elucidate how the different environmental factors interact.

In this study, we used chemical and physical data from 75 Scandinavian lakes to estimate in-lake CO_2 production. The lakes spanned close to orthogonal ecosystem gradients in DOC and TP, allowing us to assess the interactive effects of these two parameters on CO_2 production. To test for dynamic responses of bacterioplankton respiration to allochthonous DOC concentrations, nutrient availability, and temperature, we additionally performed experimental incubations. During 1-week incubations, we monitored respiration in two experimental set-ups, one addressing CO_2 production and the other O_2 consumption. A gradient of DOC concentrations was achieved by adding natural organic matter (NOM; isolates from a Norwegian humic lake obtained through reverse osmosis) to clear lake water.

MATERIALS AND METHODS

Field Sites

During July and August of 2011, a set of 75 large lakes spread out over a geographical gradient from western Norway to eastern Sweden was sampled (**Figure 1**). The lakes were chosen to represent wide and close to orthogonal gradients in dissolved organic matter (DOM) and TP. To avoid strong temperature gradients the lakes were chosen within a narrow latitudinal and altitudinal range. All lakes met the following criteria: latitude 57–64°N, altitude <600 m, surface area > 1 km^2, pH > 5, TP < 30 µg L^{-1}, and DOC <30 mg L^{-1}. The lakes were sampled by plane in a synoptic survey,

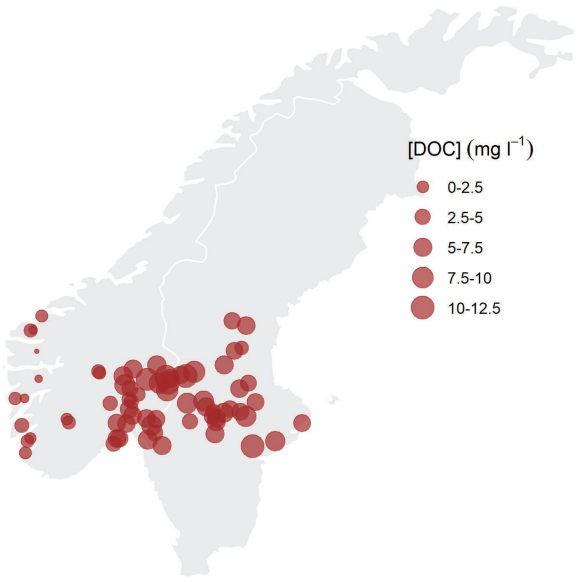

FIGURE 1 | Map of the survey lakes, the size of the circles indicates the concentrations of dissolved organic carbon (DOC; mg L^{-1}).

and composite samples of a total of 15 L were taken from 0 to 5 m in the central part of each lake during daytime, using an integrating water sampler (Hydro-BIOS, Germany). Vertical temperature profiles and vertical profiles of scalar irradiance (see SI for more detail) were measured using XRX-620 10-channel CTD (RBR Ltd., Canada). Vertical temperature profiles indicated that the thermocline was deeper than 5 m in all lakes. The integrated 0–5 m samples could thus be considered representative of the mixed layers of the lakes.

Laboratory Analyses of Lake Samples

Concentrations of TP, total organic carbon (TOC), and TN were measured in two accredited laboratories, at the Norwegian Institute for Water Research (NIVA) and at the University of Oslo (UiO). Total inorganic carbon (TIC) was measured at UiO (see SI and Thrane et al., 2014 for details).

Dissolved CO_2 and O_2 were measured as headspace concentrations in acid (0.2% HgCl) fixed samples by gas chromatography (GC) analysis (see SI and Yang et al., 2015 for details). Chlorophyll *a* (chl *a*) concentration was measured in two different ways, both by high performance liquid chromatography (HPLC; Schagerl and Donabuam, 2003) and by fluorescence spectrometry after extraction in 96% ethanol. The averages of the two methods (which generally matched well) were used in further analyses. Chromophoric dissolved organic matter (CDOM) optical density [ODCDOM(λ)] of 20 ml filtered lake water (Acrodisc 0.2 µm polyethersulfone membrane syringe filter, Pall Life Sciences) was measured from 400 to 750 nm in steps of 1 nm. According to Mitchell et al. (2002), from which we calculated the absorption coefficient spectra of CDOM [aCDOM(λ); m^{-1}].

Area-specific primary production (PP_A; mg C m^{-2} d^{-1}) was calculated using a bio-optical model based on lake-specific phytoplankton absorption coefficients, daily *in situ* irradiance, and the light dependent quantum yield of photosystem II measured by a Pulse Amplitude Modulated (PAM) fluorometer (AquaPen-C 100, PSI Czech Republic; for details see SI and Thrane et al., 2014). As PP_A here is a measure of CO_2 consumption, we can note it as the CO_2 flux from water to primary producers F_{PP}.

Water-air flux of CO_2 (F_{net}) represents the net degassing of CO_2 from the surface and was calculated from surface CO_2 concentrations of each lake using Fick's law of diffusion.

$$F_{net} = k_{CO2}\Delta_{CO2} \quad (1)$$

where the CO_2 gas exchange (kCO_2) coefficient was obtained according to Jähne et al. (1987) and Cole and Caraco (1998; for details see SI and Yang et al., 2015).

Total CO_2 Production

From the dataset, it was not possible to distinguish between lateral input of CO_2 (F_{lat}; surface and ground water inflow) and in-lake production of CO_2 (F_{min}; microbial and photochemical mineralization of DOC). The sum of in-lake DOC mineralization and lateral input was therefore used as an estimate of total CO_2 production ($F_{tot} = F_{lat} + F_{min}$). Assuming a steady state

of the CO_2 saturation deficit, the mass balance due to production, lateral input, consumption, and evasion can be written as:

$$F_{net} = F_{tot} - F_{PP} \quad (2)$$

And therefore

$$F_{tot} = F_{\min} + F_{lat} = F_{net} + F_{PP} \quad (3)$$

Experimental Design

To investigate the effects of DOC and P additions on bacterioplankton respiration in more detail, we incubated water samples with a gradient in dissolved NOM concentrations crossing it with two levels of inorganic P. Samples were incubated in the dark using two different experimental set-ups and methods. During the incubations, we monitored bacterioplankton respiration through measurements of either CO_2 production or O_2 consumption, depending on the set-up. Samples for microbial biomass were taken upon termination of the experiments with the aim of assessing biomass from a flow-cytometer equipped with a plate reader set-up. However, despite trying with different stains and protocols, the samples were obscured by background scatter from the added DOC, and hence did not provide reliable counts. Ideally, the dynamic responses in CO_2 and O_2 should have been verified not only with bacterial counts but also assessment of community response by genetic screening and transcriptomics. This does, however, require a different set-up with larger volumes and a more frequent sampling regime that does not compromise the semi-continuous gas analysis. With the current set-up, we prioritized the gas analysis as the ultimate response output but assessed final microbial biomass from quantitative PCR (qPCR) on filtered samples when terminating the experiment.

SOURCE OF DOM

The DOM gradient was obtained using a NOM isolates from the DOC-rich boreal bog/lake Hellerudmyra close to Oslo, produced within the NOM-typing and the NOMiNiC projects (see Gjessing et al., 1999 and Vogt et al., 2001 for isolation protocol and characterization). This is a powder material up-concentrated from freshwater through reverse osmosis and isolated by freeze-drying of the concentrate. While also containing non-humic material, the major fraction of the NOM isolate consists of humic substances. The carbon fraction of the isolate is 33.7%. The NOM powder was mixed in deionized water to a stock solution of DOM with a DOC concentration of 1,000 mg C L^{-1} and filter sterilized through a 0.2 µm pore size Supor membrane filter (Gelman, CO, USA). While the isolation and up-concentration of the material enriches various elements, the DOM retains its "natural" properties (Gjessing et al., 1999; Vogt et al., 2001), and should be superior to artificial sources of DOC.

Preparation of the Media

The DOM stock solution was diluted to the desired DOC concentrations in sterile filtered (0.2 µm pore size Supor membrane filter; Gelman, CO, United States) drinking water from the tap. This water comes from the oligotrophic and pristine lake Maridalsvannet in the municipality of Oslo, Norway. The water is treated following protocols for drinking water. The processing includes alkalization/carbonazation by marble and CO_2, coagulation and particle separation in Actiflo followed by two media filter, and UV irradiation for disinfection. Besides disinfecting, the UV treatment also lowers the CDOM content in the water. The treatments do not eliminate essential trace metals and macronutrients in the water, giving background concentrations of DOC and total N of 2 mg L^{-1} and 0.01 mg L^{-1}, respectively, while the background total P was below detection limits.

The samples were inoculated with 1% of the total sample volume of fresh water from a stream draining Hellerudmyra from where the DOM was isolated. The inoculum was filtered (2 µm) to remove large particles and protists.

Experimental Set-Up 1: CO_2 Production

We used 14 levels of DOC additions between 0 and 50 mg L^{-1} (0 mg L^{-1}, 2.5 mg L^{-1}, 5 mg L^{-1}, 7.5 mg L^{-1}, 10 mg L^{-1}, 12.5 mg L^{-1}, 15 mg L^{-1}, 17.5 mg L^{-1}, 20 mg L^{-1}, 22.5 mg L^{-1}, 25 mg L^{-1}, 34 mg L^{-1}, 41 mg L^{-1}, and 50 mg L^{-1}). The DOC gradient was crossed with two levels of PO_4-P additions (0 and 2 µmol L^{-1}). To make sure that N was not limiting, 30 µmol L^{-1} each of NO_3-N and NH_4-N, resulting in a total of 60 µmol L^{-1} N, were added to all samples. In samples with P additions, the C:N:P ratio thus ranged between 82:30:1 and 2160:30:1.

The incubations were carried out in the dark in a temperature-controlled water bath at 20°C. Samples of 50 ml were transferred into 122 ml, acid washed glass vials equipped with acid washed magnetic stirrers. The vials were crimp sealed with butyl rubber septa. Before incubation, the vials were washed with HeO_2 (80/20%) by 6 cycles of evacuation and filling using a manifold, while stirring the samples at 400 rpm to remove CO_2 and nitrogen gas (N_2). The samples were incubated constantly stirred (400 rpm) for 10 days at 20°C, while CO_2 production and O_2 uptake were measured automatically by GC every 6 h using the robotized set-up described by Molstad et al. (2016) with some modifications. Since these vials contained 50 ml water and 70 ml air, the O_2 uptake was small relative to the large amount of O_2 in the headspace and we could not measure uptake rates with sufficient precision.

Experimental Set-Up 1: Ribosomal RNA Gene Copy Numbers

To approximate bacterial growth yields we measured bacterial 16S ribosomal RNA (rRNA) gene copy numbers using a qPCR protocol (Savio et al., 2015). In short, 40 ml of water from each incubation were filtered through 0.2 µm Supor PES membrane filters (Pall Corporation, CA, United States) at the end of the experiment. Filters were stored at −80°C until DNA extraction was performed using the Dneasy PowerSoil kit as recommended by the manufacturer (Qiagen, Germany). Total DNA concentration was assessed

using a Qubit ds DNA Broad-Range Assay (London, United Kingdom), and 16S rRNA genes were quantified using a bacteria-specific qPCR. qPCR reactions contained 2.5 µl DNA extract as the template and 0.2 µM each of the primers 8F and 338 (Frank et al., 2007; Fierer et al., 2008) targeting the V1-V2 region of most bacterial 16S rRNA genes and iQ SYBR Green Supermix (Bio-Rad Laboratories, Hercules, USA). Samples were run in triplicates together with a dilution series of the ZymoBIOMICS Gut Microbiome Standard (Zymo Research, Irvine, USA) to obtain 16S rRNA gene copy numbers in each incubation.

Experimental Set-Up 2: Dissolved Oxygen Consumption

The second experimental set-up was designed with fewer DOC levels (0 mg L^{-1}, 25 mg L^{-1}, and 50 mg L^{-1}) plus an additional crossing with four temperatures (10, 15, 25, and 30°C). All treatments were run in quadruplicates.

The incubations were carried out in the dark, placed in a water bath in a climate chamber to assure stable temperature. Dissolved oxygen concentrations were measured over 7 days of incubation with a SensorDish Reader (SDR; resolution: ±0.4% O_2 at 20.9% O_2, PreSens GmbH, Regensburg, Germany) using non-invasive fluorescence sensor spots placed in the bottoms of 5 ml vials, which were measured by optodes. The vials were washed with 70% ethanol and baked at 80°C for 10 h before filling them with sample and leaving them in the incubator for temperature equilibration for 2 h. After the equilibration, we inoculated the samples and filled the vials to the top, leaving no headspace. The vials were then closed and additionally sealed with parafilm to avoid gas diffusion. Vials with deionized water were used as controls to check for O_2 leakage. Dissolved oxygen concentrations were recorded automatically every 15 s. O_2 consumption rates were may represent CO_2 production rates, assuming a respiratory quotient (RQ: mole CO_2 produced/mole O_2 consumed) equal to 1. Although humic-rich substances are completely oxidized at an RQ of 0.9 (Dilly, 2001), anabolic processes contributes to higher RQs than catabolic respiration alone (Dilly, 2003; Berggren et al., 2012). We therefore believe that an RQ of 1 is an appropriate assumption. However, in the analysis, we use the rates of O_2 consumption that indirectly represent CO_2 production rates (see below), and thus the RQ value does not affect the results. In some treatments, the O_2 was depleted toward anoxia, but this should not affect our analysis since the initial slopes of the uptake curves, when the incubations still were oxic, to estimate bacterial growth.

Temperature sensitivity of the respiration rates were analyzed using the Q_{10} coefficient as the relative change in rate when increasing the temperature by 10°C.

$$Q_{10} = \left(\frac{R_2}{R_1}\right)^{\left(\frac{10}{T_2 - T_1}\right)} \quad (4)$$

where R is the rate, here the respiration rate (µmol CO_2 L^{-1} h^{-1}) and T is the temperature in centigrade.

Modeling the Respiration Curves

Respiration curves and growth rates were modeled using the packages mgcv (Wood, 2011) and gratia (Simpson, 2018) in R (R Core Team, 2020). A generalized additive model (gam) with simple factor smoothers on time and grouped by experimental unit was fitted to all the measured time-series data. The fitted curves were then differentiated, using the derivatives function from the gratia package (Simpson, 2018) to estimate the time course of the net rate of change in each experimental unit. From the fitted derivatives we calculated maximum O_2 consumption or CO_2 production rates for each experimental unit. The time until the maximum rate was reached was used as a measure of the lag phase.

Statistics

All data analysis was performed using the open-source software R version 4.0.2 (R Core Team, 2020). Lake variables were checked for normality and log-transformed where needed. Correlations are reported using Pearson's correlation coefficients and all error estimates are given in standard errors. For the statistical modeling, we used the mgcv package (Wood, 2011) fitting gam models for prediction of the dependent variables. To test the dependency of total CO_2 production (F_{tot}; mg C m^{-2} d^{-1}), we used a gam model with smoothers on each of the explanatory variables DOC (mg L^{-1}), TP (µg L^{-1}), TN (mg L^{-1}), TIC (mg L^{-1}), $SUVA_{400}$ (L mg-C^{-1} m^{-1}), and temperature (°C). Predictive variable selection was done by applying additional shrinkage on the null space of the penalty with the select = TRUE argument in the mgcv::gam function, as recommended by Marra and Wood (2011). The resulting model has all smoothers that are not necessary for the fit as close to zero as possible.

For the analysis of the experimental results, individual gam models were fitted to samples with and without P additions (and the three levels of DOC concentrations in the second experiment), respectively. In the case of experimental set-up 1, gams were fitted with DOC concentration as the explanatory variable, while in experimental set-up 2 temperature was used. We also performed an analysis of covariance to test for treatment effects of P (experimental set-up 1) or P and temperature (experimental set-up 2).

RESULTS

Lake Survey

Concentrations of both DOC and TP varied largely among lakes, with DOC concentrations ranging between 0.25 and 12.9 mg L^{-1} and TP between 0.5 and 27.5 µg L^{-1}. Although lakes had been selected for orthogonality between DOC and TP, there was a correlation between the two variables ($p < 0.001$, $r = 0.61$, log-log). Still a considerable scatter indicates reasonable orthogonality. Other important cross-correlations that need to be considered in data interpretation are positive relationships of TN with both TP and DOC concentrations (**Supplementary Figure S1**).

Dissolved CO_2 concentrations spanned two orders of magnitude (0.82–133 µmol L^{-1}) with the majority of the lakes

being strongly supersaturated with CO_2 as indicated by an average CO_2 of more than twice that at atmospheric equilibrium. This supersaturation conveys evasion of CO_2 to the atmosphere from most lakes and net-heterotrophy of the lake systems during the sampling campaign. As expected, the level of CO_2 saturation was positively correlated with DOC concentration ($p < 0.001$; $r = 0.52$) and negatively correlated with O_2 saturation ($p < 0.001$; $r = -0.69$; **Supplementary Figure S2**) and thus reflects the role of DOC as a driver of heterotrophy. There was no correlation between TIC and CO_2 saturation deficit, suggesting that in-lake processes were the main cause of CO_2 supersaturation.

Areal primary production (PP_A) was not significantly correlated to CO_2 concentrations, providing no support for primary production being boosted by CO_2 in CO_2 rich lakes. Still, PP_A was weakly but negatively related to DOC concentrations ($p = 0.05$; $r = -0.23$, log-log; Thrane et al., 2014), and somewhat (but non-significant) lower in high CO_2 lakes than in lakes with low CO_2 concentrations. In addition, PP_A was negatively related to the DOC: TP ratio ($p < 0.001$; $r = -0.60$; **Supplementary Figure S3A**). Total CO_2 (F_{tot}) production here represents both CO_2 produced in lakes and CO_2 coming into lakes from the surroundings *via* ground water and run-off and was estimated as the sum of net CO_2 evasion and a real primary production ($F_{tot} = F_{min} + F_{lat} = F_{net} + F_{PP}$). The gam model explained 77% of the total deviance in total CO_2 production with strong effects of DOC, TP, and TN. TIC and temperature had weak effects and SUVA had no effect on total CO_2 production (**Figure 2**). Relating total CO_2 production to DOC concentration revealed a unimodal response to increased DOC concentrations with a minimum value at around 5 mg L^{-1} (**Figure 2**). Carbon concentration-specific CO_2 production [F_{tot}: (mg C m^{-2} d^{-1})/ DOC(mg C m^{-2})] was positively related to PP_A ($p < 0.001$, $r = 0.60$, log-log) and was thus, similar to PP_A, decreasing with an increasing DOC:TP ratio (**Supplementary Figure S3B**).

Incubation Experiments

To test for dynamic responses underlying the patterns observed across lakes, two experimental incubations were performed, one addressing the production of CO_2, and the other the consumption of O_2. Both incubations were performed in the dark, hence they reflect heterotrophic microbial mineralization.

In the CO_2 production experiment, DOC concentration had a positive effect on CO_2 production in all samples, regardless of P level. However, P had a strong effect on the kinetics of CO_2 production and hence the shape of the CO_2 accumulation curves (**Supplementary Figure S4**). While all treatments showed non-linear CO_2 accumulation similar to logistic growth, the exponential phase was more distinct and steeper in the treatments receiving P additions. CO_2 production was faster and leveled off earlier and more distinctively in P-spiked than in P-limited samples. This effect was most pronounced for initial DOC

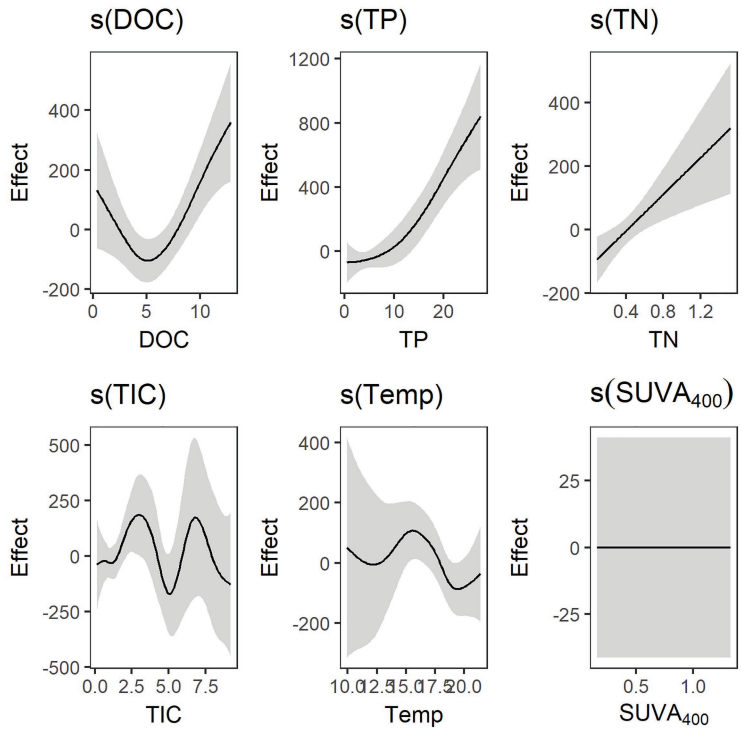

FIGURE 2 | Result plot of the generalized additive models (*gams*) predicting total carbon dioxide (CO_2) production (F_{tot}; mg C m^{-2} d^{-1}). The effect of DOC (mg L^{-1}) was strong and clearly unimodal with a minimum around 5 mg L^{-1}. Total phosphorus (TP; µg L^{-1}) and total nitrogen (TN; mg L^{-1}) had strong linear effects. The effects of total inorganic carbon (TIC; mg L^{-1}) and temperature (°C) were weak, while $SUVA_{400}$ (L mg-C^{-1} m^{-1}) had no effect on total CO_2 production.

concentrations up to 25 mg L^{-1}. The lag phase was more pronounced in P-spiked samples but decreased in length with increasing DOC concentrations. At DOC concentrations >25 mg L^{-1}, CO_2 concentrations kept increasing at a slower pace after an initial exponential phase without reaching a plateau (**Supplementary Figure S4**).

The total amount of CO_2 produced during the laboratory incubation increased monotonously with initial DOC concentration until reaching a threshold value (~10 mg L^{-1}), above which cumulative CO_2 production appeared to be independent of the amount of DOC supplied, before increasing again with DOC concentration above 30 mg L^{-1}, albeit at lower rate (**Figure 3A**). Treatments with P additions had a somewhat lower threshold value than treatments without P additions. Still, the total amount of CO_2 produced during the incubations were similar in samples with or without P additions (**Supplementary Table S1**), while higher rRNA gene copy numbers were observed in P-spiked samples (**Figure 3B**; **Supplementary Table S1**). Consequently, estimates of rRNA gene copy number-specific respiration, used here as a proxy for bacterial growth yield, were lower in P-spiked than non-spiked samples (**Figure 3C**; **Supplementary Table S1**), indicating less respiration per unit biomass produced and hence larger growth yields due to P addition. There was also an increase in rRNA gene copy numbers with increasing DOC concentrations in P-spiked and non-spiked samples (**Figure 3B**), while estimates of rRNA gene copy number-specific respiration showed no clear trends with regards to DOC concentrations (**Figure 3C**).

Similar to total CO_2 production, the maximum observed respiration rates at any time during the incubation, increased steadily with increasing DOC up to 20 mg L^{-1} (**Figure 3D**). Below this threshold value, maximum inducible respiration rates were clearly higher in P spiked than in P limited samples. Maximum inducible respiration rates increased by about 9% for each mg DOC L^{-1} up to 20 mg L^{-1}, regardless of P level. At DOC concentrations >20 mg L^{-1}, the increase in respiration rates with increasing DOC halted abruptly and stayed constant with similar rates at the two P levels.

The fraction of the DOC pool that was respired to CO_2 during the course of the experiments was similar across the P levels, but decreased with DOC concentration. At concentrations above the threshold of 20 mg L^{-1}, the respired fraction of the DOC pool was about 5% (**Supplementary Figure S6**).

In the O_2 consumption experiment, the dynamic response in O_2 uptake to DOC and P as well as temperature was tested. Similar to the CO_2 production curves, the shapes of the O_2 consumption curves differed substantially depending on P level with a more pronounced exponential phase in samples receiving P additions than in samples without P additions (**Supplementary Figure S5**). Respiration rate was also highly dependent on

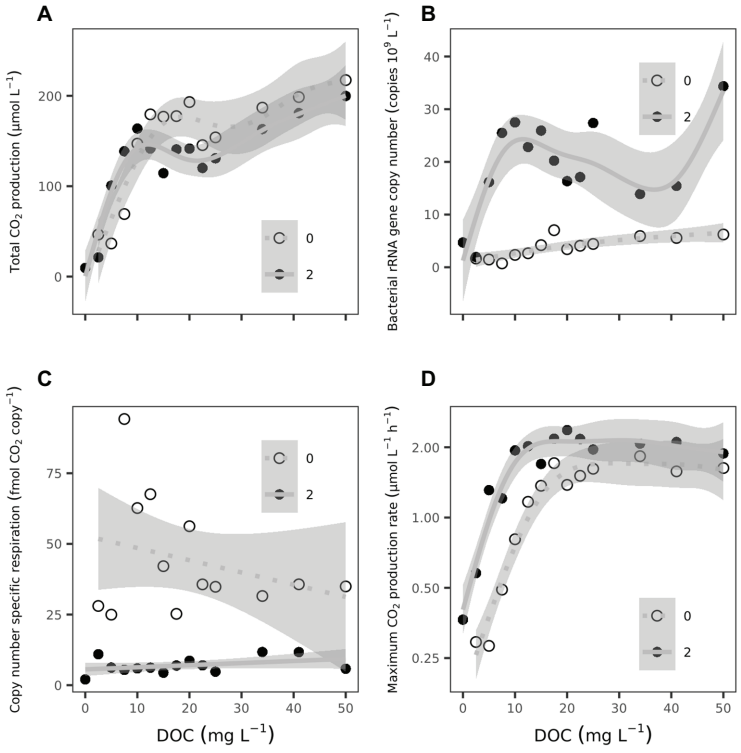

FIGURE 3 | The response of **(A)** total CO_2 production (µmol L^{-1}) during the entire incubation (240 h), **(B)** yield in bacterial 16S ribosomal RNA (rRNA) gene copy number (copies L^{-1}), **(C)** bacterial 16S rRNA gene copy number-specific respiration (fmol CO_2 $copy^{-1}$), and **(D)** maximum CO_2 production rates (µmol L^{-1} h^{-1}) to increased DOC concentrations (mg L^{-1}). The solid and dotted lines are fitted *gams* to samples with and without phosphorus (P) additions, respectively, with shaded areas representing the confidence interval of the *gams*. Statistics of the *gams* can be found in **Supplementary Table S1**.

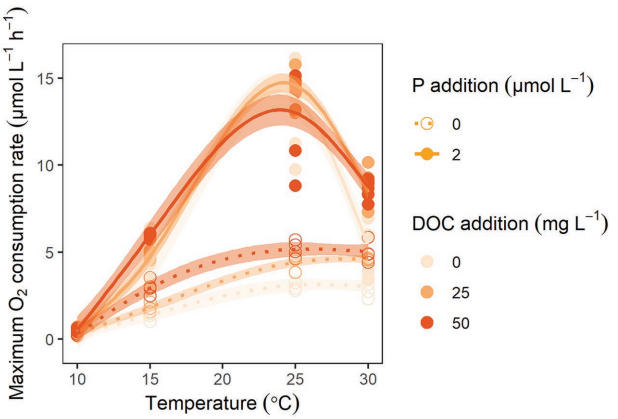

FIGURE 4 | The response of maximum oxygen (O_2; µmol L^{-1} h^{-1}) consumption rates to increased temperatures. The solid and dotted lines are fitted gam curves [y ~ s(x)] curves to samples with and without P additions, respectively. The color gradient represents DOC additions, going from light for no additions to dark for 50 mg C L^{-1}.

temperature (**Figure 4**). Maximum O_2 consumption rates were mainly related to P level and temperature (**Supplementary Table S1**), while the regression estimate of the DOC concentration effect was non-significant (**Supplementary Table S1**).

Respiration rates in the 10°C incubation were close to zero, possibly reflecting that respiration had not started to increase before the incubation was stopped and that the incubation time thus was too short with the lowest temperature. Respiration rates increased from 15 to 25°C with a Q_{10} of 2.6 (±0.2) and no significant difference in Q_{10} between samples of different P levels. From 25 to 30°C, the respiration rates decreased with a $Q_{10} < 1$. Here the Q_{10} also differed between P spiked (0.44 ± 0.09) and P limited (0.94 ± 0.05) samples.

DISCUSSION

DOC and P Availability Regulating Total CO_2 Production in Lakes

In this study, we analyzed data from a lake survey comprising 75 Scandinavian lakes chosen to represent gradients in DOM and P concentrations. Chemical and physical data from the lakes were used to estimate total CO_2 production. As it was not possible to distinguish between in-lake production and lateral input of CO_2 (from inflowing rivers or groundwater input), total CO_2 production was used to lump both sources. Notwithstanding, we found a strong relationship between O_2 and CO_2 saturation deficits ($r = -0.70$; **Supplementary Figure S2**). The intercept was not significantly different from zero and lakes that were saturated with O_2 were thus also saturated with CO_2, indicating that microbial respiration was the predominant source of CO_2 in the lakes. Furthermore, we found no correlation between TIC and CO_2 deficit, suggesting that processes within the lakes rather than lateral input regulate the CO_2 supersaturation. Although some studies have shown that DIC input from the catchment plays a larger role for explaining CO_2 evasion from lakes than previously thought (Maberly et al., 2013; Leith et al., 2015; Weyhenmeyer et al., 2015), the largest contributor to CO_2 supersaturation in the studied lakes was most probably microbial mineralization.

The observed unimodal response of total CO_2 production to increased DOC concentrations (**Figure 2**), however, suggests a shift in substrate from mainly autochthonous to predominantly allochthonous DOC. Autochthonous DOC is generally more bioavailable and of higher nutritious value with a lower C:P ratio (Søndergaard et al., 1995). When DOC of both phytoplankton and terrestrial origin is available, heterotrophic bacteria prefer the former as substrate for catabolic processes (Kritzberg et al., 2004). Estimated CO_2 production rates decreased with increasing DOC concentration until a minimum was reached at around 5 mg L^{-1}. Correspondingly, primary production rates are commonly reported to increase with DOC concentrations until around 5 mg C L^{-1}, after which the rates are declining (Karlsson et al., 2007; Seekell et al., 2015; Tanentzap et al., 2017). This unimodal response is likely reflecting a trade-off between nutrients associated with DOC and the increasing light attenuation caused by CDOM. Modest increases in DOC may also be beneficial by blocking out short-wave UV-radiation (Palen et al., 2002). Above 5 mg L^{-1}, an increasing portion of the DOC pool is of terrestrial origin and CO_2 production rates thus increase linearly with increasing DOC concentrations.

The DOC concentration-specific CO_2 production, i.e., the rates of CO_2 production per unit of DOC concentration, was positively related to PP_A, indicating that a larger share of the DOC pool was respired in more productive lakes. The DOC:TP ratio had a negative effect on PP_A, and consequently, the DOC:TP ratio also had a negative effect on the DOC concentration-specific CO_2 production (**Supplementary Figure S3**). This may seem to contradict the notion that BR increases with increased C:P ratios (Jansson et al., 2006). However, on a community level low BGE at high C:P ratios has been coupled to decreasing BP rates rather than increasing BR rates (Smith and Prairie, 2004). Higher DOC concentration-specific CO_2 production indicates faster DOC turnover in the low than in the high C:P lakes. A larger share of the DOC pool is degraded, probably accompanied with higher bacterial density in productive than in unproductive lakes. This implies a more bioavailable DOC pool in productive than in unproductive lakes, and could also suggest that this is explained by a lower C:P ratio of the substrate.

Experimental Validation of Drivers

While lake gradients may provide general patterns, the mechanistic drivers can only be revealed experimentally. To disentangle the role of DOC relative to P, we conducted two experiments. First, we measured BR along a gradient of DOC concentrations crossed with two levels of inorganic P concentrations. Since this DOC was an isolate from a humic lake (see section "Materials and Methods"), it represented primarily allochthonous C. We found clear differences in the kinetics of CO_2 production between P spiked and P-limited samples. The CO_2 accumulation curves of P-spiked samples

showed a pronounced exponential phase until reaching a plateau, similar to a bacterial growth curve reaching substrate limitation (**Supplementary Figure S4**). The kinetic patterns suggested that P-spiking boosted respiratory rates leading to substrate limitation earlier during incubation. The longer lag phase in P-spiked samples could be explained by a major shift in community composition. P-limited samples would represent a situation with minor shifts in community composition. The rRNA gene copy number-specific respiration suggests that cell-specific respiration increased under P-limited conditions. Accordingly, Smith and Prairie (2004) found cell-specific respiration to be negatively related to P supply. They further report that on a per cell basis, BR explained the greatest amount of variation in BGE. This would suggest a higher BGE in P-spiked than in P-limited samples in our experiment, provided a higher BR cell^{-1} in P-limited compared to P-spiked samples, as reflected by the lower rRNA gene copy number-specific respiration in P-spiked samples. More P, however, also releases the bacteria from P-limitation, hence causing higher metabolic activity. The balance between respiration due to excess C (i.e., under high substrate C:P) or respiration powered by increased metabolic activity under elevated P (i.e., low C:P) is not straight forward, since increased P also would stimulate bacterial growth and thus community metabolism. This unpredictability is corroborated by our results as rRNA gene copy number-specific respiration in non-spiked samples showed a negative trend with increasing DOC concentrations, while under P addition a significant increase in rRNA gene copy number-specific respiration could be observed. Previous studies with C and P manipulations, showed good correspondence between bacterial biomass and CO_2 production (Hessen et al., 1994), but in the absence of reliable day-to-day microbial counts we cannot fully resolve this stoichiometric response at the cellular versus the community level.

The cumulative amount of CO_2 produced during the incubation was higher in P-spiked than in P-limited samples at low initial DOC concentrations (<10 mg L^{-1}; **Figure 3A**). In the intermediate DOC range (12.5–25 mg L^{-1}), however, this trend shifted and more of the available DOC was respired in P-limited than in P-spiked samples (**Supplementary Figure S4**). The larger cumulative CO_2 production in P-limited samples above ~20 mg L^{-1} initial DOC could reflect that the slow-growing population assimilated the substrate at a slower pace and that the major share of the assimilated DOC was used for maintenance and hence was respired. However, this is not corroborated by rRNA gene copy number-specific respiration. The bioavailable fraction of DOC was consumed more rapidly when P was available than when P was limiting, reflecting faster DOC turnover similar to the findings in the lake survey.

We added a fixed amount of naturally isolated DOC at the beginning of the experiment, and microbial assimilation and respiration depleted a large share of the bioavailable fraction of this DOC during the course of the experiment. In a natural environment, however, fresh DOC would enter the aquatic system, e.g., by rainfall and influx from the catchment *via* rivers, brooks, or surface run-off, eventually by vertical mixing, constantly refreshing the DOC pool. Further, recalcitrant DOC would undergo photochemical processing that breaks down high molecular weight humic acids into more bioavailable substrates (Bertilsson and Tranvik, 1998). Under such conditions, mineralization would continue to increase with increasing DOC concentrations, and continuous supply of P would support higher rates of mineralization. This is in accordance with the findings from the lake survey where total CO_2 production rates increased with decreasing DOC:TP ratios (**Supplementary Figure S3B**) and increasing TP.

In the laboratory experiments, respiration rates increased with increasing DOC concentration up to 20 mg L^{-1}. This increase in respiration with DOC was in accordance with the increase in total CO_2 production rates at increased DOC concentration >5 mg L^{-1} found in the lake survey (**Figure 2**). Many boreal lakes have DOC concentrations below 20 mg L^{-1} (in our lake survey, for instance, the maximum value was 12.9 mg C L^{-1}) and a continued increase in BR with increased terrestrially derived DOC up to about 20 mg L^{-1} could be expected.

The respired fraction of DOC in the laboratory experiment was small (max 18%) and decreased with increased DOC concentration beyond a distinct peak at 12.5 mg DOC L^{-1} (**Supplementary Figure S6**). Since the source of DOC and thus the bioavailable share was the same in all samples, this suggests a lower mineralization efficiency with increased concentrations of DOC. In high DOC (>25 mg L^{-1}) treatments, the CO_2 accumulation curves of neither P-spiked nor P-limited samples reached a plateau (**Supplementary Figure S4**), suggesting that mineralization would continue beyond the 200 h of incubation, although at lower pace.

In the experiment using O_2-consumption as proxy for microbial activity (**Supplementary Figure S5**), temperature and P were strong predictors of O_2 while DOC was a poor predictor. A temperature increase from 15 to 25°C yielded an increase in respiration rates by a factor of 2.6 (±0.2) with no significant difference between P levels. This Q_{10} value is in accordance with reported Q_{10} values for physiological processes (Pomeroy and Wiebe, 2001). While respiration rates did not increase further at temperatures >25°C in P-limited samples, they decreased in P-spiked samples. Between 25 and 30°C the Q_{10} thus differed significantly between P spiked (0.44 ± 0.09) and P limited (0.94 ± 0.05) samples. This difference in Q_{10} may reflect a difference in bacterial taxonomic composition between treatments of different P levels with a faster growing and less robust community in P spiked than in P limited samples. Although there is a trend of increasing water temperatures (O'Reilly et al., 2015), an increase in temperature >25°C is unlikely to occur within the nearest future. Around 15–25°C may therefore be the most relevant temperature range for natural systems.

The observed temperature response together with the temperature sensitivity of secondary production being higher than that of primary production (Brown et al., 2004; Apple et al., 2006), further reinforce the idea that net heterotrophy in lakes will increase with increasing temperatures, which also would lead to increased emissions of CO_2 (Sobek et al., 2003). While we found no temperature effect on neither lake CO_2

production, nor CO_2 flux in the lake survey, likely reflecting that temperature measurements were snapshots, we further speculate that the narrow temperature gradient sampled in our study is overridden by a dynamic natural environment with several potentially confounding and fluctuating factors. Moreover, the role of primary production as a regulator of CO_2 is minor in these lakes. Given the positive temperature effect on microbial metabolism (Farrell and Rose, 1967), the ongoing rise in temperature, along with current browning (O'Reilly et al., 2015; Solomon et al., 2015), means that an increased CO_2 output from boreal lakes and rivers can be expected. The availability of P will serve as an additional regulator of carbon emissions, with increased respiration rates and DOC turnover rates in DOC-rich lakes where the role of primary production is small, and vice versa in cases where P is declining (Thrane et al., 2014).

Bacterioplankton respiration is a key process for converting organic carbon to CO_2 in aquatic ecosystems (Williams and Del Giorgio, 2005). This mineralization of DOC driven by microbial respiration is accompanied by O_2 consumption, often with an assumed RQ of 1, yet this quotient depends on substrate properties and metabolic states (Dilly, 2003; Berggren et al., 2012; Allesson et al., 2016). Similar to the CO_2 production rates in experimental set-up 1 and the higher O_2 consumption rates in P-spiked samples in experimental set-up 2 could represent a situation with higher BGE than in P-limited samples. As anabolic processes often are accompanied with elevated RQ's, we can expect some differences in RQ between samples of different P levels and possibly some underestimation of respiration rates in P-spiked samples by the use of an RQ value of 1. However, such differences in RQ values between P levels would make the differences in respiration rates between treatments more pronounced and the conclusions thus are still valid. High rates of heterotrophic respiration together with low rates of primary production promote oxygen depletion with major consequences for aquatic life as well as redox processes and biogeochemical cycling of C, N, P, and other elements. While increased respiration rates following increased DOC concentrations may favor primary production due to increased access to CO_2 as well as nutrients associated with DOC, increased browning and thereby increased light attenuation would most probably result in a net decline in primary production and thus increased net heterotrophy (Thrane et al., 2014; Seekell et al., 2015), with a tentative turning point around 5 mg C L^{-1}.

In conclusion, the DOC concentration regulates the overall respiratory output of CO_2 (and consumption of O_2), while additions of P changes the dynamics by boosting respiration, as did elevated temperatures. The overall respiratory outcome depends on substrate stoichiometry and the potentially different cell-specific responses versus community responses; i.e., larger biomass will generate a larger total CO_2 output despite lower cell-specific respiration. The dynamic responses revealed in the small-scale batch experiments do not necessarily capture inter-lake responses to changing DOC:TP ratios, partly because "fresh" DOC becomes available for microbial respiration due to inflow and mixing *in situ*, and partly because phytoplankton responses will impact the net CO_2 balance. Also the full nature of biotic uptake and recycling can clearly not be captured, but the combination of a gradient lake surveys together with the laboratory experiments revealed DOC as the major determinant of CO_2 production in boreal lakes, with P as a significant modulator.

DATA AVAILABILITY STATEMENT

The raw data supporting the conclusions of this article will be made available by the authors, without undue reservation.

AUTHOR CONTRIBUTIONS

LA and DH conceived the idea. LA, DH, PD, and AE conducted the experiments. All authors were involved in the analysis of data and final writing. All authors contributed to the article and approved the submitted version.

ACKNOWLEDGMENTS

We are most grateful to our colleagues Rolf Vogt for providing the DOM-isolates used in the incubation experiments, to Jan-Erik Thrane for providing the PPA estimates, and our colleagues in the Comsat-project (Norwegian Research Council, Grant/Award Number: 196336). We are also indebted to the two reviewers who provided unusually careful and helpful comments and suggestions.

SUPPLEMENTARY MATERIAL

The Supplementary Material for this article can be found online at: https://www.frontiersin.org/articles/10.3389/fmicb.2020.569879/full#supplementary-material

REFERENCES

Allesson, L., Ström, L., and Berggren, M. (2016). Impact of photochemical processing of DOC on the bacterioplankton respiratory quotient in aquatic ecosystems. *Geophys. Res. Lett.* 43, 7538–7545. doi: 10.1002/2016GL069621

Apple, J. K., Del Giorgio, P. A., and Kemp, W. M. (2006). Temperature regulation of bacterial production, respiration, and growth efficiency in a temperate salt-marsh estuary. *Aquat. Microb. Ecol.* 43, 243–254. doi: 10.3354/ame043243

Berggren, M., Lapierre, J. -F., and Del Giorgio, P. A. (2012). Magnitude and regulation of bacterioplankton respiratory quotient across freshwater environmental gradients. *ISME J.* 6, 984–993. doi: 10.1038/ismej.2011.157

Berggren, M., Laudon, H., Haei, M., Ström, L., and Jansson, M. (2010). Efficient aquatic bacterial metabolism of dissolved low-molecular-weight compounds from terrestrial sources. *ISME J.* 4, 408–416. doi: 10.1038/ismej.2009.120

Bertilsson, S., and Tranvik, L. J. (1998). Photochemically produced carboxylic acids as substrates for freshwater bacterioplankton>. *Limnol. Oceanogr.* 43, 885–895. doi: 10.4319/lo.1998.43.5.0885

Brown, J. H., Gillooly, J. F., Allen, A. P., Savage, V. M., and West, G. B. (2004). Toward a metabolic theory of ecology. *Ecology* 85, 1771–1789. doi: 10.1890/03-9000

Cole, J. J., and Caraco, N. F. (1998). Atmospheric exchange of carbon dioxide in a low-wind oligotrophic lake measured by the addition of SF6. *Limnol. Oceanogr.* 43, 647–656. doi: 10.4319/lo.1998.43.4.0647

Cole, J. J., Caraco, N. F., Kling, G. W., and Kratz, T. K. (1994). Carbon dioxide supersaturation in the surface waters of lakes. *Science* 265, 1568–1570. doi: 10.1126/science.265.5178.1568

Del Giorgio, P. A., and Cole, J. J. (1998). Bacterial growth efficiency in natural aquatic systems. *Annu. Rev. Ecol. Syst.* 29, 503–541. doi: 10.1146/annurev.ecolsys.29.1.503

Del Giorgio, P. A., Cole, J. J., and Cimbleris, A. (1997). Respiration rates in bacteria exceed phytoplankton production in unproductive aquatic systems. *Nature* 385, 148–151. doi: 10.1038/385148a0

Del Giorgio, P., and Williams, P. (eds.) (2005). *Respiration in aquatic ecosystems*. NY, USA: OUP Oxford.

Dilly, O. (2001). Microbial respiratory quotient during basal metabolism and after glucose amendment in soils and litter. *Soil Biol. Biochem.* 33, 117–127. doi: 10.1016/S0038-0717(00)00123-1

Dilly, O. (2003). Regulation of the respiratory quotient of soil microbiota by availability of nutrients. *FEMS Microbiol. Ecol.* 43, 375–381. doi: 10.1111/j.1574-6941.2003.tb01078.x

Drake, T. W., Raymond, P. A., and Spencer, R. G. (2018). Terrestrial carbon inputs to inland waters: a current synthesis of estimates and uncertainty. *Limnol. Oceanogr. Lett.* 3, 132–142. doi: 10.1002/lol2.10055

Duarte, C. M., and Prairie, Y. T. (2005). Prevalence of heterotrophy and atmospheric CO_2 emissions from aquatic ecosystems. *Ecosystems* 8, 862–870. doi: 10.1007/s10021-005-0177-4

Farrell, J., and Rose, A. (1967). Temperature effects on microorganisms. *Annu. Rev. Microbiol.* 21, 101–120. doi: 10.1146/annurev.mi.21.100167.000533

Fierer, N., Hamady, M., Lauber, C. L., and Knight, R. (2008). The influence of sex, handedness, and washing on the diversity of hand surface bacteria. *Proc. Natl. Acad. Sci. U. S. A.* 105, 17994–17999. doi: 10.1073/pnas.0807920105

Finstad, A. G., Andersen, T., Larsen, S., Tominaga, K., Blumentrath, S., De Wit, H. A., et al. (2016). From greening to browning: catchment vegetation development and reduced S-deposition promote organic carbon load on decadal time scales in Nordic lakes. *Sci. Rep.* 6:31944. doi: 10.1038/srep31944

Frank, D. N., Amand, A. L. S., Feldman, R. A., Boedeker, E. C., Harpaz, N., and Pace, N. R. (2007). Molecular-phylogenetic characterization of microbial community imbalances in human inflammatory bowel diseases. *Proc. Natl. Acad. Sci. U. S. A.* 104, 13780–13785. doi: 10.1073/pnas.0706625104

Gjessing, E., Egeberg, P., and Håkedal, J. (1999). Natural organic matter in drinking water—the "NOM-typing project", background and basic characteristics of original water samples and NOM isolates. *Environ. Int.* 25, 145–159. doi: 10.1016/S0160-4120(98)00119-6

Hessen, D. O. (1992). Dissolved organic carbon in a humic lake: effects on bacterial production and respiration. *Hydrobiologia* 229, 115–123. doi: 10.1007/BF00006995

Hessen, D., Andersen, T., and Lyche, A. (1990). Carbon metabolism in a humic lake: pool sizes and cycling through zooplankton. *Limnol. Oceanogr.* 35, 84–99. doi: 10.4319/lo.1990.35.1.0084

Hessen, D. O., and Anderson, T. R. (2008). Excess carbon in aquatic organisms and ecosystems: physiological, ecological, and evolutionary implications. *Limnol. Oceanogr.* 53, 1685–1696. doi: 10.4319/lo.2008.53.4.1685

Hessen, D. O., Nygaard, K., Salonen, K., and Vähätalo, A. (1994). The effect of substrate stoichiometry on microbial activity and carbon degradation in humic lakes. *Environ. Int.* 20, 67–76. doi: 10.1016/0160-4120(94)90068-X

Humborg, C., Mörth, C. M., Sundbom, M., Borg, H., Blenckner, T., Giesler, R., et al. (2010). CO_2 supersaturation along the aquatic conduit in Swedish watersheds as constrained by terrestrial respiration, aquatic respiration and weathering. *Glob. Chang. Biol.* 16, 1966–1978. doi: 10.1111/j.1365-2486.2009.02092.x

Jähne, B., Münnich, K. O., Bösinger, R., Dutzi, A., Huber, W., and Libner, P. (1987). On the parameters influencing air-water gas exchange. *J. Geophys. Res.* 92, 1937–1949. doi: 10.1029/JC092iC02p01937

Jane, S. F., and Rose, K. C. (2018). Carbon quality regulates the temperature dependence of aquatic ecosystem respiration. *Freshwater Biol.* 63, 1407–1419. doi: 10.1111/fwb.13168

Jansson, M., Bergström, A. -K., Blomqvist, P., and Drakare, S. (2000). Allochthonous organic carbon and phytoplankton/bacterioplankton production relationships in lakes. *Ecology* 81, 3250–3255. doi: 10.1890/0012-9658(2000)081[3250:AOCAPB]2.0.CO;2

Jansson, M., Bergström, A. -K., Lymer, D., Vrede, K., and Karlsson, J. (2006). Bacterioplankton growth and nutrient use efficiencies under variable organic carbon and inorganic phosphorus ratios. *Microb. Ecol.* 52, 358–364. doi: 10.1007/s00248-006-9013-4

Jones, R. I. (1992). The influence of humic substances on lacustrine planktonic food chains. *Hydrobiologia* 229, 73–91. doi: 10.1007/BF00006992

Karlsson, J., Jansson, M., and Jonsson, A. (2007). Respiration of allochthonous organic carbon in unproductive forest lakes determined by the keeling plot method. *Limnol. Oceanogr.* 52, 603–608. doi: 10.4319/lo.2007.52.2.0603

Kellerman, A. M., Kothawala, D. N., Dittmar, T., and Tranvik, L. J. (2015). Persistence of dissolved organic matter in lakes related to its molecular characteristics. *Nat. Geosci.* 8, 454–457. doi: 10.1038/ngeo2440

Kritzberg, E. S. (2017). Centennial-long trends of lake browning show major effect of afforestation. *Limnol. Oceanogr. Lett.* 2, 105–112. doi: 10.1002/lol2.10041

Kritzberg, E. S., Arrieta, J. M., and Duarte, C. M. (2010). Temperature and phosphorus regulating carbon flux through bacteria in a coastal marine system. *Aquat. Microb. Ecol.* 58, 141–151. doi: 10.3354/ame01368

Kritzberg, E. S., Cole, J. J., Pace, M. L., Granéli, W., and Bade, D. L. (2004). Autochthonous versus allochthonous carbon sources of bacteria: results from whole-lake 13C addition experiments. *Limnol. Oceanogr.* 49, 588–596. doi: 10.4319/lo.2004.49.2.0588

Larsen, S., Andersen, T., and Hessen, D. (2011). The pCO_2 in boreal lakes: organic carbon as a universal predictor? *Global Biogeochem. Cy.* 25:GB2012. doi: 10.1029/2010GB003864

Leith, F. I., Dinsmore, K. J., Wallin, M. B., Billett, M., Heal, K. V., Laudon, H., et al. (2015). Carbon dioxide transport across the hillslope-riparian-stream continuum in a boreal headwater catchment. *Biogeosciences* 12, 1881–1892. doi: 10.5194/bg-12-1881-2015

Maberly, S. C., Barker, P. A., Stott, A. W., and De Ville, M. M. (2013). Catchment productivity controls CO_2 emissions from lakes. *Nat. Clim. Change* 3, 391–394. doi: 10.1038/nclimate1748

Madigan, M. T., Martinko, J. M., and Parker, J. (1997). *Brock biology of microorganisms*. Upper Saddle River, NJ: Prentice Hall.

Marra, G., and Wood, S. N. (2011). Practical variable selection for generalized additive models. *Comput. Stat. Data An.* 55, 2372–2387. doi: 10.1016/j.csda.2011.02.004

Mcknight, D. M., and Aiken, G. R. (1998). "Sources and age of aquatic humus" in *Aquatic humic substances*. eds. D. O. Hessen and L. J. Tranvik (NY, USA: Springer).

Mitchell, B., Kahru, M., Wieland, J., and Stramska, M. (2002). "Determination of spectral absorption coefficients of particles, dissolved material and phytoplankton for discrete water samples" in *Ocean optics protocols for satellite ocean color sensor validation*. eds. G. S. Mueller and J. L. Tranvik (MD, USA: NASA Goddard Space Flight Center).

Molstad, L., Dörsch, P., and Bakken, L. (2016). Improved robotized incubation system for gas kinetics in batch cultures. Technical report.

Monteith, D. T., Stoddard, J. L., Evans, C. D., De Wit, H. A., Forsius, M., Høgåsen, T., et al. (2007). Dissolved organic carbon trends resulting from changes in atmospheric deposition chemistry. *Nature* 450, 537–540. doi: 10.1038/nature06316

Neff, J. C., and Asner, G. P. (2001). Dissolved organic carbon in terrestrial ecosystems: synthesis and a model. *Ecosystems* 4, 29–48. doi: 10.1007/s100210000058

O'Reilly, C. M., Sharma, S., Gray, D. K., Hampton, S. E., Read, J. S., Rowley, R. J., et al. (2015). Rapid and highly variable warming of lake surface waters around the globe. *Geophys. Res. Lett.* 42, 10773–10781. doi: 10.1002/2015GL066235

Palen, W. J., Schindler, D. E., Adams, M. J., Pearl, C. A., Bury, R. B., and Diamond, S. A. (2002). Optical characteristics of natural waters protect amphibians from UV-B in the US Pacific northwest. *Ecology* 83, 2951–2957. doi: 10.1890/0012-9658(2002)083[2951:OCONWP]2.0.CO;2

Pomeroy, L. R., and Wiebe, W. J. (2001). Temperature and substrates as interactive limiting factors for marine heterotrophic bacteria. *Aquat. Microb. Ecol.* 23, 187–204. doi: 10.3354/ame023187

R Core Team (2020). R: A language and environment for statistical computing. R foundation for statistical computing, Vienna, Austria. Avialable at: http://www.R-project.org/

Rivkin, R. B., and Legendre, L. (2001). Biogenic carbon cycling in the upper ocean: effects of microbial respiration. *Science* 291, 2398–2400. doi: 10.1126/science.291.5512.2398

Savio, D., Sinclair, L., Ijaz, U. Z., Parajka, J., Reischer, G. H., Stadler, P., et al. (2015). Bacterial diversity along a 2600 km river continuum. *Environ. Microbiol.* 17, 4994–5007. doi: 10.1111/1462-2920.12886

Schagerl, M., and Donabaum, K. (2003). Patterns of major photosynthetic pigments in freshwater algae. 1. Cyanoprokaryota, rhodophyta and cryptophyta. *Ann. Limnol. Int. J. Lim.* 39, 35–47. doi: 10.1051/limn/2003003

Schneider, P., and Hook, S. J. (2010). Space observations of inland water bodies show rapid surface warming since 1985. *Geophys. Res. Lett.* 37:L22405. doi: 10.1029/2010GL045059

Seekell, D. A., Lapierre, J. -F., Ask, J., Bergström, A. -K., Deininger, A., Rodríguez, P., et al. (2015). The influence of dissolved organic carbon on primary production in northern lakes. *Limnol. Oceanogr.* 60, 1276–1285. doi: 10.1002/lno.10096

Simpson, G. (2018). Introducing gratia. From the bottom of the heap.

Škerlep, M., Steiner, E., Axelsson, A. L., and Kritzberg, E. S. (2020). Afforestation driving long-term surface water browning. *Glob. Chang. Biol.* 26, 1390–1399. doi: 10.1111/gcb.14891

Smith, E. M., and Prairie, Y. T. (2004). Bacterial metabolism and growth efficiency in lakes: the importance of phosphorus availability. *Limnol. Oceanogr.* 49, 137–147. doi: 10.4319/lo.2004.49.1.0137

Sobek, S., Algesten, G., Bergström, A. K., Jansson, M., and Tranvik, L. J. (2003). The catchment and climate regulation of pCO_2 in boreal lakes. *Glob. Chang. Biol.* 9, 630–641. doi: 10.1046/j.1365-2486.2003.00619.x

Solomon, C. T., Jones, S. E., Weidel, B. C., Buffam, I., Fork, M. L., Karlsson, J., et al. (2015). Ecosystem consequences of changing inputs of terrestrial dissolved organic matter to lakes: current knowledge and future challenges. *Ecosystems* 18, 376–389. doi: 10.1007/s10021-015-9848-y

Søndergaard, M., Hansen, B., and Markager, S. (1995). Dynamics of dissolved organic car-bon lability in a eutrophic lake. *Limnol. Oceanogr.* 40, 46–54. doi: 10.4319/lo.1995.40.1.0046

Sterner, R. W., and Elser, J. J. (2002). *Ecological stoichiometry: The biology of elements from molecules to the biosphere*. NJ, USA: Princeton university press.

Tanentzap, A. J., Kielstra, B. W., Wilkinson, G. M., Berggren, M., Craig, N., Del Giorgio, P. A., et al. (2017). Terrestrial support of lake food webs: synthesis reveals controls over cross-ecosystem resource use. *Sci. Adv.* 3:e1601765. doi: 10.1126/sciadv.1601765

Thrane, J. -E., Hessen, D. O., and Andersen, T. (2014). The absorption of light in lakes: negative impact of dissolved organic carbon on primary productivity. *Ecosystems* 17, 1040–1052. doi: 10.1007/s10021-014-9776-2

Vadstein, O. (2000). "Heterotrophic, planktonic bacteria and cycling of phosphorus" in *Advances in microbial ecology*. ed. B. Schink (Springer).

Vallino, J., Hopkinson, C., and Hobbie, J. (1996). Modeling bacterial utilization of dissolved organic matter: optimization replaces Monod growth kinetics. *Limnol. Oceanogr.* 41, 1591–1609. doi: 10.4319/lo.1996.41.8.1591

Vogt, R. D., Gjessing, E., Andersen, D. O., Clarke, N., Gadmar, T., Bishop, K., et al. (2001). Natural organic matter in the nordic countries. Nordtest Report, 479, 150.

Weyhenmeyer, G., Kosten, S., Wallin, M., Tranvik, L., Jeppesen, E., and Roland, F. (2015). Significant fraction of CO_2 emissions from boreal lakes derived from hydrologic inorganic carbon inputs. *Nat. Geosci.* 8, 933–936. doi: 10.1038/ngeo2582

Williams, P. L. B., and Del Giorgio, P. A. (eds.) (2005). "Respiration in aquatic ecosystems: history and background" in *Respiration in aquatic ecosystems* (NY, USA: Oxford university press), 1–17.

Wood, S. N. (2011). Fast stable restricted maximum likelihood and marginal likelihood estimation of semiparametric generalized linear models. *J. R Statist. Soc. B* 73, 3–36. doi: 10.1111/j.1467-9868.2010.00749.x

Yang, H., Andersen, T., Dörsch, P., Tominaga, K., Thrane, J. -E., and Hessen, D. O. (2015). Greenhouse gas metabolism in Nordic boreal lakes. *Biogeochemistry* 126, 211–225. doi: 10.1007/s10533-015-0154-8

Ylla, I., Romaní, A. M., and Sabater, S. (2012). Labile and recalcitrant organic matter utilization by river biofilm under increasing water temperature. *Microb. Ecol.* 64, 593–604. doi: 10.1007/s00248-012-0062-6

Conflict of Interest: The authors declare that the research was conducted in the absence of any commercial or financial relationships that could be construed as a potential conflict of interest.

Supporting information materials and methods

Vertical profiles of scalar irradiance in the photosynthetically active radiation (PAR) region (400 -700 nm; E_0) were measured using a spherical irradiance sensor (BioSpherical instruments) attached to a 10 channel CTD profiler (WRW620. RBR Ltd., Canada). The sensor was lowered at a rate of approximately 20 cm s^{-1} with a sampling rate of 6 Hz. In order to correct for temporal changes in irradiance caused by for example wave action and clouds during the CTD cast, we regressed the log-transformed E_0 against depth (z) for each ten sampling point (i.e. sliding windows). The vertical attenuation coefficient for scalar PAR (K_0PAR) was then estimated by taking the median of the distribution of these slopes.

Measurements of concentrations of total phosphorus (TP), total organic carbon (TOC) and total nitrogen (TN) were carried out both at the Norwegian Institute for Water Research (NIVA) and at the University of Oslo (UiO). Regressions between the measurements at the two laboratories showed no systematic differences (TP: R^2 = 0.77, residual standard error (*RSE*) = 2.27 µg l^{-1}; TOC: R^2 = 0.99, *RSE* = 0.25 mg l^{-1}; TN: R^2 = 0.91, *RSE* = 81 µg l^{-1}) and the averages of the results were used in the subsequent analysis. DOC was calculated as the difference between the total organic carbon (TOC) and particulate organic carbon (POC). TOC was measured by infrared CO_2 detection after catalytic high temperature combustion (Shimadzu TOC-VWP analyser (UiO), or Phoenix 8000 TOC-TC analyser (NIVA)).
POC was measured on an elemental analyser (Flash EA 1112 NC, Thermo Fisher Scientific, Waltham, Massachusetts, USA) through rapid combustion in pure oxygen of particulates captured on a pre-combusted GF/C-filter. The major part (> 95 %) of the TOC was in dissolved

form (DOC). At UiO, TOC was measured together with total inorganic carbon (TIC). TP was measured on an auto-analyser as phosphate after wet oxidation with peroxodisulfate. The two labs measured TN in different ways. UiO measured TN on unfiltered samples by detecting nitrogen monoxide by chemiluminescence using a TNM-1 unit attached to the Shimadzu TOC-VWP analyser, and NIVA measured TN through detection of nitrate after wet oxidation with peroxodisulfate in a segmented flow auto-analyser.

For gas analyses, water from the composite water sample (integrated from 0 to 5 m depth) was gently let into 120 ml glass serum vials without bubbling. The samples were fixed with 0.2% HgCl and sealed with gas-tight butyl rubber stoppers (see Yang et al. (2015) for details). Prior to analysis, the vials were stored dark and cold (4 ºC). In order to prepare a 20-30 ml headspace, a gentle helium pressure (needle valve) was applied to the top of the bottle volume replacing ca. 40 ml of sample with pure He, before venting the bottles to 1 atmosphere. Equilibration between liquid and headspace was achieved by shaking the bottles horizontally at 150 rpm for 2 h at room temperature. Headspace concentrations of CO_2 and O_2 were determined by automated gas chromatography (GC; Model 7890A, Agilent, CA, USA).

In brief, the bio-optical model calculating area specific primary production (PP_A) is based on estimating the in vivo rate of light absorption by phytoplankton, and subsequently electron transport rates (ETRs) through photosystem II (PSII) using information about the light-dependent quantum yield of the PSII photochemistry. ETR can further be converted to a rate of gross carbon fixation by assuming an appropriate value for the quantum yield of CO_2 fixation (Kromkamp and Forster, 2003, Suggett et al., 2010). While the method could be sensitive to phytoplankton community composition, it has gained increased interest over the last two decades because it offers a fast and inexpensive way of obtaining PP_A estimates (see Thrane et al (2014)

for details). A comparison of this method and empirical estimates for PP_A in boreal lakes demonstrated good accordance (Thrane et al., 2014). The method is thus a feasible tool for assessment of primary production across a large number of sites. It also avoids many of the pitfalls of ^{14}C-bottle incubation, which in any case could not have been applied in this kind of synoptic survey.

CO_2 flux

We used Fick's law of diffusion to calculate the water-air flux of CO_2 (F_{net}; mmol m^{-2} d^{-1}) from lake surface CO_2 concentrations.:

$$F_{net} = k_{CO2}\Delta_{CO2} \quad (1)$$

where k_{CO2} (m d^{-1}) is the CO_2 gas exchange coefficient at a given temperature and Δ_{CO2} (mmol m^{-3}) is the CO_2 deficit from concentrations at equilibrium with the atmosphere, obtained using Henry's law. k_{CO2} was estimated for each lake using the gas transfer velocity (m d^{-1}) for a gas-temperature combination with a Schmidt number of 600 (k_{600}; CO_2 at 20 °C) according to Jähne et al. (1987):

$$k_{CO2} = k_{600}\left(\frac{Sc_{CO2}}{600}\right)^{-x} \quad (2)$$

where x = 2/3 if wind speed ≤ 3ms^{-1} and x = 0.5 if wind speed > 3m s^{-1}, Sc is the temperature dependent Schmidt number for CO_2. k_{600} is estimated from the wind speed according to Cole and Caraco (1998):

$$k_{600} = 2.07 + 0.215\,U_{10}^{1.7} \quad (3)$$

Hourly wind speed data at 10 m above ground (U_{10} in equation 9) at all 75 lakes were extracted from the Norwegian Reanalysis Archive (NORA10) and aggregated into July-August means.

COLE, J. J. & CARACO, N. F. 1998. Atmospheric exchange of carbon dioxide in a low-wind oligotrophic lake measured by the addition of SF6. *Limnology and Oceanography,* 43**,** 647-656.

JÄHNE, B., MÜNNICH, K. O., BÖSINGER, R., DUTZI, A., HUBER, W. & LIBNER, P. 1987. On the parameters influencing air-water gas exchange. *Journal of Geophysical Research: Oceans,* 92**,** 1937-1949.

KROMKAMP, J. C. & FORSTER, R. M. 2003. The use of variable fluorescence measurements in aquatic ecosystems: differences between multiple and single turnover measuring protocols and suggested terminology. *European Journal of Phycology,* 38**,** 103-112.

SUGGETT, D. J., PRÁŠIL, O. & BOROWITZKA, M. A. 2010. *Chlorophyll a fluorescence in aquatic sciences: methods and applications*, Springer.

THRANE, J.-E., HESSEN, D. O. & ANDERSEN, T. 2014. The Absorption of Light in Lakes: Negative Impact of Dissolved Organic Carbon on Primary Productivity. *Ecosystems,* 17**,** 1040-1052.

YANG, H., ANDERSEN, T., DÖRSCH, P., TOMINAGA, K., THRANE, J.-E. & HESSEN, D. O. 2015. Greenhouse gas metabolism in Nordic boreal lakes. *Biogeochemistry,* 126**,** 211-225.

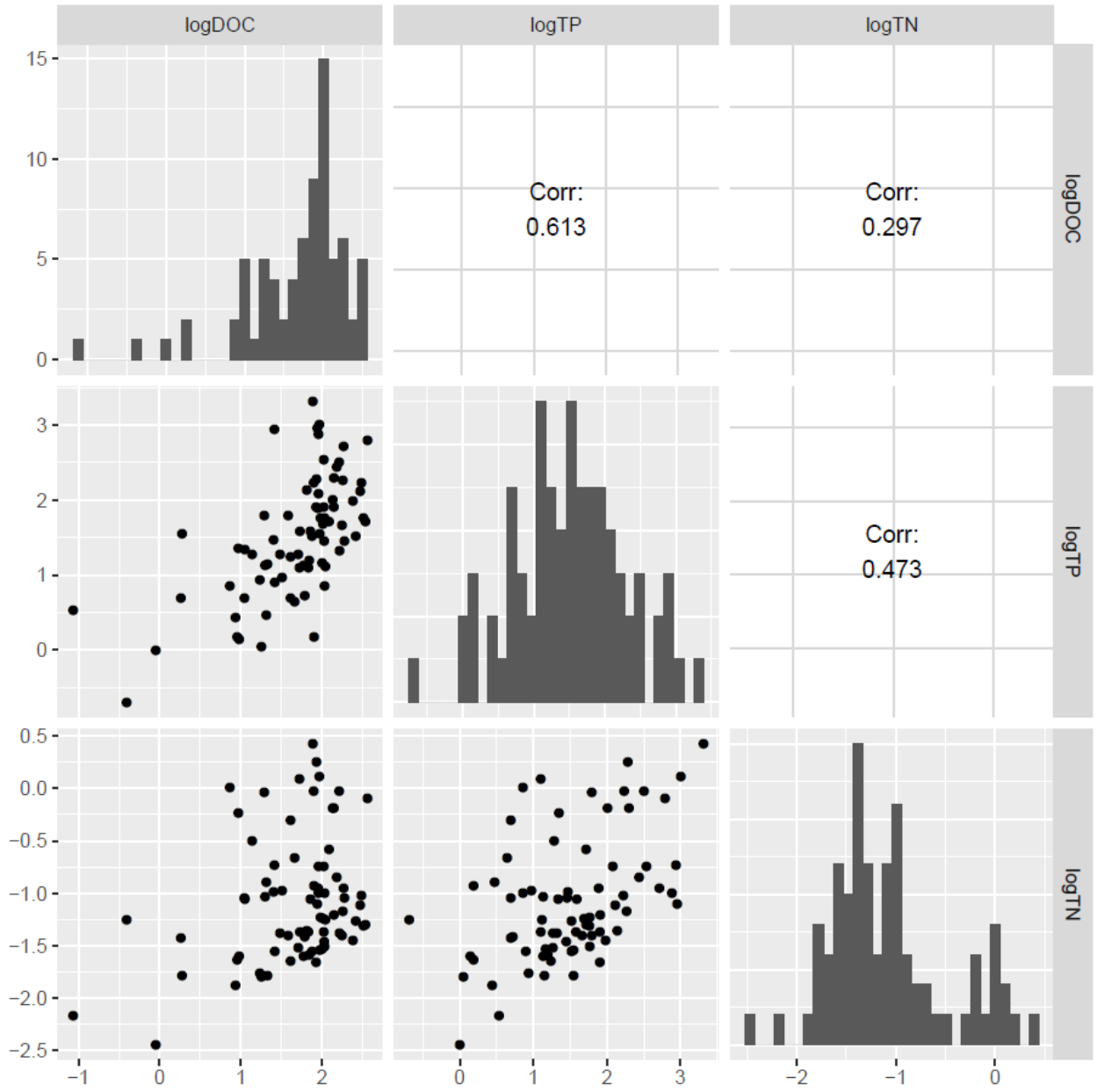

Figure S1. Correlation matrix between dissolved organic carbon (DOC; mg L^{-1}), total phosphorus (TP; µg L^{-1}), and total nitrogen (TN; mg L^{-1}). All variables are log-transformed.

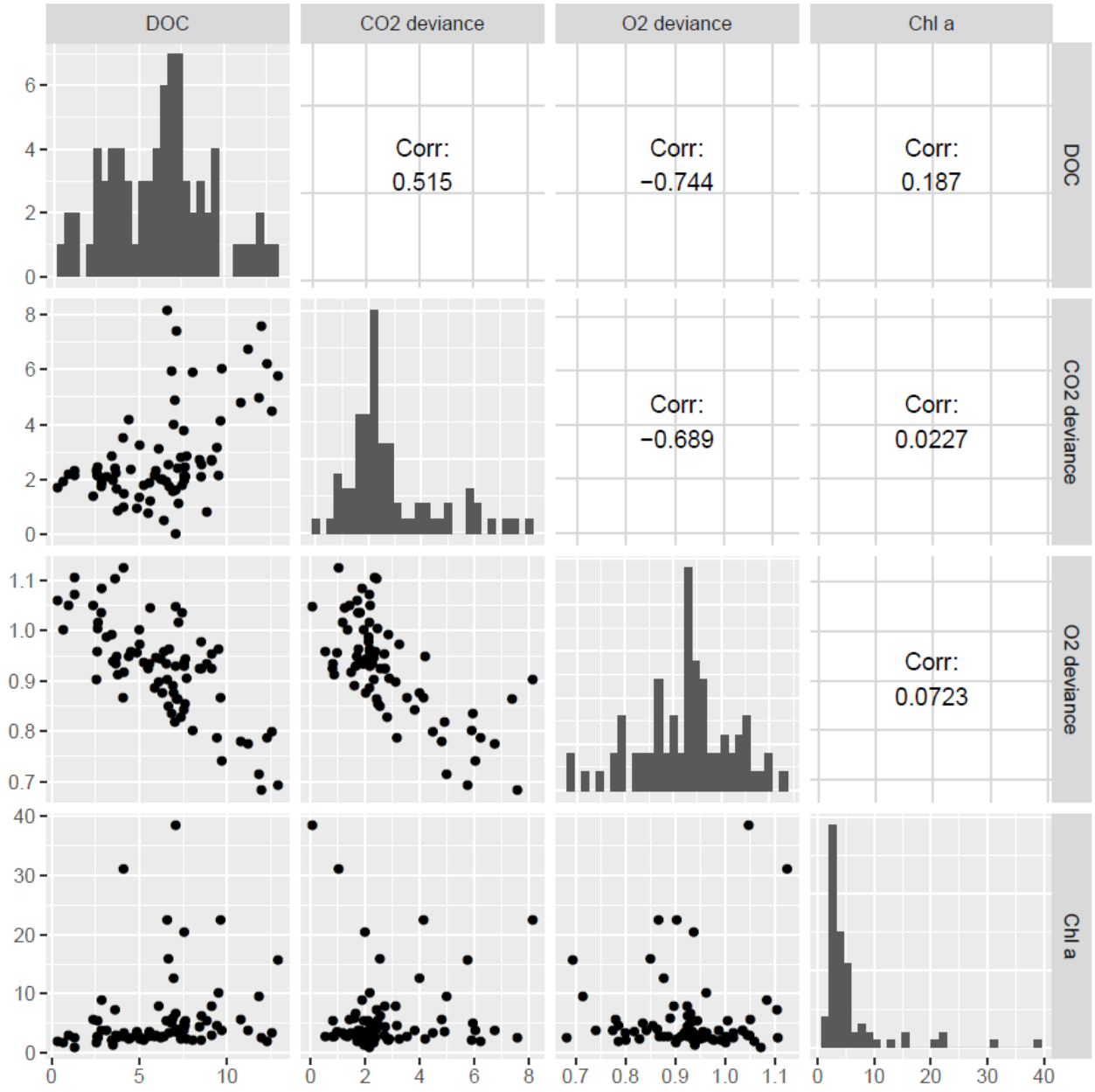

Figure S2. Correlation matrix between DOC (mg L^{-1}), CO_2 deviance from saturaion (%), O_2 deviance from saturation (%), and concentration of chlorophyll *a* (chl *a*; µg L^{-1}).

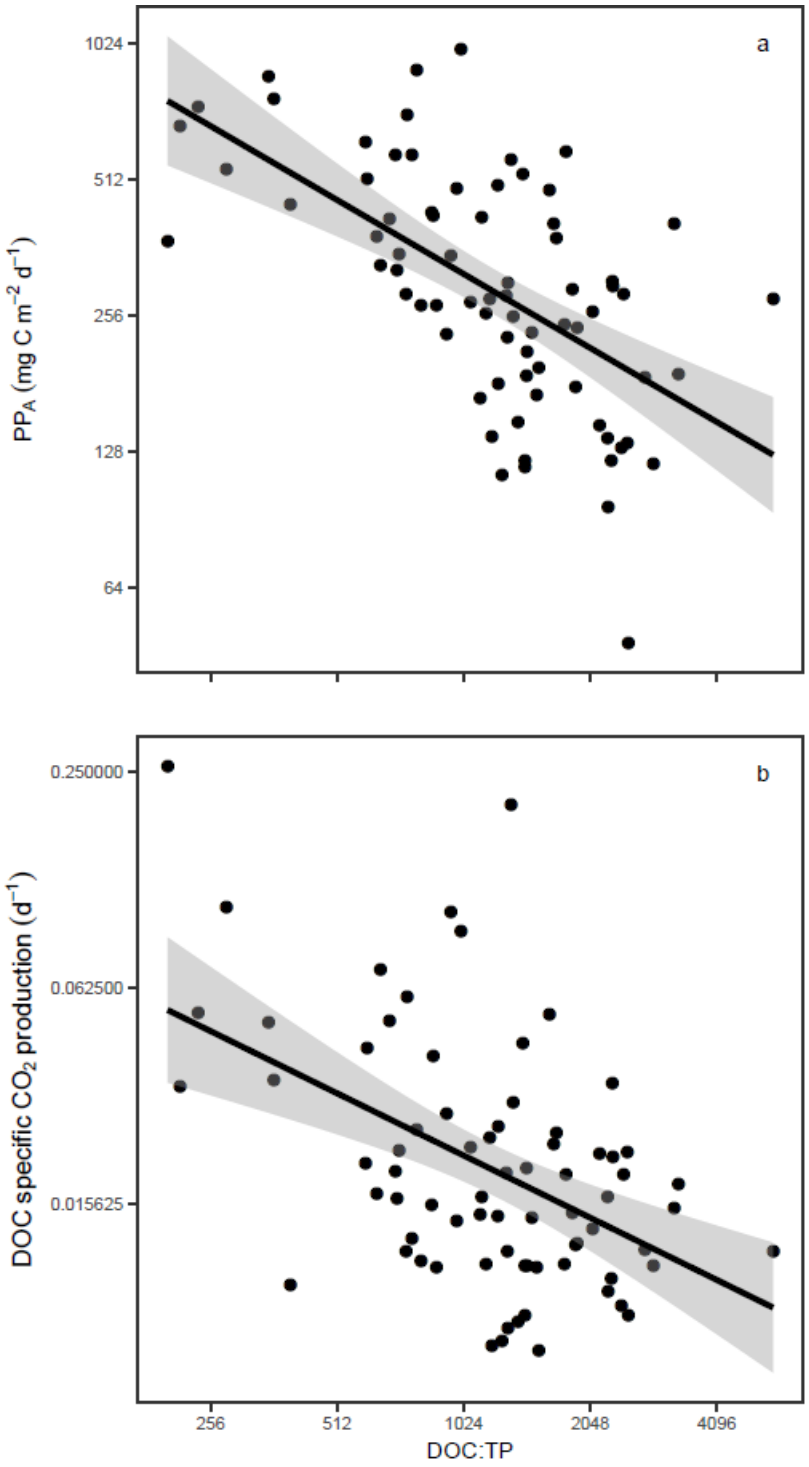

Figure S3. The response of a) area specific primary production (PP_A; mg C m^{-2} d^{-1}), and b) DOC specific CO_2 production rates (F_{tot} (mg C m^{-2} d^{-1})/DOC (mg C m^{-2})) to increased DOC:TP ratio.

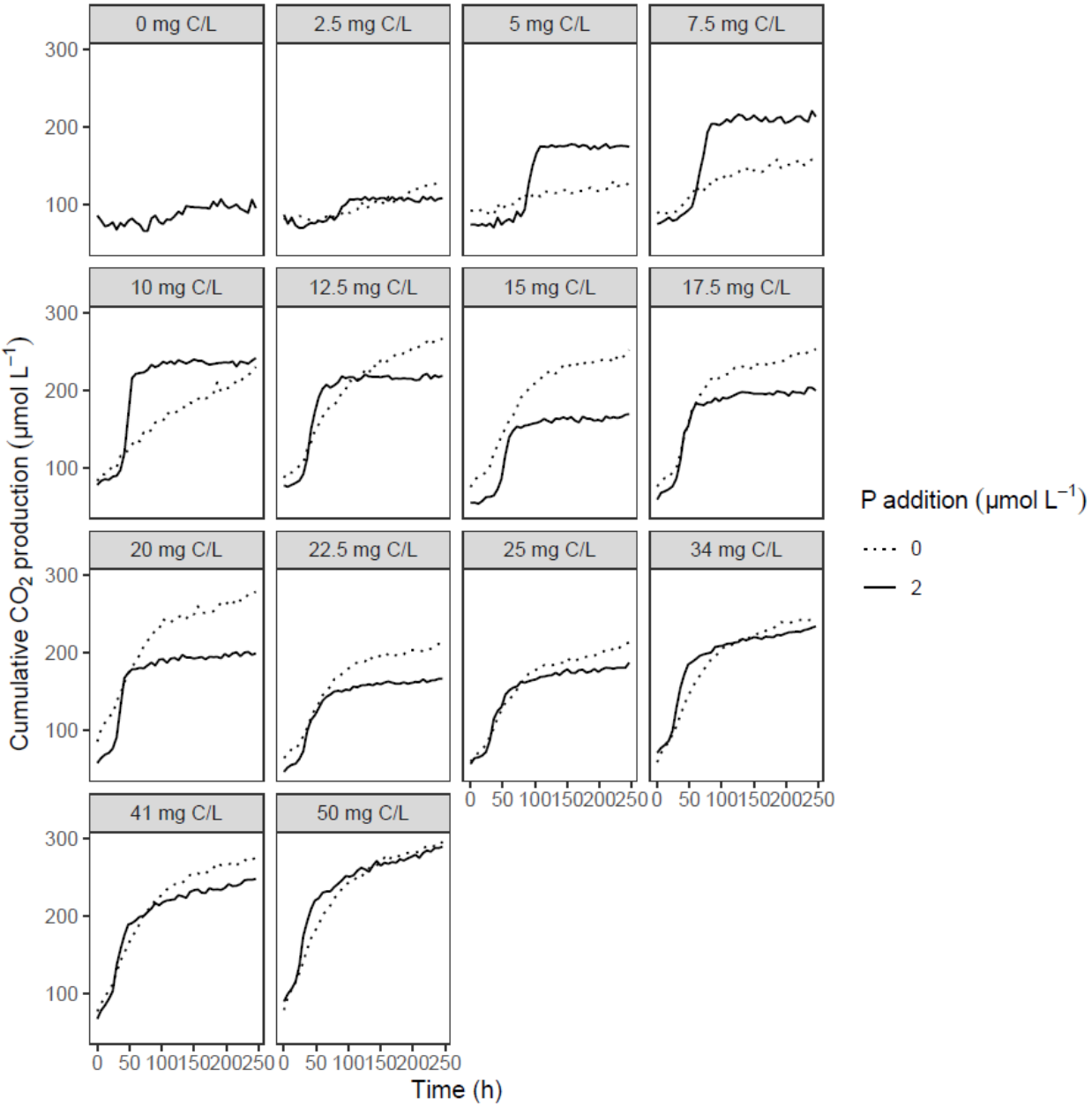

Figure S4. Cumulative CO_2 production over incubation time. The figure is divided into boxes of DOC additions starting from top left with no additions to bottom right with 50 mg C L^{-1}. Dotted and solid lines represent treatments without and with P additions, respectively.

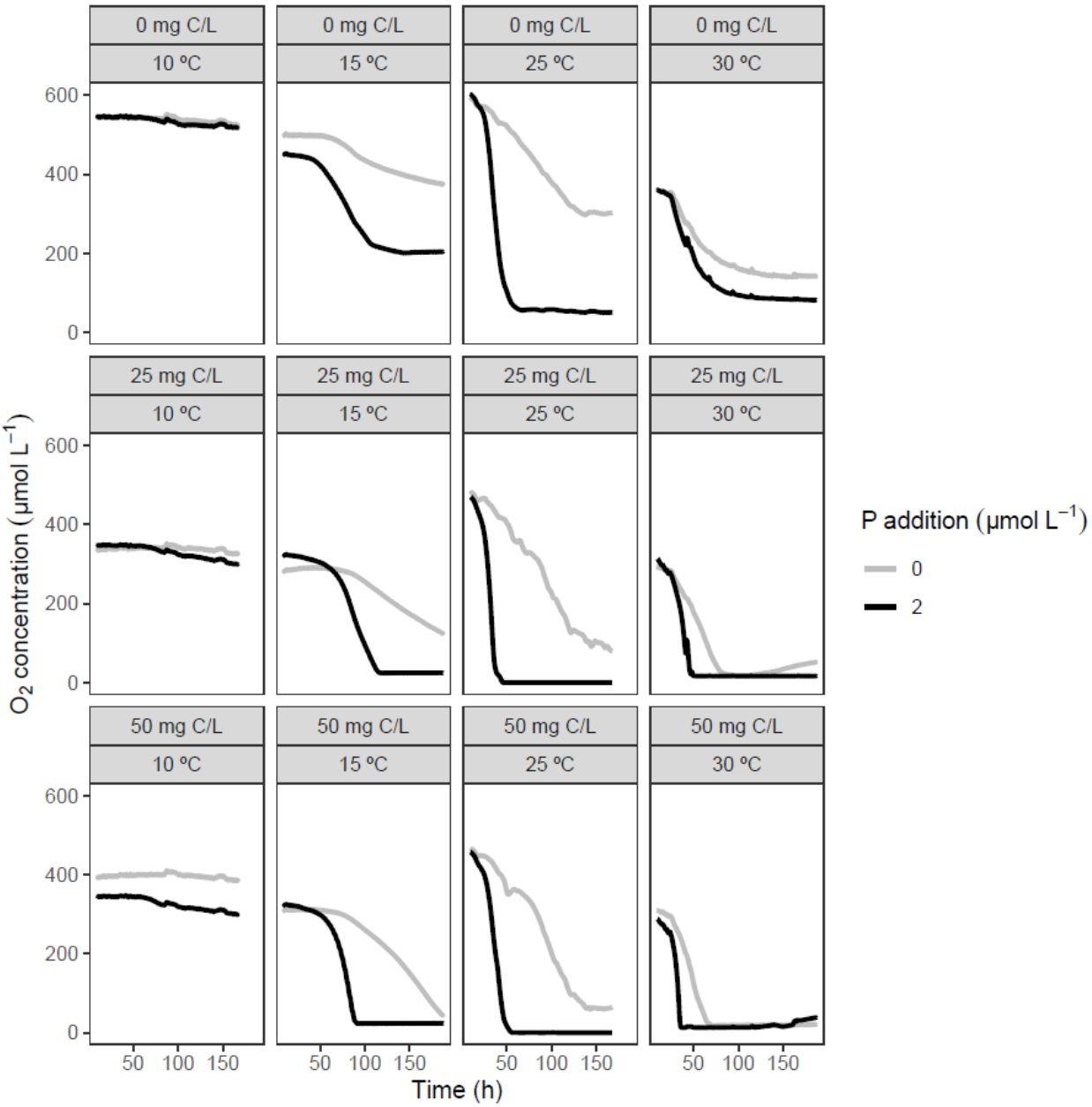

Figure S5. Cumaltive O_2 consumption over incubation time. The figure is divided into boxes of DOC (top row: no addition; middle row: 25 mg C L^{-1}; bottom 50 mg C L^{-1}), and temperature (from 10 ºC in the left column to 30 ºC in the right column). The colors represent treatments without (red) and with (blue) P additions, respectively.

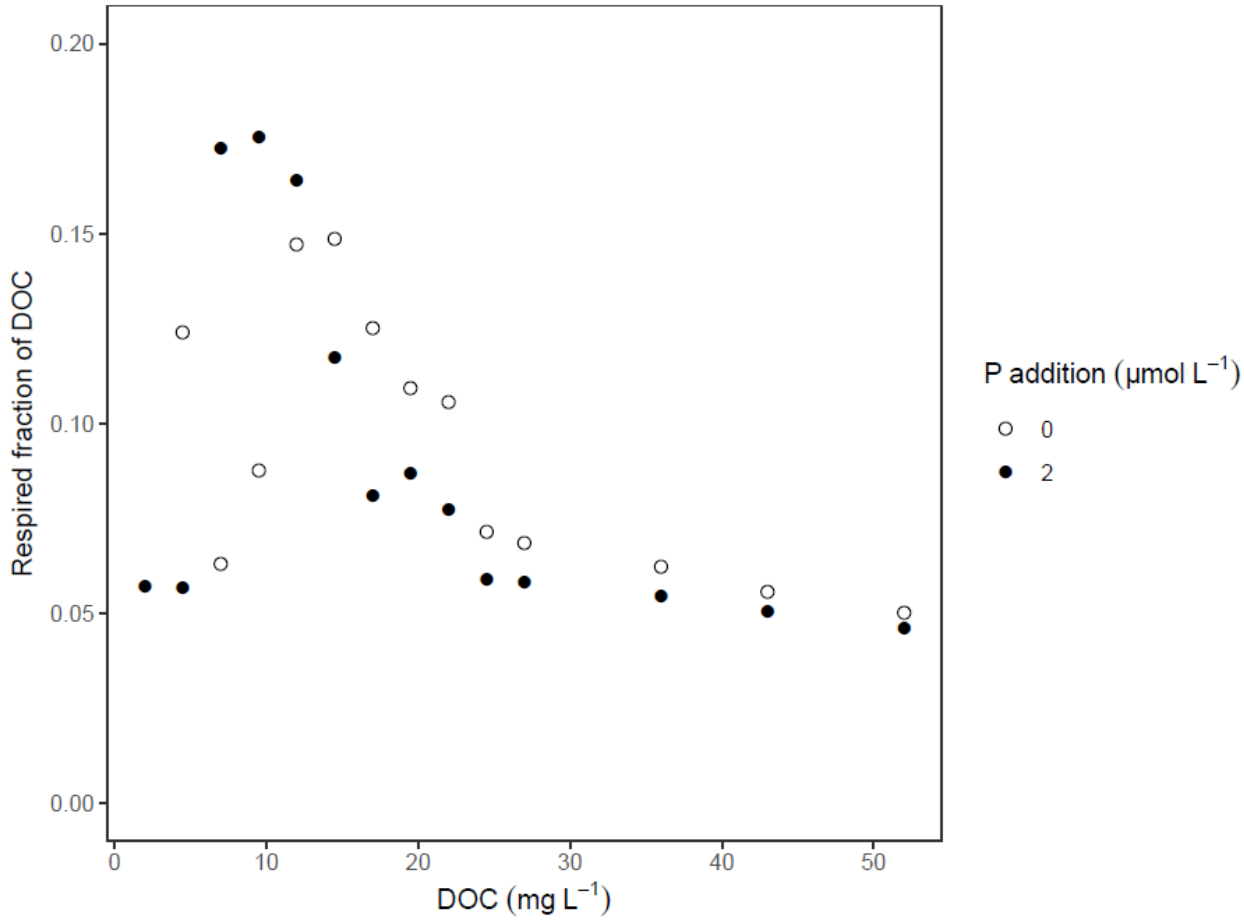

Figure S6. The respired fraction of the added DOC versus DOC concentration (mg L^{-1}) open circles are treatments without P and filled circles are treatments with 2 µmol L^{-1} P addition.

Table S1. Results of a generalized additive model (GAM) from the two experiments using non-parametric smoothers.

Response variable	**Factor**	**edf***	**F-value**	**R^2_{adj}**	**Dev. Expl.#**	**Effect§**
Experimental set-up 1						
total CO_2 production	s(DOC):P0	7.372	23.98	0.935	97.5 %	P*
	s(DOC):P2	7.731	20.27			
16S rRNA gene copy number	s(DOC):P0	1.493	7.273	0.98	98.9 %	P***
	s(DOC):P2	8.931	56.04			
copy number specific respiration	s(DOC):P0	7.548	3.748	0.813	88.2 %	P***
	s(DOC):P2	1.000	0.703			
maximum CO_2 production rate	s(DOC):P0	2.825	26.46	0.91	93.6 %	P***
	s(DOC):P2	3.689	26.89			
Experimental set-up 2						
maximum O_2 consumption rate	s(temp):P0:DOC0	1.000	6.49	0.844	84.8%	P***
	s(temp):P2:DOC0					DOC*
	s(temp):P0:DOC25	1.990	92.98			
	s(temp):P2:DOC25					
	s(temp):P0:DOC50	1.000	15.04			
	s(temp):P2:DOC50					
		1.983	104.18			
		1.608	11.13			
		1.982	89.71			

* edf is the estimated degree of freedom accounting for the smoothing function.
# Deviance explained by the model with all factors.
§ Significance of P-level (experimental set-up 1) and P and DOC levels (experimental set-up 2) on the response variable. Significant codes: *** <0.001; ** <0.01; * <0.05.

Table S2. Results from analysis of covariance (ANCOVA) using data from the two experiments.

Variable tested	explanatory	Estimate	t-value	p-value	R^2_{adj}	p-value
Experimental set-up 1						
total CO_2 production	DOC	2.946	5.650	<0.001	0.553	<0.001
	P	-17.90	-1.227	0.232		
16S rRNA gene copy number	DOC	1.93×10^8	2.305	0.0301	0.642	<0.001
	P	1.57×10^{10}	6.690	<0.001		
copy number specific respiration	DOC	-16.1	-0.811	0.425	0.626	<0.001
	P	0.374	-6.730	<0.001		
maximum CO_2 production rates	DOC	0.028	4.724	<0.001	0.531	<0.001
	P	0.539	3.257	<0.005		
Experimental set-up 2						
maximum O_2 consumption rate	DOC	0.554	1.784	0.077	0.563	<0.001
	P	0.365	11.415	<0.001		
	Temperature	3.903	7.270	<0.001		

Paper III

AGU PUBLICATIONS

Geophysical Research Letters

RESEARCH LETTER
10.1002/2016GL069621

Key Points:
- Photoprocessed DOC is consumed at higher bacterioplankton RQ than nonphotoprocessed DOC
- Bacterioplankton RQ depends on the chemical composition of the assimilated organic substrate pool
- Faulty assumption of RQ = 1 in light-exposed water greatly underestimates bacterioplankton respiration

Supporting Information:
- Supporting Information S1

Correspondence to:
L. Allesson,
lina.allesson@ibv.uio.no

Citation:
Allesson, L., L. Ström, and M. Berggren (2016), Impact of photochemical processing of DOC on the bacterioplankton respiratory quotient in aquatic ecosystems, *Geophys. Res. Lett.*, *43*, 7538–7545, doi:10.1002/2016GL069621.

Received 18 MAY 2016
Accepted 27 JUN 2016
Accepted article online 29 JUN 2016
Published online 16 JUL 2016

Impact of photochemical processing of DOC on the bacterioplankton respiratory quotient in aquatic ecosystems

Lina Allesson[1,2], Lena Ström[1], and Martin Berggren[1]

[1]Department of Physical Geography and Ecosystem Science, Lund University, Lund, Sweden, [2]Department of Biosciences, University of Oslo, Oslo, Norway

Abstract Many studies assume a respiratory quotient (RQ = molar ratio of CO_2 produced to O_2 consumed) close to 1 when calculating bacterioplankton respiration. However, evidence suggests that RQ depends on the chemical composition of the respired substrate pool that may be altered by photochemical production of oxygen-rich substrates, resulting in elevated RQs. Here we conducted a novel study of the impact of photochemical processing of dissolved organic carbon (DOC) on RQ. We monitored the bacterial RQ in bioassays of both ultraviolet light irradiated and nonirradiated humic lake water, using optic gas-pressure sensors. In the experimentally irradiated samples the average RQ value was significantly higher (3.4–3.5 [±0.4 standard error (SE)]) than that in the dark controls (1.3 [±0.1 SE]). Our results show that the RQ is systematically higher than 1 when the bacterial metabolism in large part is based on photoproducts. By assuming an RQ of 1, bacterioplankton respiration in freshwater ecosystems may be greatly underestimated.

1. Introduction

Most inland waters worldwide are supersaturated with carbon dioxide (CO_2), driving a globally significant (~ 1–2 Pg C yr^{-1}) CO_2 flux to the atmosphere [*Cole et al.*, 1994; *Raymond et al.*, 2013]. Several processes contribute to this CO_2, including groundwater input [*Humborg et al.*, 2010], sediment respiration [*Gudasz et al.*, 2010], and photochemical mineralization of dissolved organic carbon (DOC) [*Koehler et al.*, 2014], but often bacterioplankton respiration (BR; release of CO_2 per unit water volume and time) fueled by DOC is dominating the CO_2 production in the water column [*Jansson et al.*, 2000; *Sobek et al.*, 2003; *Yang et al.*, 2015]. It has been estimated that BR could be the single most important organic carbon mineralization process in the biosphere [*Williams and del Giorgio*, 2005]. However, there are methodological uncertainties in the measurement of BR, leading to a lack of understanding of the carbon cycle, especially in freshwaters [*Humborg et al.*, 2010]. A key uncertainty in the determination of BR is the assumption of a respiratory quotient (RQ), i.e., a certain fixed amount of respiratory CO_2 produced per unit measured O_2 consumption [*Gaarder and Gran*, 1927].

Throughout the history of BR assessments, indirect assessments based on dissolved oxygen (O_2) consumption measurements [*Winkler*, 1888] have been favored over direct CO_2 production measurements [*del Giorgio et al.*, 2011; *Marchand et al.*, 2009]. The O_2 method is advantageous because it can be performed on the aqueous phase, without gas extraction, and it avoids the need to correct for changing equilibria within the carbonic acid system ($CO_2 \leftrightarrow HCO_3^- \leftrightarrow CO_3^{2-}$). Moreover, the predominant analytical techniques for O_2 are typically cost efficient, accurate, and easy to use (Winkler, electrode, and optode methods) or in some cases extremely highly resolved, e.g., using membrane inlet mass spectroscopy [*Kana et al.*, 1994]. Therefore, still today the RQ remains a required conversion factor to transform respiration rates measured as O_2 consumption into carbon units.

Although generically assumed at a fixed value close to 1, true bacterioplankton RQ can vary greatly [*Berggren et al.*, 2012; *Cimbleris and Kalff*, 1998; *Romero-Kutzner et al.*, 2015]. For example, the RQ is affected by biochemical pathways of metabolism, where anabolic processes (cell growth) contribute to higher RQs than catabolic respiration alone [*Berggren et al.*, 2012; *Dilly*, 2003]. More importantly, RQ is strongly dependent on the composition of the assimilated organic substrate [*Berggren et al.*, 2012; *Romero-Kutzner et al.*, 2015], especially the O and H content [*Dilly*, 2001]. Assimilation of organic substrates with large O content and high O:H ratio requires less O_2 from the surroundings, and hence, respiration is performed at a relatively high RQ.

Photochemical processes in aquatic ecosystems may represent the most important source of oxygen-rich low molecular weight (LMW) compounds available for consumption by bacterioplankton [*Bertilsson and*

Table 1. Stoichiometry of Complete Aerobic Oxidation of Selected Compounds

Compound	Chemical Equation	CO_2 Produced	O_2 Consumed	RQ
Methane	$CH_4 + 2\ O_2 \rightarrow CO_2 + 2\ H_2O$	1	2	0.5
Glucose	$C_6H_{12}O_6 + 6\ O_2 \rightarrow 6\ CO_2 + 6\ H_2O$	6	6	1
Succinic acid[a]	$C_4H_6O_4 + 3.5\ O_2 \rightarrow 4\ CO_2 + 3\ H_2O$	4	3.5	1.14
Citric acid[a]	$C_6H_8O_7 + 4.5\ O_2 \rightarrow 6\ CO_2 + 4\ H_2O$	6	4.5	1.33
Glycolic acid[a]	$C_2H_4O_3 + 1.5\ O_2 \rightarrow 2\ CO_2 + 2\ H_2O$	2	1.5	1.33
Malic acid[a]	$C_4H_6O_5 + 3\ O_2 \rightarrow 4\ CO_2 + 3\ H_2O$	4	3	1.33
Tartaric acid[a]	$C_4H_6O_6 + 2.5\ O_2 \rightarrow 4\ CO_2 + 3\ H_2O$	4	2.5	1.6
Formic acid[a]	$CH_2O_2 + 0.5\ O_2 \rightarrow CO_2 + H_2O$	1	0.5	2
Oxalic acid[a]	$C_2H_2O_4 + 0.5\ O_2 \rightarrow 2\ CO_2 + H_2O$	2	0.5	4

[a]LMW organic acids detected in this study.

Tranvik, 1998]. Several of the most common LMW compounds that are released from reactions between DOC and ultraviolet (UV) sunlight are theoretically oxidized at RQs between 1.3 and 4 (see examples in Table 1). Although photooxidation is known to be an important process in natural freshwater systems, e.g., directly contributing to up to about 10% of the CO_2 efflux from lakes and reservoirs to the atmosphere [*Koehler et al*., 2014], its potential role as RQ regulator has to our knowledge never been addressed. If partial photooxidized DOC compounds represent a major source of carbon for inland water bacteria, then the natural RQs are likely higher than 1 and the CO_2 production is systematically underestimated even on a global scale [*Williams and del Giorgio*, 2005].

The commonly applied RQ of 1 corresponds to complete oxidation of glucose (Table 1), but it is also close to the theoretical RQ for complete oxidation of bulk natural DOC [*Dilly*, 2001]. However, bacterioplankton do not normally make use of the bulk pool of DOC, especially not humic fractions, but instead use small selected fractions that are easy to assimilate [*Berggren et al*., 2007]. These compounds contain various proportions of O and H, resulting in a potential range in RQ from 0.7 to 0.8 for phytoplankton-derived DOC [*Berggren et al*., 2012] to far above 1 for many photoproduced organic acids (Table 1). Thus, the theoretical RQ for complete oxidation of bulk DOC pools may tell us little about the actual RQs, resulting in errors when estimating BR.

In this study, we therefore test the impact of UV radiation on bacterioplankton RQ hypothesizing that photochemically processed DOC is used at a higher RQ than nonirradiated DOC because bacteria assimilate highly oxidized photoproducts such as organic acids. To test this hypothesis, we conducted biological incubations of both irradiated and nonirradiated samples of natural lake water, simultaneously measuring the changes in O_2 and CO_2 to obtain the RQ. To confirm that the photochemical processes contributed to increased concentrations of LMW organic acids (LMWOAs), we also measured concentrations of common LMWOAs in all samples, before and after UV treatment. We expected that the bacterioplankton RQ would be significantly higher than 1 after UV treatment and around 1 in nonirradiated samples (obtained from natural humic lake waters).

2. Methods

2.1. Study Site and Sampling

Samples were collected from four brown-water, humic lakes in northern Sweden during 14 and 21 August 2014 (for lake data see supporting information Table S1). The catchments are dominated by coniferous forest, mainly Norway spruce (*Picea abies*, *L*.; 80%) and *Sphagnum* peatmires (20%). The lakes can be considered representative for unproductive humic lakes in the boreal zone, characterized by low productivity and high degrees of CO_2 supersaturation [*Jansson et al*., 2000]. We can assume that DOC in the samples was dominated by allochthonous sources [*Karlsson et al*., 2012]. In the laboratory, the water was sterile filtered through a 0.22 μm pore size filter (Sartorius Stedim Biotech, NY) and kept cold 4°C until further analyses.

2.2. Study Design

Before the experiments, the samples were transferred into 300 mL acid washed Ehrlenmeyer flasks and sparged with synthetic air (N_2 and O_2) to remove CO_2 supersaturation. The samples were then inoculated with 1 mL of a fresh unfiltered mix of water from the study lakes and their inlets, in equal proportions. The

filled flasks were closed using ground glass joints, leaving no headspace, and additionally sealed with parafilm to avoid diffusion of CO_2. Biological incubations were carried out in the dark with both irradiated water and ambient lake water controls in a climate chamber (PU-3 J high performance chamber, ESPEC, Japan) keeping a stable temperature of 20°C (±0.1°C). In each experiment, one sample per lake was incubated.

The experiment consisted of three parts. (1) *Irradiated*: the water was first irradiated during 48 h followed by 48 h of biological incubation. (2) *Biological + irradiated*: the samples were first incubated in the dark for 48 h followed by 48 h of UV treatment and then finally biologically incubated for 48 h. (3) *Dark control*: the samples were biologically incubated in the dark for 144 h. The longer incubation time was chosen to mirror the time of the second treatment, controlling that a possible change in RQ was due to bacterial consumption of photochemical processed DOC and not incubation time.

2.3. Biological Incubations and Bacterial Respiration

Depending on the alkalinity and pH in the system, a certain share of the respiratory CO_2 dissociates in the water, forming bicarbonate and carbonate ions [*Stumm and Morgan*, 1996]. To cover the total CO_2 ($TCO_2 = CO_2 + HCO_3^- + CO_3^{2-}$) production during BR measurements, the impact of the carbonate system on CO_2 hence needs to be corrected for. Either the CO_2 concentrations can be measured and used to calculate the pH-induced changes in ionization fractions, or the change in pH during a bioassay can be measured and used directly to calculate the TCO_2 production (see supporting information Text S1 for details). In this study, we measured BR through changes in pH (decreasing as CO_2 is produced) in the water samples using noninvasive optical pH sensor spots placed in the bottom of each flask with a SensorDish Reader (SDR: resolution: 0.05 units; PreSens GmbH, Regensburg, Germany). Each lake was considered a replicate. In order to obtain the same starting point pH was standardized to the range 6.5–7, by adding 0.2 M NaOH. Bacterial O_2 consumption was measured with an "oxy-10 system" (resolution: best: ± 0.14 μM at 2.83 μM and worst: ± 1.14 μM at 283 μM; PreSens GmbH, Regensburg, Germany), recording the concentration of dissolved oxygen every 5 min with optic sensor spots glued on to the inside of the flasks [*Marchand et al*., 2009].

Bacterial communities have a short establishment time and previous studies have shown that a total of 48 h of incubation time is sufficient to acquire enough data to analyze the bacterial respiration [*Berggren et al*., 2012; *Cimbleris and Kalff*, 1998]. To let the sensors equilibrate and reach a stable reading and allow the bacteria to establish, we waited 10–12 h before starting any gas measurements. The impact of photoproduced hydrogen peroxide and other reactive oxygen species could be neglected in our measurements due to their relatively short half-life under nonsterile, aerobic conditions [*Tranvik and Kokalj*, 1998], assuming they disappeared during the sensor equilibration time. Since the measurement range of the optical pH sensors was 5.5–8.5, some data points in irradiated samples with high rates of CO_2 production were lost, as the incubation pH in these samples sometimes reached very low values ($pH < 5.5$).

2.4. Irradiation Incubations

Before irradiation the water samples were transferred to 1000 mL quartz glass bottles (Chemglass Life Sciences, Vineland, NJ). The samples were thereafter placed vertically on a spinning disk (0.67 rpm) under UV lamps and incubated for 48 h in a climate chamber kept at 20 ± 1°C. The radiation was within 3.64–6.89 Wm^{-2} for UV-A and 0.06–0.1 Wm^{-2} for UV-B, which is roughly representative to average daytime radiation during summer in northern Sweden. Since the disk was spinning, all samples received the same amount of light. Photochemical processing produces CO2, alters the gas equilibration and may damage the microorganisms [*Anesio and Granéli*, 2003]. Therefore, inoculation was performed again following each UV treatment.

2.5. Chemical Analyses

Determination of LMWOAs was made using a liquid ion chromatography-ionspray tandem mass spectrometry system (IC-MS). The system consisted of a Dionex (Sunnyvale, CA, USA) ICS-2500 liquid chromatography system and an Applied Biosystems (Foster City, CA, USA) 2000 Q-trap triple quadrupole mass spectrometer. The method is described in further detail in *Ström et al*. [2012].

For IC-MS analysis of LMWOA, subsamples of ~ 10 mL were sampled before start of each irradiation treatment (data not shown) and twice during each biological treatment, at the beginning and end, respectively. To replenish the water in the Ehrlenmeyer flasks after subsampling, water treated identically and in parallel to the water samples being monitored were incubated at the side and used for this purpose. The subsamples

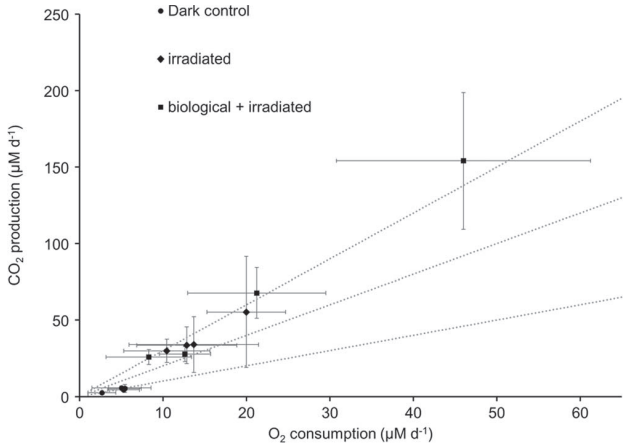

Figure 1. Plot of the daily increase in CO_2 concentration versus the daily decrease in O_2 concentration (in absolute numbers). Error bars represent the standard error and grey dotted reference lines from below represent RQs of 1, 2, and 3, respectively.

were filtered through 0.22 µm pore size filters, prerinsed with 30 mL of distilled water to remove any LMWOA contaminants, and deep frozen until further analysis.

Analyses of DOC were performed on 0.45 µm filtered water samples (30 mm Polyethersulfone (PES) membrane filters, Thermo scientific, MA, USA) using a TOC-VCPN (Shimadzu, Japan). Alkalinity (µeq L^{-1}) was defined and measured as the amount HCl (µmol) that was consumed per liter sample water during titration with 0.1 M HCl to an endpoint of pH 4.5.

2.6. Calculations and Statistics

The TCO_2 production was calculated from the change in pH together with the known alkalinity in the water samples, using the equations from *Stumm and Morgan* [1996]. We thus accounted for all CO_2 production in the samples, i.e., both the share that was transformed into carbonates and the share that stayed as dissolved CO_2. The concentrations of the different species were calculated using well-established temperature-dependent empirical equilibration constants (the uncertainty in these constants was considered negligible). The pH measurements were averaged over 5 h and TCO_2 concentrations were calculated for each 5 h pH value with the standard deviation (SD) representing the spread in the measurements (Figure 1). The RQ was then calculated as the TCO_2 production divided by the O_2 consumption during the five hour intervals in each sample and incubation. The standard error (SE) of the RQ was calculated as the SD divided by the square root of the number of observations.

The calculated RQs were compared through a repeated measures analysis of variance (ANOVA) followed by a Tukey HSD post hoc test to compare the RQs of the different treatments. In order to test whether the RQs obtained were significantly different from 1, a one sample *t* test (two tailed) was performed.

The concentrations of the different LMWOAs that would give rise to a theoretical RQ $>$ 1 were summed and converted to concentrations of carbon per liter (µM C) in the samples for each incubation period. A correlation analysis between the concentrations and the RQ values was then performed. All statistical tests were performed using R [*R Development Core Team*, 2015].

3. Results

The pH decreased significantly over time in all bioassays, allowing us to calculate the release of CO_2 from BR. In bioassays with irradiated water, the CO_2 production was remarkably high. With a range between lakes of 27–52 µM d^{-1} in the first trial (irradiated) and of 25–130 µM d^{-1} in the second trial (biological and irradiated), the CO_2 production was one order of magnitude higher than the nonirradiated dark controls (range 2.6–6.6 µM d^{-1}). Therefore, although intended to be 48 h, some of these bioassays had to be aborted after 20–30 h (depending on the alkalinity of the lake water; Table S1 and Figure S1 in the supporting information) as the lower limit of the pH sensors was approached.

Similar to the pattern for CO_2, the O_2 consumption rates were consistently higher in irradiated samples than in nonirradiated dark controls. The highest rates were measured in the second trial (biological + irradiated) ranging between 8.7 and 46.0 µM d^{-1} (Figure 1). Following the initial equilibration time, the O_2 consumption rates were stable and linear. Similarly, the CO_2 production rates were mostly stable throughout the experiment, although showing some increase toward the end of the incubation time in bioassays with especially high rates (Figure S1 in the supporting information).

Table 2. RQ Values With Standard Deviations and Organic Acids Carbon Concentration During the Different Treatments and for All Four Lakes[a]

Lake and Treatment	RQ (± SE)	Organic Acids[b] (μM C)
	Övre Björntjärn	
Dark control	1.2 (±0.1)	5.6
Irradiated	4.1 (±1.0)	8.0
Biological + irradiated	3.9 (±0.9)	8.0
	Nedre Björntjärn	
Dark control	1.0 (±0.1)	6.1
Irradiated	3.5 (±0.4)	11.5
Biological + irradiated	2.3 (±0.2)	7.6
	Lillsjöliden	
Dark control	1.6 (±0.2)	5.7
Irradiated	3.5 (±0.5)	10.3
Biological + irradiated	3.7 (±0.7)	10.5
	Stortjärn	
Dark control	1.3 (±0.2)	6.1
Irradiated	3.1 (±0.6)	7.8
Biological + irradiated	4.1 (±0.5)	6.4
	All Lakes	
Dark control	1.3 (±0.1)	
Irradiated	3.5[a] (±0. 4)	
Biological + irradiated	3.4[a] (±0.4)	

[a]The analysis was performed using repeated measures ANOVA ($F_{2,6} = 32.32$, $p < 0.001$) with a Tukey HSD post hoc test. RQ in irradiated samples were significantly higher than in dark controls (dark control—irradiated $p < 0.0001$, $df = 28$; dark control—biological + irradiated $p < 0.0001$, $df = 26$).
[b]Organic acid concentrations represent the mean of two measurements performed during different time points of the bioassays. Concentrations were not systematically different between these time points.

Dark controls showed an average RQ of 1.3, significantly different from 1 (one sample t test, $t = 2.96$, $p = 0.004$). Furthermore, the RQ in irradiated samples was significantly ($p < 0.0001$) higher than the dark controls, with mean values of 3.5 (±0.4 SE) and 3.4 (±0.4 SE) for water irradiated directly (irradiated) and water irradiated after biological incubation (biological + irradiated) respectively (Table 2). Thus, also in the second trial (biological + irradiated) we could see a shift in the RQ from before to after UV treatment.

A number of LMWOAs that theoretically are oxidized at an RQ above 1 were found in the IC-MS analysis (Table 1). The concentrations of these acids were slightly higher in irradiated than in nonirradiated samples (Table 2) indicating that there was a production of LMWOAs due to photochemical processing of DOC. There was a significant positive correlation between bacterioplankton RQ and the concentration of LMWOAs ($r^2 = 0.718$; $p < 0.01$; $n = 12$; Figure S2 in the supporting information). However, the apparent production of LMWOA during UV treatment (difference in concentrations measured before and after) was relatively low compared to the large amount of CO_2 production that was recorded during biological incubation of irradiated samples. In the nonirradiated dark controls, the concentration of LMWOAs was 5.6–6.1 μM C, while in the irradiated samples the ranges were 7.7–11.2 μM C in the first trial (irradiated) and 6.5–10.5 μM C in the second trial (biological + irradiated) (Table 2 and Figure S2 in the supporting information). These organic acid concentrations corresponded to 19–48% of the cumulative CO_2 production in nonirradiated samples and 6–24% of the corresponding production in irradiated water.

4. Discussion

Our results clearly show that the bacterioplankton respiratory quotient (RQ) is elevated during degradation of photochemically processed DOC compared to dark controls. The RQ in the same lake water samples shifted from slightly above 1 before irradiation to exceeding 3 after UV light treatment of the water. We further found that the irradiation greatly boosted the CO_2 production rates during biological incubations (approximately tenfold increase, on average, compared to nonirradiated dark control incubations), which implies that photoaltered DOC was strongly dominating as substrate after irradiation. In agreement with our hypothesis, we observed relatively high concentrations of LMWOAs in UV light treated water, in parallel to the elevated RQs, and there was an overall positive correlation between RQ and the total LMWOA concentration. These results imply that the estimates of the contribution to CO_2 by bacterioplankton are greatly underestimated assuming an RQ of 1 in naturally light-exposed aquatic ecosystems.

From a mass balance perspective, however, the elevated RQ values found in irradiated samples could only partially be explained by bacterial use of LMWOAs, because the measured photoproduction of LMWOAs was too small to account for the photostimulated CO_2 release. Moreover, we systematically observed photostimulated RQs above 3, which is higher than the expected theoretical RQs—mostly below 2—for oxidation of the LMWOAs that were produced (Table 1). Although other studies have observed higher photoproduction

rates of LMWOAs than we did [*Bertilsson and Tranvik*, 2000], it is evident from our results that analyses of organic acids alone provide limited possibilities for explaining the large amounts of CO_2 released during biological processing of irradiated water (Figure S2 in the supporting information). Thus, the change in RQ that we observed was not only dependent on LMWOA production but most likely also by production and modification of a broader range of DOC molecules. This conclusion is supported by the previous study by *Miller and Moran* [1997] which observed biological degradation of photoaltered DOC exceeding the detected LMWOA production by 90%. Therefore, a recommendation for future RQ studies is to combine LMWOA measurements with chemical characterizations of the bulk DOC pool and to assess changes in the oxidation state of the entire substrate pool by performing a redox balance.

In highly humic (dark) lakes, natural UV light only penetrates a few centimeters into the water column and the majority of photochemical reactions hence take place at the surface layers. Nonetheless, photochemically produced carboxylic acids have been shown to be a major source of labile DOC over the entire mixed zone [*Bertilsson and Tranvik*, 1998]. The dark control RQ exceeded 1 (1.3 ± 0.1), which is in agreement with the average RQ of a number of humic rich lakes in Québec [*Berggren et al*., 2012] and may reflect the downward mixing of photochemically altered DOC in the lakes.

It should be noted that all substrates that are assimilated are not oxidized by the microorganisms into CO_2 but instead used for production of biomass [*Biddanda et al*., 1994; *del Giorgio and Cole*, 1998]. In soil ecosystems, increases in microbial growth under glucose amended conditions have resulted in elevated RQs up to 1.5 [*Dilly*, 2003]. In lakes, bacterial consumption of photoprocessed DOC has been shown to result in enhanced microbial biomass production [*Amado et al*., 2015; *Anesio et al*., 2005], which could give a positive marginal effect on RQ similar to what has been observed in soils. However, in this study bacterial production was not measured and it can only be speculated that enhanced biomass production might have partly contributed to the high RQ values observed in UV treated compared to dark samples. Nonetheless, considering the vastly elevated RQs that we observed, a shift in substrate pool due to partial photooxidation is more likely to have had an overriding impact on the bacterial RQ than physiological processes that tend to have only marginal effects [*Romero-Kutzner et al*., 2015].

The consistently much higher RQ values that we observed in the irradiated samples reflect a mechanism that should be present in all light-exposed DOC-rich aquatic ecosystems around the globe. The relative importance of photomineralization to partial photooxidation of DOC is dependent on the age of the compounds and the intensity of the incoming solar radiation [*Cory et al*., 2013, 2014; *Vähätalo et al*., 2003]. Photochemical mineralization of DOC to CO_2 represents up to about 10% of the total CO_2 emissions from lakes and reservoirs globally [*Koehler et al*., 2014] and studies of photochemical processing of DOC have reported partial photooxidation possibly be as important as photomineralization [*Bertilsson and Tranvik*, 2000]. In water samples from a coastal marine environment, *Miller and Moran* [1997] found DOC losses from photochemical gas formation to be approximately equal to the losses from microbial consumption of labile photoproducts. Applying an underestimated RQ value would thus lead to large amounts of CO_2 from BR being missed, given that labile photoproducts require little dissolved oxygen to degrade. There is extensive evidence of microbial consumption of photoproduced LMW compounds [*Bertilsson and Tranvik*, 2000; *Judd et al*., 2007]. In long term bioassays (years), simulating water residence times in lakes, *Vähätalo and Wetzel* [2008] showed that exposure to solar radiation followed by bacterial degradation depleted all humic DOC (99.7%). It must thus be expected that bacterioplankton in natural waters will consume photoproducts and most likely, according to our results, at an RQ significantly exceeding 1.

5. Summary, Conclusions, and Recommendations

Biological incubations of water with photochemically processed DOC lead to enhanced RQ values compared to nonirradiated dark controls. The RQ was consistently higher than 1 in irradiated samples and the CO_2 production rates exceeded the rates in nonirradiated dark controls several fold. In fact, we could see a clear shift in RQ from slightly above 1 before to exceeding 3 after UV treatment. The elevated RQ values may partly be explained by bacterial consumption of single photoproduced LMWOAs but, more likely, also by a general shift in oxidation state of the bulk substrate pool. Our results indicate that by the use of a fixed RQ value of 1, bacterioplankton respiration in inland waters may be globally underestimated. Therefore, we cannot recommend the a priori assumption of an RQ value for a lake to estimate the BR from dissolved oxygen

consumption. For future respiration studies we suggest to either determine the RQ or to measure the CO_2 production directly instead of measuring the O_2 consumption. The possible loss of information due to less accurate and more cumbersome methods for measuring CO_2 compared to measuring O_2 is most probably not as severe as the uncertainty accompanying the assumption of a faulty RQ value.

Acknowledgments
We would like to thank Marcin Jackowicz-Korczynski, Oskar Ström, and Julia Jakobsson for their assistance in sample analysis. Ander Jonsson, Marcus Klaus, and Erik Lundin assisted in the sample collection. We further thank Jan Karlsson for valuable discussions. The work was financially supported through project grants from KSLA (grant H13-0020-GBN), Helge Ax:son Johnson's Foundation (grant 140622), FORMAS (project "Managing multiple stressors in the Baltic sea," 217-2010-126) and LUCCI (Lund University Centre for studies of Carbon cycle and Climate Interactions). The data used are listed in the references, tables, and supporting information.

References

Amado, A., J. Cotner, R. Cory, B. Edhlund, and K. McNeill (2015), Disentangling the interactions between photochemical and bacterial degradation of dissolved organic matter: Amino acids play a central role, *Microb. Ecol.*, *69*(3), 554–566, doi:10.1007/s00248-014-0512-4.

Anesio, A. M., and W. Granéli (2003), Increased photoreactivity of DOC by acidification: Implications for the carbon cycle in humic lakes, *Limnol. Oceanogr.*, *48*(2), 735–744.

Anesio, A. M., W. Granéli, G. R. Aiken, D. J. Kieber, and K. Mopper (2005), Effect of humic substance photodegradation on bacterial growth and respiration in lake water, *Appl. Environ. Microbiol.*, *71*(10), 6267–6275, doi:10.1128/AEM.71.10.6267-6275.2005.

Berggren, M., H. Laudon, and M. Jansson (2007), Landscape regulation of bacterial growth efficiency in boreal freshwaters, *Global Biogeochem. Cycles*, *21*, GB4002, doi:10.1029/2006GB002844.

Berggren, M., J.-F. Lapierre, and P. A. del Giorgio (2012), Magnitude and regulation of bacterioplankton respiratory quotient across freshwater environmental gradients, *ISME J.*, *6*(5), 984–993, doi:10.1038/ismej.2011.157.

Bertilsson, S., and L. J. Tranvik (1998), Photochemically produced carboxylic acids as substrates for freshwater bacterioplankton, *Limnol. Oceanogr.*, *43*(5), 885–895, doi:10.4319/lo.1998.43.5.0885.

Bertilsson, S., and L. J. Tranvik (2000), Photochemical transformation of dissolved organic matter in lakes, *Limnol. Oceanogr.*, *45*(4), 753–762, doi:10.4319/lo.2000.45.4.0753.

Biddanda, B., S. Opsahl, and R. Benner (1994), Plankton respiration and carbon flux through bacterioplankton on the Louisiana shelf, *Limnol. Oceanogr.*, *39*(6), 1259–1275.

Cimbleris, A. P., and J. Kalff (1998), Planktonic bacterial respiration as a function of C:N:P ratios across temperate lakes, *Hydrobiologia*, *384*(1-3), 89–100, doi:10.1023/A:1003496815969.

Cole, J. J., N. F. Caraco, G. W. Kling, and T. K. Kratz (1994), Carbon dioxide supersaturation in the surface waters of lakes, *Science*, *265*(5178), 1568–1570, doi:10.1126/science.265.5178.1568.

Cory, R. M., B. C. Crump, J. A. Dobkowski, and G. W. Kling (2013), Surface exposure to sunlight stimulates CO_2 release from permafrost soil carbon in the Arctic, *Proc. Natl. Acad. Sci. U.S.A.*, *110*(9), 3429–3434, doi:10.1073/pnas.1214104110.

Cory, R. M., C. P. Ward, B. C. Crump, and G. W. Kling (2014), Sunlight controls water column processing of carbon in arctic fresh waters, *Science*, *345*(6199), 925–928, doi:10.1126/science.1253119.

del Giorgio, P. A., and J. J. Cole (1998), Bacterial growth efficiency in natural aquatic systems, *Annu. Rev. Ecol. Syst.*, *29*, 503–541, doi:10.1146/annurev.ecolsys.29.1.503.

del Giorgio, P. A., R. Condon, T. Bouvier, K. Longnecker, C. Bouvier, E. Sherr, and J. M. Gasol (2011), Coherent patterns in bacterial growth, growth efficiency, and leucine metabolism along a northeastern Pacific inshore-offshore transect, *Limnol. Oceanogr.*, *56*(1), 1–16, doi:10.4319/lo.2011.56.1.0001.

Dilly, O. (2001), Microbial respiratory quotient during basal metabolism and after glucose amendment in soils and litter, *Soil Biol. Biochem.*, *33*(1), 117–127.

Dilly, O. (2003), Regulation of the respiratory quotient of soil microbiota by availability of nutrients, *FEMS Microbiol. Ecol.*, *43*(3), 375–381, doi:10.1016/s0168-6496(02)00437-3.

Gaarder, T., and H. H. Gran (1927), *Investigations of the Production of Plankton in the Oslo Fjord*, Copenhague Høst en comm.

Gudasz, C., D. Bastviken, K. Steger, K. Premke, S. Sobek, and L. J. Tranvik (2010), Temperature-controlled organic carbon mineralization in lake sediments, *Nature*, *466*(7305), 478–481, doi:10.1038/nature09186.

Humborg, C., C.-M. Morth, M. Sundbom, H. Borg, T. Blenckner, R. Giesler, and V. Ittekkot (2010), CO_2 supersaturation along the aquatic conduit in Swedish watersheds as constrained by terrestrial respiration, aquatic respiration and weathering, *Global Change Biol.*, *16*(7), 1966–1978, doi:10.1111/j.1365-2486.2009.02092.x.

Jansson, M., A.-K. Bergström, P. Blomqvist, and S. Drakare (2000), Allochthonous organic carbon and phytoplankton/bacterioplankton production relationships in lakes, *Ecology*, *81*(11), 3250–3255, doi:10.1890/0012-9658(2000)081[3250:AOCAPB]2.0.CO;2.

Judd, K., B. Crump, and G. Kling (2007), Bacterial responses in activity and community composition to photo-oxidation of dissolved organic matter from soil and surface waters, *Aquat. Sci.*, *69*(1), 96–107, doi:10.1007/s00027-006-0908-4.

Kana, T. M., C. Darkangelo, M. D. Hunt, J. B. Oldham, G. E. Bennett, and J. C. Cornwell (1994), Membrane inlet mass spectrometer for rapid high-precision determination of N_2, O_2, and Ar in environmental water samples, *Anal. Chem.*, *66*(23), 4166–4170, doi:10.1021/ac00095a009.

Karlsson, J., M. Berggren, J. Ask, P. Byström, A. Jonsson, H. Laudon, and M. Jansson (2012), Terrestrial organic matter support of lake food webs: Evidence from lake metabolism and stable hydrogen isotopes of consumers, *Limnol. Oceanogr.*, *57*(4), 1042–1048, doi:10.4319/lo.2012.57.4.1042.

Koehler, B., T. Landelius, G. A. Weyhenmeyer, N. Machida, and L. J. Tranvik (2014), Sunlight-induced carbon dioxide emissions from inland waters, *Global Biogeochem. Cycles*, *28*, 696–711, doi:10.1002/2014GB004850.

Marchand, D., Y. T. Prairie, and P. A. Del Giorgio (2009), Linking forest fires to lake metabolism and carbon dioxide emissions in the boreal region of Northern Québec, *Global Change Biol.*, *15*(12), 2861–2873, doi:10.1111/j.1365-2486.2009.01979.x.

Miller, W. L., and M. A. Moran (1997), Interaction of photochemical and microbial processes in the degradation of refractory dissolved organic matter from a coastal marine environment, *Limnol. Oceanogr.*, *42*(6), 1317–1324, doi:10.4319/lo.1997.42.6.1317.

Raymond, P. A., et al. (2013), Global carbon dioxide emissions from inland waters, *Nature*, *503*(7476), 355–359, doi:10.1038/nature12760.

R Core Team (2015), R: A language and environment for statistical computing. R Foundation for statistical Computing, Vienna, Austria. [Available athttps://www.R-project.org/.]

Romero-Kutzner, V., T. T. Packard, E. Berdalet, S. O. Roy, J. P. Gagne, and M. Gomez (2015), Respiration quotient variability: Bacterial evidence, *Mar. Ecol. Prog. Ser.*, *519*, 47–59, doi:10.3354/meps11062.

Sobek, S., G. Algesten, A.-K. BergstrÖM, M. Jansson, and L. J. Tranvik (2003), The catchment and climate regulation of pCO2 in boreal lakes, *Global Change Biol.*, *9*(4), 630–641, doi:10.1046/j.1365-2486.2003.00619.x.

Ström, L., T. Tagesson, M. Mastepanov, and T. R. Christensen (2012), Presence of Eriophorum scheuchzeri enhances substrate availability and methane emission in an Arctic wetland, *Soil Biol. Biochem.*, *45*, 61–70, doi:10.1016/j.soilbio.2011.09.005.

Stumm, W., and J. Morgan (1996), *Chemical Equilibria and Rates in Natural Waters*, Interscience, New York.
Tranvik, L., and S. Kokalj (1998), Decreased biodegradability of algal DOC due to interactive effects of UV radiation and humic matter, *Aquat. Microb. Ecol.*, *14*(3), 301–307, doi:10.3354/ame014301.
Vähätalo, A. V., and R. G. Wetzel (2008), Long-term photochemical and microbial decomposition of wetland-derived dissolved organic matter with alteration of C-13 : C-12 mass ratio, *Limnol. Oceanogr.*, *53*(4), 1387–1392, doi:10.4319/lo.2008.53.4.1387.
Vähätalo, A. V., K. Salonen, U. Munster, M. Jarvinen, and R. G. Wetzel (2003), Photochemical transformation of allochthonous organic matter provides bioavailable nutrients in a humic lake, *Arch. Hydrobiol.*, *156*(3), 287–314, doi:10.1127/0003-9136/2003/0156-0287.
Williams, P. J. l. B., and P. A. del Giorgio (2005), Respiration in aquatic ecosystems: History and background, in *Respiration in Aquatic Ecosystems*, pp. 1–17, Oxford Univ. Press, Oxford, U. K., doi:10.1093/acprof:oso/9780198527084.003.0001.
Winkler, L. W. (1888), Die Bestimmung des im Wasser gelösten Sauerstoffes, *Ber. Dtsch. Chem. Ges.*, *21*(2), 2843–2854, doi:10.1002/cber.188802102122.
Yang, H., T. Andersen, P. Dörsch, K. Tominaga, J.-E. Thrane, and D. Hessen (2015), Greenhouse gas metabolism in Nordic boreal lakes, *Biogeochemistry*, *126*(1-2), 211–225, doi:10.1007/s10533-015-0154-8.

[Geophysical Research Letters]

Supporting Information for

[Impact of photo-chemical processing of DOC on the bacterial respiratory quotient in aquatic ecosystems]

[Lina Allesson, Lena Ström, Martin Berggren]

[Department of Physical Geography and Ecosystem Science, Lund University, Sweden]

Contents of this file

Description

In Methods S1 we describe how the pH and alkalinity of the lake water samples was used to assess the carbonic system and to calculate total CO_2 release from bacterial respiration. Table S1 contains information of the lake characteristics, such as DOC concentrations, alkalinity, lake area and depth. In Figure S1, the cumulative CO_2 production is plotted against the cumulative O_2 consumption for each lake and bioassay. Finally, Figure S2 shows the relationship between RQ and the total concentrations of organic acids during the bioassays.

Supporting Methods S1 – TCO_2 calculations from pH measurements

The carbonate system was modeled from the known pH, alkalinity and temperature of the samples, using the equations in Stumm and Morgan [1996]. The release of CO_2 by bacterial respiration (BR) causes formation of carbonate acid (H_2CO_3), in turn dissociating into HCO_3^-, CO_3^{2-} and H^+, lowering the pH of the system. Therefore, the BR was calculated as the change in TCO_2 ($CO_2 + HCO_3^- + CO_3^{2-}$) concentrations over time. In this study we used closed systems with no headspace, implying that any change in pCO_2 was caused by mineralization of DOC to CO_2. We considered that the release of CO_2 to the water did not affect the alkalinity since dissociation of CO_2 produces the same amount of negative and positive charges [*Stumm and Morgan*, 1996]. We further assumed that dissolved organic carbon (DOC) did not contribute significantly to the alkalinity. Thus, alkalinity was assumed to be constant during the bioassays, equaling the total charge of bicarbonate and carbonate ions. The concentrations and the ionization fractions of the different dissoved inorganic carbon species in the solution were obtained using existing empirical, temperature dependent constants of high accuracy [*Stumm and Morgan*, 1996].

Although the pH sensors had been recently calibrated by the manufacturer, we noted a slight systematic difference between measured output values and the true pH values for a range of buffer solutions, possibly caused by the optical properties of our incubation flasks. Therefore we used the measurements from the buffer solutions (pH 5.5, 6.5, 7.5, and 8.5) to perform a four point linear recalibration ($y = 0.9608*x + 0.5826$; $R^2 = 0.9942$).

Table S1. Study site information**.** Variables are self-explanatory or described elsewhere in the paper.

Lake name	Location	Elevation (m.a.s.l.)	Lake area (ha)	Lake depth, mean/max (m)	Lake peri-meter (m)	Catchment area (ha)	DOC (mM C)	Alkalinity (μeq L^{-1})	$CDOM_{440nm}$ (m^{-1})
Övre Björntjärn	64°12'N 18°78'E	336	4.8	4.0/8.0	1178	284.0	1.8	37	19.1
Nedre Björntjärn	64°12'N 18°78'E	336	3.2	6.0/9.7	893	324.9	2.3	75	17.0
Lillsjöliden	63°85'N 16°62'E	317	0.8	3.8/5.2	407	25.4	1.6	300	11.7
Stortjärn	64°26'N 19°76'E	284	3.9	2.7/6.7	1089	81.7	2.1	80	21.7

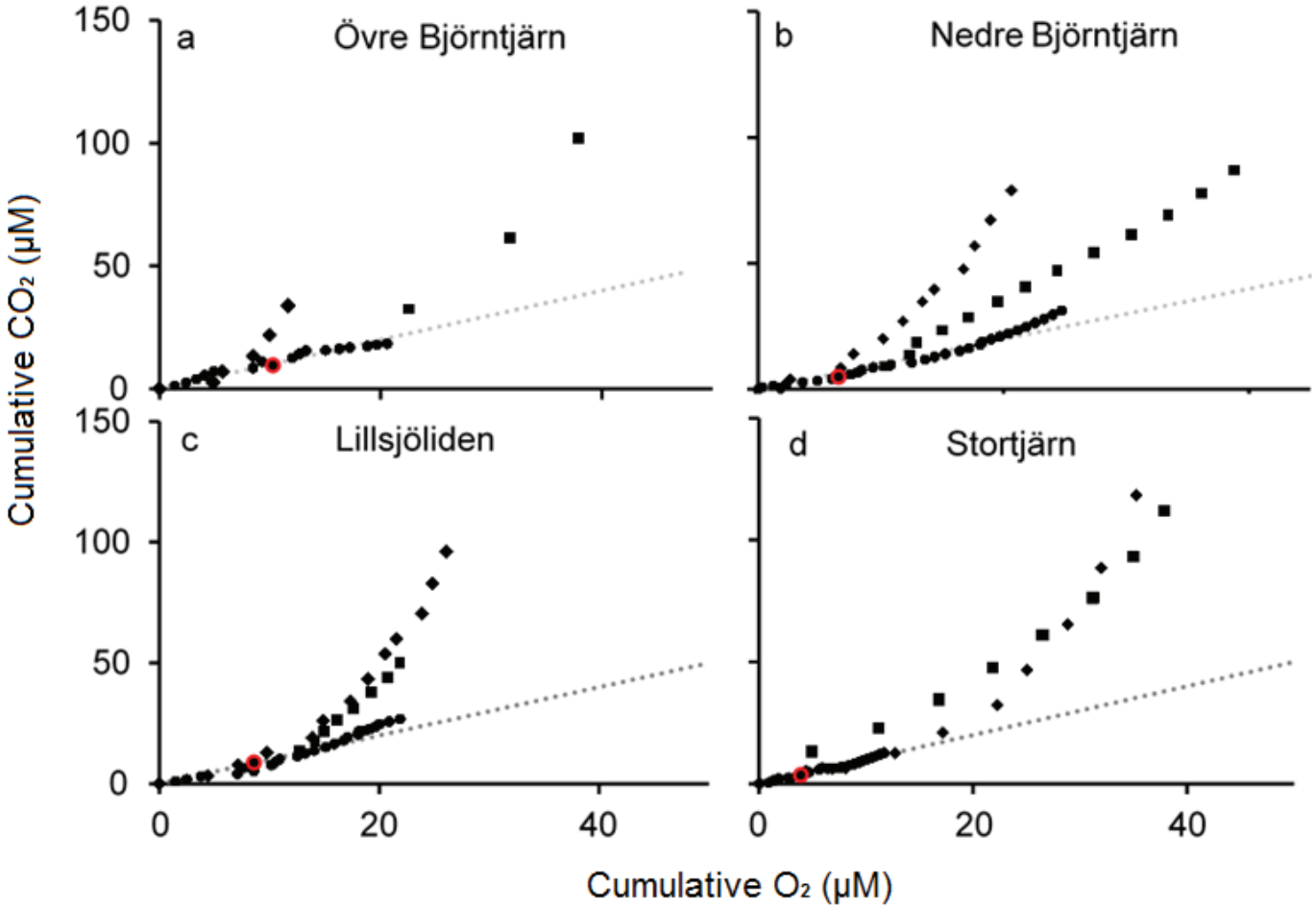

Figure S1. The cumulative CO_2 production plotted against the cumulative O_2 consumption in the bioassays. Circles represent 'dark controls', diamonds the 'irradiated' treatment and squares the 'biological + irradiated' samples (see main paper for explanations). The first 48 h of dark incubation in the 'biological + irradiated' treatment are overlapping with the dark control treatment. These curves therefore start after 48 h, at the points marked with red circles, illustrating the shift in RQ in these samples from before to after UV-treatment. The grey dotted line is the 1:1 reference line representing an RQ of 1.

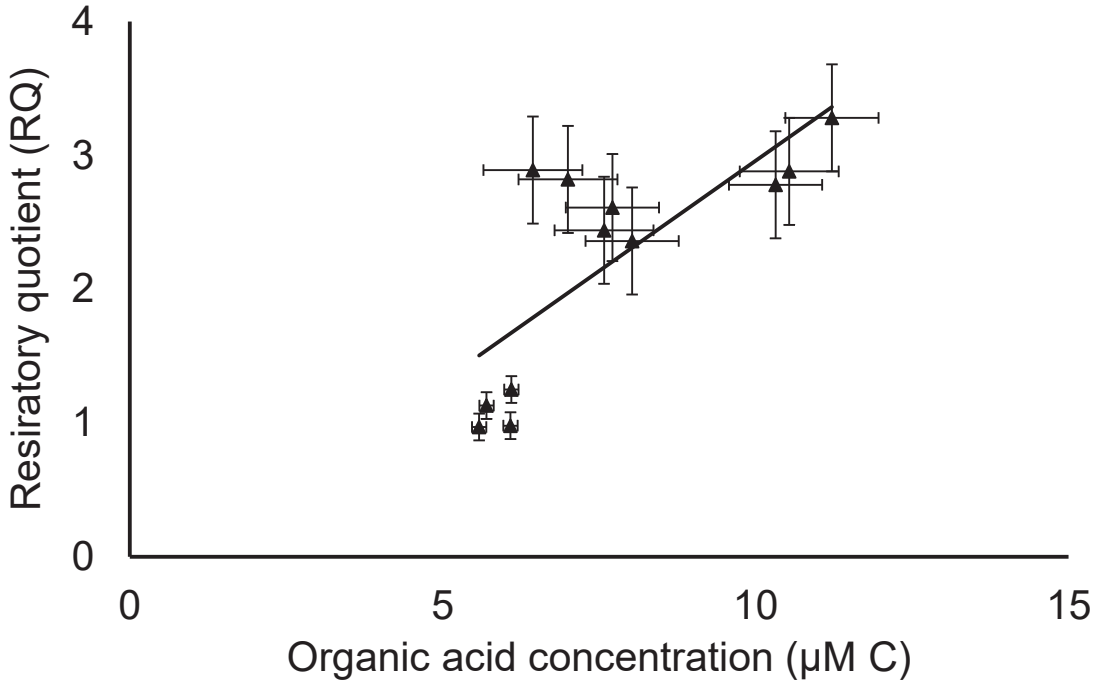

Figure S2. Correlation (r^2= 0.718; $p < 0.01$; n=12) between respiratory quotient (RQ) and the total concentration of carbon in measured organic acids. Symbols show means across the four study lakes and error bars display ± 1 standard errors of the means (see Table 2 in main paper).

Paper IV

Drivers and variability of CO_2:O_2 saturation along a gradient from boreal to Arctic lakes

Lina Allesson[1], Nicolas Valiente[1,2], Peter Dörsch[3], Tom Andersen[1], Alexander Eiler[1], Dag O. Hessen[1*]

[1]Centre for Biogeochemistry in the Anthropocene, Department of Biosciences, Section for Aquatic Biology and Toxicology, University of Oslo, 0316 Oslo, Norway

[2]Division of Terrestrial Ecosystem Research, Centre for Microbiology and Environmental Systems Science, University of Vienna, 1030 Vienna, Austria

[3]Faculty of Environmental Sciences and Natural Resource Management, Norwegian University of Life Sciences, 1432 Ås, Norway

[*]Corresponding author: Dag O. Hessen do.hessen@mn.uio.no

Abstract

Lakes are significant players for the global climate since they sequester terrestrially derived dissolved organic carbon (DOC), and emit greenhouse gases like CO_2 to the atmosphere. However, the differences in environmental drivers of CO_2 concentrations are not well constrained along latitudinal and thus climate gradients. Our aim here is to provide a better understanding of net heterotrophy and gas balance at the catchment scale. We assessed water chemistry and concentrations of dissolved O_2 and CO_2, as well as the CO_2:O_2 ratio in three groups of lakes separated by steps of approximately 10 degrees latitude in South-Eastern Norway (near 60 ^oN), sub-Arctic lakes in the northernmost part of the Norwegian mainland (near 70 ^oN) and high-Arctic lakes on Svalbard (near 80 ^oN). Across all regions, CO_2 saturation levels varied more (6 – 1374 %) than O_2 saturation levels (85 – 148 %) and hence CO_2 saturation governed the CO_2:O_2 ratio. The boreal lakes were generally undersaturated with O_2, while the sub-Arctic and high-Arctic lakes ranged from O_2 saturated to oversaturated. Regardless of location, the majority of the lakes were CO_2 supersaturated. In the boreal lakes the CO_2:O_2 ratio was mainly related to DOC concentration, in contrast to the

sub-Arctic and high-Arctic localities, where conductivity was the major statistical determinant. While the southern part is dominated by granitic and metamorphic bedrock, the sub-Arctic sites are scattered across a range of granitic to sedimentary bed rocks, and the majority of the high-Arctic lakes are situated on limestone, resulting in contrasting lake alkalinities between the regions. DOC dependency of the CO_2:O_2 ratio in the boreal region together with low alkalinity suggests that in-lake heterotrophic respiration was a major source of lake CO_2. Contrastingly, the conductivity dependency indicates that CO_2 saturation in the sub-Arctic and high-Arctic lakes was to a large part explained by DIC input from catchment respiration and carbonate weathering.

Keywords: Aquatic Biogeochemistry, CO_2 saturation, O_2 saturation, Lake Heterotrophy, Geology, Dissolved Organic Carbon

Acknowledgements
We are most grateful to our colleagues Camille Crapart, Jing Wei, Even Werner, and Laurent Fontaine for sampling assistance. The project has received grants from Centre for Biogeochemistry in the Anthropocene and the Belmont Forum project BiodivERsA, project no. 295367

Introduction

Oxygen (O_2) and carbon dioxide (CO_2) are key gases for life on Earth. Their ratio is mainly determined by the balance between heterotrophic and autotrophic processes in the biosphere. Under net autotrophic conditions, CO_2 is sequestrated in both terrestrial and aquatic ecosystems, thus decreasing atmospheric CO_2 concentrations and greenhouse effects on global climate. Lakes, and notably boreal lakes, are key players in this context since they convert a significant part of terrestrially derived organic carbon to CO_2 and CH_4 [1, 2]. A large share of CH_4 may also be converted to CO_2 by methanotrophs in the water column [3]. Simultaneous and complementary biological processes thus drive variations in O_2 and CO_2 concentrations [4, 5] and this coupling has led to the assumption that O_2 and CO_2 can be used interchangeably when studying metabolism of aquatic ecosystems. O_2 is advantageous over CO_2 because it can be measured directly in the aqueous phase without gas extraction. Therefore, indirect assessments of CO_2 based on dissolved O_2 are often favored over direct CO_2 measurements [6, 7]. However, combined CO_2 and O_2 measurements have shown decoupling over time [8-10]. This may in part be explained by decoupling of production and consumption of these gases across the aquatic-terrestrial interface and thus reflect the catchment type of the aquatic ecosystem [9]. Other explanations for the deviations in CO_2:O_2 coupling could be inputs of CO_2-rich water and anaerobic CO_2 cycling [11]. Simultaneous measurements of CO_2 and O_2 concentrations thus increase the understanding of lake ecosystem functioning. Ratios of CO_2:O_2 may in turn give a better indication of lake net heterotrophy than CO_2 or O_2 saturation alone, since it encompass the net balance between autotrophic and heterotrophic and well as physical and chemical processes. It will also provide insight in spatial drivers of CO_2 emissions that could allow a space-for-time approach to address future changes in e.g. climate, hydrology and forest cover.

74 Biological oxidation of dissolved organic matter (DOM) is a main source of aquatic CO_2 [12-
75 14] while photochemical oxidation plays a smaller role [14, 15]. Other sources may be CO_2
76 from catchment processes like root exudation or supersaturated groundwater (Raymond et al.,
77 2013). Depending on the pH and buffering capacity of the water, inorganic carbon is either
78 present as CO_2 or reacts with water forming bicarbonate or carbonate. Lake chemistry and
79 notably pH thus plays a key role in determining the CO_2 concentration in the water. Similarly,
80 elevated temperatures will reduce concentrations while not necessarily the level of saturation
81 or the CO_2:O_2 ratio, as the dissolution of both gases depends similarly on temperature.
82 The Boreal zone is characterized by extensive land-water interfaces. Forests with large
83 above- and below-ground C-pools as well as abundant bogs and wetlands, export terrestrial
84 DOM and dissolved inorganic carbon (DIC) to waters, making boreal aquatic ecosystems an
85 especially important component of the global carbon cycle [2]. In certain areas also
86 agricultural areas may be important sources of organic C. Climate change, changes in land
87 use, most notably afforestation, and the recovery from acidification [16] have led to increased
88 export of terrestrial DOM and a shift in water color towards brown in many boreal
89 freshwaters [17, 18]. This "browning" may affect lake metabolism in various ways.
90 Terrestrially derived DOM provides energy and nutrients to heterotrophs, stimulating
91 bacterial metabolism and CO_2 production [19, 20]. Nutrients associated to DOM may also
92 benefit autotrophs. However, the beneficial effect of enhanced nutrient loadings is overridden
93 by enhanced light attenuation inhibiting primary production as DOM concentration increases
94 [20, 21]. This trade-off between positive and negative effects of increasing DOM inputs on
95 photosynthesis may yield a unimodal response in primary production with a maximum around
96 5-10 mg DOC l^{-1} [22, 23].
97 In contrast to boreal lakes, Arctic lakes have generally unforested catchments with less
98 developed soils, yet there is a gradient from sub-Arctic to high-Arctic sites. Still they are

generally supersaturated with and net emitters of CO_2 to the atmosphere [24]. Lake abundancy is higher in the Arctic than in any other region of the world with high complexity in lake type ranging from clear, pristine, mountain lakes to brown, DOM rich thermokarst lakes formed by thawing permafrost [25-27]. Climate warming in the Arctic has led to increased biomass and production of terrestrial plants and schrubs, so called Arctic greening, leading to increased loads of DOM to Arctic lakes [28-30]. At the same time, thawing permafrost results in inputs of old organic carbon to Arctic lakes that may undergo microbial oxidation [31-33]. Increased DOM loadings in Arctic lakes are thus expected to result in enhanced CO_2 production and emission [30, 34, 35].

Autochthonous (in-lake) production is however not the only source of DIC. Lateral flux of inorganic carbon produced in the catchment may account for a sizeable share of lake CO_2, especially in small lakes with short retention times and long ice-free seasons [36]. In-lake DOM mineralization together with DIC inputs make most lakes worldwide supersaturated with- and net emitters of CO_2 to the atmosphere [1, 37].

Whether a lake is a net conduit of CO_2 is however not necessarily a sign of net heterotrophy but could also reflect that catchment derived CO_2 exceeds photosynthetic uptake. Likewise, the magnitude of atmospheric CO_2 uptake in a net autotrophic system may be reduced by inputs of terrestrial CO_2. There are conflicting reports of whether CO_2 produced in aquatic environments via DOM mineralization or exported from terrestrial environments is the main regulator of lake CO_2 flux [36, 38-40]. Some of the contradictory findings likely depend on climate, local hydrology, catchment slopes, water retention time, and not the least catchment properties like lake size or fraction and type of forest, bogs and wetlands [41, 42].

In this paper, we aim to gain understanding of lake CO_2 source, whether it is dominated by in-lake processes or by allochthonous inputs and whether there is a latitudinal difference in drivers of lake CO_2:O_2 ratio, notably related to forested or unforested catchments. To do so,

we couple surface CO_2 and O_2 concentrations in 103 Norwegian lakes to environmental variables along a geographical gradient ranging from the boreal zone in southern Norway (58^o N) through sub-Arctic northern Norway (69 ^{o} N) to the high Arctic at Svalbard (79^o N). The gradient reflects different catchment properties varying from dense spruce forest, via open birch forest to totally unforested catchments with thin soils in the high Arctic. We believe that this wide spatial gradient across climatic regions and catchment properties could provide insights relevant to larger parts of both the boreal and the arctic biome, yet with the proviso that there clearly may be pronounced regional differences within this vast area.

Materials and methods

Study lakes

During fall 2019, 73 lakes in South-Eastern Norway (Boreal) and 22 Arctic lakes on Svalbard (high-Arctic) were sampled and a number of water chemistry parameters and dissolved gases were measured. In fall 2020, additionally 14 sub-Arctic lakes in the Finnmark county (Northern Norway; sub-Arctic) were sampled (Fig. 1). Sampling was performed at, or shortly after, fall overturn, to secure a maximum vertical homogenization of the water masses and gases. Since onset of fall differs with latitude, the samplings were performed during October, September and August for the three clusters of lakes (Boreal, sub-Arctic and high-Arctic, respectively), reflecting their geographical position from south to north. The boreal, southern cluster of lakes is within the coniferous forest zone but covers locations differing in size and altitude. The sub-Arctic lakes have sparsely forested catchments with birch, less topographic variation and larger areas of bogs and wetlands, while the high Arctic sites are treeless and also with very sparely developed soils. Granitic and metamorphic bedrock dominate in the southern zone, yielding low alkalinity lakes (Fig. S1). The catchments of these lakes are also characterized by well-developed soils. The sub-Arctic lakes are situated on granitic to

sedimentary rocks (slate) giving rise to a wide range in alkalinity. The sub-Arctic lakes were chosen to span a geographical gradient from the southern inland to the costal northeast, reflecting a gradient in biome domination from taiga to Arctic tundra. A high proportion of the high-Arctic lakes are situated on limestone bedrock, with elevated alkalinity (Fig. S1). The high-Arctic lakes are mostly small with catchments devoid of soil and vegetation beyond scrubs and mosses, covering a gradient from rocky terrain from glacier fronts to shore sites, the latter influenced by birds and with some vegetation [43].

Sampling and field sample preparations

The lakes were sampled in early fall, after mixing but before ice-on. Sampling was performed from the shore using a sampling rod with a beaker, collecting surface water in a bucket. At the sampling sites, *in situ* measurements of temperature (T), pH and electrical conductivity (EC) were taken using a portable multimeter (Hach HQ40D). Samples were processed *in situ* for further analysis of lake chemistry: 50 ml of unfiltered water was taken for the analysis of total organic carbon (TOC), total nitrogen (TN) and total phosphorus (TP). For analysis of DOC, dissolved nitrogen (DN) and phosphorus (DP), surface water from the bucket was filtered in the field through Sterivex 0.22 µm pore size filters (Millipore). All samples were frozen until further analysis.

Dissolved CO_2, O_2 and argon (Ar; all sites except Svalbard) were analyzed using the headspace method after acidification [44]. The samples were prepared in the field by filling 30 ml water in a syringe, creating an in-situ headspace with air (20 ml) and adding 0.6 ml of 3% HCl (≈ 1M). Syringes were closed and equilibrated by shaking the syringes for 3 min. *In situ* lake temperature was used as equilibration temperature and caution was exercised to not warm the syringes during shaking. The equilibrated headspace gas was then injected into He-

washed and pre-evacuated glass vials crimp sealed with butyl rubber septa, and then kept at room temperature until analysis by gas chromatography.

Laboratory analysis

TOC and DOC were measured by infrared CO_2 detection after catalytic high temperature combustion (Shimadzu TOC-VWP analyser). TP was measured on an Autoanalyser (Thermo Finnigan EA 1112 series flash elemental analyser) as phosphate after wet oxidation with peroxodisulfate. TN was measured on unfiltered samples by detecting nitrogen monoxide by chemiluminescence using a TNM-1 unit attached to the Shimadzu TOC-VWP analyser. Concentrations of CO_2, O_2 and Ar were determined by automated gas chromatography (GC) analysis with He back-flushing as described by Yang et al. [13]. The level of saturation of each gas relative to equilibrium with ambient air was calculated from measured concentrations using Henry's law with temperature-dependent solubility constants. In the sites where Ar was measured, O_2 was normalized to Ar saturation for a more stable and accurate estimate of O_2 saturation [45].

Statistical analysis

All data analysis was performed using the open-source software R version 3.4.1 [46]. We use Spearman's rank correlation as a measure of association between continuous variables. To calculate DIC from pH and CO_2 at the *in situ* temperature, we used the AquaEnv package [47]. For the statistical modelling, we used the mgcv package [48] to fit generalized additive models (gam) of the gaussian family to the dependent variables. To test the dependency of CO_2:O_2 ratio and O_2 saturation, we used a gam model with smoothers on each of the explanatory variables DOC (mg L^{-1}), TP (µg L^{-1}), TN (mg L^{-1}), and conductivity (EC; µS cm^{-1}). Predictive variable selection was done by applying additional shrinkage on the null space

of the penalty with the select=TRUE argument in the mgcv::gam function, as recommended by Marra and Wood [49]. The resulting models have all smoothers that are not necessary for the fit as close to zero as possible.

Results

Saturation levels of O_2 varied with geographical location (Fig. 2). By contrast, CO_2 saturation covered a much wider range with both undersaturated and supersaturated lakes in the sub-Arctic and saturation or supersaturation in the boreal and the high-Arctic lakes (Table 1; Fig. 2).

The majority of the boreal lakes were supersaturated with CO_2 and undersaturated with O_2, with a weak but significantly negative correlation between CO_2 and O_2 saturation levels ($\rho = -0.42$, $p < 0.001$). The sub-Arctic and high-Arctic lakes, which were all saturated or supersaturated with O_2 showed deviating patterns of CO_2 saturation with no significant correlation between CO_2 and O_2 saturation levels (Fig. S2). Across all three latitudinal zones, lake O_2 saturation levels showed lower variation than CO_2 saturation levels. Hence, the variation in CO_2:O_2 ratio was mainly governed by CO_2 saturation (Fig. 2).

General patterns among nutrients and conductivity

While high Arctic lakes had lower DOC concentrations than boreal lakes on the mainland, there were no major differences in DOC concentrations among the boreal and the sub-Arctic mainland lakes (Table 1). In the boreal lakes, DOC concentrations correlated positively with TN and total conductivity ($\rho = 0.48$ and $\rho = 0.45$, respectively; Fig. S3). The relation between DOC and TP was also positive but weak. Conductivity ranged between 6 and 243 µS cm^{-1} with a median value at 24 µS cm^{-1} (Table 1) and correlated best with TN ($\rho = 0.72$; Fig. S3).

Similar to the boreal lakes, DOC was positively correlated to TN in both the sub-Arctic and in the high-Arctic lakes ($\rho = 0.42$ and $\rho = 0.65$, respectively). However, there was no significant relation between DOC and conductivity in the high-Arctic while in the sub-Arctic, the relation was weak but negative (Fig. S3). DOC and pH correlated positively in the high-Artic ($\rho = 0.65$) and in the sub-Arctic lakes there was a positive correlation between conductivity and pH ($\rho = 0.59$). TP was generally lower in the high-Arctic than in the boreal and sub-Arctic lakes and 12 of the 22 lakes in the high-Arctic had TP concentrations below detection limit. Conductivity in the high-Artic lakes was generally higher and had a wider range than in the boreal lakes (Table 1).

In all lakes, there was a strong positive correlation between conductivity and DIC concentrations (Fig. S3). In the boreal lakes, DIC concentrations were generally low. Contrastingly, in the Arctic the relationship between DOC and DIC was either negative (sub-Arctic) or non-existing (high-Arctic) and thus inorganic compounds are the main sources of alkalinity in the arctic lakes. Including all lakes in the full model with DOC, TP, TN, and conductivity as independent variables, the model explained 42 % of the deviance, with conductivity, TP and DOC concentration as significant predictors (Table 2). Since the variables predicting the CO_2:O_2 ratio differed with geographic location, the models were also run for each zone separately.

Boreal zone

As stated, the CO_2 and O_2 saturation were negatively related with each other in the boreal lakes. A model with DOC as the only explanatory variable explained 35 % of the deviance. The full model, including TN, TP, and conductivity, improved the deviance explained to 73 % (Table 2; Fig. 3a). DOC and conductivity were the strongest predictors, both having positive

effects on the CO_2:O_2 ratio. O_2 saturation in the boreal lakes was negatively related to DOC concentrations and positively related to TN (Fig. S3).

High-and sub-Arctic lakes

CO_2:O_2 ratios in the Arctic lakes were primarily driven by conductivity (positive) and TN (negative) with the models explaining 75 % and 98 % of the deviance for the sub-Arctic and the high-Arctic, respectively (Table 2; Fig. 3b and 3c). In the high-Arctic, DOC was a weak ($p = 0.04$), mainly negative predictor of CO_2:O_2 ratio while TP was below detection limit in most lakes and excluded from the analysis. In the sub-Arctic, neither DOC nor TP were significant predictors of CO_2:O_2 ratio.

All lakes in the Arctic were saturated with O_2. In the sub-Arctic, O_2 saturation was at 100 % in all lakes without variation among lakes and, hence, no correlation was found between O_2 saturation and any other variable. In the high-Arctic, O_2 saturation spanned a wider range from saturation to oversaturation. The only variable that correlated with O_2 saturation was conductivity ($\rho = -0.48$). Modelling the CO_2:O_2 ratio in the high-Arctic lakes with conductivity as the only independent variable explained 69 % of the deviance. In the sub-Arctic, 70 % of the deviance was explained with conductivity as the only explanatory variable.

Discussion

O_2 and CO_2 saturation

We analyzed saturation levels of O_2 and CO_2 as well as CO_2:O_2 ratios in surface lake waters of three different regions of Norway to assess regional differences in lake metabolism related to catchment properties and key water quality parameters. The study revealed striking differences between boreal on the one hand, and sub-Arctic and high-Arctic sites on the other

hand. The boreal lakes (n = 73) all had catchments dominated by coniferous forests, primarily spruce and pine and the terrestrial C-fixation by forests enrich also lake water with DOC [17, 18, 50], which in turn promote the biogenic production of CO_2 from bacterial respiration [1, 2, 14, 38]. The positive relationship between CO_2 saturation and DOC concentration indicates in-lake CO_2 production by DOC mineralization, but could also reflect a negative relation between DOC and retention time, and that more CO_2 is flushed in from the catchment in systems with low retention times. On the other hand, short retention times are associated with inputs of highly reactive DOC [51], yielding enhanced CO_2 production rates. The two explanations are thus not mutually exclusive, and in the high-Arctic sites, the CO_2:O_2-ratio was primarily driven by input of allochthonous CO_2.

The corresponding negative relationship between DOC concentration and O_2 saturation suggests enhanced microbial O_2 consumption, which may go along with a decrease in primary production when DOC inputs rise [21, 52]. The net heterotrophy that is prevailing in boreal DOC-rich lakes is attributed both to reduced photosynthesis in the water column and enhanced microbial respiration [53]. Together with the negative relation between CO_2 and O_2 saturation, such findings indicate that in-lake processes are the main drives of the CO_2:O_2 balance and that the level of net heterotrophy increases with increasing DOC concentration in the boreal lakes.

Besides biological processes and air-water exchange, lateral input via groundwater and surface run-off contribute to lake CO_2 [54, 55]. Groundwater input has been shown to correlate well with conductivity, as water in contact with bedrock is likely to become enriched in ions and minerals. The positive relationship between CO_2 saturation and conductivity may thus indicate lateral input of CO_2 [56]. Further, lake pH may regulate the CO_2 concentration with a higher proportion of the DIC staying as free CO_2 at low pH values while at higher pH values, more CO_2 enters the carbonate cycle, forming carbonate and bicarbonate. Boreal lakes

296 are low in alkalinity (Fig. S1) and sensitive to changes in pH. Therefore, besides serving as a
297 substratum for heterotrophic bacteria, enhanced input of humic acids may result in a decline
298 in pH and an additional increase in CO_2 saturation [57].
299
300 *The role of nutrients*
301 Phosphorus is the major limiting nutrient of bacterioplankton and has been previously shown
302 to be a strong driver of lake CO_2 supersaturation [13, 58, 59]. The influence of TP on the
303 CO_2:O_2 ratio in the boreal lakes was positive up to about 15 µg DOC l^{-1}, above which the
304 effect declined and became negative. However, there were only few observations with high
305 TP concentrations resulting in wide confidence interval in the second half of the curve (Fig.
306 3a). The ratio of CO_2:O_2 could also be affected by the bacterial carbon use efficiency which
307 depends on the nutrient to C ratio of the substrate with high ratios allowing to allocate more C
308 to growth while with low ratios, bacteria may dispose excess C as enhanced respiration [60,
309 61]. Accordingly, CO_2 saturation was negatively related to the TP:DOC ratio in boreal lakes
310 (Fig. S4), suggesting enhanced rates of CO_2 production in lakes where DOC concentrations
311 were high in relation to TP concentrations.
312 Primary production in boreal lakes has been shown to be strongly affected by nitrogen
313 availability in areas receiving low input of N [62] and the positive effect of TN on O_2
314 saturation likely reflects increased primary production with increased TN concentrations.
315
316 *Different dynamics in high-latitude lakes*
317 A main result of our study was the difference between boreal and Arctic catchments in terms
318 of CO_2 and thus CO_2:O_2-ratio. In contrast to the boreal lakes, DOC concentration did not
319 appear to drive the CO_2:O_2 ratio in Arctic lakes, and there was no significant difference in
320 CO_2 saturation between lakes with high and low DOC concentrations. This was consistent

both for sub-Arctic and high-Arctic sites despite the difference in soils and bogs, and points to absence or presence of coniferous forests in the catchment as a major determinant. This is also in support of a recent comparison between boreal (forested) and Arctic sites [41]. The majority of the studied Arctic lakes were saturated or oversaturated with both O_2 and CO_2 without any relation between O_2 and CO_2 saturation level. These lakes are generally shallow and low in productivity. Hence, O_2 saturation is most likely a result of downward mixing rather than primary production.

Among the significant predictors of the CO_2:O_2 ratio in the Arctic, conductivity was clearly predominant (Table 2; Fig. 3b and 3c). This suggests that the majority of lake CO_2 in the Arctic entered from the surrounding mineral soils [63] and was not produced through in-lake DOC mineralization. For some high-Arctic sites, conductivity can also be coupled to their proximity to the sea. The lakes closest to the sea are also the lakes most influenced by vegetation and most frequently visited by birds, yielding enhanced DOC and nutrient input via bird feces [43].

While CO_2 saturation increased with conductivity, we observed no correlation between conductivity and DOC concentration in neither the sub-Arctic nor the high-Arctic. Instead, conductivity was closely correlated with DIC concentrations and total alkalinity in both Arctic regions. In the sub-Arctic, CO_2 saturation spanned from undersaturated to supersaturated. Saturation level was closely related to conductivity and thus also to total alkalinity. Alkalinity in turn could be coupled to bedrock, indicating weathering to be a source of lake DIC. Likewise, the relatively high alkalinity together with the lime-rich bedrock suggests carbonate weathering to be a DIC source also in the high-Arctic lakes [41, 64].

In the high-Arctic lakes, O_2 saturation correlated negatively with conductivity. While all lakes were supersaturated with O_2, there was more variation in CO_2 saturation with 7 out of 22 lakes being undersaturated or close to saturation and the rest supersaturated. The seven CO_2

346 undersaturated lakes were all high in DOC and TN and highly influenced by birds. Many high
347 latitude lakes are naturally poor in nutrients and although there was no significant relation
348 between TN and O_2 saturation, additions of N via birds may stimulate primary production
349 with a concomitant drawdown of CO_2.
350 The sub-Arctic lakes were all close to O_2 saturation with little variation among lakes (95 % -
351 99 %), meaning that the variability in CO_2:O_2 ratio was determined by CO_2 alone. Most
352 studies suggest that arctic lakes are net heterotrophic, as they are net emitters of CO_2 to the
353 atmosphere [2, 65]. The majority of Arctic lakes in our study was indeed supersaturated and
354 net emitters of CO_2 at the time of sampling. However, the uncoupling of CO_2:O2 ratio from
355 DOC and of CO_2 and O_2 saturation indicate an allochthonous CO_2 source rather than in-lake
356 heterotrophic respiration. The high O_2 saturation levels together with a dominance of
357 allochthonous DIC suggest autotrophy rather than heterotrophy in the arctic lakes studied
358 here. In contrast to other parts of the arctic where permafrost cover vast areas, permafrost in
359 the Scandinavian arctic is generally found in palsas or in mountainous areas. Although
360 allochthonous DIC may gouvern the CO_2 in the arctic lakes in this study, heterotrophic
361 mineralization of DOC may thus have an impact on CO_2 saturation in arctic lakes affected by
362 permafrost thawing.
363
364 *Conclusion*
365 Based on a large number of (mostly) boreal lakes, Larsen et al [38] claimed DOC to be a
366 universal predictor of lake pCO_2, while groundwater influx was a minor contributor.
367 However, including also sub- and high-Arctic lakes, we found a clear distinction in drivers of
368 CO_2 saturation along a latitudinal gradient. The boreal lakes followed the expected pattern
369 with both CO_2 and O_2 saturation being largely dependent on DOC concentrations and relating
370 negatively to each other, suggesting enhanced net heterotrophy with increased DOC inputs. In

the Arctic lakes, despite the differences between sub-Arctic and high-Arctic sites, there was no correlation between DOC and CO_2, yet these sites were also to a large degree supersaturated with CO_2 and thus could be considered net heterotrophic. However, most of these lakes were also saturated or supersaturated with O_2, indicative of low respiratory activity in agreement with generally nutrient-poor conditions and low levels of primary production. This is supported by the positive correlation between CO_2:O_2 ratio and conductivity, while the influence of DOC concentration was weak or non-significant. This may suggest that the major share of CO_2 in these lakes is of allochthonous origin, likely from organic carbon mineralization and carbonate weathering in the catchment soils, entering via groundwater flow [41, 56]. This points to fundamentally different links between DOC and CO_2 in boreal and Arctic catchments, pinpointing the fundamental role of coniferous forests for organic and inorganic carbon dynamics in lakes.

Funding

This work was supported by the Centre of Biogeochemistry in the Anthropocene (CBA) and Belmont Forum project ArcticBiodiversity

The authors have no relevant financial or non-financial interests to disclose.

Author contribution

Lina Allesson and Dag Hessen conceived the idea. Lina Allesson, Peter Dörsch and Nicolas Valiente Parra performed material preparation and data collection. All authors were involved in the analysis of data and final writing and approved the submitted version.

Data availability statement

All data will be made available upon request, or if demanded, stored in a UiO repository (GitHUB)

1. Cole, J.J., et al., *Plumbing the Global Carbon Cycle: Integrating Inland Waters into the Terrestrial Carbon Budget.* Ecosystems, 2007. **10**(1): p. 172-185.
2. Tranvik, L.J., et al., *Lakes and reservoirs as regulators of carbon cycling and climate.* Limnology and oceanography, 2009. **54**(6part2): p. 2298-2314.
3. Bastviken, D., et al., *Fates of methane from different lake habitats: Connecting whole-lake budgets and CH4 emissions.* Journal of Geophysical Research: Biogeosciences, 2008. **113**(G2).
4. Cole, J.J. and N.F. Caraco, *Carbon in catchments: connecting terrestrial carbon losses with aquatic metabolism.* Marine and Freshwater Research, 2001. **52**(1): p. 101-110.
5. Hanson, P.C., et al., *Lake dissolved inorganic carbon and dissolved oxygen: changing drivers from days to decades.* Ecological Monographs, 2006. **76**(3): p. 343-363.
6. Marchand, D., Y.T. Prairie, and P.A. Del Giorgio, *Linking forest fires to lake metabolism and carbon dioxide emissions in the boreal region of Northern Quebec.* Global Change Biology, 2009. **15**(12): p. 2861-2873.
7. Del Giorgio, P.A., et al., *Coherent patterns in bacterial growth, growth efficiency, and leucine metabolism along a northeastern Pacific inshore-offshore transect.* Limnology and Oceanography, 2011. **56**(1): p. 1-16.
8. Torgersen, T. and B. Branco, *Carbon and oxygen fluxes from a small pond to the atmosphere: Temporal variability and the CO2/O2 imbalance.* Water Resources Research, 2008. **44**(2).
9. Crawford, J.T., et al., *CO2 and CH4 emissions from streams in a lake-rich landscape: Patterns, controls, and regional significance.* Global Biogeochemical Cycles, 2014. **28**(3): p. 197-210.
10. Stets, E.G., et al., *Carbonate buffering and metabolic controls on carbon dioxide in rivers.* Global Biogeochemical Cycles, 2017. **31**(4): p. 663-677.
11. Vachon, D., J.-F. Lapierre, and P.A. del Giorgio, *Seasonality of photochemical dissolved organic carbon mineralization and its relative contribution to pelagic CO2 production in northern lakes.* Journal of Geophysical Research: Biogeosciences, 2016. **121**(3): p. 864-878.
12. Jansson, M., et al., *Allochthonous organic carbon and phytoplankton/bacterioplankton production relationships in lakes.* Ecology, 2000. **81**(11): p. 3250-3255.
13. Yang, H., et al., *Greenhouse gas metabolism in Nordic boreal lakes.* Biogeochemistry, 2015. **126**(1): p. 211-225.
14. Allesson, L., et al., *The role of photomineralization for CO2 emissions in boreal lakes along a gradient of dissolved organic matter.* Limnology and Oceanography, 2020.
15. Koehler, B., et al., *Sunlight-induced carbon dioxide emissions from inland waters.* Global Biogeochemical Cycles, 2014. **28**(7): p. 696-711.
16. De Wit, H.A., et al., *Long-term increase in dissolved organic carbon in streamwaters in Norway is response to reduced acid deposition.* Environmental Science & Technology, 2007. **41**(22): p. 7706-7713.
17. Finstad, A.G., et al., *From greening to browning: Catchment vegetation development and reduced S-deposition promote organic carbon load on decadal time scales in Nordic lakes.* Scientific Reports, 2016. **6**(1): p. 1-8.
18. Škerlep, M., et al., *Afforestation driving long-term surface water browning.* Global change biology, 2020. **26**(3): p. 1390-1399.
19. Hessen, D., T. Andersen, and A. Lyehe, *Carbon metabolism in a humic lake: Pool sires and cycling through zooplankton.* Limnology and Oceanography, 1990. **35**(1): p. 84-99.
20. Karlsson, J., M. Jansson, and A. Jonsson, *Respiration of allochthonous organic carbon in unproductive forest lakes determined by the Keeling plot method.* Limnology and Oceanography, 2007. **52**(2): p. 603-608.
21. Karlsson, J., et al., *Light limitation of nutrient-poor lake ecosystems.* Nature, 2009. **460**: p. 506-9.
22. Seekell, D.A., et al., *The influence of dissolved organic carbon on primary production in northern lakes.* Limnology and Oceanography, 2015. **60**(4): p. 1276-1285.
23. Tanentzap, A.J., et al., *Terrestrial support of lake food webs: Synthesis reveals controls over cross-ecosystem resource use.* Science advances, 2017. **3**(3): p. e1601765.

24. Tan, Z., et al., *Modeling CO 2 emissions from A rctic lakes: Model development and site-level study.* Journal of Advances in Modeling Earth Systems, 2017. **9**(5): p. 2190-2213.
25. Downing, J.A., et al., *The global abundance and size distribution of lakes, ponds, and impoundments.* Limnology and Oceanography, 2006. **51**(5): p. 2388-2397.
26. Verpoorter, C., et al., *A global inventory of lakes based on high-resolution satellite imagery.* Geophysical Research Letters, 2014. **41**(18): p. 6396-6402.
27. Matveev, A., I. Laurion, and W.F. Vincent, *Methane and carbon dioxide emissions from thermokarst lakes on mineral soils.* Arctic Science, 2018. **4**(4): p. 584-604.
28. Myers-Smith, I.H., et al., *Shrub expansion in tundra ecosystems: dynamics, impacts and research priorities.* Environmental Research Letters, 2011. **6**(4): p. 045509.
29. Kaiser, K., et al., *Origins and transformations of dissolved organic matter in large Arctic rivers.* Scientific reports, 2017. **7**(1): p. 1-11.
30. Elder, C.D., et al., *Greenhouse gas emissions from diverse Arctic Alaskan lakes are dominated by young carbon.* Nature Climate Change, 2018. **8**(2): p. 166-171.
31. Drake, T.W., et al., *Ancient low–molecular-weight organic acids in permafrost fuel rapid carbon dioxide production upon thaw.* Proceedings of the National Academy of Sciences, 2015. **112**(45): p. 13946-13951.
32. Vonk, J.E., et al., *Reviews and syntheses: Effects of permafrost thaw on Arctic aquatic ecosystems.* Biogeosciences, 2015. **12**(23): p. 7129-7167.
33. Wauthy, M., et al., *Increasing dominance of terrigenous organic matter in circumpolar freshwaters due to permafrost thaw.* Limnology and Oceanography Letters, 2018. **3**(3): p. 186-198.
34. Tank, S.E., et al., *Landscape matters: Predicting the biogeochemical effects of permafrost thaw on aquatic networks with a state factor approach.* Permafrost and Periglacial Processes, 2020. **31**(3): p. 358-370.
35. Waldrop, M., et al., *Carbon fluxes and microbial activities from boreal peatlands experiencing permafrost thaw.* Journal of Geophysical Research: Biogeosciences, 2021. **126**(3): p. e2020JG005869.
36. Weyhenmeyer, G., et al., *Significant fraction of CO2 emissions from boreal lakes derived from hydrologic inorganic carbon inputs.* Nature Geoscience, 2015. **8**: p. 933-936.
37. Raymond, P.A., et al., *Global carbon dioxide emissions from inland waters.* Nature, 2013. **503**(7476): p. 355-359.
38. Larsen, S., T. Andersen, and D. Hessen, *The pCO2 in boreal lakes: Organic carbon as a universal predictor?* Global Biogeochemical Cycles - GLOBAL BIOGEOCHEM CYCLE, 2011. **25**.
39. Nydahl, A.C., M.B. Wallin, and G.A. Weyhenmeyer, *Diverse drivers of long-term p CO2 increases across thirteen boreal lakes and streams.* Inland Waters, 2020. **10**(3): p. 360-372.
40. Jonsson, A., et al., *Whole-lake mineralization of allochthonous and autochthonous organic carbon in a large humic lake (örträsket, N. Sweden).* Limnology and Oceanography, 2001. **46**(7): p. 1691-1700.
41. Puts, I.C., et al., *Landscape determinants of pelagic and benthic primary production in northern lakes.* Global Change Biology, 2022.
42. Valiente, N., et al., *Catchment properties as predictors of greenhouse gas concentrations across a gradient of boreal lakes.* Frontiers in Environmental Science, 2022: p. 1668.
43. Hessen, D.O., et al., *Global change and ecosystem connectivity: How geese link fields of central Europe to eutrophication of Arctic freshwaters.* Ambio, 2017. **46**(1): p. 40-47.
44. Åberg, J. and B. Wallin, *Evaluating a fast headspace method for measuring DIC and subsequent calculation of p CO2 in freshwater systems.* Inland Waters, 2014. **4**(2): p. 157-166.
45. Stanley, R.H. and W.J. Jenkins, *Noble gases in seawater as tracers for physical and biogeochemical ocean processes*, in *The Noble Gases as Geochemical Tracers*. 2013, Springer. p. 55-79.

46. Team, R.C., *R Core Team (2017). R: A language and environment for statistical computing.* R Found. Stat. Comput. Vienna, Austria. URL http://www. R-project. org/., page R Foundation for Statistical Computing, 2017.
47. Hofmann, A.F., et al., *AquaEnv: An Aqua tic Acid–Base Modelling Env ironment in R.* Aquatic Geochemistry, 2010. **16**(4): p. 507-546.
48. Wood, S.N., *Fast stable restricted maximum likelihood and marginal likelihood estimation of semiparametric generalized linear models.* Journal of the Royal Statistical Society: Series B (Statistical Methodology), 2011. **73**(1): p. 3-36.
49. Marra, G. and S.N. Wood, *Practical variable selection for generalized additive models.* Computational Statistics & Data Analysis, 2011. **55**(7): p. 2372-2387.
50. Larsen, S., T. Andersen, and D.O. Hessen, *Climate change predicted to cause severe increase of organic carbon in lakes.* Global Change Biology, 2011. **17**(2): p. 1186-1192.
51. Catalán, N., et al., *Organic carbon decomposition rates controlled by water retention time across inland waters.* Nature Geoscience, 2016. **9**(7): p. 501-504.
52. Thrane, J.-E., D.O. Hessen, and T. Andersen, *The Absorption of Light in Lakes: Negative Impact of Dissolved Organic Carbon on Primary Productivity.* Ecosystems, 2014. **17**(6): p. 1040-1052.
53. Ask, J., J. Karlsson, and M. Jansson, *Net ecosystem production in clear-water and brown-water lakes.* Global Biogeochemical Cycles, 2012. **26**(1).
54. Ojala, A., et al., *Carbon gas fluxes from a brown-water and a clear-water lake in the boreal zone during a summer with extreme rain events.* Limnology and Oceanography, 2011. **56**(1): p. 61-76.
55. Vachon, D. and P.A. Del Giorgio, *Whole-lake CO 2 dynamics in response to storm events in two morphologically different lakes.* Ecosystems, 2014. **17**(8): p. 1338-1353.
56. Rodríguez-Rodríguez, M., et al., *Using water temperature, electrical conductivity, and pH to Characterize surface–groundwater relations in a shallow ponds system (Doñana National Park, SW Spain).* Water, 2018. **10**(10): p. 1406.
57. Nydahl, A.C., et al., *Colored organic matter increases CO2 in meso-eutrophic lake water through altered light climate and acidity.* Limnology and Oceanography, 2019. **64**(2): p. 744-756.
58. Vadstein, O., *Heterotrophic, planktonic bacteria and cycling of phosphorus*, in *Advances in microbial ecology*. 2000, Springer. p. 115-167.
59. Allesson, L., et al., *Phosphorus Availability Promotes Bacterial DOC-Mineralization, but Not Cumulative CO2-Production.* Frontiers in microbiology, 2020. **11**: p. 2272.
60. Hessen, D.O., *Dissolved organic carbon in a humic lake: effects on bacterial production and respiration.* Hydrobiologia, 1992. **229**(1): p. 115-123.
61. Hessen, D.O. and T.R. Anderson, *Excess carbon in aquatic organisms and ecosystems: physiological, ecological, and evolutionary implications.* Limnology and Oceanography, 2008. **53**(4): p. 1685-1696.
62. Elser, J.J., et al., *Shifts in lake N: P stoichiometry and nutrient limitation driven by atmospheric nitrogen deposition.* science, 2009. **326**(5954): p. 835-837.
63. Dean, J.F., et al., *Biogeochemistry of "pristine" freshwater stream and lake systems in the western Canadian Arctic.* Biogeochemistry, 2016. **130**(3): p. 191-213.
64. Marcé, R., et al., *Carbonate weathering as a driver of CO2 supersaturation in lakes.* Nature Geoscience, 2015. **8**(2): p. 107-111.
65. Kling, G.W., G.W. Kipphut, and M.C. Miller, *The flux of CO 2 and CH 4 from lakes and rivers in arctic Alaska.* Hydrobiologia, 1992. **240**(1): p. 23-36.

Figures

Figure 1

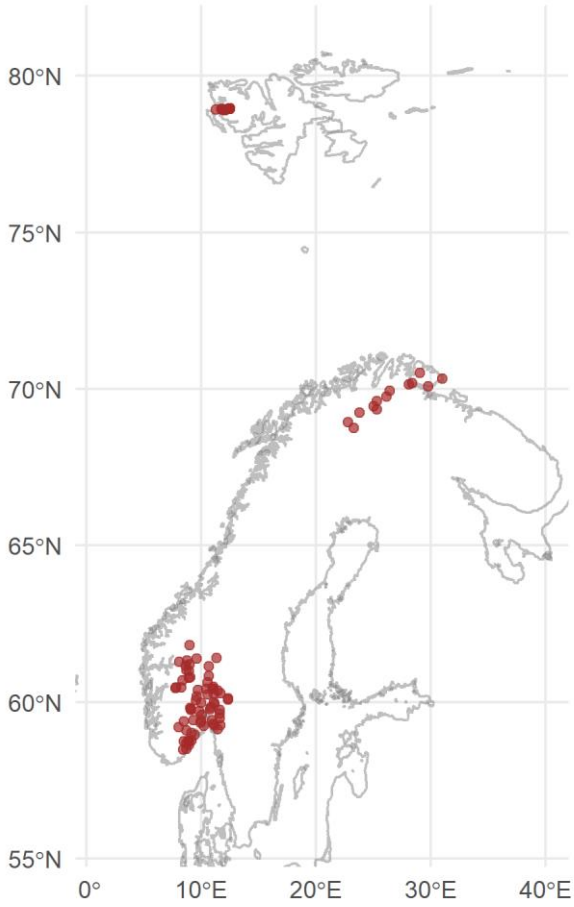

Figure 2

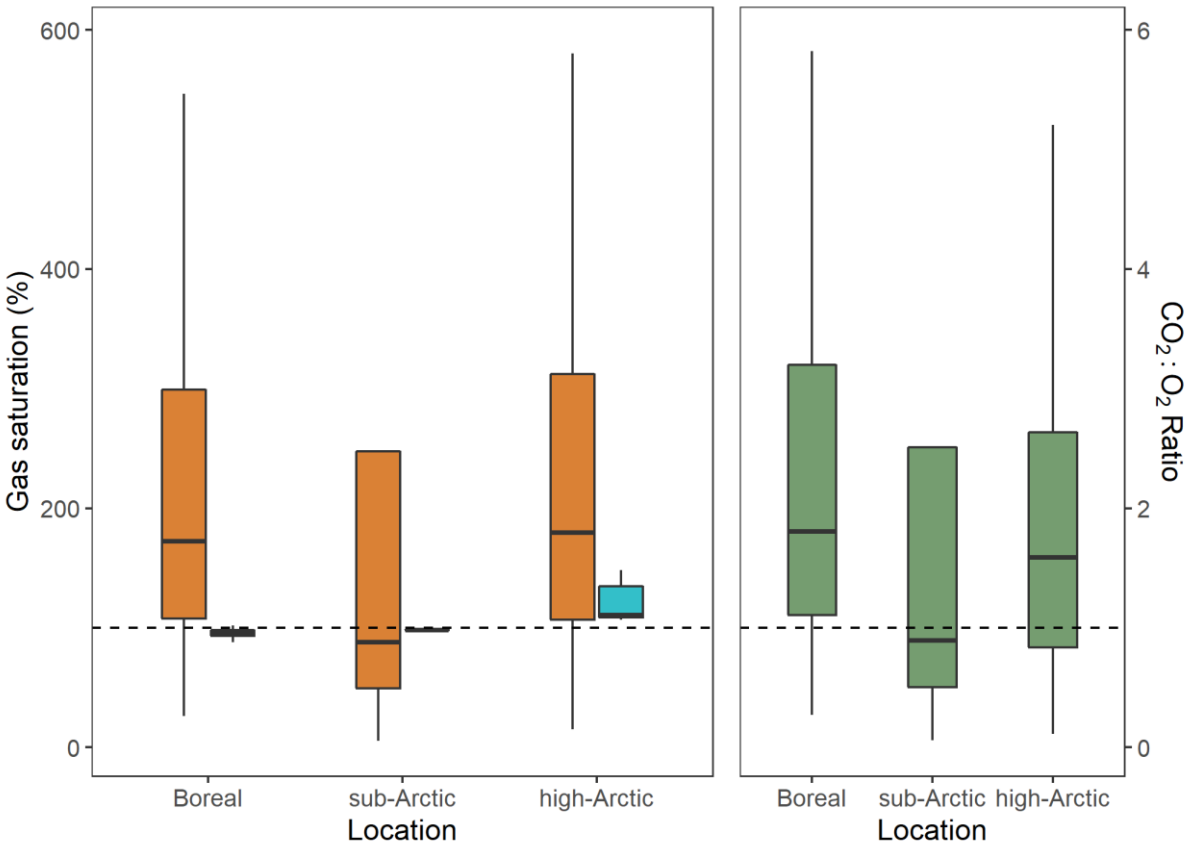
600
400
200
0
Gas saturation (%)
Boreal
sub-Arctic
high-Arctic
Location
6
4
2
0
$CO_2 : O_2$ Ratio
Boreal
sub-Arctic
high-Arctic
Location

Figure 3

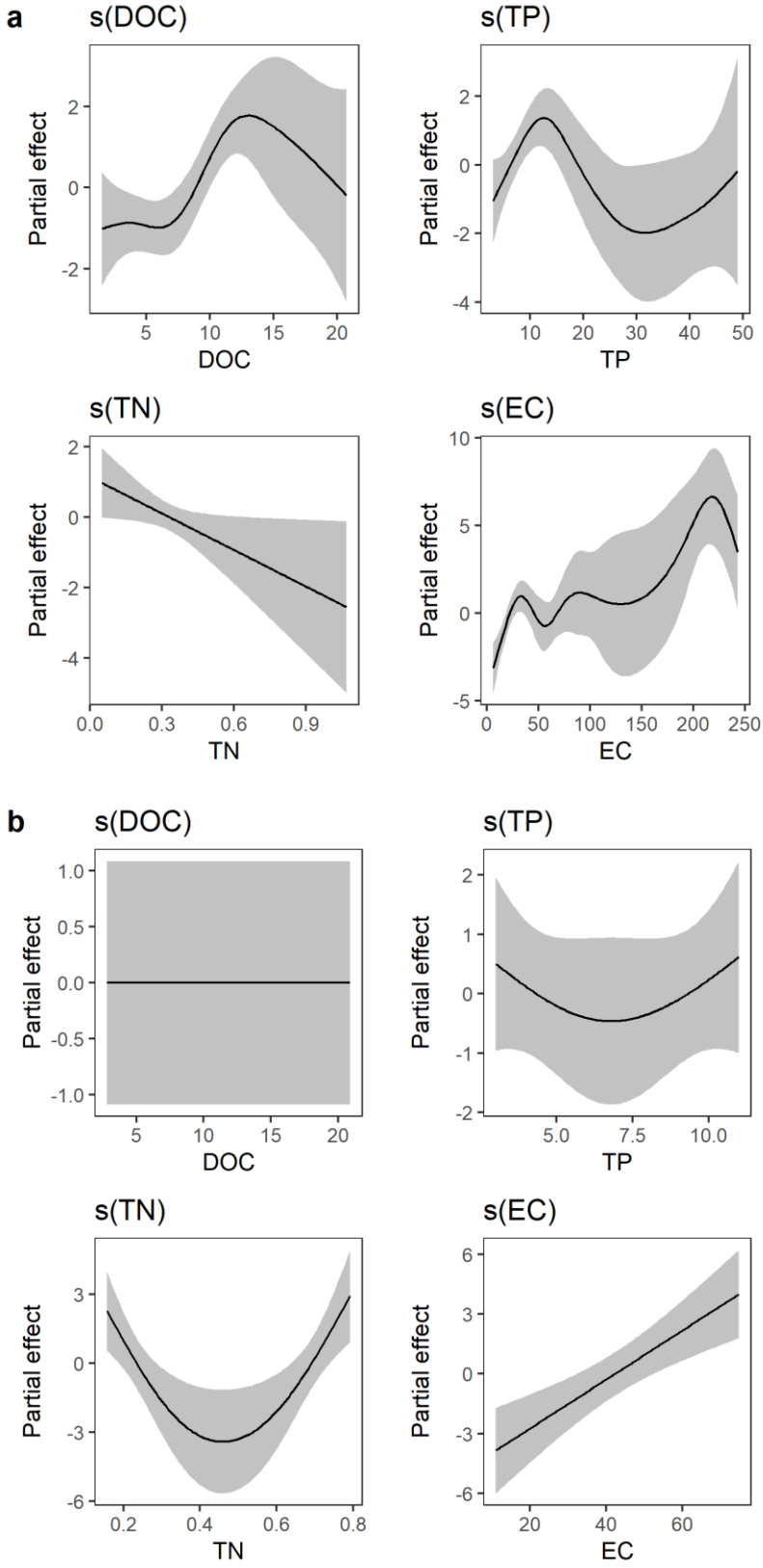
a
s(DOC)
Partial effect
DOC
s(TP)
TP
s(TN)
TN
s(EC)
EC
b
s(DOC)
Partial effect
DOC
s(TP)
TP
s(TN)
TN
s(EC)
EC

c

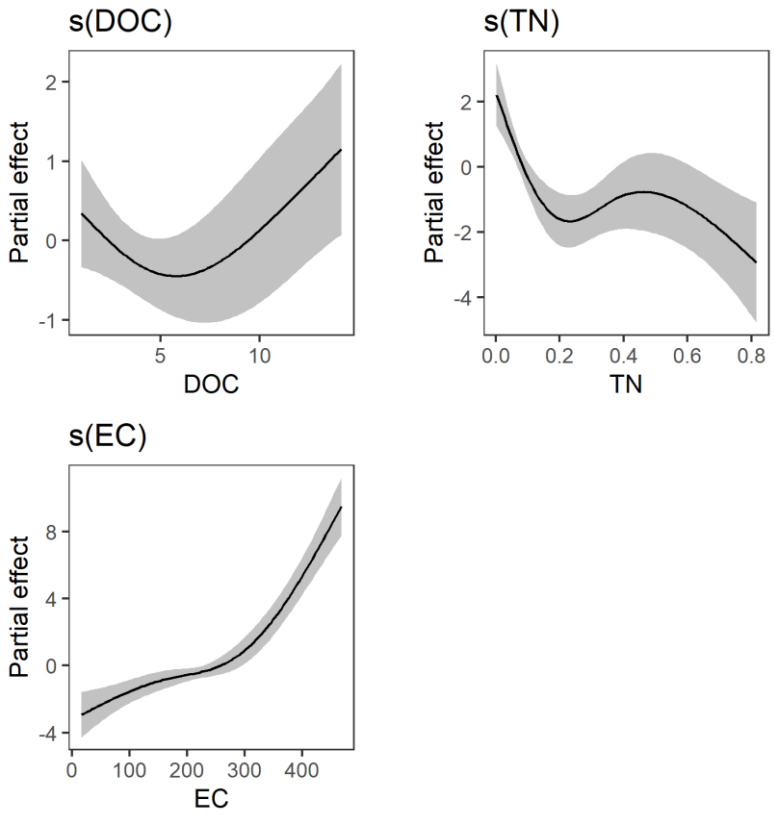
s(DOC)
Partial effect
2
1
0
-1
5
10
DOC
s(TN)
Partial effect
2
0
-2
-4
0.0
0.2
0.4
0.6
0.8
TN
s(EC)
Partial effect
8
4
0
-4
0
100
200
300
400
EC

Table 1. Statistics of the lake chemistry variables used in the analyses.

	Boreal	Sub-Arctic	High-Arctic
CO_2 saturation range (%; median; average)	26 – 1374 (175; 260)	6 – 1218 (88; 262)	15 – 1121 (180; 245)
O_2 saturation range (%; median; average)	85 – 102 (96; 95)	95 – 99 (98; 98)	107 – 148 (111; 120)
DOC range (mg l^{-1}; median; average)	1.5 – 20.7 (7.3; 7.7)	2.8 – 20.9 (6.6; 8)	1 – 14 (4; 4.9)
TP range (µg l^{-1}; median; average)	3 – 49 (9; 12)	3 – 11 (6; 6.5)	2 – 19 (3; 6.2) **
TN range (mg l^{-1}; median; average)	0.05 – 1.07 (0.27; 0.33)	0.16 – 0.79 (0.27; 0.35)	0.003 – 0.8 (0.08; 0.2)
Conductivity range (µS cm^{-1}; median; average)	6 – 243 (24.5; 42)	11 – 74.8 (40; 44.4)	16.5 – 1410 (212; 269)

**12 out of 22 lakes with concentrations below detection limit.

Table 2. Model outputs of the general additive models (CO_2:O_2~ s(DOC) + s(TP) + s(TN) + s(EC)) for the different regions. Significance codes: *** p < 0.001, ** p < 0.01, * p < 0.05, $^{non\text{-}sig}$ p > 0.05.

	Variance explained (%)	Significant predictors
All lakes	42	EC***, DOC*, TP*, $TN^{non\text{-}sig}$
Boreal lakes	73	DOC***, TP**, EC**, TN*
Sub- Arctic lakes	75	EC***, TN**, $DOC^{non\text{-}sig}$, $TP^{non\text{-}sig}$
High-Arctic lakes	94	EC***, TN**, DOC*

Figure captions

Fig. 1 Map of the site locations

Fig. 2 Box plot of lake CO_2 saturation (red), O_2 saturation (blue), and CO_2:O_2 ratio (green) in the different geographical regions. Dashed line represents the 100 % saturation (to the left) and a CO_2:O_2 ratio of 1 (to the right)

Fig. 3 Result plots of the generalized additive models (gams) predicting CO_2:O_2 saturation ratio for the three regions. In the Boreal lakes (a), the best predictor was DOC concentration followed by conductivity. In both the sub-Arctic (b) and high-Arctic (c), conductivity was the best predictor for CO_2:O_2 saturation ratio

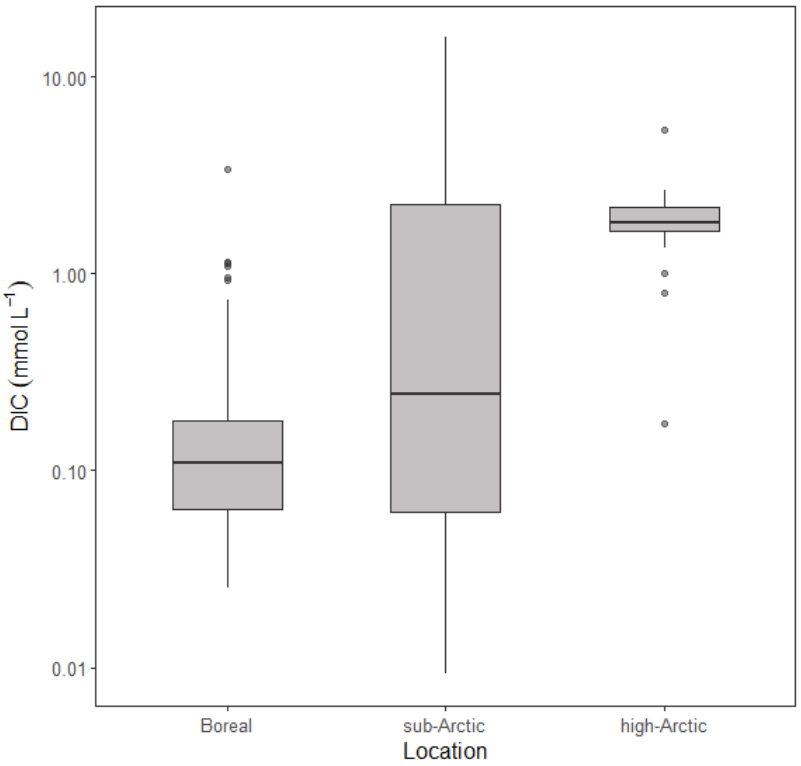

Fig. S1 Boxplot of total DIC concentration in the three regions. In the Boreal part, where granitic and metamorphic bedrock dominates, the alkalinity is generally low. The wide variability in alkalinity in the sub-Arctic is a result of the variability in bedrock from granitic to sedimentary (slate). In the high-Arctic, the majority of the lakes are situated on limestone bedrock giving elevated alkalinity.

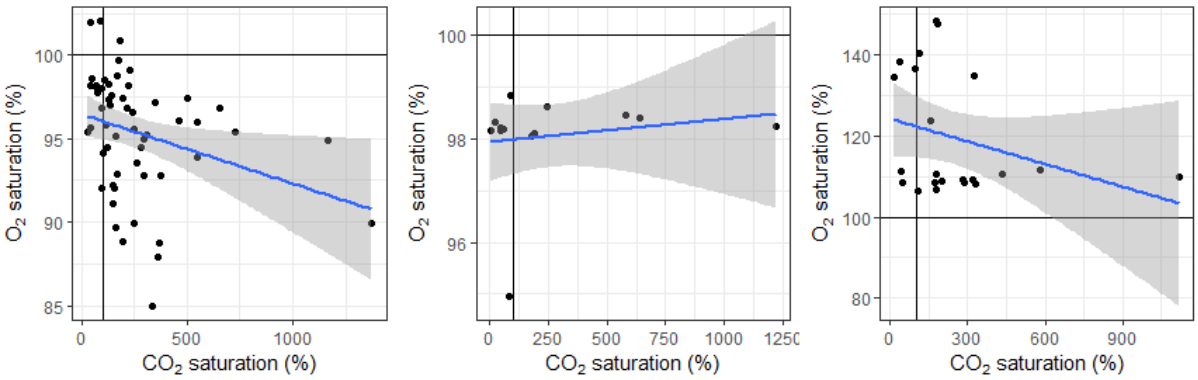

Fig. S2 Scatterplots of O_2 saturation vs. CO_2 saturation. From left to right Boreal lakes, sub-Arctic lakes, high-Arctic lakes. Although quite some scattering, there was a weak but significant negative relation between O_2 saturation and CO_2 saturation in the boreal lakes ($\rho = -0.42$). The relation was stronger in lakes with CO_2 saturation below 500 %. In the northern lakes (sub-Arctic and high-Arctic) where all lakes were saturated or subsaturated with O_2, there was no significant relation between O_2 and CO_2 saturation. Note differences in axes, lines indicate 100 % saturation.

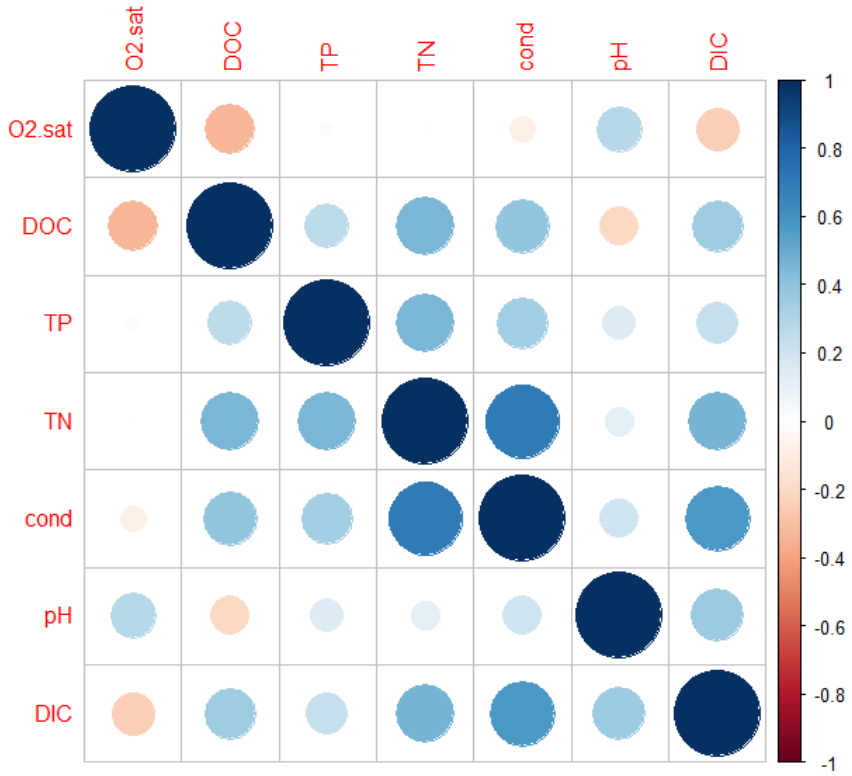
O2.sat
DOC
TP
TN
cond
pH
DIC
1
0.8
0.6
0.4
0.2
0
-0.2
-0.4
-0.6
-0.8
-1

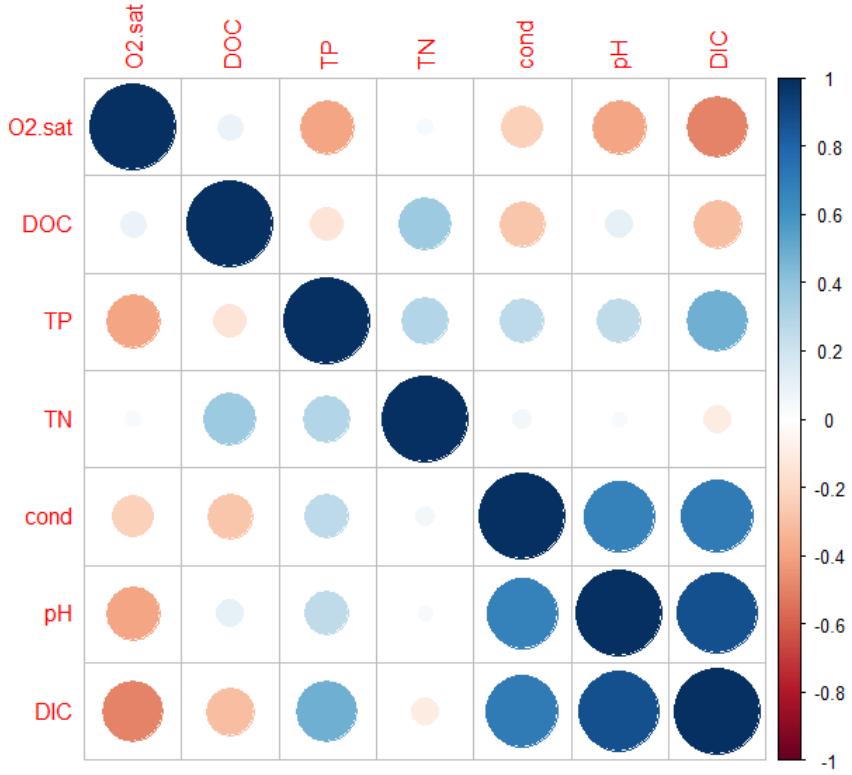
O2.sat
DOC
TP
TN
cond
pH
DIC
1
0.8
0.6
0.4
0.2
0
-0.2
-0.4
-0.6
-0.8
-1

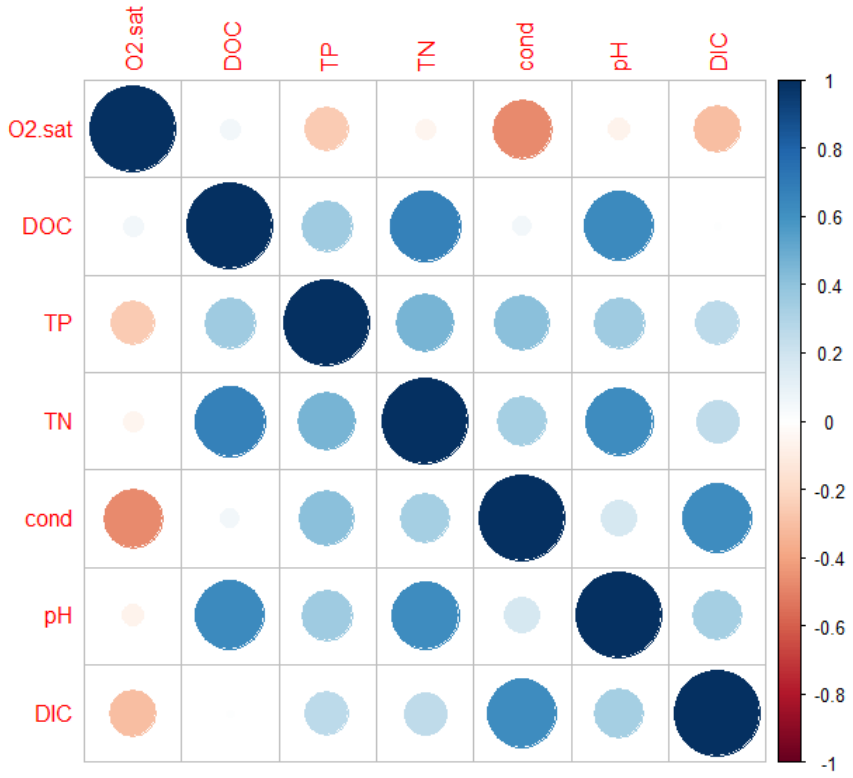

Fig. S3 Spearsman's correlation matrices of lake chemistry variables and O_2 saturation. Top to bottom: Boreal lakes, sub-Arctic lakes, high-Arctic lakes.

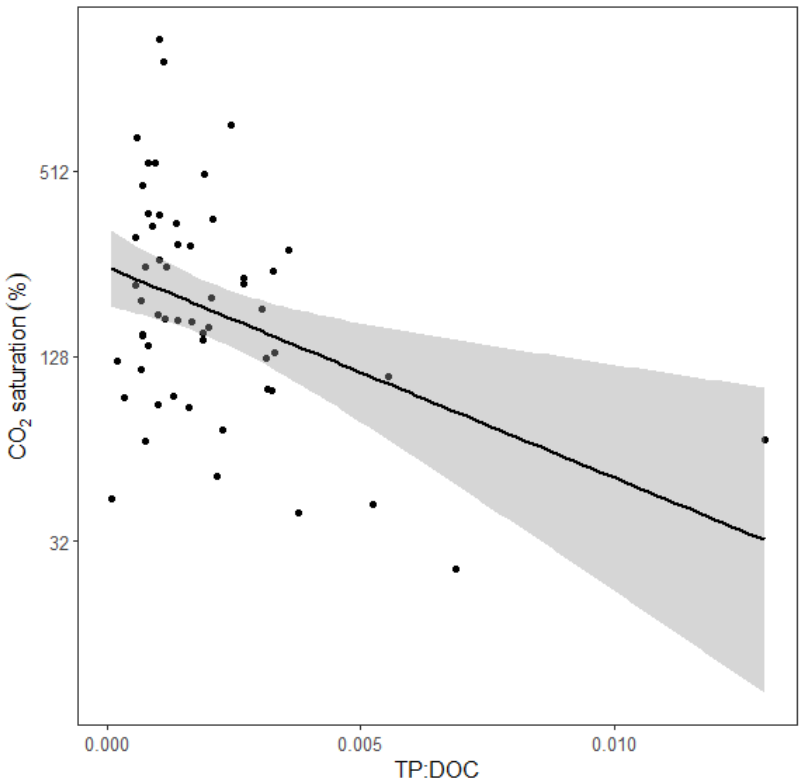

Fig. S4 CO_2 saturation vs TP:DOC ratio in the boreal lakes. The CO2 saturation level decreases as TP:DOC increases.